

Identification and validation of seedling powdery mildew resistance genes

**Dissertation
zur Erlangung des
Doktorgrades der Naturwissenschaften (Dr. rer. nat.)**

der

Naturwissenschaftlichen Fakultät III
Agrar- und Ernährungswissenschaften,
Geowissenschaften und Informatik

der Martin-Luther-Universität Halle-Wittenberg

vorgelegt von

Frau Maria Pogoda

Geb. am 06. August 1991 in Quedlinburg

Gutachter: Prof. Dr. Jochen C. Reif
Prof. Dr. Ralph Panstruga

Verteidigt am 28.10.2019

Table of context

Table of context	I
Abbreviations	IV
List of figures	VII
List of tables	VIII
1. Introduction	1
1.1. The importance of barley in agriculture and science.....	1
1.2. Resistance mechanisms of plants against microorganisms.....	2
1.3. A common plant disease: powdery mildew.....	6
1.3.1. The life cycle of cereal powdery mildew fungus.....	7
1.3.2. Race-specific powdery mildew resistance.....	9
1.3.3. Race-nonspecific powdery mildew resistance.....	11
1.4. Strengths and weaknesses of genome-wide-association studies.....	13
1.5. Identification and functional validation of candidates.....	19
1.6. The aims of this study.....	21
2. Material and methods	23
2.1. Plant material.....	23
2.1.1. Whealbi barley collection.....	23
2.1.2. Barley cultivars for powdery mildew maintenance.....	23
2.1.3. Plant growth conditions.....	23
2.2. Barley powdery mildew isolates and their maintenance.....	24
2.3. Screening for powdery mildew resistance.....	26
2.3.1. Resistance screening based on detached seedling leaves (detached leaf assay).....	26
2.3.2. Resistance screening of identified resistant genotypes with additional mildew powdery isolates (isolate tests).....	27
2.3.3. Resistance screening based on natural powdery mildew infection (field trial).....	28
2.4. Characterization of the <i>Mlo</i> -alleles in identified resistant genotypes.....	29
2.4.1. DNA isolation from seedling leaves of identified resistant genotypes.....	30
2.4.2. Screening for the <i>mlo-11</i> allele based on polymerase chain reaction.....	30
2.4.3. Determination of the <i>Mlo</i> allele status of selected genotypes based on full-length genomic sequences.....	31
2.4.4. Expression of <i>Mlo</i> of selected genotypes as semi-quantitative PCR.....	31
2.4.5. Conformation of WB 352-specific <i>Mlo</i> fragments by Sanger sequencing.....	32
2.5. Genome-wide-association study.....	33
2.5.1. Exome capture data.....	33
2.5.2. Processing of the phenotypic resistance data.....	33
2.5.3. Specifications of the mixed linear model.....	33
2.6. Characterization of candidate genes identified in the genome-wide-association study.....	34
2.6.1. Identification of candidate genes putatively involved in powdery mildew resistance.....	34
2.6.2. Determination of the allele status of selected candidate genes (allele mining).....	35
2.6.3. Relative quantification of the expression of selected candidate genes.....	36

2.7. Particle bombardment.....	37
2.7.1. Preparation of chemical competent cells.....	38
2.7.2. Generation of constructs for the functional validation tests.....	38
2.7.3. Preparation of plasmid DNA.....	40
2.7.4. Preparation of the gold suspension.....	41
2.7.5. Biolistic gene transfer.....	41
2.7.6. Inoculation with powdery mildew.....	42
2.7.7. Glucuronidase assay.....	42
2.7.8. Microscopic and statistical analysis.....	43
2.8. Additional information.....	44
3. Results.....	45
3.1. Biological status and growth habit of the Whealbi population.....	45
3.2. Screening for powdery mildew resistance in the Whealbi population.....	46
3.2.1. Evaluation of the seedling powdery mildew resistance in controlled environmental conditions.....	46
3.2.2. Association of the adult plant resistance under natural powdery mildew infection and the determined seedling resistance based on detached leaves	48
3.3. Identification of known powdery mildew resistance genes in resistant varieties..	50
3.4. Characterization of two putative novel natural mlo mutants.....	54
3.5. Identification of candidate genes involved in powdery mildew resistance based on a genome-wide-association study.....	64
3.6. Evaluation of the identified candidate genes involved in powdery mildew resistance based on in silico and in vitro analyses.....	67
3.6.1. <i>In silico</i> determination of alleles of the identified candidate genes.....	67
3.6.2. Expression and amplification of the defined candidate alleles in various genotypes.....	68
3.6.3. Determination of the allele effect on powdery mildew resistance.....	72
3.7. Functional assessments of the four most promising candidate genes.....	74
3.7.1. Functional analysis of selected candidates based on in silico data.....	74
3.7.2. Functional validation of selected candidates based on transient silencing and overexpression.....	79
3.8. Selection of the best promoter_GUS construct for transient validation assays.....	81
4. Discussion.....	84
4.1. Evaluation of the observed powdery mildew resistance.....	84
4.1.1. A critical view on the phenotyping approach.....	84
4.1.2. Confirmation and postulation of resistance genes and their importance for barley breeding.....	90
4.2. Population structure in diverse barley material.....	96
4.3. Pitfalls of genome-wide-association studies.....	99
4.4. Possible new players in the regulation of defence responses in the barley- powdery mildew pathosystem.....	103
4.4.1. Relevance of the identified candidate genes.....	103
4.4.2. Are the four selected candidate genes casual genes?	105
5. Summary.....	113
6. Zusammenfassung.....	114

References.....	X
Appendix A: additional material and methods.....	XXX
a) Important equipment and consumables.....	XXX
b) Important chemicals.....	XXXI
c) Marker and proteins.....	XXXII
d) Kits.....	XXXIII
e) Solutions.....	XXXIV
f) Culture media.....	XXXVI
g) Software and databases.....	XXXVII
h) Vectors.....	XXXIX
i) Additional figures.....	XLI
j) Additional tables.....	XLIII
Appendix B: additional results.....	LXXIV
a) Additional figures.....	LXXIV
b) Additional tables.....	LXXXVII
Acknowledgment.....	CXXII
Curriculum vitae.....	CXXIII
List of publications/Oral presentations and posters.....	CXXIV
Eidesstattliche Erklärung /Declaration under oath.....	CXXV

Abbreviations

Abbreviation	Meaning
A	alternative-intermediate growth habit
AC/IC	advanced/improved cultivar
<i>Act</i>	<i>actin</i>
AGP	arabinogalactan protein
<i>At</i>	<i>Arabidopsis thaliana</i>
Avr	avirulence
BACK domain	BTB And C-terminal Kelch domain
<i>Bgh</i>	<i>Blumeria graminis</i> (DC) Speer f. sp. <i>hordei</i> (Marchal)
<i>Bgt</i>	<i>Blumeria graminis</i> (DC) Speer f. sp. <i>tritici</i> (Marchal)
BHQ [®] -1	Black Hole Quencher [®] -1
BLUE	best linear unbiased estimation
BM	breeder's material
BM/RM	breeding/research material
bp	base pairs
BTB domain	Bric-a-Brac/-Tramtrack/-Broad Complex domain
CaMV	Cauliflower mosaic virus
CFU	colony forming units
Cq	quantification cycle
Ct	threshold cycle
CTAB	hexadecyltrimethylammonium bromide
CRISPR	clustered regularly interspaced short palindromic repeats
cv.	cultivar
CXR	carboxy-X-rhodamine
d35S	enhanced Cauliflower mosaic virus 35S promoter
DPM3	dolichol-phosphate mannosyltransferase subunit 3
DPMS3	dolichol phosphate mannose synthase 3
DPMT	dolichol-phosphate mannosyl-transferase
<i>E. coli</i>	<i>Escherichia coli</i>
EDTA	ethylenediaminetetraacetic acid disodium salt dihydrate
EST	expressed sequence tag
f	forward primer
F	facultative growth habit
FAO	Food and Agriculture Organization
F/W	Facultative/winter growth habit
FEN	flap endonuclease
<i>f. sp.</i>	<i>formae speciales</i>
GxG	Gene-by-Gene
GxE	Gene-by-Environment
GAPDH	glyceraldehyd-3-phosphatdehydrogenase
GRAM domain	glucosyltransferases, Rab-like GTPase activators and Myotubularins domain
<i>GstA1</i>	<i>glutathione S-transferase A1</i>
GUS	β-glucuronidase
GWA	genome-wide-association
GWAS	genome-wide-association study
HR	hypersensitive response
IPK	Leibniz Institute of Plant Genetics and Crop Plant Research
JKI	Julius Kühn-Institute
kb	kilo base pairs

Abbreviations

Abbreviation	Meaning
LD	linkage disequilibrium
LRB	Light-Response BTB
LS	light step
M	size standard
MAF	minor allele frequency
MAMP	microbial-associated molecular pattern
Mla	Mildew resistance locus a
Mlo	Mildew resistance locus o
m. r.	moderately resistant
m. s.	moderately susceptible
n	total number
n.	not specified allele
NA	not analysed
NB-LRR	nucleotide-binding and leucine-rich repeat
NLS	nuclear localization signal
n. sp.	not specified
NTC	no-template-control
ON	overnight
OX	overexpression
PAMP	pathogen-associated molecular pattern
PCR	polymerase chain reaction
PIF3	Phytochrome Interacting Factor 3
PH domain	Pleckstrin Homology domain
Phy	phytochrome
POB	POZ/BTB Containing Protein
POZ	POxvirus and Zinc finger domain
PRR	pattern-recognition receptors
<i>PRX</i>	<i>peroxidase</i>
PUB	Plant U-box
qPCR	quantitative PCR
QTL	quantitative trait locus
R	reverse primer
r.	resistant
<i>R-gene</i>	<i>resistance-gene</i>
Rar1	Required for Mla-dependent resistance 1
RNAi	RNA interference
<i>Ror1</i>	<i>Required for mlo-specified resistance 1</i>
ROS	reactive oxygen species
<i>RPW8</i>	<i>Resistance to powdery mildew 8</i>
RQ	relative quantification
S	spring growth habit
s.	susceptible
SD	standard deviation
SEM	standard error of the mean
S/F	Spring/facultative growth habit
SGT1	suppressor of the G2 allele of S phase kinase associated protein 1
SI	susceptibility index
siRNA	small interfering RNA
SNP	single nucleotide polymorphism
syn	synonymous
T _a	annealing temperature

Abbreviations

Abbreviation	Meaning
TC	traditional cultivar
TC/L	traditional cultivar/landrace
TIGS	transient-induced gene silencing
TL	traditional landrace
T _m	melting temperature
<i>UBC</i>	<i>ubiquitin-conjugating enzyme 3</i>
<i>Ubi</i>	<i>ubiquitin</i>
<i>uidA</i>	β -glucuronidase
UTR	untranslated region
vol	volume
W	winter growth habit
Wi	wild material
Whealbi	Wheat and barley legacy for breeding improvement
WBP2 domain	WW binding protein 2 domain
X-Gluc	5-bromo-4-chloro-3-indolyl glucuronide
XPG domain	Xeroderma Pigmentosum Complementation Group G domain

List of figures

Figure I 1: The asexual life cycle of <i>Blumeria graminis</i> f. sp. <i>hordei</i>	8
Figure I 2: Basic approach for the conduct of a genome-wide-association study.....	14
Figure I 3: Spectrum of allele effects.....	16
Figure I 4: Overview of possible aberrant associations.....	17
Figure R 1: Composition of the selected genotype panels in regard of the biological status and the growth habit.....	45
Figure R 2: Distribution of the 459 Whealbi genotypes in regard of the resistance response against the powdery mildew isolate D35/3.....	46
Figure R 3: Distribution of the 267 selected Whealbi genotypes in regard of the resistance response against the powdery mildew isolates D35/3 and RiIII..	47
Figure R 4: Evaluation of the powdery mildew resistance of selected Whealbi genotypes under natural field infection	49
Figure R 5: Resistance response of the four indicated genotypes against 27 European powdery mildew isolates.....	51
Figure R 6: Amplification test for the presence of the mlo-11 allele in the resistant genotypes.....	52
Figure R 7: Effect of the biolistic complementation of the indicated genotypes with a construct overexpressing a functional Mlo allele.....	54
Figure R 8: Schematic representation of the Mlo Sanger sequencing results for the indicated genotypes.....	55
Figure R 9: Amplification of the indicated genotypes with Mlo or UBC specific primers.....	58
Figure R 10: Determination of the length of the presumed WB-352-specific Mlo duplicate.....	60
Figure R 11: Schematic representation of the Sanger sequencing results of the WB-352-specific Mlo amplification products.....	62
Figure R 12: Manhattan plots of the $-\log_{10}$ -transformed p-values for the three traits (Max, RiIII and D35/3).....	65
Figure R 13: Relative quantification of the transcripts of WB-CG_17 and WB-CG_23....	70
Figure R 14: Relative expression of the four candidate genes as mean signal intensities of microarray data.....	71
Figure R 15: Box plots of the average infected leaf area for the defined alleles.....	73
Figure D 1: Classification of the 33 candidate genes according to their annotated functions.....	103
Figure A 1: Scheme of the experimental procedure of a detached leaf assay.....	XLI
Figure A 2: Recorded weather data during the growth period of the field trials at both locations.....	XLII
Figure B 1: Countries of origin of the 459 barley genotypes of the Whealbi collection	LXXIV
Figure B 2: Amplification of the indicated genotypes with Mlo or UBC specific primers for the remaining two biological replicates	LXXV
Figure B 3: Overview of the repeatability and the heritability of the phenotypic data..	LXXVI
Figure B 4: Heat map of the calculated Rogers' distance from 201 genotypes.....	LXXVII
Figure B 5: Linkage disequilibrium plot for the significant SNPs of the Max trait.....	LXXVIII
Figure B 6: Results of the allele amplification and the expression analysis of selected candidates.....	LXXIX
Figure B 7: Multiple sequence alignment of the WB-CG_17 homologs.....	LXXXI
Figure B 8: Multiple sequence alignment of the WB-CG_19 homologs.....	LXXXII
Figure B 9: Multiple sequence alignment of the WB-CG_23 homologs.....	LXXXIV
Figure B 10: Multiple sequence alignment of the WB-CG_28 homologs.....	LXXXVI

List of tables

Table M 1: Cultivars used for the maintenance of the powdery mildew isolates.....	23
Table M 2: Virulence spectra of the powdery mildew isolates D35/3 and RiIII used for the resistance screening on a differential set of 33 barley lines and the in silico generated spectrum for the mixed inoculation (Max trait).....	24
Table M 3: Definition of the resistance classes for the complete powdery mildew resistance screening.....	26
Table M 4: Definition of the resistance classes for the field trials and the assumed corresponding infected leaf area ranges, which were used for transformation during correlation analysis.....	28
Table M 5: Composition of the ligation mixture for one reaction.....	39
Table R 1: Quantification of the seedling resistance of the indicated genotypes in response to seven powdery mildew isolates based on the development of macroscopic disease symptoms.....	53
Table R 2: Overview of the 33 identified candidate genes.....	66
Table R 3: Summary of the predicted functions of potential candidate homologs.....	75
Table R 4: Effect of the transient silencing of the candidate genes on the resistance of a resistant and a susceptible genotype against powdery mildew isolate CH4.8.....	79
Table R 5: Effect of the transient overexpression of the candidate genes on resistance of a resistant and a susceptible genotype against powdery mildew isolate CH4.8.....	80
Table R 6: Effect of the different promoter_GUS constructs on the total number of GUS stained cells.....	82
Table R 7: Effect of the different promoters_GUS constructs on the staining/colour intensity of GUS stained cells.....	83
Table A 1: Specifications of the 459 used barley Whealbi genotypes.....	XLIII
Table A 2: Virulence spectra of the seven powdery mildew isolates used for the small isolate test on a differential set of 33 barley lines.....	LIV
Table A 3: Virulence spectra of the additional 18 powdery mildew isolates used for the comprehensive isolate test on a differential set of 33 barley lines.....	LVI
Table A 4: Spore densities and age of the spores for the three different biological replicates of the small isolate test.....	LVIII
Table A 5: Chemicals applied during the field trials.....	LIX
Table A 6: Primers used for the determination of the <i>mlo-11</i> status and the semi-quantitative PCR.....	LX
Table A 7: General composition of the Taq-Mastermix for one reaction and the general Taq-PCR cycling program.....	LXI
Table A 8: Primers used for <i>Mlo</i> sequencing.....	LXII
Table A 9: General Phusion-Mastermix for one reaction.....	LXIV
Table A 10: General Phusion-PCR cycling program.....	LXV
Table A 11: Primers used for functional validation assays.....	LXVI
Table A 12: General qPCR-Mastermix for one reaction and the general qPCR cycling program.....	LXVIII
Table A 13: Primers and probes used for the qPCR.....	LXIX
Table A 14: Overview of the shooting experiments.....	LXX
Table A 15: Primers used for the colony PCRs.....	LXXII
Table A 16: Primers used for the sequencing of the generated constructs.....	LXXIII

Table B 1: Quantification of the resistance response of the 459 barley Whealbi genotypes against the powdery mildew isolates D35/3 based on the development of macroscopic disease symptoms.....	LXXXVII
Table B 2: Quantification of the resistance response of the 267 barley Whealbi genotypes against the powdery mildew isolates D35/3 and RiIII based on the development of macroscopic disease symptoms.....	XCII
Table B 3: Quantification of the resistance response of 102 barley genotypes against natural powdery mildew infection under field conditions and against the powdery mildew isolates D35/3 and RiIII under controlled conditions.....	XCVIII
Table B 4: Resistance spectra of the four resistant field genotypes defined by the infection of detached seedling leaves with 27 powdery mildew isolates.....	CI
Table B 5: Overview of all significant single nucleotide polymorphisms.....	CII
Table B 6: Overview of the sequence identifiers for the defined candidates.....	CVII
Table B 7: Overview of the defined alleles of 33 candidates.....	CXI
Table B 8: Effect of the defined alleles on the infected leaf area.....	CXXI

1. Introduction

1.1. The importance of barley in agriculture and science

The production of sufficient amounts of food for the ever-growing human population is a major issue not only of modern society. Instead it is discussed since more than 200 years (Malthus, 1798). Particularly, in times of climate change, water shortage and increasing loss of fruitful cultivation area due to soil erosion, the efficiency of agronomy is a controversial discussed topic in society and politics. Necessary amounts of food staples are required to ensure the major proportion of the energy and nutritional needs of a person (Rutledge *et al.*, 2011). The production of these food staples is an important part of modern agriculture because the majority of them are plant-based. Commonly, food staples are constituted by cereal grains and tubers (Rutledge *et al.*, 2011). Barley (*Hordeum vulgare* L. subsp. *vulgare*) is besides maize (*Zea mays* L.), wheat (*Triticum aestivum* L.) and rice (*Oryza sativa* L.), the fourth most produced grain worldwide (<http://www.fao.org/faostat/en/#data/QC>). The worldwide production of barley amounted to 147 million metric tons in the growing season 2017 and Germany is the second largest producing nation (with 7.8 % of the worldwide production). Barley is mainly used for food, feed, and alcohol production (Zhou, 2010). The crop plant belongs to the *Triticeae* tribe of the *Poaceae* family (Pourkheirandish & Komatsuda, 2007) and it has a long domestication history, which originates in the 'Fertile Crescent' (Allaby, 2015; Schmid *et al.*, 2018). The precursors of our modern crop are associated with the emergence of agriculture in the Neolithic age about 10 000 BC (Zohary *et al.*, 2012). The growing regions of the closest wild relative, *Hordeum vulgare* subsp. *spontaneum* (C. Koch) Thell. (Schmid *et al.*, 2018) span a wide range of habitats (Allaby, 2015). This species can grow from grasslands of varying altitude up to very arid/desert-like regions (Allaby, 2015). In this respect, local adapted ecotypes that can tolerate pests and abiotic stresses such as high temperatures are of interest for modern plant breeding to confront climate change. Nevertheless, only a small part of the natural wild diversity is preserved in modern elite material (Killian *et al.*, 2006), which led to high susceptibility against biotic and abiotic stresses. Unfortunately, the introduction of wild material into the modern gene pool is complicated and time-consuming, although often worthwhile (McCouch *et al.*, 2013; Zhang *et al.* 2017). For instance, progress has been achieved in the introgression of desirable alleles from wild material into modern material in regard of disease resistance, abiotic stress response and root architecture (Schmid *et al.*, 2018). Nevertheless, also within cultivated barley an adaptation to diverse climatic conditions occurred (Russell *et al.*, 2016). This adaptation is represented in the positive correlation between genetic and geographic distances (Russell *et al.*, 2016). The majority of the diversity of cultivated barley is preserved in landraces (Schmid *et al.*, 2018). Landraces are traditional, locally adapted varieties which lack formal genetic improvement (Camacho Villa *et al.*, 2005). The unlocking of the natural

diversity is one of the major goals from modern research (McCouch *et al.*, 2013; Milner *et al.*, 2019).

Besides these recent advances, barley has a long tradition as model research plant. In particular, it is investigated in respect of resistance responses and plant-pathogen interactions with powdery mildew (Peterhänsel & Lahaye, 2005). In respect of this model function, a wide range of (phenotyping) assays are established. Moreover, the propagation of the self-fertilizing crop is relatively simple and fast. Cultivated barley varieties display mostly a spring or winter annual growth habit, but wild barleys display a predominant winter growth habit (Pourkheirandish & Komatsuda, 2007). During domestication, the six-rowed as well as two-rowed spikes were persevered (Pourkheirandish & Komatsuda, 2007; Zhou, 2010). In general, six-rowed barleys produce three times more grains per spike (Zhou, 2010). Nonetheless, the spike morphology conditioned the production of smaller grains in comparison to the grains grown on two-rowed spikes (Zhou, 2010). In addition, the protein content of grains grown at two-rowed spikes is higher as in six-rowed spikes but the starch content is lower (Frégeau-Reid *et al.*, 2001). In this respect, two-rowed barleys were mainly used for the production of animal feed (Zhou, 2010).

The diploid character ($2n = 2x = 14$) of the crop facilitated the assembly of a good reference genome (Mascher *et al.*, 2017). This reference genome will further boost the identification of interesting genes and alleles. Particularly, in combination with the increasing amount of next generation sequencing results from various varieties. Besides, barley is used, together with the related grass species *Aegilops tauschii* subsp. *tauschii* and *Brachypodium distachyon*, as model for allohexaploid wheat (Brenchley *et al.*, 2012; Harwood, 2012). Wheat is the second most frequent produced cereal crop (<http://www.fao.org/faostat/en/#data/QC>).

1.2. Resistance mechanisms of plants against microorganisms

As sessile organisms, plants have to cope with many different abiotic as well as biotic stresses which can result in high yield losses. Severe infections with plant pathogens can decrease yield between 20-40 % (Savary *et al.*, 2012). Besides herbivores like aphids and nematodes, microorganisms are the main causing agents of plant diseases. The term microorganism summarizes bacterial, viral, fungal and oomycete plant pathogens and history taught us that they share a high devastating potential (Dangl *et al.*, 2013). Plants and their corresponding pathogens share a long evolutionary history. In this regard, plants developed different layers of protection. Some of these defences are constitutive (bark, waxy epidermal cuticles and cell walls) while other types are inducible (Freeman & Beattie, 2008). The interplay between plant and pathogen responses was described as zigzag model (Jones & Dangl, 2006). The first line of the resistance responses is often referred as basal resistance or innate immunity (Freeman & Beattie, 2008). The invading microorganism is usually perceived by diverse cell surface pattern-recognition receptors

(PRR) which detect pathogen- or microbial-associated molecular pattern (PAMP, MAMP; Jones & Dangl, 2006). Various molecules can act as PAMP/MAMP, for example the bacterial flagellin (Jones & Dangl, 2006). Cutin monomers act as another classical PAMP/MAMP (Hückelhoven, 2007). They are generated during the attack of fungal pathogens, when the plant cuticula is degraded (Hückelhoven, 2007). After its perception by the plant, the oxidative burst as well as cell wall-associated defence alterations like callose depositions are triggered (Hückelhoven, 2007). Oxidative burst describes the massive production of reactive oxygen species (ROS; Stael *et al.*, 2015). The initial contact between pathogen and plant cell takes place at the cell wall/plasma membrane and *N*-glycosylated proteins like arabinogalactan proteins (AGPs) or glycosylphosphatidylinositol anchor proteins were proposed as PRRs (Häweker *et al.*, 2010; Ellis *et al.*, 2010; Jadid *et al.*, 2011). The activation of PRRs lead to alterations in the transcriptome as well as in the proteome to ensure the limitation of microbial growth (Dangl *et al.*, 2013). Nonetheless, a, in evolutionary terms, successful pathogen can suppress this early resistance responses by effector molecules (Jones & Dangl, 2006). It was reported that effectors act via various mechanisms. As examples, some effectors can alter the transcription level of defence-related genes or they interact with defence-related proteins (Niks *et al.*, 2015).

To counteract the pathogens, a wide range of resistance genes evolved in plants. In this sense, every gene that is related to resistance responses can be considered as resistance gene. Nevertheless, the most studied major *resistance* (*R*-) genes encode for nucleotide-binding, leucine-rich repeat (NB-LRR) proteins which recognize directly or indirectly pathogen effectors (Dangl & Jones, 2001; Jones & Dangl, 2006). The term major refers here to the effect size in regard of the explained genetic variance of resistance used by quantitative geneticists (Falconer & Mackay, 1996). The segregation of major *R*-genes can be easily followed in the progenies (St. Clair, 2010; Niks *et al.*, 2015). If an *R*-gene product recognizes a corresponding effector, this effector is then referred as avirulence (*Avr*) protein (St. Clair, 2010). This interaction results in an incompatible response, which usually leads to little or no development of disease symptoms (St. Clair, 2010). In contrast, a plant can become fully susceptible when this interaction is compatible (Freeman & Beattie, 2008). The interaction between *R*-gene product and the corresponding effector is often described as 'qualitative' resistance (St. Clair, 2010). Nevertheless, this term can be misleading. It has to be distinguished between phenotypically qualitative resistance and genetically qualitative resistance (Niks *et al.*, 2015). The described situation refers to phenotypically qualitative as well as genetically qualitative resistance response (Niks *et al.*, 2015). Phenotypically qualitative resistance describes the discrete (categorical) distribution of the resistance response and genetically qualitative resistance refers to a Mendelian inheritance of the (major) effect gene (St. Clair, 2010; Niks *et al.*, 2015). In analogy, phenotypically quantitative

resistance can be measured as continuum because it leads to reduction rather than absence of disease symptoms (Falconer & Mackay, 1996; St. Clair, 2010; Niks *et al.*, 2015). The quantitative contribution of several minor effects to the resistance response is described as genetically quantitative resistance (Brown, 2015; Niks *et al.*, 2015). Hereafter, the term quantitative disease resistance is used to designate the phenotypical resistance response and the genetically quantitative resistance is referred as polygenic. The combination of both types of quantitative and polygenic resistances is sometimes referred as partial resistance (Niks *et al.*, 2015).

Several minor effect genes have been described as active specifically during the adult plant stage, while showing only little or even no effect in the seedlings (Li *et al.*, 2014a; Chen, 2013). They are designated as adult plant resistance (Chen, 2013), sometimes also as slow-rusting (or slow-mildewing) resistance genes (Li *et al.*, 2014a). An example of this type is the *Lr43* resistance gene in wheat (Niks *et al.*, 2015). The majority of the described genes confer race-nonspecific sometimes also broad resistance (Li *et al.*, 2014a; St. Clair, 2010). Race-specificity denotes the resistance to a particular pathogen species (race) and thus, race-nonspecific resistance describes the effective resistance response independently of the pathogen race/isolate (Chen, 2013; Parlevliet, 1985). Race-nonspecific resistance can be conferred by major as well as minor effect genes with mono- or polygenic inheritance (Parlevliet, 1985). Additionally, the time of its onset as well as its effectiveness is independent of the plant age or the environment (Li *et al.*, 2014a). In contrast, race-specific resistance relies on the presence of a particular *Avr* gene in the pathogen (Lindhout, 2002). This is often the case for classical NB-LRR based resistance responses (St. Clair, 2010). In contrast, broad (spectrum) resistance is designated as effective resistance against different pathogen species or the majority of races of the same species (Parlevliet, 1985; Kou & Wang, 2010). In addition to this type, also nonhost resistance provides a wide range of protection. Nonhost resistance is a highly discussed topic, but the exact definition changes within the literature (Niks & Marcel, 2009). Usually, this resistance type describes the resistance of all genotypes of a plant species to all genetic variants of a pathogen (Niks & Marcel, 2009). In this regard, it can be considered as the inability of a pathogen to cause disease symptoms in a specific plant (species), the host (Parlevliet, 1985; Freeman & Beattie, 2008; Niks *et al.*, 2015). Additionally, nonhost resistance is sometimes referred as basal resistance (Niks & Marcel, 2009). Nevertheless, the underlying resistance mechanisms are from high interest in respect of its expected durability (Fan & Doerner, 2012, Niks & Marcel, 2009). Durable resistance is described as effective resistance while it is widely used in an environment that favour disease (Johnson, 1983). In particular, qualitative major *R*-gene based resistance is often rapidly overcome by a pathogen due to coevolution (St. Clair, 2010; Brown, 2015). It was proposed that durability is

related to the complexity of the trait as well as by fitness penalties on the host and/or pathogen site (Brown, 2015; Niks *et al.*, 2015).

The resistance of inducible plant defence reactions relies on a wide variety of mechanisms. One of the most common responses is the hypersensitive response (HR) based on programmed cell death (Jones & Dangl, 2006). This mechanism is mostly active against biotrophic pathogens, which can survive and proliferate only on living plant tissue (Freeman & Beattie, 2008). It is based on elevated salicylic acid levels and the corresponding activation of systemic acquired resistance in relation to the transcription of various pathogenesis-related genes (Craig *et al.*, 2009; Conrath, 2006; Jones & Dangl, 2006). In contrast, the defence mechanisms against necrotrophs, those pathogens that can survive and proliferate on non-living tissue, rely on jasmonate and ethylene signalling (Jones & Dangl, 2006). Because of the antagonistic effects, a sensible balance between the different resistance signalling pathways is necessary which is ensured by the tight regulation through the redox state of the cells (Craig *et al.*, 2009; Karapetyan & Dong, 2018).

Many of the triggered defence mechanisms are based on degradation processes either of nucleic acids or proteins. This is especially the case for the defence against viruses, in which RNA silencing is most efficient (Baulcombe, 2015). The underlying mechanism is known as RNA interference (RNAi) and it relies on the production of small interfering (si)RNAs based on double stranded RNA molecules (Agrawal *et al.*, 2003). Besides the virus-induced gene silencing, also filamentous organism- and host-induced gene silencing exists (Baulcombe, 2015). The latter two mechanisms describe the gene silencing either in the plant cell directed from the pathogen or in the pathogen directed from the plant site, respectively (Baulcombe, 2015). The key player of the defence related protein degradation is the ubiquitin-26S proteasome system (Craig *et al.*, 2009). Protein degradation is usually based on the tagging of the target protein with ubiquitin moieties via the E1-E2-E3 enzyme cascade (Callis, 2014). The activated ubiquitin is bound to the E1 (ubiquitin-activating enzyme) and transferred to the E2 (ubiquitin-conjugating enzyme, Callis, 2014). The ubiquitin is then transferred directly or indirectly, based on the type of the E3 ligase, to the target protein (Callis, 2014). There exists a huge variety of ubiquitin E3 ligases and they can be classified in single- or multi-subunit groups (Callis, 2014; Shu & Yang, 2017). Particularly, U-box-type E3 ligase like PUB (Plant U-box) ligases are involved in the plant defence (Craig *et al.*, 2009).

In the last decades, it became more and more obvious that also light and temperature responsive pathways, the circadian clock and the overall cellular redox state are involved in regulation of defence responses (Roden & Ingle, 2009, Mazza & Ballaré, 2015; Hua, 2013). The production of ROS and its signalling pathway are coupled tightly to photosynthesis (Karapetyan & Dong, 2018; Stael *et al.*, 2015). Additionally, the induction of ROS during pathogen attack is required for the full activation of the plant immune system in dependence of calcium-signalling (Stael *et al.*, 2015;

Poovaiah *et al.*, 2013). The expression of many defence-related genes is under control of the circadian clock (Lu *et al.*, 2017). In respect of the conflict between defence responses and growth activities, it is necessary to restrict the costly defence responses to the timepoints with the highest infection risks (Karapetyan & Dong, 2018; Lu *et al.*, 2017). The integration of the ratios between ultraviolet as well as red and far-red light signals is a main regulatory process of plant development and growth (Xu *et al.*, 2015; Ballaré, 2014). Additionally, these signals are also important for the regulation of plant defence responses (Mazza & Ballaré, 2015; Xu *et al.*, 2015; Ballaré, 2014; Hua, 2013). For the perception of the ratio between red and far-red light, five phytochromes are responsible in *Arabidopsis* (Xu *et al.*, 2015). For instance, phytochrome B is involved in the regulation of diverse growth processes (Ballaré, 2014; Legris *et al.*, 2016). Furthermore, it is a key regulator of the salicylic acid signalling pathway and it is necessary for the uncoupling of plant growth-defence trade-offs mediated by jasmonate (Ballaré, 2014; Genoud *et al.*, 2002; Campos *et al.*, 2016; Cerrudo *et al.*, 2017). It was proposed that phytochrome B could act as temperature sensor (Legris *et al.*, 2016).

All in all, plant resistance signalling pathways are tightly regulated. This is necessary because of the high costs for the production of defence-related proteins (hydrolytic proteins or defensins) as well as for the production of chemical defence compounds like terpenoids (saponins), phenolics (phytoalexins and lignin) and alkaloids (glucosinolates, Freeman & Beattie, 2008). Moreover, there are many indications that the defence-related genes/proteins are involved in various other pathway like wounding and temperature stress (van Loon *et al.*, 2006).

1.3. A common plant disease: powdery mildew

The common plant disease powdery mildew is caused by ascomycete fungi which infect leaves, stems, flowers and fruits of almost 10,000 species (Glawe, 2008). In this respect, important cereals like barley and wheat are not the exception. The fungus *Blumeria graminis* (DC Speer) is the causal agent of cereal powdery mildew and evolved in eight distinct *formae speciales* (*f. sp.*) with strict host specifications (Glawe, 2008; Heffer *et al.*, 2006; Wyand & Brown, 2003). The fungus *Blumeria graminis* (DC Speer) *f. sp. hordei* (Marchal) (*Bgh*) causes powdery mildew specifically on barley whereas *Blumeria graminis* (DC Speer) *f. sp. tritici* (Marchal) (*Bgt*) is the causal agent of this disease on wheat (Wyand & Brown, 2003). Both fungi can usually only develop on the corresponding host, although under specific conditions like a highly susceptible genotype, a partial reproduction on the nonhost cereal is possible (Ferreira *et al.*, 2006; Romero *et al.*, 2018). Besides monocot plants like cereals, also the dicot model plant *Arabidopsis* can be infected by the powdery mildew fungi *Golovinomyces orontii* and *Golovinomyces cichoracearum* (Humphry *et al.*, 2006).

Besides the application of fungicides, the planting of resistant cultivars can provide sufficient protection against the pathogen. The risk of severe yield losses caused by *Bgh* is nowadays decreased based on the extensive use of a race-nonspecific resistance gene in spring barleys (Kusch & Panstruga, 2017). In the late 1970s and early 1980s the gene was introgressed in about 50 % of the commercially available varieties (Kusch & Panstruga, 2017). This was a quite important breeding improvement because before this, an infection with *Bgh* could lead to yield losses between 5-30 % due to the reduced single grain weight (Smith & Smith, 1974). Nevertheless, on winter barleys *Bgh* is still a devastating disease especially in China (Zhu *et al.*, 2016). The exploration of the diversity of natural resistance genes/alleles is from high importance for the further plant breeding. In this sense, landraces, wild relatives and crop ancestors potentially provide valuable sources of resistance (Zhang *et al.* 2017; Schmid *et al.*, 2018). For instance, several important *Bgh* and *Bgt* resistance genes originated in related species (Jørgensen & Wolfe, 1994).

1.3.1. The life cycle of cereal powdery mildew fungi

Based on the obligate biotrophic life cycle of powdery mildews, they reproduce only on/in living host cells (Heffer *et al.*, 2006). Like most powdery mildew fungi, *Bgh* as well as *Bgt* grow on plant tissue (Glawe, 2008; Heffer *et al.*, 2006, Both *et al.*, 2005) and the epiphytically mycelium forms the typical white fluffy pustules (Figure A 1). The epidemic spread of powdery mildew is a result of the massive production of asexual conidia spores (Glawe, 2008). These spores can be airborne dispersed over large distances, under ideal conditions up to several hundred kilometres (Hermansen *et al.*, 1978; Zhu *et al.*, 2016).

The life cycle of *Bgh* (Figure I 1) starts with the landing of a conidium on a barley leaf (Zhang *et al.*, 2005) and within 20 sec, droplets of extracellular material are secreted (Carver *et al.*, 1999). This substance binds the spore to the host tissue and exhibits unspecific esterase and cutinase activity (Green *et al.*, 2002; Glawe, 2008). The conidium germinates within an hour and a short primary germ tube is formed (Zhang *et al.*, 2005; Glawe, 2008). The formed cuticular peg penetrates the plant cuticle but not the cell wall (Green *et al.*, 2002; Glawe, 2008). It tightens the attachment of the spore to the host and is involved in water uptake, which is necessary for the further development (Green *et al.*, 2002). Moreover, it recognizes the host surface features with focus on the hydrophobicity of the surface but independently of the presence of epicuticular wax (Zhang *et al.*, 2005). The termination of the elongation of the primary germ tube triggers the development of the appressorial germ tube (Yamaoka *et al.*, 2006). This normally happens 9-10 h after the first contact. This elongated germ tube is also tightly attached to the host surface via extracellular material (Zhang *et al.*, 2005). The end of this hypha swells to form a hooked appressorium and 2 h after its emergence, the penetration peg evolves (Zhang *et al.*, 2005). It

penetrates the cell wall based on mechanical pressure and cell wall degradation by enzymes like cellulases (Zhang *et al.*, 2005; Pryce-Jones *et al.*, 1999). The differentiation of the appressorium is regulated by the composition of the cuticular wax (Tsuba *et al.*, 2002).

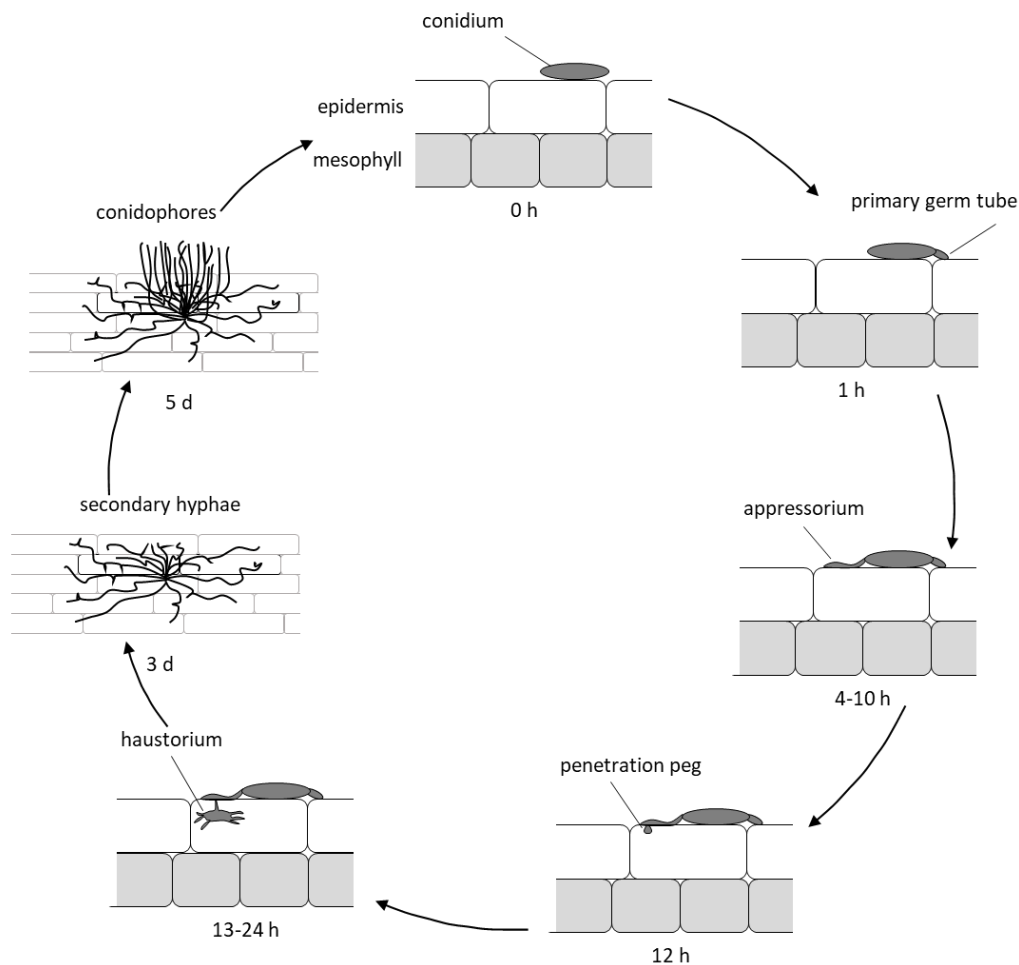


Figure I 1: The asexual life cycle of *Blumeria graminis* f. sp. *hordei*

The asexual life cycle starts with the landing of a conidium on a barley leaf (0 h after inoculation), followed by the germination of the primary germ tube within one hour and development of the appressorial germ tube (up to 10 h after infection). These stages were summarized as pre-penetration stages. With begin of the formation the penetration peg (12 h post inoculation) the post-penetration stages starts. Within the next 24 h, the haustorium is developed after successful penetration of an epidermal cell. The epiphytic mycelium is based on secondary hyphae (3 d after infection) and the colony is visible by eye. The asexual life cycle is completed with release of new conidia from the mature conidiophores. (Modified after Both *et al.*, 2005; Zhang *et al.*, 2005 and Hoseinzadeh, 2018).

Within the next 24 h, the growing penetration peg invaginates the plant plasma membrane and a finger-shaped feed structure, the haustorium, is formed (Zhang *et al.*, 2005; Green *et al.*, 2002). The membrane surrounding the haustorium is called extrahaustorial membrane because its composition differs remarkably from a normal plant plasma membrane (Hückelhoven & Panstruga, 2011). It is the place where the interaction and the molecular signalling between plant cell and fungus takes place (Glawe, 2008). Independently of the success of the penetration, the

conidium is able to form additional appressorial germ tubes and these secondary hyphae form the mycelium (Zhang *et al.*, 2005).

Several days after the successful infection, the asexual reproduction of the fungus begins with the development of conidiophores from vegetative hyphae. At this phase, mature conidia are able to start the next infection cycle (Glawe, 2008). The sexual spores of powdery mildew fungi are called ascospores and they are produced from chasmothecium at the end of the growing season. This allows the fungus to endure difficult environmental conditions like high or cold temperatures (Glawe, 2008; Heffer *et al.*, 2006; Zhang *et al.*, 2005). A former term for chasmothecia is cleistothecia (Heffer *et al.*, 2006).

1.3.2. Race-specific powdery mildew resistance

The key feature of race-specific resistance is the fact that the protection is only provided for a sub-set of the respective pathogen species (Parlevliet, 1985) because each (major) *R*-gene provides only protection if the corresponding *Avr* gene is present in the respective pathogen isolate (Lindhout, 2002). This monogenetic resistance can be explained by the gene-for-gene hypothesis (Flor, 1971) and it displays usually a qualitative resistance response (St. Clair, 2010; Niks *et al.*, 2015). As mentioned before, several major *R*-genes encode for NB-LRR proteins, and these, in turn, can be classified based on their nucleotide binding domain (Dangl & Jones, 2001). The most frequently used model system relies on Arabidopsis interacting with various pathogens and resistance responses seem to be well conserved (Schulze-Lefert & Vogel, 2000). Nevertheless, it is still not specified if the salicylic acid signalling pathway, including the corresponding activation of systemic acquired resistance, is similarly regulated in monocot crops as it is in Arabidopsis. Although several studies provided evidence for the conservation of the signalling pathway in barley and wheat (Gao *et al.*, 2018; van Loon *et al.*, 2006). In case of barley, the application of salicylic acid led to locally as well as systemically reduced *Bgh* propagation (Lenk *et al.*, 2018).

The barley-*Bgh* pathosystem has a long tradition as resistance model and early studies were already performed in the 1930s (Wiberg, 1974; Peterhänsel & Lahaye, 2005). Recently, 175 potential NB-LRR genes of barley were identified which were classified into three distinct clades (Andersen *et al.*, 2016). The best characterized *R*-gene locus against *Bgh* is called *Mla* (*Mildew resistance locus a*) and more than 30 annotated resistance specificities have been described for it (Jørgensen & Wolfe, 1994; Seeholzer *et al.*, 2010). The majority of these alleles/haplotypes were introgressed from the wild ancestor *Hordeum spontaneum* (Schulze-Lefert & Vogel, 2000). In a 240 kb long interval on chromosome 1HS at least eleven NB-LRRs were identified (Wei *et al.*, 1999) and the NB-LRR gene *RGH1bcd* of Morex was proposed as non-functional allele of *Mla* because it lacks the corresponding resistance specificity but displays high sequence identity (Wei *et al.*, 2002). If the corresponding *Avr* protein of the pathogen is perceived by *Mla*, the typical HR

reactions take place within 24 h and the infected cells die (Schulze-Lefert & Vogel, 2000). Recent results indicated the direct interaction between receptor and corresponding avirulence effector (Saur *et al.*, 2019).

The regulation of plant defence responses involves many signalling molecules. In particular, ROS in form of hydrogen peroxide and nitrogen monoxide are important signalling molecules during the whole plant-pathogen interaction (Karapetyan & Dong, 2018, Hüchelhoven, 2007; Stael *et al.*, 2015). The importance of superoxide dismutases (Lightfoot *et al.*, 2017; Xu *et al.*, 2014), oxalate oxidases or germin-like proteins (Zimmermann *et al.*, 2006) and peroxidases (González *et al.*, 2010; Johrde & Schweizer, 2008) for race-specific as well as race-nonspecific resistance responses have been demonstrated over the last decades (Karapetyan & Dong, 2018). The function of most *Mla* proteins is related to Rar1 (Required for *Mla*-dependent resistance 1) and Rar2 proteins with *Mla1* and *Mla7* being the exception to this (Schulze-Lefert & Vogel, 2000; Jones, 2001; Freialdenhoven *et al.*, 1994). The interaction of Rar1 with SGT1 (suppressor of the G2 allele of S phase kinase associated Protein 1) relates the *Mla* resistance with ubiquitination processes because SGT1 is a cell cycle regulator involved in the 26S proteasome mediated protein degradation (Azevedo *et al.*, 2002). The regulation of the *Mla* genes is complex and indications hint to the involvement of different micro RNAs (Xu *et al.*, 2014; Liu *et al.*, 2016). Besides *Mla*, several other resistance loci were identified on different barley chromosomes (Jørgensen & Wolfe, 1994) and the relative positions of them were presented on the integrated map published by Aghnoum *et al.* (2010). The genes *Mlra*, *Mlk*, *Mlnn* and *Mlga* are annotated on chromosome 1H, *MILa* on 2H, *Mlg* on 4H, *Mlj* on 5H and *mlt* as well as *Mlf* on 7H, respectively (Aghnoum *et al.*, 2010). The function of a part of these *R*-genes/resistance specificities is also coupled to Rar1 and Rar2 (Schulze-Lefert & Vogel, 2000). Like *Mla1* and *Mla7*, *Mlg* acts independently of these two proteins (Schulze-Lefert & Vogel, 2000) and it confers prehaustorial resistance (Görg *et al.*, 1993). The majority of the published studies are focused on the host site of the powdery mildew pathosystems, which led to an underrepresentation of pathogen genes (effectors). In the recent years, several new *Avr* genes of known *R*-genes/resistance specificities were identified. Some examples are *AVRa1*, *AVRa7*, *AVRa9*, *AVRa10*, *AVRa13* and *AVRa22* from *Bgh* (Lu *et al.*, 2016; Saur *et al.*, 2019) and *AvrPm2* and *AvrPm3^{a2/f2}* of *Bgt* (Praz *et al.*, 2017; Bourras *et al.*, 2015). The identification of pathogen effectors could be versatile for plant breeding because the corresponding host targets are often disease susceptibility genes or susceptibility factors (Dangl *et al.*, 2013). A disease susceptibility gene is a gene that makes a plant susceptible to a pathogen (Fan & Doerner, 2012) and is often reprogrammed by the pathogen to its own benefits (Dangl *et al.*, 2013). In contrast, a susceptibility factor is a host factor that is necessary for the pathogen development and growth but not involved in defence suppression (Fan & Doerner, 2012).

Nevertheless, the major problem of the strong monogenetic resistance is its fast break down. The analysis of several typical *R*-genes of barley revealed that their provided protection against *Bgh* lasted only for three to four years (Brown, 2015). This effect is caused by the rapid coevolution of plant and pathogen. Often only small mutations of the Avr proteins (effectors) are necessary to escape the detection by the *R*-gene or the corresponding effector is lost completely due to redundancy among the effectors (Mundt, 2014; Niks *et al.*, 2015; Dangl *et al.*, 2013). The durability of the monogenetic resistance can be increased if mixtures of cultivars rather than monocultures were grown (Brown, 2015). This method prevents the typical 'boom-and-bust' cycle that occurs if only one prevalent *R*-gene is planted on huge areas (Brown, 2015). Another possibility to increase the durability is the *R*-gene stacking (Dangl *et al.*, 2013).

1.3.3. Race-nonspecific powdery mildew resistance

In contrast to the often short-lived race-specific resistance, the race-nonspecific resistance in form of nonhost and basal resistance provides long termed protection and the underlying mechanisms are of high interest for breeders (Fan & Doerner, 2012, Niks & Marcel, 2009). Interestingly, there are several indications that relate the typical race-specific monogenetic resistance signalling pathways with the race-nonspecific resistance responses (Kou & Wang, 2010; Schweizer, 2007). Examples for these indications are the production of ROS (Hückelhoven, 2007; Stael *et al.*, 2015) and the protein degradation via the 26S proteasome (Dong *et al.*, 2006; Reiner *et al.*, 2016; Craig *et al.*, 2009). The first layer of resistance responses or basal resistance is usually race-nonspecific and it is activated by the detection of MAMPs/PAMPs (Jones & Dangl, 2006). Various molecules can act as MAMPs/PAMPs. As an example, components of the plant cell wall, which is degraded during the penetration attempt of powdery mildew fungi (Zhao & Dixon, 2014; Zhang *et al.*, 2005). To protect the cell wall three strategies have evolved: (1) inhibition of cell wall degrading enzymes; (2) structural and chemical reorganization of the cell wall; and (3) killing of potential intruders by antimicrobial chemicals (Hückelhoven, 2007). All three strategies are related with ROS, nitrogen monoxide and calcium signalling (Stael *et al.*, 2015; Poovaiah *et al.*, 2013). To prevent a fungal penetration, a further crosslinking of the cell wall and the formation of cell-wall appositions (or papillae) directly underneath the primary germ tube as well as the appressorial germ tube, are initiated (Hückelhoven, 2007; Schulze-Lefert, 2004; Houston *et al.*, 2016; Zhang *et al.*, 2005). The major component of papillae is callose (β -1,3-glucan) and its exact composition is important for their functionality (Chowdhury *et al.*, 2014). In general, enzymes related to callose or cellulose synthesis are important factors for the penetration resistance (Chowdhury *et al.*, 2016; Douchkov *et al.*, 2016; Hückelhoven, 2007). In addition, secondary metabolites are important for the defence. For instance, phytoalexins and phenolic compounds (like lignin) that accumulate within the papillae (Zhao & Dixon, 2014). Moreover, cell wall degrading enzymes (like chitinases) are

released (Hückelhoven, 2007). The penetration attempt leads to re-organization of the cytoplasm, increased vesicular transport of cellular components depending on actin filaments and enhanced peroxisome activity (Park *et al.*, 2018; Moral *et al.*, 2017; Schulze-Lefert, 2004). Only adapted pathogens are able to suppress or circumvent all these prehaustorial defence mechanisms and are able to establish feeding structures (Niks & Rubiales, 2002).

The two resistance genes that confer broad spectrum resistance against powdery mildews rely on different defence pathways but they are related to the described mechanisms. On the one hand, there is the *RPW8* (*Resistance to powdery mildew 8*) gene of *Arabidopsis* (Xiao *et al.*, 2001) and on the other hand the *Mlo* (*Mildew resistance locus O*) gene that is conserved in mono- as well as in dicot plants (Appiano *et al.*, 2015; Kusch *et al.*, 2016). The resistance of *RPW8* seems to rely on hydrogen peroxide production and salicylic acid induced HRs (Xiao *et al.*, 2001; Wang *et al.*, 2009a; Jones, 2001). In contrast, the recessive loss-of function *mlo* mutation leads to a prehaustorial resistance similar to the described basal defence responses (Jørgensen, 1992; Büschges *et al.*, 1997). The *mlo*-based resistance was discovered in 1937 and since then, it is widely used in spring barleys (Peterhänsel & Lahaye, 2005). Particularly in the last 40 years, *mlo* alleles were introgressed in a huge variety of cultivars and they provide still stable resistance at the field level (Peterhänsel & Lahaye, 2005; Brown, 2015). Despite extensive studies, the real biochemical function of the seven-transmembrane *Mlo* proteins remains unclear (Acevedo-Garcia *et al.*, 2014; Devoto *et al.*, 2003). In case of barley, it is a single copy gene, but in other plant species it occurs in medium sized families with seven to 39 members (Kusch *et al.*, 2016). Nevertheless, the function as powdery mildew disease susceptibility factor/gene is conserved in plants (Appiano *et al.*, 2015; Kusch & Panstruga, 2017). In barley *mlo* mutants, the papillae formation set in earlier and is stronger than in other resistant genotypes (Skou *et al.*, 1984) and also defence-related compounds like hydrogen peroxide and defence-related transcript levels in them appear elevated (Hückelhoven *et al.* 2000; Piffanelli *et al.*, 2002; Zierold *et al.*, 2005). Several genes which participate in the *mlo*-mediated resistance were identified, some examples being *Ror1* (*Required for mlo-specified resistance 1*) and *Ror2* as well as *BAX INHIBITOR-1* and *calmodulin* (Freialdenhoven *et al.*, 1996; Collins *et al.*, 2003; Eichmann *et al.*, 2010; Kim *et al.*, 2002a; Kim *et al.*, 2002b). These genes further relate the *mlo* resistance with vesicle transport, ROS production and calcium signalling (Hückelhoven, 2007; Kusch & Panstruga, 2017). Additionally, the actin filament based re-organization of the cytoskeleton was enhanced in *mlo* mutants (Opalski *et al.*, 2005). Together, this evidence indicates that the *mlo*-mediated resistance is part of the basal and/or nonhost resistance (Humphry *et al.*, 2006).

In total, 40 *mlo* mutants of barley were characterized (Reinstädler *et al.*, 2010), but only one natural allele was described (Peterhänsel & Lahaye, 2005; Piffanelli *et al.*, 2004). The *mlo-11*

mutant was discovered in an Ethiopian barley landrace (Eth295) and it is still one of two prevalent *mlo* alleles (Kusch & Panstruga, 2017). The causative mutation of *mlo-11* is not located within the coding sequence, in contrast to the chemical induced mutations where the protein sequence is altered (Piffanelli *et al.*, 2004; Reinstädler *et al.*, 2010). The transcription of a *mlo-11* specific repeat array, which is located upstream of the functional *Mlo* allele, leads to aberrant transcripts and blocks the transcription of the functional copy (Piffanelli *et al.*, 2004; Peterhänsel & Lahaye, 2005). The repeat array encodes for a part of the promoter, the 5' untranslated region (UTR) and the first five exons and introns (Piffanelli *et al.*, 2004; Peterhänsel & Lahaye, 2005). Recently, an alternative *mlo-11* allele (*mlo-11 cnv2*) was identified, which display a reduced number of repeat copies (Ge *et al.*, 2016).

Besides the nearly complete race-nonspecific resistance of *mlo* mutants, also negative trade-offs of the mutation were described (Piffanelli *et al.*, 2002). The major negative trade-offs resulting in yield penalties are early leaf senescence and spontaneous mesophyll cell death (Piffanelli *et al.*, 2002). These trade-offs occur in the natural as well as chemical induced *mlo* mutants (Kusch & Panstruga, 2017). In general, the susceptibility against necrotrophic pathogens is increased in *mlo* mutants, probably because of the accumulation of necrosis (Kusch & Panstruga, 2017). Brown (2015) speculated that these negative effects are the reason why natural *mlo* alleles were not more frequent in nature.

1.4. Strengths and weaknesses of genome-wide-association studies

The identification of a casual gene in regard of the trait of interest is a major goal in scientific research. Such information provide valuable resources for plant breeding (Brachi *et al.*, 2011). Because of the reduced genetic diversity in our modern crops compared to the wild ancestors, valuable genes or alleles (for example resistance related genes) were lost during domestication (Killian *et al.*, 2006). In this respect, the assessment of the natural diversity is important for modern crop plant breeding (McCouch *et al.*, 2013; Schmid *et al.*, 2018). To provide access to the often complex traits of interest, two major strategies evolved in plant science; on the one hand, linkage mapping also referred as quantitative trait locus (QTL) mapping and on the other hand genome-wide-association (GWA) studies (Burghardt *et al.*, 2017; Brachi *et al.*, 2011). A QTL is the chromosomal region with the highest probability where one or more genes are located that affect a quantitative trait (Niks *et al.*, 2015). Linkage mapping, relies on biparental mapping populations (Sehgal *et al.*, 2016) and many important chromosomal regions of essential agronomic traits could be identified with this method. It is a very time-consuming method since several generations are needed to fix alleles in the progenies of initial biparental crosses (Muluaem & Bekeko, 2016). Another major issue of the method is its low resolution because it is restricted to the few recombination events that occurred in the biparental mapping population (Huang & Wang, 2014).

In this regard, labour intensive fine-mapping is necessary to improve the resolution (Burghardt *et al.*, 2017). Another flaw of the method is the limited allele diversity that can be evaluated because it is limited by the selected parents (Burghardt *et al.*, 2017). To overcome these obstacles, several techniques were developed (Korte & Farlow, 2013). Nevertheless, traditional and advanced QTL mapping methods are still in use and recent studies identified important resistance QTLs using these methods (Romero *et al.*, 2018; Hoseinzadeh *et al.*, 2019).

Besides QTL mapping, GWA studies are versatile for the identification of candidates. The method was first applied in humans nearly 20 years ago (Hirschhorn & Daly, 2005). Nevertheless, it proved to be also effective in plant science (Brachi *et al.*, 2011; Huang & Wang, 2014; Bartoli & Roux, 2017). The principle of an association study is the statistically evaluation of the correlation between an observed phenotype and the determined genotypic variants (Hirschhorn & Daly, 2005). A major advantage of the method is that it favours diverse (natural) populations (Figure I 2) because they provide a higher degree of genomic variants than biparental crosses (Brachi *et al.*, 2011; Burghardt *et al.*, 2017). In crops like barley, most diversity is found in wild relatives and traditional landraces (McCouch *et al.*, 2013; Killian *et al.*, 2006), which can be assessed more easily in a GWAS (GWA study) than in a biparental mapping population. For instance, a recent analysis of genebank material revealed the (hidden) potential of the stored material in regard of natural diversity (Milner *et al.*, 2019).

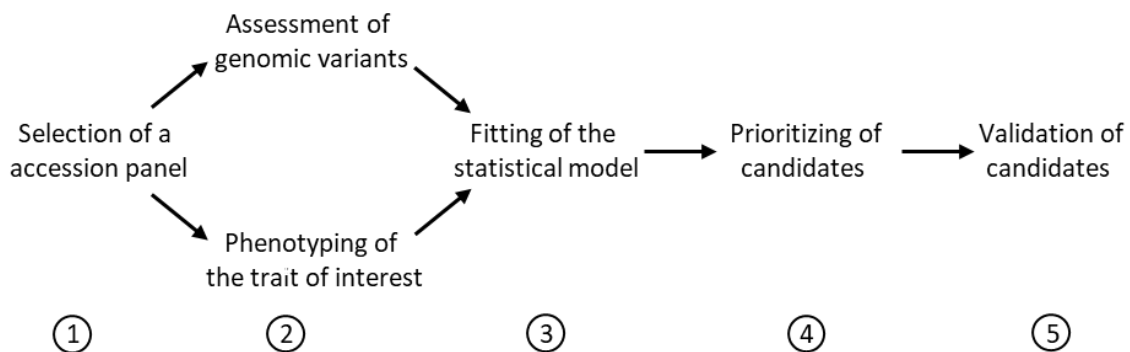


Figure I 2: Basic approach for the conduct of a genome-wide-association study

(1) The selection of a diverse accession panel in form of a natural or a mapping population. (2) Determination of the genomic and phenotypic variation. The higher the marker density and the more precise the phenotyping, the more accurate the results will be. (3) Performance of the statistical analysis to link the genomic variants to the phenotypic variation. (4) Prioritizing of the candidates for the follow-up work. (5) Validation of selected candidate genes. (Modified after Burghardt *et al.*, 2017).

The main pillars of a GWAS are the provision of reliable phenotype and genotype data of the selected accessions (Figure I 2; Burghardt *et al.*, 2017). The phenotype of a trait usually depends highly on the environment but this causes in plant GWA studies less problems than in human studies because the phenotyping can be performed under controlled, reproducible conditions like greenhouse experiments (Burghardt *et al.*, 2017).

For the provision of the genomic variants several aspects have to be considered. The complete genotyping from many accessions is still hardly affordable because most crop plants have large, highly complex and repetitive genomes due to their polyploid nature (Warr *et al.*, 2015). The barley genome is for example around 5 giga base pairs large but almost 81 % of it consists of repetitive elements (Mascher *et al.*, 2017). In contrast, the human genome is almost half that size (3 giga base pairs) and the proportion of repetitive elements is estimated between 50-70 % (Frith *et al.*, 2005; de Koning *et al.*, 2011). A possible alternative to a complete re-sequencing, is the analysis of the exome which is defined by all sequences of the annotated exons and partially by sequences of noncoding elements like functional RNAs and promoters (Warr *et al.*, 2015). Normally, it represents 1-2 % of the genome, although this represented proportion highly depends on the studied species (Warr *et al.*, 2015). Even though a great majority of genomic variants occur in noncoding region (Huang & Han, 2014; Barker & Edwards, 2009), exome capture data proved as suitable for genome-wide studies (Pankin *et al.*, 2014; Russell *et al.*, 2016; Bustos-Korts *et al.*, accepted). The accessibility of single-nucleotide polymorphisms (SNPs) as markers boosted further the application of GWA studies (Nadeem *et al.*, 2018). SNPs are single base pair changes that occur in a specific genome, which could represent base pair transitions or transversions as well as single nucleotide insertions or deletions (Nadeem *et al.*, 2018). Besides the huge variety of genetic markers, SNPs provide several advantages: (1) they are the most abundant genetic markers; (2) they are highly reproducible; and (3) they can be found in the proximity of almost every gene which covers both, coding and non-coding regions (Nadeem *et al.*, 2018; Rafalski, 2002). Plants display usually a high SNP frequency, up to 10-30 SNPs/kb (Nadeem *et al.*, 2018). Nevertheless, the individual SNP rates varying from species to species. As an example, the determined SNP rates in rice (0.45-3.2 SNPs/kb) were much lower in comparison to maize (8.34-23.3 SNPs/kb, Huq *et al.*, 2016).

The basis of an association study is the estimation of the proportion of the phenotypic variation that is explained by the genotype and the method compares (in its simplest form) phenotype frequencies as a function of allele frequencies (Hirschhorn & Daly, 2005). Association studies use the principle of linkage disequilibrium (LD) which describes the non-random association of alleles at different loci (Flint-Garcia *et al.*, 2003; Korte & Farlow, 2013). The LD represents the correlation between polymorphisms like SNPs that is caused by their shared mutation, selection and recombination history (Flint-Garcia *et al.*, 2003). Its persistence or decay defines the number and the density of markers that are necessary for a GWAS (Flint-Garcia *et al.*, 2003). LD is closely related to chromosomal/physical linkage (the correlated inheritance of loci because of a physical connection), but it refers to the correlation of alleles in a population on the basis of differences between the observed and expected frequencies (Busch & Moore, 2012; Flint-Garcia *et al.*, 2003).

It can be reported in several ways, but one of the most common ones is as correlation coefficient r^2 between two loci and the corresponding statistical significance is usually evaluated by a Fischer's exact test (Flint-Garcia *et al.*, 2003).

To determine the associations between genotype and phenotype (Figure I 2), many different statistical models were developed. In plants, it proved to be most suitable to fit a mixed linear model (Huang & Han, 2014; Wang *et al.*, 2012; Li *et al.*, 2014b) which was first described in animals (Henderson, 1975) and were later adapted to plants (Yu *et al.*, 2006).

In general, the power of a GWAS depends on the phenotypic variation within the selected accession panel that is explained by the genetic markers (Korte & Farlow, 2013). In more detail, GWAS power is related to five main factor: (1) the genetic complexity of the trait of interest; (2) the heritability of the trait; (3) the number of accessions that are investigated; (4) the relatedness of these accessions; and (5) the density of the genetic markers (Burghardt *et al.*, 2017). The complexity of the trait is defined by its genetic architecture and several scenarios are possible (Figure I 3; Gibson, 2012). If a suitable accession panel is selected also rare variants with small effects can be detected because of an enrichment of the rare variants if the sample size is large enough (Brachi *et al.*, 2011). Nevertheless, rare variants, for example so-called 'private' SNPs, can lead to synthetic associations which are defined as significant associations of noncausal markers (SNPs) based on (complete) LD to the causal one (Figure I 4A; Dickson *et al.*, 2010; Korte & Farlow, 2013). To prevent this type of confounding, often a minor allele frequency (MAF) of 5 % is used (Figure I 3, Gibson, 2012; Brachi *et al.*, 2011).

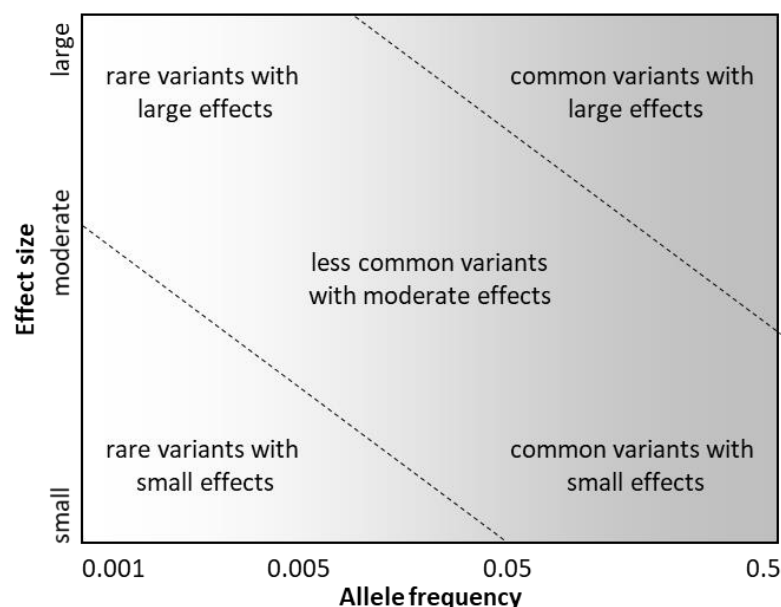


Figure I 3: Spectrum of allele effects

Associations are often classified in regard of the allele frequency and the effect size. The majority of the discovered associations lie within the diagonal region framed by dashed lines. (Modified after Bush & Moore, 2012).

The heritability in general describes how strong a phenotype is determined by the genotype in a specific environment and population (Burghardt *et al.*, 2017). The broad sense heritability H^2 is defined as proportion of the phenotypic variance that can attribute to the variance of the genotype (additive and nonadditive components) and the narrow sense heritability h^2 is a measure of the contribution of the additive genetic (or breeding) value to the phenotypic variance (Korte & Farlow, 2013; Falconer & Mackay, 1996). In a mixed linear model, the observed phenotypic variance can be divided in additive and nonadditive genetic components (Korte & Farlow, 2013). The additive genetic variance component describes the variance in the sum of the average effects of alleles caused by a particular allele substitution. In respect of the population mean, the average effect of a gene (allele) is the mean deviation from the population mean of individuals (Falconer & Mackay, 1996). Often only a small part of the heritability is explained by the significant associations and this issue is referred as ‘missing heritability problem’ (Brachi *et al.*, 2011, Gibson, 2012).

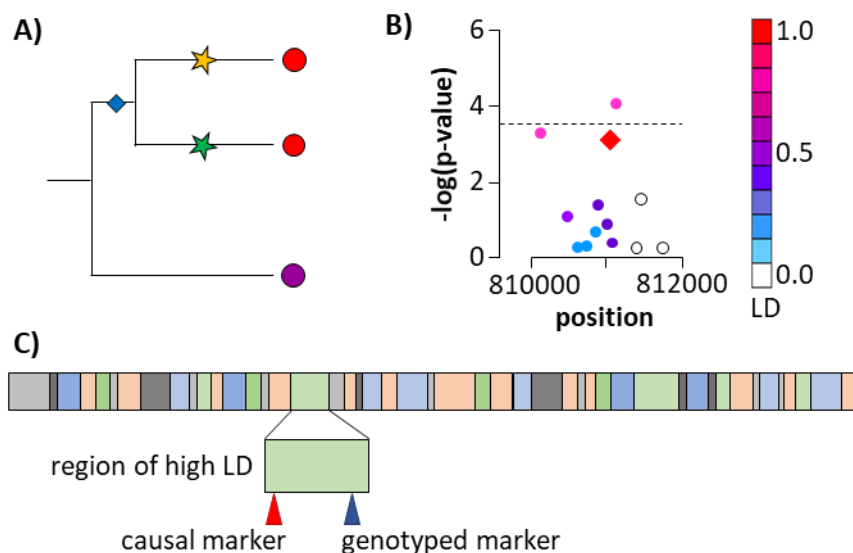


Figure I 4: Overview of possible aberrant associations

A) The example presents how synthetic associations can be caused by genetic heterogeneity. In the phylogenetic tree of the three individuals, three mutations occurred. The two most recent mutations (stars) causes a phenotypic change (from violet to red colour) but the blue mutation has per se no effect on the phenotype, but because of its perfect correlation with the trait, it will be significantly associated. The causal markers were bad predictors of the trait. (Modified after Korte & Farlow, 2013)

B) An example Manhattan plot were synthetic associations, instead of the causal marker (red diamond), are most significantly associated. The pink markers represent noncausal markers where the association is caused by their high linkage disequilibrium (LD) to the causal one or an unmeasured error source. The markers were coloured according to their LD to the causal one and the dashed line represents the significant threshold. (Modified after Korte & Farlow, 2013)

C) The genotyped marker for example a single nucleotide polymorphism (SNP) will be statistically associated with the trait of interest through an indirect association because both markers (SNPs) are located together in a chromosomal region with high LD based on physical linkage. (Modified after Bush & Moore, 2012).

The 'missing heritability problem' can be caused by several factors (1) rare variants: because no population can include all possible variants; (2) genetic heterogeneity (Figure 1.4): when different markers within one gene (allelic heterogeneity) or in different genes (locus heterogeneity) generate the same phenotype in separate individuals or when multiple alleles of one marker exist, which were associated with different phenotypes; (3) epistatic or Gene-by-Gene (GxG) interactions can result in a higher or lower phenotype than expected because of conditional effects in unlinked loci; (4) epigenetic variations causing different phenotypes because of the impact of chromatin modifications like DNA methylations; and (5) Gene-by-Environment (GxE) interactions are important when the phenotyping was performed in several locations and/or years or under less controlled conditions like field trials (Brachi *et al.*, 2011, Gibson, 2012; Korte & Farlow, 2013). The latter three points contribute to the non-additive components of the phenotypic variance (Gibson, 2012).

In general, the genetic background plays an important role because the phenotype correlates always with the relatedness of the genotypes (Korte & Farlow, 2013; Burghardt *et al.*, 2017). The major confounders of GWAS are the genetic relatedness (number of shared alleles between genotypes) and/or the population structure (subpopulations caused by shared genetic ancestry, Vilhjálmsson & Nordberg, 2013; Price *et al.*, 2010). Population substructures classify groups of individuals within a population where the allele frequencies differ from the population itself because of some degree of reproductive isolation (Weir *et al.*, 2006). When the relatedness of the accessions and the population structure are not adequately corrected, spurious associations can occur since the genotypes in a population share both causal and noncausal markers (Price *et al.*, 2010; Vilhjálmsson & Nordberg, 2013; Korte & Farlow, 2013). The membership to a specific subpopulation can be estimated by a set of allele frequencies at each locus (Pritchard *et al.*, 2000) or in form of genetic relatedness matrices (Melchinger *et al.*, 1991; Burghardt *et al.*, 2017). In a mixed linear model, a measure of the familial relatedness (a kinship matrix as part of the variance-covariance structure between random background genotype effects) and the population structure (as fixed effect) can be included (Yu *et al.*, 2006). To further reduce the effect of allelic heterogeneity, it was proposed to restrict the selection of the accession panel to a geographical region because if all genotypes belong to the same genetic cluster, the resolution and the power might be increased (Brachi *et al.*, 2013; Bartoli & Roux, 2017).

Because a GWAS is a statistical approach that determines the probability of non-random associations of markers for the trait of interest, the evaluation of the significance is important (Burghardt *et al.*, 2017). It is necessary to correct for multiple testing because with increasing test numbers, the risk of obtaining false positives (random significantly associated but unlinked noncausal markers) increases (Platt *et al.*, 2010). The most common correction methods of the

experiment-wise Type I error in the context of GWAS are the false discovery rate (Benjamini-Hochberg procedure) and the Bonferroni correction (McDonald, 2014). The Bonferroni correction is often too conservative so that the power of the association study is reduced due to an excessive negation of true positives (Korte & Farlow, 2013). The Bonferroni correction assumes that the several tests being corrected, which total number equals the total number of markers, are fully orthogonal (independent). Nonetheless, this is often not the case, because the LD between the tested markers makes tests non-independent (Gao *et al.*, 2008). In consequence, methods that estimate the significance threshold based on independent tests were developed (Gao *et al.*, 2008). After identification of significantly associated markers, the candidate genes can be defined (Figure I 2).

1.5. Identification and functional validation of candidates

To identify the most promising candidate genes, the right associated markers have to be selected. In regard of the experimental design of the performed GWAS, it is either possible to identify QTLs or causal genes (Korte & Farlow, 2013). The fundamentals were based on the selected genotype panel, the marker density and the LD decay within the population (Korte & Farlow, 2013; Flint-Garcia *et al.*, 2003).

In case of QTL, it is irrelevant for most breeding applications if the associations have direct or indirect nature (Figure I 4C, Platt *et al.*, 2010; Sehgal *et al.*, 2016). Nevertheless, the identification of a causal marker can be difficult because the most significant marker does not have to be the causal one (Figure I 4A & 4B, Platt *et al.*, 2010). These synthetic associations often represent statistically true associations and it is possible to reproduce them in independent studies regardless of the sample size and the marker density (Platt *et al.*, 2010). The phenomenon is related to genetic heterogeneity and in contrast to the real randomly occurring false positive associations, they can be caused by (1) correlations between causal and noncausal markers; (2) more than a single causal marker; or (3) epistasis (Platt *et al.*, 2010). In case of the correlation with unlinked markers, the error source is often insufficient correction for population structure or unexpected LD blocks, but also interactions between different genes or pleiotropy can be a reason (Ioannidis *et al.*, 2009; Platt *et al.*, 2010). Pleiotropy describes the effect of a gene on more than one phenotype (Ioannidis *et al.*, 2009) and the related indirect associations are not random instead they are specifically linked to the causal markers (Platt *et al.*, 2010). If more than one locus is causal, the highest associations could be observed for unlinked markers that are genetically linked to several causal regions (Platt *et al.*, 2010). Moreover, epistatic interactions can even lead to the absence of significant associations with the causal marker, resulting in only indirect associations (Platt *et al.*, 2010; Burghardt *et al.*, 2017). These effects play normally only minor

roles in a GWAS, but for a highly polygenic trait under strong selection, like pathogen resistance, it could be important (Platt *et al.*, 2010).

The most important information for the identification of candidate genes is provided by (prior) knowledge of the trait biology, for example genes that are expressed in the relevant tissue could be prioritized (Burghardt *et al.*, 2017). Moreover, the peak shape and the strength of the statistical association could be used as criteria (Burghardt *et al.*, 2017; Cantor *et al.*, 2010). Wider peaks could represent simply strong clusters of LD or regions where more than one causal marker is located (Burghardt *et al.*, 2017). Additionally, *in silico* analyses could provide valuable information about complementary mapping data and genomic annotations (Burghardt *et al.*, 2017).

The validation of the identified candidates should be obvious (Figure 1 2), but it is actually less common (Burghardt *et al.*, 2017; Bartoli & Roux, 2017). Many reports about GWAS results end with a notification about further possible exploitations or confirmations (Wang *et al.*, 2012; Pasam *et al.*, 2012; Zhou *et al.*, 2016; Bengtsson *et al.*, 2017; Jabbari *et al.*, 2018). Nonetheless, only in rare cases these functional validations were reported in additional studies (Bartoli & Roux, 2017). In particular, in plant pathogen interactions several functional validation methods are established. In general, functional validation methods can be divided in statistical and experimental approaches (Burghardt *et al.*, 2017). Statistical approaches encompass the application of further mathematical models, the replication of the GWAS design with another population and the re-examination of already published data (Cantor *et al.*, 2010; Ioannidis *et al.*, 2009; Bush & Moore, 2012). Nevertheless, a negative result in a replication study or a meta-analysis does not mean necessarily that the initial results were false positives because often the so-called winners curse (inflation of the effect size) can be observed or the alterations in the population strongly influences the phenotype (Ioannidis *et al.*, 2009; Bush & Moore, 2012; Burghardt *et al.*, 2017).

On the other hand, classical forward or reverse genetic approaches allow functional validation in an empirical way by using the principles of gain or loss of function, respectively. In this sense, it could be worthwhile to analyse existing mutant collections or to introduce specially mutations in the identified candidates (Jankowicz-Cieslak & Till, 2015). Additionally, allele swapping experiments could be used to validate the identified candidates respectively candidate alleles (Genissel *et al.*, 2017). Many experimental approaches rely on the miss-expression or regulation of the candidate gene in regard of the transcriptional or protein level (silencing or overexpression) to analyse the function (Burghardt *et al.*, 2017).

In case of the barley system, stable as well as transient assays are established. The crop can be efficiently stably transformed via *Agrobacteria* in a genotype specific manner and also the transgene expression can be controlled specifically via various promoters (constitutive, inducible as well as tissue-specific promoters, Harwood, 2012). On the other hand, the silencing of the gene

of interest is usually based on RNAi (Harwood, 2012) or the clustered regularly interspaced short palindromic repeats (CRISPR)/Cas system (Lawrenson & Harwood, 2019).

Besides several advantages of stable transformed plants, a major issue is the long generation time. In particular for the functional validation in the barley-*Bgh* pathosystem, transient methods are well established (Panstruga, 2004). There are several methods available that rely on virus-mediated silencing or overexpression (Delventhal *et al.*, 2011; Lee *et al.*, 2012) as well as on particle bombardment (Douchkov *et al.*, 2005; Zimmermann *et al.*, 2006). During particle bombardment, DNA coated gold particles were transferred to single epidermis cells via high pressure (Panstruga, 2004). The method has been routinely used during the last 20 years (Schweizer *et al.*, 1999a+b; Rajaraman *et al.*, 2018) because it provides reproducible results specifically in the attacked tissue (Panstruga, 2004). The coexpression of the candidate and a suitable reporter gene like the β -glucuronidase (GUS) allows the study of the penetration resistance (Panstruga, 2004). Over the time, specific approaches were developed to either silence the candidate gene based on RNAi (Douchkov *et al.*, 2005) or to overexpress it under various promoters (Zimmermann *et al.*, 2006; Himmelbach *et al.*, 2007).

1.6. The aims of this study

One of the most important goals of plant breeding is the generation of varieties resistant against a wide range of abiotic as well as biotic stresses. In view of the negative effects on biodiversity and human health, the extensive application of pesticides should be avoided in future sustainable agriculture. To protect the crops from their attackers, one of the most reliable and environmentally friendly approaches is the use of the genetic resistance present in a species (Niks *et al.*, 2015). In comparison to wild ancestors, the genetic diversity of the modern gene pool was reduced during domestication (Killian *et al.*, 2006). Besides wild material, also landraces provided a high genetic diversity (McCouch *et al.*, 2013) and the exploitation of these resources is important for the future plant breeding (Schmid *et al.*, 2018). Particularly as source for disease resistance genes, wild material and landraces had proved to be versatile (Zhang *et al.* 2017; Schmid *et al.*, 2018). For instance, several of the most important race-specific *Bgh* resistance genes were found such material (Jørgensen & Wolfe, 1994; Schulze-Lefert & Vogel, 2000; Czembor *et al.*, 2000-2002). In this respect, the Whealbi (**W**heat and barley **l**egacy for **b**reeding **i**mprovement) collection was selected for the present study. One of the major criteria for the sampling of the material was to give access to the most relevant genetic diversity for European agriculture (<https://www.whealbi.eu/plant-diversity/key-facts/>).

To unlock the genetic diversity, several approaches were developed. In particular, GWA studies were a powerful tool to identify QTL or candidate genes in large and diverse populations (Huang & Wang, 2014). The reliability of the used phenotype and genotype data are essential for the success

of a GWAS (Burghardt *et al.*, 2017). The precision of the phenotyping is a highly discussed topic in science, particularly for the application in high-resolution approaches (Cobb *et al.*, 2013). Additionally, the effect of the environment on the trait of interest has to be considered (Korte & Farlow, 2013). Powdery mildew resistance was reported as reproducible trait where a high percentage of the phenotypic variation is explained genetically (Hoseinzadeh *et al.*, 2019; Bengtsson *et al.*, 2017). Nevertheless, it has to be considered that quantitative (polygenic) powdery resistance is dependent on the environment and the developmental stage of the examined material (Aghnoum *et al.*, 2010). Race-nonspecific resistance is difficult to assess regarding the small effect sizes of the causal genes (Niks *et al.*, 2015). Nevertheless, it is valuable because of the assumed higher durability compared to the monogenic major *R*-gene based resistance. The protection of this resistance type lasts often only three to four years (Brown, 2015; Niks *et al.*, 2015).

In consideration of this background, the main aims of the present study were the assessment of the feasibility of an association study in plant genetic resources to identify novel resistance genes or new alleles of known genes against the barley powdery mildew fungus and the validation of the most promising candidate alleles. Additionally, new insights about the genetic background of the barley powdery mildew resistance should be obtained. In regard of the special focus of study on the identification of race-nonspecific resistance genes, the following milestones should be achieved:

- Characterization of the Whealbi collection regarding the seedling and adult plant powdery mildew resistance;
- Identification of known major *R*-genes present in the collection;
- Identification of potential novel powdery mildew resistance genes;
- Functional validation of the most promising candidate alleles;
- Evaluation of different reporter constructs for their application in transient validation assays.

2. Material and methods

2.1. Plant material

2.1.1. Whealbi barley collection

For the powdery mildew resistance screening, 459 genotypes of the barley Whealbi (**W**heat and **b**arley legacy for **b**reeding improvement) collection were selected. The Whealbi project (<http://www.whealbi.eu/project/>) was founded in the frame of the European Community's Seventh Framework Programme (FP7/ 2007-2013, grant agreement n°FP7- 613556). Information for the complete germplasm collection can be retrieved through the URGI website (<https://urgi.versailles.inra.fr/siregal/siregal/accesionAction.do?collectionId=126>). One of the major criteria for the selection of the plant material was to give access to maximized genetic diversity (<https://www.whealbi.eu/plant-diversity/key-facts/>). To ensure a better description of such diverse material, the FAO and Biodiversity International released a set of descriptors for plant genetic resources. In respect of these 'FAO/IPGRI multicrop passport descriptors' (<http://www.fao.org/plant-treaty/news/news-detail/en/c/358465/>), the growth habit and biological status were selected to describe the present material (Appendix Table A 1). The biological status or cultivation status (<https://terms.tdwg.org/wiki/germplasm:biologicalstatus>) distinguish the material into wild, weedy or breeding/research material. Additionally, the material can be classified as traditional cultivar/landraces or advanced/improved cultivar.

2.1.2. Barley cultivars for powdery mildew maintenance

For the powdery mildew maintenance, several cultivars were used because of specific requirements of the nine fungal isolates and to minimize the risk of cross-contaminations (Table M 1).

Table M 1: Cultivars used for the maintenance of the powdery mildew isolates

Powdery mildew isolate		Cultivar
CH4.8 ¹	247 ²	Maythorpe: Ingrid: Golden Promise (2:2:1)
D2/4	227	KWS Bambina
D4/6	240	Ingrid
D35/2	233	JB Flavour
D35/3	242	JB Flavour
MH21	125	Ingrid
RiIII	75	Roland
Ro23a	78	Roland
Si1	224	Hanna

¹ work name of the powdery mildew isolate

² official isolate number of the Julius Kühn-Institute (JKI)

2.1.3. Plant growth conditions

For the powdery mildew resistance screenings, the barley genotypes were sown in plastic pallets (with 9x6 wells and one seed per well) filled with compost soil (from the IPK nursery). With the exceptions of the controls Roland and Morex, 12 seeds per genotype were used and the plants

were grown in a green house chamber under long-day conditions (16 h light at 20 °C/ 8 h dark at 16 °C) for 12 d.

The plants for the powdery mildew maintenance, the transient assays and amplification tests were sown in plastic pots (Ø 12 cm) filled with compost soil (from the IPK nursery) and were grown usually for 7 d under long-day conditions (16 h light / 8 h dark at 20 °C) in a Biomedical MLR-350 plant growth chamber (SANYO) or in a MLR-352H-PE Plant Growth Chamber (Panasonic). Only the plants for the transient silencing assay were grown for 8 d under the same conditions. In the case of the powdery mildew isolate CH4.8, the plants were grown in a greenhouse chamber (16 h light at 22 °C / 8 h dark at 20 °C).

2.2. Barley powdery mildew isolates and their maintenance

For the powdery mildew resistance screenings of the collection several powdery mildew isolates were used. The pathogen causing barley powdery mildew is the fungus *Blumeria graminis* (DC) Speer f. sp. *hordei* (Bgh). The used isolates were provided by the Institute for Plant Protection in Field Crops and Grassland, Julius Kühn-Institute (JKI) Kleinmachnow, except the powdery mildew isolate CH4.8, which was collected separately in Switzerland. The JKI provided all information about the used 27 European powdery mildew isolates and their virulence spectra were determined on a differential set of 33 barley accessions. In this set 35 known or postulated resistance genes/specificities and one (so far) unknown resistance gene are present (Table M 2). The infection types were scored on a scale from 0-4 and the additional symbol O(P) represents a *mlo* (*Mildew resistance locus o*)-like phenotype. An Infection type above two is considered as susceptible. Further methodical details were reported by Silvar *et al.* (2011). The powdery mildew isolates D35/3 and RiIII were selected for the powdery mildew resistance screening because of their high virulence (Table M 2). Additionally, seven (Table A 2) and 18 (Table A 3) powdery mildew isolates were used in the small and comprehensive isolate tests, respectively.

Table M 2: Virulence spectra of the powdery mildew isolates D35/3 and RiIII used for the resistance screening on a differential set of 33 barley lines and the *in silico* generated spectrum for the mixed inoculation (*Max* trait)

Accession	Gene ²	Code	Powdery mildew isolates ¹		<i>Max</i> ³
			D35/3 242 DEU	RiIII 75 DNK	
Alexis	<i>mlo9</i>	Mlo	0	0(P)	0
Antalja (WI/7)	<i>MI(WI-7)</i>	WI-7	2	2	2
Borwina	<i>MI(Bw)</i>	Bw	2.5	2.5	2.5
Camilla	<i>U</i> ⁴	U	1	1	1
Kredit	<i>MI(Kr)</i>	Kr	3	2.5	3
Laverda (U)	<i>MI(Lv)</i>	Lv	0	0	0
Lotta	<i>MI(Ab)</i>	Ab	3	2.5	3
P01	<i>Mla1</i>	Al	0	1	1

Table M 2 (continued)

Accession	Gene ²	Code	Powdery mildew isolates ¹		Max ³
			D35/3	RiIII	
			242 DEU	75 DNK	
P02	<i>Mla3</i>	Ri	1.5	3	3
P03	<i>Mla6, (Mla14)</i>	Sp	3	3	3
P04 B	<i>Mla7, Mlu</i>	Ly,u	3	3	3
P06	<i>Mla7, (Mlk)</i>	Ly	3	2.5	3
P08B	<i>Mla9</i>	MC	3	3	3
P10	<i>Mla12</i>	Ar	3	2.5	3
P11	<i>Mla13, MI(Ru3)</i>	Ru	0	3	3
P12	<i>Mla22</i>	-	3	0	3
P14	<i>Mlra</i>	Ra	3	2.5	3
P17	<i>Mlk</i>	Kw	3	3	3
P20	<i>Mlat</i>	At	2	2	2
P21	<i>Mlg, (MI(CP))</i>	We	3	2.5	3
P22	<i>mlo5</i>	Mlo	2	0	2
P23	<i>MILa</i>	La	3	2.5	3
P24	<i>Mlh</i>	Ha	3	3	3
SI-1 (RS1-12)	<i>MI(SI-1)</i>	SI-1	1	1	1
SI-2	<i>MI(SI-2)</i>	SI-2	1	0	1
SI-3	<i>MI(SI-3)</i>	SI-3	0	1	1
SI-4 (1-B-87)	<i>MI(SI-4)</i>	SI-4	0	3	3
SI-5	<i>MI(SI-5)</i>	SI-5	3	2.5	3
SI-6	<i>Mlf, mlt</i>	SI-6	2	2	2
SI-7	<i>MI(SI-7)</i>	SI-7	2	2	2
Steffi	<i>MI(St)</i>	St	2.5	3	3
WI-1 (RS142-29)	<i>MI(WI-1)</i>	WI-1	0	0	0
Hanna	-	-	3	2.5	3

¹ represented by the work names, the official JKI numbers and the country of origin on the basis of the NATO Codification System Country Codes

² annotated resistance genes

³ artificial virulence spectrum that was assumed for the *in silico* generated maximal infection. The higher infection type from both isolates (in bold) was selected.

⁴ until now unknown resistance gene

The infection types and the information about the resistance genes of the differential were provided by the JKI Kleinmachnow and the infection types were scored on a scale from 0-4 (0= resistant; 4=highly susceptible) and the additional symbol 0(P) was included for a *mlo* (*mildew resistance locus o*)-like phenotype.

Because of the obligate biotrophic life cycle of the fungus, the maintenance of the isolates is only possible on living vegetal tissue and it was performed weekly to have always fresh spores for the powdery mildew resistance screening. Otherwise the maintenance was performed every two to three weeks. Because of specific requirements of the fungal isolates, several plant cultivars were used to maintain them (Table M 1). The leaves of 7-8 d old plants were cut and placed with the adaxial surface up on petri dishes filled with 1 % Phytoagar solution supplemented with

benzimidazole [35 mg/l] and silver nitrate [1 mg/l]. For the inoculation, three plates were put under a 5 L-bucket with three holes at the top and the spores were blown inside with a pipette. To minimize the risk of cross-contamination, the inoculation was conducted under the laminar flow and all devices were cleaned with soapy water. The plates were incubated for 7 d under long-day conditions (16 h light / 8 h dark at 20 °C, 1 LS [light step]) in a MLR-352H-PE Plant Growth Chamber (Panasonic). The Swiss isolate CH4.8 was additionally maintained on whole plants (6 d) and the fungus grew at least for 7 d under long-day conditions (16 h light/ 8 h dark at 20 °C) in a Biomedical MLR-350 plant growth chamber (SANYO) or MLR-352H-PE Plant Growth Chamber (Panasonic).

The maintenance of the 27 powdery mildew isolates at the JKI were performed similarly at leaf segments of the cultivar Igri.

2.3. Screening for powdery mildew resistance

2.3.1. Resistance screening based on detached seedling leaves (detached leaf assay)

For the first powdery mildew resistance screening, 459 genotypes of the Whealbi collection and two susceptible controls (the genotypes Roland and Morex) were selected. The control plants were interspersed between the growing test genotypes. The second leaves of 12 d old plants were harvested and the basal part of each leaf was placed with the adaxial surface up on a 4-well plate (Greiner Bio-One, Figure A 1). The plate was filled with 1 % Phytoagar solution supplemented with benzimidazole [20 mg/l]. A special Teflon frame was positioned above all leaves per plate column to fix the leaves in their position and to keep them flat (Figure A 1). For the inoculation, 7 d old spores of the powdery mildew isolate D35/3 from infected leaves were blown into a settling tower containing the plates. To monitor the inoculation density, which was set to 8-9 spores/mm², a glass slide was placed inside the settling tower and the plates were incubated for 7 d under long-day conditions (16 h light / 8 h dark at 20 °C, 1 LS) in a MLR-352H-PE Plant Growth Chamber (Panasonic, Figure A 1). Afterwards, the macroscopic disease symptoms were scored as percentage of the infected leaf area and the median per genotype was calculated (Table B 1). The calculation of the median was selected to minimize the risk that single outliers skew the results in regard of the small sample size. The leaves displaying huge brown spots were excluded from the analysis because these spots could hint to an unspecific stress reaction of the leaves.

Table M 3: Definition of the resistance classes for the complete powdery mildew resistance screening

Resistance Class	Percentage of the infected leaf area
Resistant	≤ 2.5 %
Moderately resistant	≤ 25 %
Moderately susceptible	< 51 %
Susceptible	≥ 51 %

The genotypes with an infected leaf area < 31 % or > 50 % were selected for the complete powdery mildew resistance screening and they were analysed due to the assigned biological status and their growth habit (Table A 1). In total, 267 genotypes (Table A 1 and B 1) were tested with the powdery mildew isolates D35/3 and RiIII in at least three independent experiments. The procedure was very similar to the first resistance screening (scheme in Figure A 1). The harvested second leaves were halved horizontally and the basal half of each leaf was inoculated with D35/3 spores. The inoculation density was set to 8-10 spores/mm² whereas the inoculation and incubation were performed as described for the first screening.

Because the screening was conducted as several sub-experiments, the control Morex was used for normalization. Each leaf was normalized and after outlier test (ROUT Q= 1 %, performed with GraphPad Prism7.01 for Windows) the means and the standard deviations were calculated. In the next step, the genotypes were grouped into resistance classes (Table M 3) based on artificial maximal infection of both isolates. This *in silico* generated trait was named *Max* because always the higher infected leaf area value from the two isolates was selected.

2.3.2. Resistance screening of identified resistant genotypes with additional powdery mildew isolates (isolate tests)

A small isolate test with additional seven powdery mildew isolates (Table A 2) was performed. In this detached leaf assay, the ten resistant genotypes that do not harbour the *mlo-11* allele, and the controls Roland and Morex were tested. The determination of the *Mlo* status is described in section 2.4. The second leaves of 11-12 d old plants were harvested and cut horizontally into two to three segments. Each leaf segment was used for the inoculation with a different powdery mildew isolate (further details in section 2.3.1 and Figure A 1). The inoculation densities and spore age vary compared to the procedure described in section 2.3.1 (Table A 4). On the basis of at least nine values per genotype, the mean and the standard deviation per isolate and genotype were calculated to determine the resistance. The control Morex was used for normalization.

In cooperation with the JKI Kleinmachnow, a comprehensive isolate test with 27 powdery mildew isolates was performed. The resistance spectra of the four genotypes (WB-052, WB-066, WB-400 and WB-476) that were resistant or only weakly infected in the field experiments (section 2.3.3) should be analysed in more details. The comprehensive isolate test was performed also as detached leaf assay and the complete experimental procedure was described by Silvar *et al.* (2011). The virulence spectra of the 27 powdery mildew isolates are presented in the Table M 2, A 2 and A 3. The data were analysed manually for the distribution of infection types and the resistance spectra of the genotypes was determined.

2.3.3. Resistance screening based on natural powdery mildew infection (field trial)

The field trial was performed at two locations and in cooperation with KWS Lochow GmbH. One hundred Whealbi genotypes as well as the controls Morex and Roland (Table B 3) were planted in spring 2017 at the IPK (Leibniz Institute of Plant Genetics and Crop Plant Research) campus in Gatersleben (51°49'35.7"N 11°16'49.7"E, 110 m) and at a field in Bergen/Wohlde (52°48'32.1"N 9°59'53.7"E, 80 m). Due to the planting time, only genotypes that show a spring or facultative growth habit were selected and the lines were sampled from all resistance classes to cover the complete resistance spectrum of the population. Moreover, only a difference of 10 % of the arithmetic means of the infected leaf area between the isolates was allowed, in order to favour the scoring of potential race-nonspecific rather than race-specific resistances. The genotypes were sown in separated rows in observation plots following a completely randomized block design. For each row per genotype, ~40-50 grains were used for field trials. Each test line was sown twice per location (in total in two blocks). Additionally, the controls Morex and Roland were planted ten-times each within each block. The elite cultivar Milford (Saatzucht Breun) was utilized as experiment border at the Gatersleben field, while no border stripe was considered for Bergen. During the growth period, the plants were treated with fertilizer and protection agents (Table A 5). Additionally, the temperature, the relative air humidity and the rainfall was recorded (Figure A 2).

Table M 4: Definition of the resistance classes for the field trials and the assumed corresponding infected leaf area ranges, which were used for transformation during correlation analysis

Resistance class	Phenotype	infected leaf area range
1	Complete resistant or a few small colonies	0 %-10 %
1-2	Subclass between class 1 & 2	10 %-20 %
2	Weak infection	20 %-30 %
2-3	Subclass between class 2 & 3	30 %-40 %
3	Moderate infection	40 %-50 %
3-4	Subclass between class 3 & 4	50 %-60 %
4	Strong infection	60 %-100 %

The disease scoring was based on four major resistant classes (Table M 4) including three possible subclasses and the macroscopic disease symptoms of all plants (as whole plant) in a row were evaluated. Potential hypersensitive reactions were not taken into account during the visual scoring. The plants were 10-11 weeks old while the scoring was performed. Nevertheless, due to the different growth rates of the genotypes it was not possible to define a specific growth stage for the time point of scoring. The development ranged from stage 4.9 (first visible awns) to 6.1 (beginning of flowering) on the Zadoks two-digit code system (Zadok *et al.*, 1974).

In the first step, the detached leaf assay data were transformed into classes based on the assumed infected leaf area ranges (Table M 4) and the complete resistant genotypes were excluded from the analysis to focus on race-nonspecific resistance. In the second step, the arithmetic means of

all leaves belonging to a particular genotype \times experiment combination were computed in order to have only one data point per genotype per experiment for further analyses. These data were subsequently used to obtain the best linear unbiased estimations (BLUEs) of each genotype by fitting the following linear mixed model (Henderson, 1975 & Piepho *et al.*, 2003):

$$y_{ij} = \mu + \xi_i + g_j + e_{ij}, \quad (1)$$

where y_{ij} is the arithmetic mean of the detached leaf assay values calculated from up to five leaves for the j th genotype evaluated in the i th experiment, μ corresponds to the common mean of the material under study, ξ_i denotes the effect of the i th experiment, g_j is the effect of j th genotype, and e_{ij} is the residual variation. The common mean and genotypic effects were assumed as fixed factors, while the rest of the factors were considered as random. On the basis of the calculated BLUEs, also the artificial maximal infection was generated by the selection of the higher infection values of the two isolates (transformed *Max BLUE*).

The BLUEs of genotypes were calculated from the field data by fitting a linear mixed model as follows:

$$y_{ijk} = \mu + E_i + \beta_{j(i)} + g_k + E_i \times g_k + e_{ijk}, \quad (2)$$

where y_{ijk} is the disease score of the k th genotype tested in the j th block within the i th environment, μ denotes the common mean of the plant material tested in the field, E_i corresponds to the effect of the i th environment, $\beta_{j(i)}$ is the effect of the j th block nested within the i th environment, g_k represents the effect of the k th genotype, $E_i \times g_k$ indicates the interaction between the i th environment and the k th genotype, and e_{ijk} is the residual variation of the model. Model assumptions respecting fixed and random effects were the same as in equation (1). Afterwards, BLUEs from the detached leaf assays, the field experiments as well as the transformed *Max BLUEs* were compared using the Pearson correlation coefficient in addition to a graphical approach. Significance of correlation coefficients ($H_0: \rho = 0$) was assessed by t-test. Mixed model equations were solved using the Restricted Maximum Likelihood algorithm as implemented in the ASREML-R package (Butler *et al.*, 2009). All computational methods were performed in the R environment (R Development Core Team, 2008).

2.4. Characterization of the *Mlo*-alleles in identified resistant genotypes

The powdery mildew resistance screening revealed 21 genotypes as resistant against both powdery mildew isolates (Table B 2) and their resistance was analysed regarding race-specificity. The allele status of the race-nonspecific resistance gene *Mildew resistance locus o* (*Mlo*, HORVU4Hr1G082710.2) was determined with special interest on the presence of the natural *mlo-11*-allele (Piffanelli *et al.*, 2004).

2.4.1. DNA isolation from seedling leaves of identified resistant genotypes

For the DNA isolation, 11 or 14 d old plants were used (grown under the conditions described in section 2.1.3). The second leaves were harvested manually into in 2.0 ml reaction tubes including two small metal beads. The samples were frozen in liquid nitrogen and they were grinded with a TissueLyser® (Qiagen, two times for 30 sec at a frequency of 1/30 sec). The DNA of ~200 mg leaf powder was isolated via CTAB (hexadecyltrimethylammonium bromide) extraction method. Four volume (vol) of CTAB buffer (freshly supplemented with β -mercaptoethanol) were added to the frozen leaf powder and thawed on ice. The samples were incubated for 30 min at 65 °C and 400 rpm in a thermomixer and then 800 μ l of ice-cold chloroform:isoamylalcohol (24:1) were added. They were inverted or vortexed every 2 min during a 15-min incubation period on ice, followed by a centrifugation step of 15 min at 10,000 x g and 4 °C. The supernatant was transferred into a fresh tube and 800 μ l cold chloroform was added. After vortexing, the samples were centrifuged under the same conditions as mentioned before and the supernatant was transferred into a fresh tube. Five μ l RNase A (Fermentas) were added and the samples were incubated 1 min at 250 rpm at 37 °C and then 30 min without shaking. Afterwards, the DNA was precipitated on ice by addition of 0.7 vol of ice-cold isopropanol and the tubes were inverted several times. The samples were incubated at least 1 h at -20 °C and the DNA was pelleted by centrifugation for 30 min at 1,850 x g at 4 °C. The supernatant was removed and the pellet was washed by addition of 700 μ l wash buffer I and again centrifuged under the same conditions as previously mentioned. Afterwards, a second wash step followed with 700 μ l wash buffer II and centrifugation. The pellets dried for 10-15 min at room temperature and were resuspended in 50 μ l TE-buffer overnight (ON) at 4 °C. The following day, the DNA concentration was measured by usage of the Colibri Microvolume Spectrometer (Titertek Berthold).

2.4.2. Screening for the *mlo-11* allele based on polymerase chain reaction

The generated DNA samples were used for the amplification of the *Mlo* gene and the house keeping gene *GAPDH* (HORVU6Hr1G054520.3). The glyceraldehyde 3-phosphate dehydrogenase (*GAPDH*) is part of the glycolysis pathway and it is expected to be amplified in all samples because it is highly conserved. An amplification of a 1.2 kilo base pair (kb) sized product with *mlo-11* specific primers is only possible if the *mlo-11* allele is present (Piffanelli *et al.*, 2004). For the PCRs (polymerase chain reactions), the Taq PCR Mastermix (Qiagen) and DNA dilutions (c=500 ng/ μ l in TE buffer) were used (Table A 6i and A 7). After amplification, the PCR products were separated on 1 % TAE-agarose gels (*mlo-11*) or 2 % gels (*GAPDH*) supplemented with 0.03 % ethidium bromide and visualized under UV light.

2.4.3. Determination of the *Mlo* allele status of selected genotypes based on full-length genomic sequences

The two Whealbi landraces WB-352 and WB-358 were completely resistant against all powdery mildew isolates but lack the *mlo-11* allele. They were used along with the controls Morex and Roland for the determination of the *Mlo* allele status based on full-length genomic sequences. The designed primers (Table A 8i) cover the old (MLOC 70290) gene model and amplify overlapping products. The length of the untranslated regions (UTRs) were defined differently in the MLOC model in comparison to the current gene annotation (HORVU4Hr1G082710.2; Mascher *et al.*, 2017). Additionally, two fragments from two accessions (WB-219 & WB-468), which were tested positively for the presence of the *mlo-11* allele, were amplified and sequenced. The PCRs were carried out in a 50 µl reaction based on the Phusion high-fidelity DNA polymerase and genomic DNA dilutions (c=50 ng/µl in TE buffer, Table A 9 and A 10i-ii). After amplification, 5 µl of the PCR-mix were separated on 1 % TAE-agarose gels and visualized as described in section 2.4.2. The remaining PCR-mix was purified according to the instructions of the GeneJET PCR purification Kit (Thermo Scientific™), followed by two consecutive elution steps. The DNA concentration was measured (section 2.4.1). Afterwards, 200 ng of the purified PCR products were used for Sanger sequencing. Each sample was sequenced in forward and reverse direction with 5 pmol of the corresponding primer. The generated, quality-controlled sequences from the six genotypes were used for pairwise and multiple alignments together with the public sequences of Morex (available over the BARLEX Server (Colmsee *et al.*, 2015) database: Barley Genomic HC Genes May 2016) and Ingrid (GenBank: Z83834.1 & Y14573.1). The alignments were performed with the online tools 'EMBOSS Needle – nucleotide alignment' and 'Clustal Omega'. To prove, if the detected insertion of WB-358 interrupts a functional domain, the coding sequence of WB-358 was translated *in silico* into a protein with the 'ExpASy- translate tool' and it was compared with the reference protein (Morex) via protein alignment with the 'EMBOSS Needle – protein alignment' tool.

2.4.4. Expression of *Mlo* of selected genotypes as semi-quantitative PCR

The experiment consists of three independent biological replicates. The plants were grown for 7 d under the conditions described in section 2.1.3. The first leaves were harvested and placed on petri dishes filled with 0.5 % Phytoagar solution supplemented with benzimidazole [10 mg/l]. For each genotype (WB-352, WB-358, Morex and Ingrid *BC mlo5*) two plates were set up. One plate was not treated and the second one was inoculated with 7-8 d old spores from the powdery mildew isolate CH4.8. The inoculation was performed as described for the detached leaf assay (section 2.3.1). The inoculation density was set to 60-67 spores/mm². According to Piffanelli *et al.* (2002), the *Mlo* expression is highest 6 h after powdery mildew inoculation. Thus, all plates were incubated for 6 h under long-day conditions (16 h light / 8 h dark at 20 °C, 1 LS) in a MLR-352H-PE

Plant Growth Chamber (Panasonic). Afterwards, samples of ~100 mg of tissue (based on two separate leaves per genotype) were harvested. The same harvesting and grinding procedures as described in section 2.4.1 were used. The only exception was that three instead of two small metal beads were included in the tubes. To extract the total RNA, the RNeasy® Plant Mini Kit from Qiagen was used according to the manufacturer's instructions. Prior to cDNA synthesis, the residual DNA was removed by DNase I digestion. One µg of RNA was set up together with the required volume of 10x buffer (including MgCl₂), 1 U of DNase I (Thermo Scientific™) and 20 U of Ribolock RNase Inhibitor (Thermo Scientific™) per genotype and treatment. The samples were incubated for 30 min at 37 °C and afterwards placed on ice. The DNA digestion was stopped by adding EDTA (ethylenediaminetetraacetic acid disodium salt dihydrate) according to the manufacturer's instructions. Later, the samples were incubated for 5 min at 65 °C together with the recommended volume of Oligo(dT)₁₈ primer (Thermo Scientific™) and placed on ice until the samples were chilled again. For the cDNA synthesis itself, the primed RNA mixture was set up together with the required volume of 5x buffer, dNTPs (Thermo Scientific™) and the RevertAid M-MuLV RT (200 U by Thermo Scientific™). The samples were incubated for 60 min at 42 °C, followed by heat inactivation for 10 min at 70 °C.

The quality of the produced cDNA was checked by amplification of a house keeping gene. The *ubiquitin-conjugating enzyme 3 (UBC, HORVU5Hr1G104090.1)* was chosen as reference gene because it displays a constitutive expression even after powdery mildew treatment (Skov *et al.*, 2007). For the semi-quantitative PCRs, either the Phusion high-fidelity DNA polymerase (V=10µl) or the Taq PCR Mastermix was used together with 1 µl of cDNA as template (Table A 6ii, A 7, A 9 and A 10iii). After amplification, the PCR products were separated on 1 % TAE-agarose gels (Phusion PCR) or 2 % gels (Taq-based PCRs) and visualized as described in section 2.4.2.

2.4.5. Conformation of WB-352-specific *Mlo* fragments by Sanger sequencing

During the semi-quantitative PCR, it was obvious that the Taq DNA polymerase amplifies additional WB-352-specific products. To follow this up, PCRs with different primer combinations (listed in Table A 8ii) and the Taq Mastermix (Qiagen) were conducted similarly as described for the semi-quantitative PCR (section 2.4.4, Table A 7). To confirm the specificity of the amplified products, the WB-352-specific fragments were cut out from the gels and the gel slices were purified with the GeneJET PCR purification Kit (Thermo Scientific™). This last step was performed following manufacturer's protocol with slight modifications. The DNA concentration was measured as described in section 2.4.1 after performance of two consecutive elution steps. The purified PCR products were analysed after Sanger sequencing as described in section 2.4.3. Additionally, the products were also re-sequenced with additional primer pairs located within the obtained sequences.

2.5. Genome-wide-association study

2.5.1. Exome capture data

The genotyping was done in form of exome capture sequencing (Bustos-Korts *et al.*, accepted) according to the method described by Mascher *et al.* (2013). The obtained reads were aligned to the current barley reference genome of Morex (Mascher *et al.*, 2017) and the data represent single nucleotide polymorphisms (SNPs) with eightfold coverage for at least 50 % of the samples and a minor allele frequency (MAF) of 5 %. The SNP mapping quality score (Q) cut-off was set to 30. The SNPs were filtered considering a minimum homozygosity of 98 % and multiallelic sites were not allowed. In total, genotypic data from 403 genotypes were provided, leading to an overlap of 220 genotypes with the present phenotypic data set. Thereby, the SNPs were filtered again with MAF >5 % referring the 220 genotypes and 424,567 SNPs were selected for subsequent analyses.

2.5.2. Processing of the phenotypic resistance data

The results of the powdery mildew resistance screening and the small isolate test were combined with the obtained information for the presence of the *mlo-11* allele. Due to the main focus on race-nonspecific resistance, the 19 identified *mlo*- and major *R*-gene carriers were excluded from the further analyses. From the resulting 201 genotypes, the BLUEs for each powdery mildew isolate were calculated in the R environment (R Development Core Team, 2008) using the ASReml-R package (Butler *et al.*, 2009) in the same way as described before in section 2.3.3 (Henderson, 1975; Piepho *et al.*, 2003). For the analysis, the unnormalized values from the powdery mildew resistance screening were used and each sub-experiment was treated as independent location to minimize the effects that were caused by small changes of the experimental conditions over time. Again, the maximal infection trait (*Max BLUE*) was generated by the selection of the higher BLUE value from the two isolates to favour race-nonspecific associations. Additionally, the repeatability and heritability for each sub-experiment were calculated based on Piepho & Möhring (2007).

2.5.3. Specifications of the mixed linear model

GWAS was performed separately for each powdery mildew isolate or using the *Max BLUEs* as phenotypic data. The basis of the GWAS was described by Yu *et al.* (2006) in the general form of a mixed linear model:

$$y = X\beta + Gs + Zg + e, \quad (3)$$

where y is the vector containing the phenotypes of the 201 genotypes, β denotes a vector of fixed effects containing the common population mean and the allele substitution effect of the tested marker, s represents a vector of fixed subpopulation effects, g corresponds to a vector containing the random genetic background effects of the 201 genotypes, X as well as G and Z represent design matrices that relate y to β , s and g , respectively, while e is a vector of random residual

variation. Subpopulations and the membership of genotypes to them included in the G matrix were calculated based on the Rogers' distance (Rogers, 1972). Vectors g and e were assumed as $g \sim N(0, \sigma_g^2 K)$, $e \sim N(0, \sigma_e^2 I)$, where K is a marker-derived kinship matrix based on the Rogers' distances (Melchinger *et al.*, 1991), I is an identity matrix, while σ_g^2 and σ_e^2 are the corresponding variance components. The linear mixed model in equation (3) was fitted at each of the 424,567 SNP positions using the R package ASReml-R (Butler *et al.*, 2009). The significance threshold to control the genome-wide multiple-test Type I error during whole genome scans was estimated based on the effective number of independent tests (M_{eff_G}) as described by Gao *et al.* (2008): (1) the percentage cut-off C (the proportion of linkage disequilibrium (LD) variation explained by independent markers) was set to 99.8%; (2) LD matrices were calculated chromosome wise; (3) by applying single-value decomposition to these matrices, an effective number of independent tests equals to 1,414 was estimated; and (4) the expected Type I error rate (α_e) was set to 0.05. In this respect, SNPs having a $-\log_{10}(\text{p-value})$ higher than 4.45 were considered as significant. To evaluate if the population was suitable for a GWAS approach, the association of the phenotypic distance matrix and the Rogers' distance matrix was determined. The Pearson correlation coefficient of the triangle matrices was calculated and the significance of correlation coefficients ($H_0: \rho = 0$) was assessed by t-test.

2.6. Characterization of candidate genes identified in the genome-wide-association study

2.6.1. Identification of candidate genes putatively involved in powdery mildew resistance

Because of the focus on race-nonspecific resistance, all significant SNPs from the trait *Max BLUE* were used for the determination of the candidate genes (Table B 5i). The significant SNPs that were only significant in the D35/3 or RiIII trait were treated as potential race-specific resistances (Table B 5ii). Additionally, the identified significant SNPs (*Max BLUE* trait) were analysed with TASSEL 5 for LD as sliding window. The window size was set to 50 and heterozygous SNPs were treated as missing.

At least 2 kb of the flanking genomic regions (reference genome cultivar Morex, Mascher *et al.*, 2017) of the significant SNPs for the trait *Max BLUE* were extracted with the help of the IPK Galaxy Server [database: Barley 2016 Chromosomes (IBSC 2016)] and the sequences were used for a 'blastn' analysis with the BARLEX Server (Colmsee *et al.*, 2015, database: Barley CDS HC May 2016 & Barley CDS LC May 2016). Based on these results, the corresponding Gene-IDs and gene positions were used to assign the candidates (Table R 2). To confirm the annotated gene models, the (genomic and coding) sequences of the 33 identified candidate genes were verified via 'megablast' analysis with the NCBI (National Center for Biotechnology Information, 1988) Server

[database: nucleotide collection (nr/nt)]. The candidate gene models were compared with similar sequences of (predicted) genes (Table B 6) in the related species *Aegilops tauschii* subsp. *tauschii* and *Brachypodium distachyon* to confirm especially the start and stop codons of the candidates. Moreover, only these candidates were selected for further analyses where potential cDNA clones and expressed sequence tags (ESTs) from barley could be identified with the help of the IPK Barley BLAST Server [databases: full length cDNA & ipk 206633 barley ESTs] (Table B 6).

2.6.2. Determination of the allele status of selected candidate genes (allele mining)

To select the most promising candidate genes, several further analyses were necessary. Because of the high diversity of the selected barley collection, the presence of different alleles per candidate was expected and the allele status of the twelve candidate genes with confirmed annotation was determined. All significant SNPs of the trait *Max BLUE* that were located within the respective annotated gene model, were used to define the alleles. These determined alleles should be tested functionally in a transient overexpression (OX) assay and because of this, the full-length alleles of different genotypes were tried to amplify via PCR. For the experiment, 9 d old first leaves were used and the plants were grown under similar conditions as described in section 2.1.3. The sample preparation was comparable to the semi-quantitative PCR set up (section 2.4.4). To extract the DNA, the DNeasy® Plant Mini Kit from Qiagen was used according to the manufacturer's instructions and the concentration was measured with the Colibri Microvolume Spectrometer (Titertek Berthold). The utilized PCR set up was similar to the semi-quantitative PCR approach (section 2.4.4). The reactions were carried out in a 10 or 20 µl reaction and cDNA or genomic DNA (50 ng/µl) was used as template (Tables A 9, A 10i, A 10iv and A 11i). In the section 2.7.3, a detailed description for the primer design is given.

Moreover, it was essential to test the expression of the candidate genes because of the planned transient silencing. Six out of the twelve candidate genes with confirmed annotation were analysed due to their expression in the reference genotype Morex and Ingrid *BC mlo5*. For the PCRs, the cDNAs generated as control for the semi-quantitative PCR were used. The utilized PCR set up was similar to the allele amplification approach (Tables A 9, A 10i, A 10iv and A 11ii). Again, details about the primer design is provided in the section 2.7.3.

On the basis of these results, the four most promising candidate genes were selected and for their defined alleles, the average infected leaf area was calculated from the *Max BLUEs*. To detect significant differences between the alleles, an unpaired, two-tailed t-test using GraphPad Prism 7.01 for Windows was performed. The basis of the allele definition was the inheritance of SNPs in specific clusters due to (genetic) linkage (Flint-Garcia *et al.*, 2003). Additionally, a linear model (lm function) in the R environment (R Development Core Team, 2008) was calculated to compare the

proportion of the variation of the infected leaf area, which is explained by the single SNPs with the one attributed by the alleles.

The loci 13 and 14 co-localizes with a previously mapped powdery mildew resistance locus and the nucleotide sequence of the potential causal gene (GenBank: L37358.1) was blasted against the BARLEX Server (Colmsee et al., 2015, database: Barley CDS HC May 2016) to determine the corresponding current candidate gene(s).

To check the annotated candidate gene functions, several *in silico* analyses were performed. Based on the off-target prediction of the si-Fi21 tool, potential candidate homologs in barley were identified (Table B 6). Moreover, the closest candidate gene homologs of *Arabidopsis thaliana* and rice were identified via 'blastp' analysis against the TAIR server [database: TAIR10 proteins (protein)] and the rice genome annotation project server [database: genes in MSU RGAP release 7-protein sequences], respectively (Table B 6). In case of WB-CG_28, the corresponding rice protein sequences were selected based on the results published by Kimura *et al.* (2003) (Table B 6). Additionally, the protein sequences of the closest homologs identified via 'NCBI blastn' analysis were extracted (Table B 6). These obtained protein sequences were used for pairwise and multiple protein alignments with the online tools 'EMBOSS Needle – protein alignment' and 'Clustal Omega', respectively. Moreover, the protein sequences were used for domain prediction with the 'Pfam 32.0 sequence search' and in case of WB-CG_23 also for a nuclear localization signal (NLS) prediction via 'NLS mapper' with default settings. The nucleotide sequences of the defined candidate alleles were generated on the basis of the annotated significant SNPs and the obtained sequencing results of the cloned alleles (section 2.7.3). These sequences were translated into putative proteins with 'ExpASY -Translate tool' and the different alleles were compared to each other.

2.6.3. Relative quantification of the expression of selected candidate genes

The first approach to quantify the transcript level of the selected candidate genes was based on a time course experiment with three independent biological replicates. The experimental set up was similar as described for the semi-quantitative PCR (section 2.4.4) and the 7 d old first leaves of the genotypes WB-052 and Morex were inoculated with the powdery mildew isolate CH4.8 (inoculation density 223-330 spores/mm²). For the first time point, the leaves were collected directly after the inoculation (time point 0 h) and handled as described in section 2.4.1. The remaining inoculated and not-inoculated leaves were maintained for 4 h and 24 h under the previously described conditions (section 2.4.4). The following RNA extraction and cDNA synthesis was performed as described for the semi-quantitative PCR (section 2.4.4). It was decided to perform the quantitative (q) PCR in the hydrolysis probe detection format with the GoTaq® Probe qPCR Master Mix by Promega according to manufacturer's instructions (Table A 12). The primers

and probes for the qPCR were designed with the qPCR Primer & Probe Design Tool (eurofins Genomics, Table A 13). For each biological replicate and the no-template-control (NTC), three technical replicates were set up.

The qPCR was performed as multiplex qPCR with the 7900HT Fast Real-Time PCR System (Applied Biosystems™) in 384-well plates and the analysis was performed with the SDS 2.4.1 software and the RQ manager 1.2.1 (Applied Biosystems™). The raw quantification cycle values (C_q-values, sometimes also referred as threshold cycle (C_t)-values, Bustin et al., 2009) of the three technical replicates were analysed manually for outliers. An expression quantification of the WB-CG_19 and WB-CG_28 was not possible because the generated C_q-values were partially above the threshold value (≥ 35) which is recommended in the general guidelines provided from the Genomics platform from IRIC. The samples from WB-CG_17 and WB-CG_23 were normalized to the endogenous control (*UBC*) and the biological replicates were analysed separately via the delta delta C_q method to calculate the relative quantification (RQ) values. The results were displayed relative to time point 0 h of the not-inoculated samples because it was selected as calibrator. The values were analysed statistically via an unpaired two-tailed t-test between the inoculated and the not-inoculated samples per time point.

The second approach to quantify the transcript level of the selected candidate genes was to analyse public available micro array data. The chosen data were described by Delventhal *et al.* (2017). The powdery mildew inoculated (*Blumeria graminis* f. sp. *hordei* (*Bgh*) isolate CH4.8 or *Blumeria graminis* f. sp. *tritici* (*Bgt*) isolate FAL92315) and the non-inoculated epidermis peels of the barley cultivar Vada were analysed via the custom barley microarray SCRI_Hv35_44k_v1 (Agilent design ID 20599). The data were based on three biological replicates and four different time points (6 h, 12 h, 24 h and 74 h post inoculation). The annotated coding sequences of the candidate genes were used for a 'blastn' analysis against the HarvEST barley database to identify the corresponding U35 sequence identifier and probe-IDs, respectively. It was checked via pairwise alignment if the identified probes were present in the genomic candidate sequences. The quantile-normalized signal intensities were calculated by the GeneSpring software package. The signal intensity values of the confirmed probes were analysed statistically via unpaired two-tailed t-test between the inoculated and non-inoculated samples per time point.

2.7. Particle bombardment

For the functional validation, a method called biolistic gene transfer was used. It is sometimes also referred as particle bombardment or shooting. This method is based on transient transformation of single epidermis cells via high pressure with DNA coated gold particles. Based on the selected construct, the gene of interest is either overexpressed or silenced (Panstruga, 2004). A short description of the vectors which were generated prior to this work is given in Appendix A h).

Besides the functional validation of the candidate genes, this method was also used for a *Mlo* complementation assay and the characterization of promoter_GUS constructs (Table A 14).

2.7.1. Preparation of chemical competent cells

To prepare chemical competent Top10 cells, a fresh single *Escherichia coli* (*E. coli*) colony was used to inoculate 3 ml of sterile LB medium without antibiotics and the culture was grown for 15 h at 37 °C, 220 rpm. On the next day, the starter culture was used to inoculate in total 200 ml of sterile LB medium without antibiotics but supplemented with magnesium salts. The inoculated LB medium was incubated at 37 °C and 220 rpm until the absorbance (OD₆₀₀) reached 0.4-0.5. Afterwards the cultures were distributed on pre-cooled 50 ml-tubes, cooled for 20 min on ice and centrifuged for 15 min at 3,000 rpm and 4 °C. Then, the pellets were carefully resuspended in 10 ml transformation buffer I and cooled for 2 h on ice. After centrifugation under the same conditions, the pellets were resuspended in 4 ml transformation buffer II and the bacteria were distributed on cooled tubes using 50 µl-aliquots under sterile conditions. A test transformation with four aliquots of the competent cells were performed with 50 pg of pUC19 plasmid DNA. The thawed aliquots were gently mixed with the DNA and incubated for 30 min on ice. Then, the heat shock was performed at 42 °C for 20 sec and after incubation for 1-2 min on ice; the bacteria were mixed with 100 µl of SOC medium. Before the plating on pre-warmed LB-Ampicillin plates, the bacteria were incubated for 1 h at 37 °C. On the next day the transformation efficiency was determined between 5.7×10^6 and 2.4×10^7 colony forming units per µg DNA (CFU/µg).

2.7.2. Generation of constructs for the functional validation tests

To generate the overexpression (OX) constructs, primers for the twelve candidate genes, which annotation was confirmed, were designed in order to amplify the full-length alleles. In general, the primer pairs (Table A 11i) cover the whole coding region of the candidates with begin at the start codon and end at the stop codon. The candidates WB-CG_6, WB-CG_7, WB-CG_11, WB-CG_13, WB-CG_14, WB-CG_17 and WB-CG_28 were an exception to this because also parts of the 5' and/or 3' UTRs were included. In these included regions interesting SNPs were located. The amplified PCR fragments from the four selected candidate genes were cut out of the gels and the gel slices were purified as described in the section 2.4.5.

In a one-step ligation, the vector pPKTA9 was linearized with SmaI and the purified fragments (in two concentrations) were inserted (Table M 15). The ligation mixtures were incubated for 1 h at 25 °C and the enzymes were heat inactivated for 10 min at 65 °C. Afterwards, 1 µl of SmaI was added and incubated for 30-35 min at 25 °C to reduce the background. For the transformation, a sample of the prepared chemical competent Top10 cells were gently mixed with 5 µl of the ligation mixture and incubated for 30 min on ice.

Table M 5: Composition of the ligation mixture for one reaction

Compound	Volume (V=10 µl)
pIPKTA9 [160 ng/µl]	1 µl
10x T4 DNA Ligase buffer	1 µl
PEG4000 (50%)	1 µl
T4 Ligase [5 U/µl]	0.5 µl
SmaI [10 U/µl]	0.5 µl
Purified PCR fragment	2 µl or 4 µl
Water	4 µl or 2 µl

Then, the heat shock was performed at 42 °C for 20-45 sec and after incubation for 1-2 min on ice, the bacteria were mixed with 100 µl of SOC medium. Before the plating on pre-warmed LB-Ampicillin plates, the bacteria were incubated for a maximum of 1 h at 37 °C. The bacteria were grown ON at 37 °C and the developed colonies were transferred to new LB-Ampicillin plates with a sterile tip. The same tip was used to inoculate 50 µl of water. The samples were boiled for 10 min at 98 °C in a thermomixer, cooled for 2 min on ice and then centrifuged for 5 min at 14,000 rpm. For the following colony PCRs, a similar PCR approach as described in section 2.6.2 for the 10 µl reaction volume was utilized (Table A 9 and A 10iv). The only exception was that 2 µl of the sample supernatant were used as template. It was decided to use always one vector- and one gene-specific primer (Table A 15ii). After amplification, the PCR products were separated on 1 % TAE-agarose gels as described in section 2.4.2. Independent of the cloning method, all trials to clone WB-CG_28 failed. All generated colonies were tested negatively for the presence of the full-length alleles in the colony PCRs and it was assumed that the complete candidate gene fragment is toxic for the bacteria. Because of this constant failure, the different attempts will not be further described.

To confirm the positive clones, 5 ml LB-Ampicillin medium was inoculated with a single bacteria colony and incubated for 14-16 h at 37 °C and 220 rpm. The DNA was extracted via the QIAprep® Spin Miniprep Kit (Qiagen) according to the protocol except for an additional cooling step of 1-2 h at 4 °C between the pelletisation of the bacteria and its resuspension in buffer P1. An additional elution step was also included. The concentration measurement and the Sanger sequencing were performed as described in section 2.4.3. Each sample was sequenced with vector- and gene-specific primers to confirm specifically the presence of the SNPs determining each allele (Table A 16i). The generated quality-controlled sequences were used for pairwise and multiple alignments ('EMBOSS Needle – nucleotide alignment' and 'Clustal Omega') against the created vector maps based on the confirmed gene models.

To create the hairpin constructs which should be used for the transient-induced gene silencing (TIGS), the si-Fi21 tool (Douchkov *et al.*, 2014) was used. It predicted the region of the candidate genes, where the most efficient siRNAs (small interfering RNAs) should be produced in regard of potential off-targets. Based on these predicted regions, primers were designed for the six

candidate genes (Table A 11ii) which were analysed for their expression (section 2.6.2). The utilized set up was similar to the allele amplification approach (Table A 9 and A 10iv) and 5 μ l of the 20 μ l PCR mix were separated on 2 % TAE-agarose gels as described in section 2.4.2. The remaining 15 μ l PCR mix was purified with the GeneJET PCR purification Kit (Thermo Scientific™) according to manufacturer's instructions. The PCR fragments were inserted in the vector pIPKTA38 via the same blunt-end cloning procedure as described for the OX constructs (Table M 15). The utilized restriction enzyme was *Swa*I and the transformed bacteria were always grown in LB-Kanamycin medium. The grown colonies were also tested via colony PCR as described for the OX constructs (Table A 7, A 15ii). Two μ l of the bacteria supernatant was used as template and as annealing temperature 45.3 °C was chosen. The plasmid DNA of the positive clones was extracted as described for the OX constructs and ~2.5 μ g of the DNA was digested with *Apa*I for 3 h at 37 °C, followed by heat inactivation for 10 min at 80 °C. The mixtures were separated on 2 % TAE-agarose gels as described in section 2.4.2. One positive clone per candidate gene was selected for the LR Clonase reaction. The reaction was performed according to manufacturer's instructions. The pIPKTA38_candidate construct (150 ng) served as entry vector where as pIPKTA30N (150 ng) was used as destination vector. To transform the competent cells, the aliquots were thawed on ice and gently mixed with either 1 μ l (WB-CG_17, WB-CG_19, WB-CG_23), 2 μ l or 4 μ l (WB-CG_28) of the LR mixtures, respectively. After an incubation of 30 min on ice, the bacteria were heat-shocked for 30 sec at 42 °C and cooled for less than 1 min on ice before they were mixed with 250 μ l of SOC medium. The plating was performed as described for the OX constructs. For the following colony PCR, the same set up as described for pIPKTA38 was used. Because the candidate genes fragments should be inserted twice into the destination vector, two vector-specific primer combinations were utilized (Table A 15ii). The plasmid DNA of selected positive clones was extracted as described for the OX constructs. Because the constructs form hairpin structures, ~1 μ g plasmid DNA was digested with *FastDigest Eco*32I for 10 min at 37 °C prior Sanger sequencing (described in section 2.4.3, Table A 16ii).

2.7.3. Preparation of plasmid DNA

The plasmid DNAs for shooting were extracted from single colonies of transformed bacteria. To generate single colonies, a glycerol stock (250 μ l sterile 80 % glycerol mixed with 750 μ l fresh ON culture and stored at -80 °C) of the respective construct was plated on a LB plate supplemented with the required antibiotic. After incubation ON at 37 °C, a single colony was picked and used for the inoculation of 50-100 ml liquid LB medium supplemented with the required antibiotic. The cultures were incubated for 14-16 h at 37 °C under shaking at 180-240 rpm. To extract the plasmid DNA, either the JETSTAR MIDI Kit (GENOMED) or the PureLink™ HiPure Plasmid DNA Purification Kit (Invitrogen™) was used according to an adapted protocol. The cells were harvested in two

steps. Fifty ml of the ON cultures were centrifuged for 20 min at 4,000 rpm at room temperature and the same tube was used for the centrifugation of the remaining culture. After cell lysis and neutralization, the mixtures were centrifuged for 30 min at 4,000 rpm at room temperature. To precipitate the plasmid after addition of isopropanol, the tubes were centrifuged for 60 min at 4,600 rpm at 4 °C. Afterwards, the pellets were washed with 1 ml 70 % ethanol and the pellets were transferred to 1.5 ml tubes. The solutions were centrifuged for 5 min at 14,000 rpm and 4 °C. The DNA pellets were resuspended in 50-100 µl TE buffer (5 min at 50 °C followed by ON incubation at 4 °C). As alternative plasmid extraction approach, the QIAprep Spin Miniprep Kit (Qiagen) was utilized according to the Miraprep protocol (Pronobis *et al.*, 2016).

Independent of the extraction method, the concentration was measured with the Colibri Microvolume Spectrometer (Titertek Berthold) and then adjusted to 1 µg/µl.

2.7.4. Preparation of the gold suspension

For the Preparation of the gold suspension, 27.5 mg microcarriers (1.0 µm gold particles) were transferred into a 1.5 ml reaction tube and suspended in 1 ml sterile water through extensive vortexing and ultrasonication for 20-30 sec. After centrifugation at 14,000 rpm for 30 sec, the supernatant was removed and the pellet was washed again with 1 ml sterile water and 1 ml 96 % ethanol. Then, the pellet was dried for approximal 10 min at 50 °C in a thermomixer and afterwards resuspended in 1 ml 50 % (v/v) sterile glycerol.

To coat the gold particles with DNA, 87.5 µl of the gold suspension were mixed with 7 µg plasmid DNA [1 µg/µl] of both, test and the normalization construct (Table A 14). Afterwards, calcium nitrate solution was added dropwise until a final concentration of 0.5 M was reached. The mixture was incubated for 30 min at room temperature and inverted every 2 min. After centrifugation at 14,000 rpm for 30 sec, the pellet was washed once with 500 µl 70 % ethanol and twice with 500 µl 96 % ethanol. Finally, the pellet was resuspended in 40 µl of 96 % ethanol.

2.7.5. Biolistic gene transfer

The first leaves of 7 d old plants (the genotype varies due to the assay, Table A 14) were harvested on petri dishes filled with 0.5 % Phytoagar solution supplemented with benzimidazole [10 mg/l]. On the seven leaves per petri dish, two magnetic stirrers were placed at the leaf ends to ensure that they stay flat and with the adaxial leaf side up.

The Biolistic® PDS-1000/He Particle Delivery System (BIO RAD) was used for the biolistic gene transfer. Per shot, one rupture disc (900 psi, BIO RAD) was placed into the retaining cap and one sterile stopping screening was added to the stopping screening holder. Seven macrocarriers (BIO RAD, cleaned with 96 % ethanol prior use) were fixed in the macrocarrier holder and 35-40 µl of DNA coated gold suspension were distributed on them. The complete macrocarrier launch assembly and one open petri dish with leaves were placed into the transformation chamber. After

applying ~27 mm Hg vacuum to the chamber using a vacuum pump, the rupture disk broke at a pressure about 900 psi and the macrocarries were pressed against the stopping screen. During this procedure, the DNA coated gold particles are transferred to the leaf epidermal cells. Afterwards, the magnetic stirrers were removed and water droplets on the leaf surfaces were allowed to air dry for 20-30 min.

2.7.6. Inoculation with powdery mildew

The inoculation with powdery mildew was performed at different time points according to the experimental design. In case of the evaluation of the total number of β -glucuronidase (GUS) stained cells of the promoter_GUS constructs, the leaves were inoculated after 24-28 h after particle bombardment. In contrast to this, the leaves of the silencing approach were inoculated after 3 d and the leaves of the *Mlo* complementation and OX assay were inoculated after 4 h. For the inoculation, the leaves of several shots were pinned randomly on big square plates (23.2 cm x 23.2 cm) filled with 1 % Phytoagar solution supplemented with benzimidazole [20 mg/l] and 7-12 d old spores of the powdery mildew isolate CH4.8 from infected plants were blown into a settling tower containing the plates. The different inoculation densities were listed in Table A 14 and the monitoring was described in section 2.3.1. The plates were incubated for 2 d under long-day conditions (16 h light / 8 h dark at 20 °C, 1 LS) in a MLR-352H-PE Plant Growth Chamber (Panasonic). In case of the OX approach, the randomized pinning was not performed because the use of an air compressor ensured the even distribution of the spores inside the settling tower.

2.7.7. Glucuronidase assay

The glucuronidase assay is based on the *uidA* gene of *E. coli* which is translated into the enzyme β -glucuronidase (GUS, EC:3.2.1.31). This protein is able to convert the indigogenic substrate 5-bromo-4-chloro-3-indolyl glucuronide (X-Gluc) into the blue product 5,5'-dibrom-4,4'-dichlor-indigo and the technique allows the visualization of GUS activity from single cells and small cell clusters after particle bombardment (Jefferson *et al.*, 1987; Panstruga, 2004). To stain the leaves, the leaf ends were cut to fit a Riplate® SW (10mL) deep well plate (by Ritter) or 5.0 ml screw-cap mailing tube (by VWR) and all seven leaves per shot were collected together into GUS-staining solution. A 1.4 M GUS-staining solution was used for the promoter_GUS analyses and the *Mlo* complementation assay and in contrast, a 3 M GUS-staining solution was selected for the functional validation assays. The samples were vacuum infiltrated 2-3 times in an exicator until the colour of the leaves turned dark green and the leaves went down to the bottom. The GUS-staining solution volume was adjusted to ensure that the leaves were completely covered. After an incubation step of 24 h at 37 °C in the dark, the GUS-staining solution was discarded and the samples were washed two times with distilled water. For the destaining of the leaves, they

were incubated for 3 d at room temperature in 96 % ethanol. If some chlorophyll was left, the leaves were incubated one day longer in fresh ethanol (96 %). Afterwards, the wash step was repeated and the samples were stored in water at 4 °C. In case of the evaluation of the staining/colour intensity of the GUS-stained cells, the leaves were destained with trichloroacetic acid until the chlorophyll was completely removed and the leaves were washed 2-3 times with distilled water.

2.7.8. Microscopic and statistical analysis

The manual microscopy was performed with an Axioplan 2 imaging or AxioScope A.1 (Carl Zeiss AG) equipped with one of the following objectives: EC Plan-Neofluar 5x/0.16, EC Plan-Neofluar 10x/0.3 Ph1 or EC Plan-Neofluar 10x/0.3 M27. The scoring of the stained cells was conducted usually in a 0.05 % Tween-20 solution. The anthocyanin-stained cells were scored after 3 d but prior GUS-staining, which means that the leaves were still green during the process. To test the constructs for their response to powdery mildew, the same construct was shot twice per experiment but only one shot was inoculated. The total number of the GUS-stained cells per shot was divided by the total number of the anthocyanin-stained cells per shot to normalize for the shooting efficiency. The mean values of three independent experiments per construct and treatment were calculated and analysed with GraphPad Prism7.01 for Windows. To detect possible significant differences, the log₂-transformed mean values per construct and treatment were used for an unpaired, two-tailed t-test against pUbiGUS.

In case of the evaluation of the staining/colour intensity of the GUS-stained cells, the scoring of the anthocyanin-stained cells was done as described before and the scoring of the GUS-stained cells was performed in a 50 % glycerol solution. The pictures were taken with an Axio Scan Z.1 (Carl Zeiss AG) equipped with an Objective Fluar 5x/0.25 M27 and a HV-F20SCL Hitachi camera. The original image size was 1,600 x 1,200 pix in stacks of 10 Z-levels. The pictures were analysed with a tool specifically written by S. Lück. It was used for the calculation of the background intensity (in the Lab-color space) as well as for the detection and calculation of the cell hue (in HSV-colour space) of GUS-stained cells. The first analysis step was the calculation of the normalization factor: this is the mean of the three independent experiments for the total number of detected GUS-stained cells divided by the total number of detected anthocyanin-stained cells for each promoter construct. The next step was the calculation of the average background intensities per promoter construct which were normalized with the average background intensity per experiment. Based on these results, it was decided to exclude one of the experiments because the background intensities were in a different range than the other two experiments. This could be caused by an overexposure during the process of picture taking. Finally, all cells within the defined confidence interval (25 %-75 % of the average background intensity) were selected. The

selected GUS-stained cells per promoter construct were multiplied with the corresponding normalization factor to correct for the different shooting efficiencies of the constructs and the mean of the normalized cell hue was calculated. To assess possible significant differences between the constructs and pUbiGUS, an unpaired two-tailed t-test of the normalized cell hue values was performed.

The *Mlo* complementation assay was performed as two independent experiments. The susceptibility index (SI) of all GUS-stained cells per construct (both experiments combined) was calculated according to the following equation:

$$\text{susceptibility index (SI)} = \frac{\sum \text{GUS-stained cells with haustorium}}{\sum \text{total number of GUS-stained cells}} \quad (4)$$

The analyses of the functional validation tests were performed as described by Rajaraman *et al.* (2018). One experiment of the OX assay was excluded from the analysis because the positive control displayed the opposite effect as it would be expected. The mean SI value of the three shots of the empty vector control (TIGS: pIPKTA30N or OX: pIPKTA9) were used for the calculation of the relative SI according the following equation:

$$\text{relative SI} = \left(\frac{\text{SI of test gene}}{\text{SI of empty vector control}} \right) \quad (5)$$

In order to determine possible significant differences between the constructs, an unpaired two-tailed t-test of the log₂-transformed relative SI values against the hypothetical value '0' was performed.

2.8. Additional information

Appendix A provides detailed information about important equipment and consumables; like chemicals, markers, proteins, kits, solutions, culture media and used software as well as used databases. Moreover, a short description of utilized constructs, additional figures and tables are presented.

3. Results

3.1. Biological status and growth habit of the Whealbi population

The worldwide collected barley Whealbi (**W**heat and barley legacy for **b**reeding improvement) population was assembled to provide access to the most relevant genetic diversity for European agriculture (<https://www.whealbi.eu/plant-diversity/key-facts/>, Appendix Table A 1). For this study, a panel of 459 genotypes, which originate from 71 countries (Appendix Figure B 1) were selected.

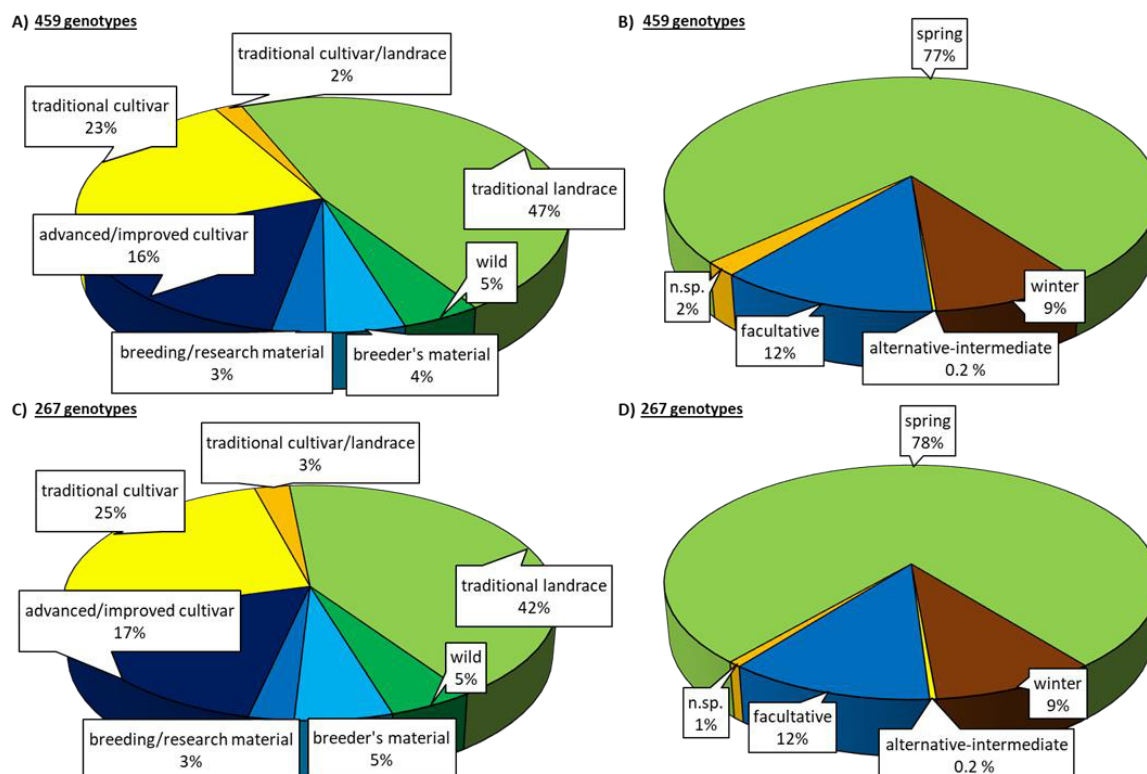


Figure R 1: Composition of the selected genotype panels in regard of the biological status and the growth habit

The composition of the collections used for the powdery mildew screenings, were depicted according to the assigned biological status (**A & C**) and the growth habit (**B & D**). The graphics **A & B** represent the results for the 459 genotypes and the graphics **C & D** illustrate the results of the 267 selected genotypes. The abbreviation 'n. sp.' stand for 'not specified'. The group 'facultative' summarizes true facultative genotypes as well as facultative/spring and facultative/winter varieties. The information of the biological status and the growth habit were extracted from the URGI website and supplemented with the information provided by the GIBIS database.

In regard of the 'FAO/IPGRI multicrop passport descriptors' (<http://www.fao.org/plant-treaty/news/news-detail/en/c/358465/>), the material was characterized concerning the biological/cultivation status and the growth habit. More than three-quarter of the population is constituted by traditional cultivars, traditional landraces, and wild genotypes (Figure R 1A). The term 'landrace' normally describes genetically diverse varieties that were locally adapted to the region of origin and/or cultivation, have historical origin, distinct identity, and lack formal genetic

improvement (Camacho Villa *et al.*, 2005). The wild material (5 %) belong to the taxon *Hordeum vulgare* subsp. *spontaneum*, which is the ancestor of the cultivated crop *Hordeum vulgare* subsp. *vulgare*. The remaining 23 % of the material encompasses modern or elite material (Figure R 1A). The analysis of the growth habit revealed that 78 % of the population were classified as spring cultivars and only 9 % were determined as winter cultivars. The group ‘facultative’ (12 %) summarizes true facultative genotypes as well as facultative/spring and facultative/winter lines (Figure R 1B).

3.2. Screening for powdery mildew resistance in the Whealbi population

3.2.1. Evaluation of the seedling powdery mildew resistance in controlled environmental conditions

For the evaluation of powdery mildew resistance several methods were established varying in plant age, infection conditions and disease quantification. In the first phenotypic screening of the diverse panel of 459 genotypes, the seedling resistance in response to the German powdery mildew isolate D35/3 (JKI-242) was evaluated for one biological replicate. The selected isolate is virulent against 12 major *R*-genes/resistance specificities commonly used in European material (Table M 2).

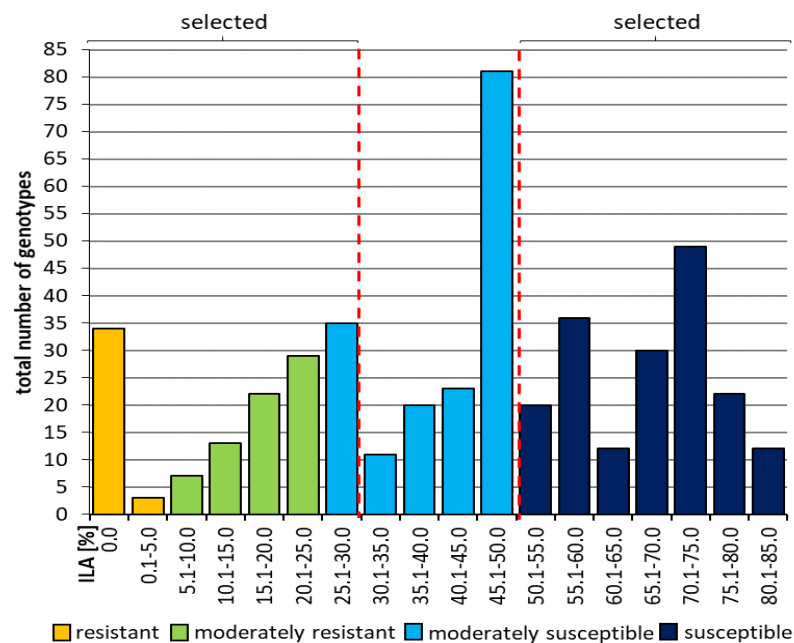


Figure R 2: Distribution of the 459 Whealbi genotypes in regard of the resistance response against the powdery mildew isolate D35/3

The 459 genotypes were inoculated with the isolate D35/3 and the distribution of genotypes per interval is given as absolute frequency. The resistance responses were evaluated based on macroscopic visible disease symptoms. They were assessed as median values of the infected leaf area [ILA in %]. The results represent one biological replicate per genotype and the classification into resistance classes (Table M 3) is visualized with colours. The indicated material was selected for further tests.

This approach was performed under controlled environmental conditions (greenhouse) based on inoculated detached seedling leaves. A scheme of the whole screening procedure is presented in Figure A 1. Seven days after controlled inoculation, the percentage of the leaf which was covered by macroscopic disease symptoms (the infected leaf area) was scored visually. This first screening revealed that the collection spans the complete range of susceptibility to the powdery mildew isolate D35/3 (Figure R 2 and Table B 1).

In account of the high virulence of the used isolate, a large proportion (76.4 %) of the genotypes was declared as susceptible. One hundred and seventy-two genotypes were either classified as moderately susceptible (37.0 %) or susceptible (39.4 %) and only 37 genotypes (8.1 %) were characterized as resistant. The remaining 15.5 % of the population (71 genotypes) were determined as moderately resistant. With focus on the more extreme phenotypes (as indicated in Figure R 2), 267 genotypes from all defined resistance classes were selected for the further screening of the seedling powdery mildew resistance (Table A 1 and B 1). The selected genotype panel was also analysed for the biological/cultivation status and the growth habit. Accordingly, a representative subset of genotypes was selected from both populations (Figure R 1C and 1D).

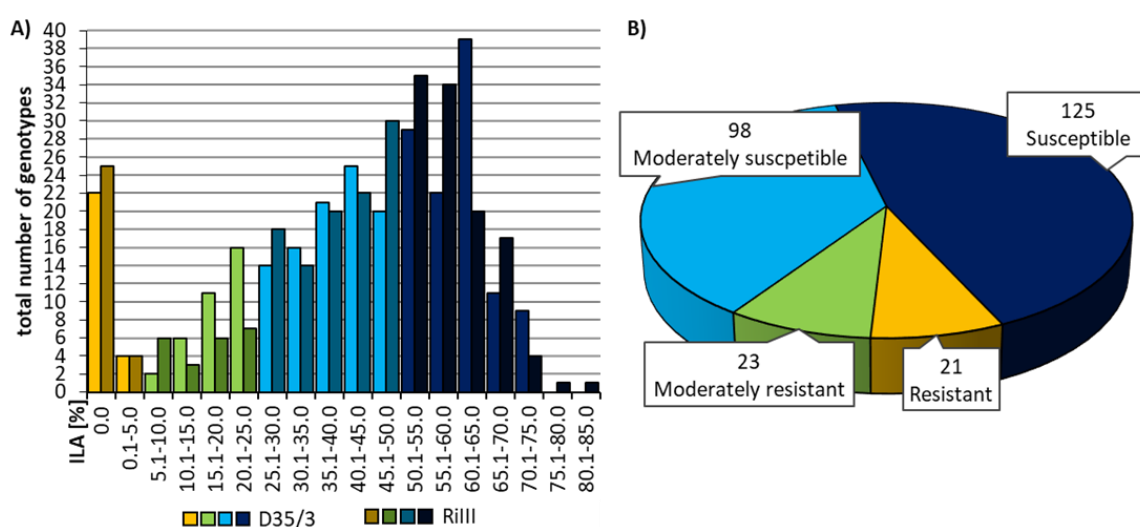


Figure R 3: Distribution of the 267 selected Whealbi genotypes in regard of the resistance response against the powdery mildew isolates D35/3 and RiIII

A) The 267 selected genotypes were inoculated either with the isolate D35/3 (light colours) or RiIII (dark colours). The distribution of genotypes per interval is given as absolute frequency per isolate. The resistance responses were determined on the basis of the macroscopically visible disease symptoms as mean values of the infected leaf area [ILA in %]. The results represent at least three biological replicates per genotype and the classification into resistance classes (Table M 3) is visualized with colours.

B) The 267 selected genotypes were grouped into the defined resistance classes (Table M 3) according to the mean values of the infected leaf area (%) for the *Max* trait. The given numbers represent the absolute frequency of genotypes per resistance class.

The further evaluation of the resistance of the selected genotypes against the German powdery mildew isolate D35/3 and the Danish isolate RiIII (JKI-75) was quantified in a detached seedling leaf assay (independent experiments: $n \geq 3$). These two isolates were selected because of their

poly-virulent nature (Table M 2). In this sense, both isolates have overcome together, 22 known major resistance (*R*)-genes/resistance specificities (data provided by the Julius Kühn Institute (JKI), 2019). Moreover, the high virulence of both isolates is also reflected by the negatively skewed genotypic distributions of the infected leaf area (Figure R 3A). In this respect, more genotypes were determined as moderately susceptible or susceptible than as (moderately) resistant. Nevertheless, more than 20 lines were completely resistant against at least one of the powdery mildew isolates. An artificial maximal infection (*Max* trait) was generated *in silico* by the selection of the higher disease score from both isolates. The distribution of the 267 genotypes per assigned resistance classes (Table M 3) was determined in regard of the *Max* trait (Figure R 3B). These results (Table B 2) represent indeed the artificial 'super-virulence' (Table M 2) of the *in silico* trait, because almost half of the population was determined as susceptible and only 7.9 % and 8.6 % of the genotypes were classified as resistant or moderately resistant, respectively.

3.2.2. Association of the adult plant resistance under natural powdery mildew infection and the determined seedling resistance based on detached leaves

Because of the focus of this study on race-nonspecific resistance, which is sometimes also referred as 'field' or 'adult plant' resistance (Niks *et al.*, 2015; Li *et al.*, 2014a), it was decided to evaluate the adult plant resistance of a subset of 100 genotypes in a field trial with natural occurring powdery mildew infection. The selected spring or facultative varieties (Table B 2), which span the complete range of powdery mildew susceptibility, were planted in spring 2017 at two locations (Gatersleben and Bergen/Wohlde) and the disease scoring was based on four major resistant classes (Table M 4). The genotype panel spans also under natural occurring infection the whole range of susceptibility against powdery mildew, although the majority of the varieties were again classified as susceptible (infection value >2), regardless the location (Figure R 4A and Table B 3). It seems that the infection rate in Bergen/Wohlde was higher as in Gatersleben because the predominant disease scores were 3-4 to 4 and 2-3 to 3-4, respectively. This effect could be related to the virulence of the infecting isolates or the developmental stage. The seeds were sown one week earlier in Bergen/Wohlde as in Gatersleben (Figure A 2). Moreover, the observed higher infection could be influenced by environmental conditions. The average air temperature per day and the relative humidity were similar at both locations, but more rainfall was recorded in Bergen/Wohlde (Figure A 2). Higher temperatures and arid conditions were observed particularly three weeks prior scoring. In the following two weeks, 53.4 mm and 12.7 mm rainfall was recorded in Bergen/Wohlde and Gatersleben, respectively.

To determine the association, the seedling resistance data were transformed into the same classification system that was used to assess the adult plant resistance. This step was included because it is easier to evaluate effects, when data were available in the same scale. After the

exclusion of the (race-specific) resistant genotypes, the transformed detached leaf assay data were used for the calculation of the best linear unbiased estimation (BLUE). This step was performed to minimize the effects that were caused by small changes of the experimental conditions over time. Afterwards, the 'transformed *Max BLUE*' trait was generated from the calculated BLUEs of the two isolate datasets (Table B 3). Additionally, the raw infection values of the field trials were used to calculate the BLUE value per variety to integrate both locations into one dataset (Table B 3). The relationship between the adult plant resistance and the transformed *Max BLUE* values of the detached seedling leaves was graphically visualized in Figure R 4B.

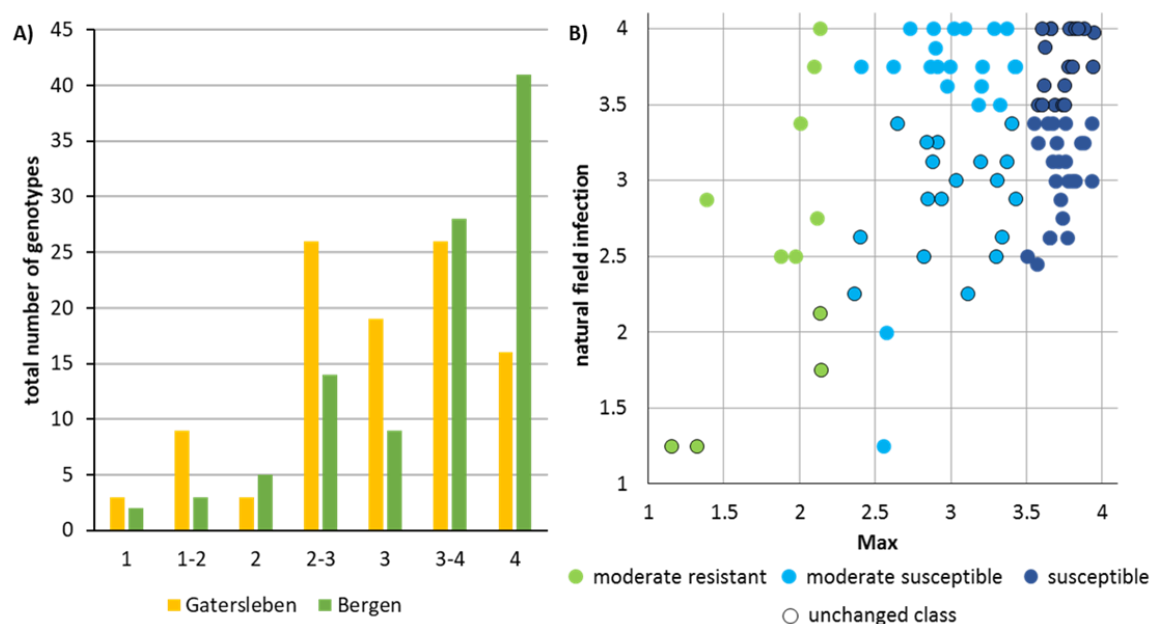


Figure R 4: Evaluation of the powdery mildew resistance of selected Whealbi genotypes under natural field infection

A) The distribution of the 100 Whealbi varieties and the control genotypes Roland and Morex under natural occurring powdery mildew infection is displayed as absolute frequency per resistance class (Table M 4) and location (Gatersleben and Bergen/ Wohlde).

B) Natural field infection of adult plants as a function of the corresponding seedling resistance data of detached leaves. The data are based on the results of 92 Whealbi varieties and the two controls. The natural field infection data represent the calculated best linear unbiased estimations (BLUEs) of the two locations. The transformed *Max BLUE* trait was generated *in silico* from the calculated BLUEs of the transformed detached leaf assay results (indicated with the colour code) by selection of the highest disease score. The encircled data points correspond to genotypes which were grouped into the same resistance class in the detached leaf assay and the field trials.

The 92 Whealbi genotypes and the control lines Morex and Roland were grouped into the resistance classes according to the transformed *Max BLUE* trait (colour code as indicated). Forty-two accessions were classified into the same resistance class by both, the detached leaf assay data and the natural infections in field trials (encircled data points in Figure R 4B). For the remaining 52 genotypes the classification changed. Five and two moderately resistant genotypes according to the seedling assay became moderately susceptible and susceptible in the field, respectively. In case of the 39 moderately susceptible genotypes, two of them proved to be more resistant and

19 of them to be more susceptible under natural occurring infection. Twenty-four of the 44 susceptible varieties were scored as moderately susceptible in the adult plant stage. Nevertheless, the detected changes in the resistance patterns of the genotypes can be caused by various factors. Besides the plant age (seedling versus adult plant resistance) and differences in the virulence of the powdery mildew isolates (D35/3 & RiIII versus natural infection in spring 2017), also a wide range of biotic and abiotic factors on the fields could influence the powdery mildew responses. As described above, the rainfall was three times higher in Bergen/Wohlde as in Gatersleben in the two weeks prior scoring (Figure A 2). Additionally, it has to be considered that the seedling data were generated by the evaluation of single detached leaves instead of several whole plants like in the field trials.

A high association between the two field locations could be determined by the Pearson correlation coefficient between BLUEs ($r = 0.81, p\text{-value} < 1 \times 10^{-7}$). In respect of the selection criteria of the genotypes for the field panel, a very high association was expected and observed between the seedling resistance data ($r = 0.95, p\text{-value} < 1 \times 10^{-7}$). Nevertheless, the association between the natural field infection and the transformed *Max BLUE* values of the detached leaves was only moderate ($r = 0.45, p\text{-value} = 6.11 \times 10^{-6}$). A similar association was determined between the natural field infection and the transformed data sets of the single isolates. The Pearson correlation coefficients of the natural infection and D35/3 was $r = 0.45, p\text{-value} = 5.45 \times 10^{-6}$ and for RiIII $r = 0.45, p\text{-value} = 4.27 \times 10^{-6}$, respectively. According to the coefficients of determination (R^2) 20 % of the variation of the adult plant resistance under natural infection is explained by the respective seedling resistance achieved under controlled conditions. The heritability of the natural field infection was determined as 0.87 and of the single powdery mildew isolates D35/3 and RiIII as 0.90 and 0.88, respectively. These results indicate that the variation of the powdery mildew resistance is mainly genetically determined.

3.3. Identification of known powdery mildew resistance genes in resistant varieties

In respect of the focus of this work on race-nonspecific resistance, it was decided to further assess the presence of known (race-specific) major *R*-genes/resistance specificities in the resistant genotypes. In addition, interesting (new) alleles of resistance genes might be hidden in the material. The characterization of the adult plant resistance under natural powdery mildew infection in combination with the seedling resistance data indicates that the four genotypes WB-052, WB-066, WB-400 and WB-476 were from higher interest for possible breeding applications. These four genotypes displayed in the detached leaf assays (score ≤ 2.6) as well as in the field experiments (score < 2) a good resistance and they were selected for a large isolate test to evaluate the stability/extent of the seedling resistance response. The four genotypes were

tested against 27 European powdery mildew isolates (Table M 2, A 2 and A 3) in an additional detached leaf assay performed in cooperation with the JKI, Kleinmachnow (Figure R 5 and Table B 4). The resistance response was scored as infection type on a scale from 0-4 and according to Silvar *et al.* (2011), an infection type > 2 is considered as susceptible interaction.

In respect of this threshold, the genotype WB-052 was resistant against all 27 isolates. The predominant infection type was an infection type = 1 (for 16 isolates). Moreover, the line was completely resistant (infection type = 0) against five powdery mildew isolates and moderately resistant against the remaining six isolates. The resistance spectrum of this Ethiopian landrace indicates the presence of a major *R*-gene/resistance specificity, which seems to be not common in Europe so far, because none of the 27 European powdery mildew isolates was able to successfully infect the genotype.

The prevalent infection type of WB-066 and WB-476 was also an infection type = 1 (for ten and eleven isolates, respectively). Additionally, WB-066 was completely resistant (infection type = 0) against isolate 122, but is susceptible (infection type > 2) against isolate 224 (Si1). In case of the remaining 15 isolates, the traditional cultivar/landrace is moderately resistant. Thus, the resistance spectrum of the Moroccan genotype indicates again the presence of a major *R*-gene/resistance specificity, which is not frequently used in Europe.

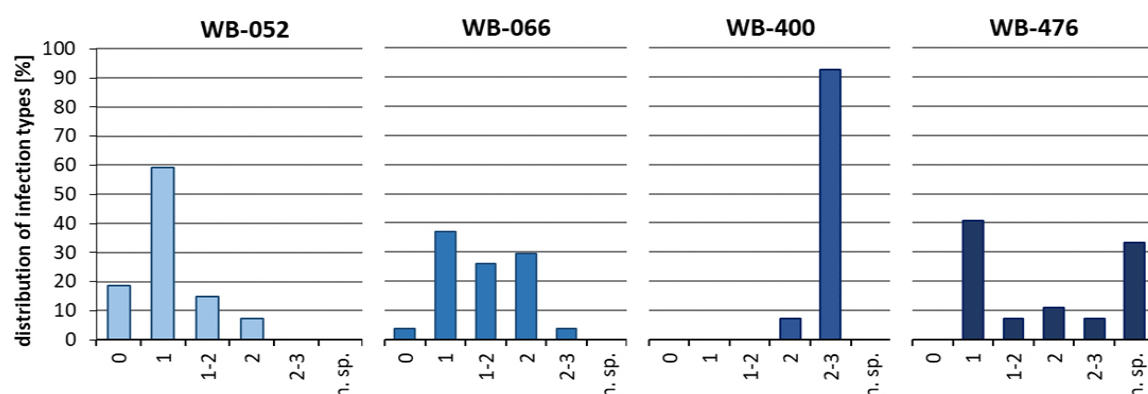


Figure R 5: Resistance response of the four indicated genotypes against 27 European powdery mildew isolates

Detached leaves of the four resistant genotypes (WB-052, WB-066, WB-400, WB-476) were infected with 27 European powdery mildew isolates. The resistance response was scored as infection type on a scale from 0-4 (0= resistant; 4=highly susceptible) and the distribution of infection types was determined as percentages for the four genotypes. The abbreviation 'n. sp.' stands for 'not specified'.

For the genotype WB-476, it is not possible to draw a valid conclusion because the results of nine isolates were inconclusive due to heterogenous responses of the tested leaf material.

The genotype WB-400 was moderately resistant against two isolates and moderately susceptible against the remaining 25 isolates. The consistent resistance spectrum of the Ethiopian landrace could be either caused by an accumulation of a range of race-nonspecific minor effect genes

(polygenic quantitative resistance) or by one or several defeated *R*-genes/resistance specificities which provide still a low level of resistance.

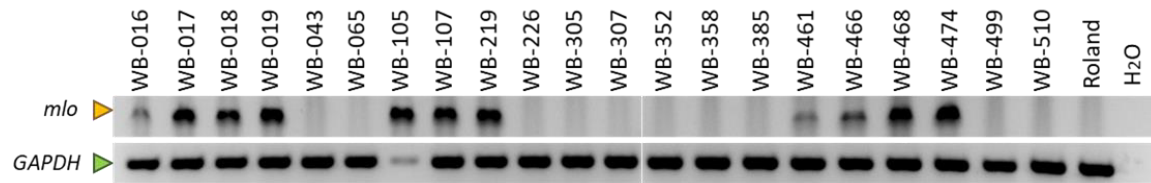


Figure R 6: Amplification test for the presence of the *mlo-11* allele in the resistant genotypes

The total leaf DNA of 21 resistant genotypes were analysed in respect to the presence of the *mlo* (*mildew resistance locus o*)-11 allele via PCR with allele-specific primers (upper panel). The expected product (1,200 base pairs, yellow arrow head) is only amplified, if this allele is present (Piffanelli *et al.*, 2004). Additionally, the DNA samples were analysed for the amplification of the house keeping gene *GAPDH* (*glyceraldehyde 3-phosphate dehydrogenase*, lower panel). The amplified fragment is 322 base pairs long (green arrow head). The DNA of the cultivar Roland and purified water were used as (negative) controls.

Besides this detailed assessment of these four genotypes, also the genotypes resistant only in the seedling stage (Figure R 3A) were analysed for the presence of known resistance genes. In respect of the resistance patterns of nine genotypes, which were resistant against only one of powdery mildew isolate (either D35/3 or RiIII), were assumed to be caused in a race-specific manner. The complete absence of disease symptoms of 21 genotypes against both powdery mildew isolates in the seedling resistance assays, hints to the presence of major effect *R*-genes/resistance specificities (St. Clair, 2010; Niks *et al.*, 2015). In particular, it hints to the race-nonspecific locus *mildew resistance locus o* (*mlo*) which is widely used in (European) spring cultivars and confers a broad-spectrum powdery mildew resistance. One of the predominant *mlo* alleles is the natural occurring *mlo-11* allele (Kusch & Panstruga, 2017). To test, if the observed resistance is based on the natural allele, the amplification of the *mlo-11* specific repeat array was analysed by PCR (polymerase-chain reaction) using genomic DNA from the 21 genotypes and specific primers designed by Piffanelli *et al.* (2004). To rule out that the absence of a PCR product is caused by poor DNA quality, an additional amplification of a short fragment from the highly conserved *glyceraldehyde 3-phosphate dehydrogenase* (*GAPDH*) was conducted. Representative gel pictures for both genes were selected from at least three technical replicates, which led to similar results (Figure R 6). The *GAPDH* fragment was amplified in all 22 lines, but the *mlo-11* specific product was only amplified from eleven genotypes. Therefore, the detected seedling resistance of these eleven genotypes (WB-016, WB-017, WB-018, WB-019, WB-105, WB-107, WB-219, WB-461, WB-466, WB-468 and WB-474) should be conferred by the *mlo-11* allele.

To evaluate if the observed resistance of ten remaining genotypes, is caused in a race-specific manner, the seedling resistance of the genotypes and the two susceptible controls Roland and Morex was assessed in response to seven additional powdery mildew isolates (Table R 1). Compared to the virulence spectra of D35/3 and RiIII (Table M 2), they have overcome nine

additional major *R*-genes/resistance specificities (Table A 2). This small isolate test was also performed as detached leaf assay and the calculated mean values and the standard deviations per genotype from three independent replications were determined (Table R 1).

Table R 1: Quantification of the seedling resistance of the indicated genotypes in response to seven powdery mildew isolates based on the development of macroscopic disease symptoms

Genotype	Powdery mildew isolates						
	CH4.8	D2/4	D4/6	D35/2	MH21	Ro93a	Si1
Morex ¹	52.8 ± 17.7 ²	57.8 ± 11.2	47.2 ± 24.5	69.4 ± 10.1	70.6 ± 16.5	45.0 ± 10.5	73.3 ± 4.3
Roland ¹	0.0 ± 0.0	0.0 ± 0.0	0.0 ± 0.0	63.7 ± 13.6	0.0 ± 0.0	26.9 ± 10.3	0.0 ± 0.0
WB-043	0.0 ± 0.0	0.0 ± 0.0	14.0 ± 15.7	43.1 ± 9.9	35.4 ± 15.1	0.0 ± 0.0	49.4 ± 10.5
WB-065	0.0 ± 0.0	0.0 ± 0.0	32.9 ± 17.0	53.4 ± 12.9	49.1 ± 8.8	0.0 ± 0.0	40.6 ± 12.7
WB-226	3.0 ± 3.5	0.0 ± 0.0	41.9 ± 24.3	58.4 ± 18.1	67.1 ± 10.4	8.2 ± 6.2	68.0 ± 10.5
WB-305	0.0 ± 0.0	12.9 ± 19.1	0.0 ± 0.0	11.5 ± 10.3	0.0 ± 0.0	0.0 ± 0.0	27.7 ± 32.0
WB-307	0.0 ± 0.0	43.1 ± 11.4	0.0 ± 0.0	6.8 ± 7.0	0.0 ± 0.0	0.0 ± 0.0	0.0 ± 0.0
WB-352	0.0 ± 0.0	0.0 ± 0.0	0.0 ± 0.0	0.0 ± 0.0	0.0 ± 0.0	0.0 ± 0.0	0.0 ± 0.0
WB-358	1.6 ± 1.9	0.0 ± 0.0	0.7 ± 1.7	3.7 ± 3.3	4.9 ± 2.6	0.0 ± 0.0	3.7 ± 2.7
WB-385	0.0 ± 0.0	0.0 ± 0.0	16.5 ± 22.8	42.4 ± 16.9	31.8 ± 14.9	0.0 ± 0.0	49.5 ± 12.8
WB-499	0.0 ± 0.0	42.1 ± 12.4	0.0 ± 0.0	5.1 ± 5.7	0.0 ± 0.0	0.0 ± 0.0	0.0 ± 0.0
WB-510	0.0 ± 0.0	0.0 ± 0.0	0.0 ± 0.0	0.0 ± 0.0	0.0 ± 0.0	0.0 ± 0.0	0.0 ± 0.0

¹ (susceptible) controls to assess the general infection quality

² normalized mean values of the infected leaf area (%) and the standard deviations from three biological replicates

As expected, the control variety Morex was susceptible against all used isolates (mean infected leaf area > 45 %). In contrast, the cultivar Roland was only susceptible against D35/2 and Ro93a, in addition to previously determined susceptibility against D35/5 and RiIII. The genotype WB-305 was moderately susceptible against the powdery mildew isolate Si1 and moderately resistant against D2/4 and D35/2. The genotypes WB-307 and WB-499 depicted similar resistance spectra. Both lines were moderately susceptible against D2/4 and moderately resistant against D35/2. The genotypes WB-043 and WB-385 display also the same resistance spectrum (moderately susceptible against D35/2, MH21 and Si1 as well as moderately resistant against D4/6). The resistance spectrum of WB-065 is highly similar to the previously described spectra of WB-043 and WB-385, but the genotype is more susceptible against D4/6 and D35/2. Moreover, the resistance spectrum of WB-226 resembles the same type. The genotype is susceptible against the same isolates (D4/6, D35/2, MH21 and Si1) and additionally it can be partially infected by CH4.8 and Ro93a. Based on these results, it can be concluded that the observed seedling resistance of these seven genotypes is caused in a race-specific manner. The test genotypes were susceptible against at least one isolate and the corresponding resistance spectra indicate the presence of common major *R*-genes or resistance specificities. In contrast, to the seven genotypes, the lines WB-352, WB-358 and WB-510 were (almost) completely resistant against all nine tested isolates. These resistance spectra resemble the one that is conferred by the race-nonspecific *mlo* locus

(Silvar *et al.*, 2011). In case of the genotype WB-510, the assumption is confirmed because WB-510 is the German cultivar Barke and the literature states the presence of the *mlo-9* allele (Silvar *et al.*, 2009). Whether WB-352 and WB-358 are actually *mlo* mutants needed further investigation.

3.4. Characterization of two putative novel natural *mlo* mutants

The genotypes WB-352 and WB-358 were resistant in the field trials as well as against the nine tested isolates. Because of the high similarity of the observed resistance spectra to the one that is conferred by the race-nonspecific *mlo* locus (Silvar *et al.*, 2011), it can be hypothesized that the two genotypes are *mlo* mutants. To test if WB-352 and WB-358 are actually *mlo* mutants, the two genotypes and the cultivars Ingrid and Ingrid BC *mlo5* were used for a *Mlo* complementation assay via particle bombardment. The resistance that is conferred by the *mlo* locus is recessive and thus it is possible to abolish the resistance of *mlo* mutants with the transient expression of a functional *Mlo* allele (Kushc & Panstruga, 2017; Spies *et al.*, 2012; Ge *et al.*, 2016). To evaluate the complementation, the susceptibility index of the four genotypes for the empty vector and the *Mlo* overexpression construct were calculated (Figure R 7).

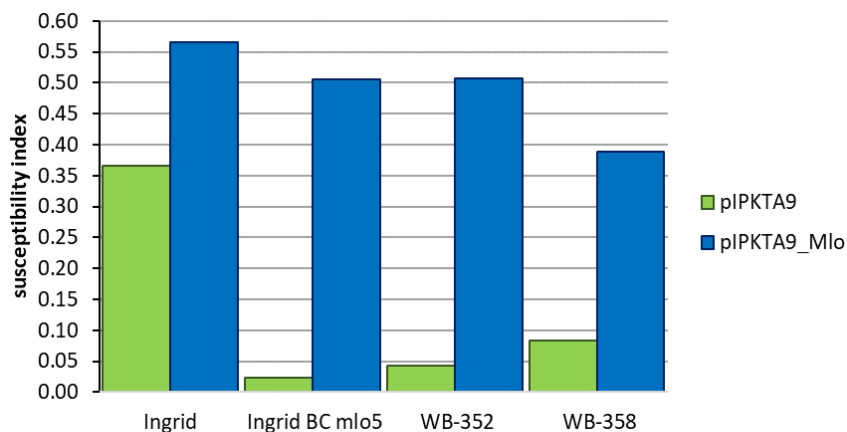


Figure R 7: Effect of the biolistic complementation of the indicated genotypes with a construct overexpressing a functional *Mlo* allele

The leaves of the control genotypes Ingrid and Ingrid BC *mlo5* as well as the putative (*mildew resistance locus o*) *mlo* mutants WB-352 and WB-358 were particle bombarded with the empty vector pIPKTA9 (green) or the *Mlo* overexpression construct pIPKTA9_Mlo (blue). The results were expressed as susceptibility index for the four genotypes and considering the average of two different bombardment experiments.

The overexpression of the *Mlo* gene in a *Mlo* wild type background under a strong constitutive promoter led to super-susceptibility (Elliott *et al.*, 2002). This effect was also observed in the control genotype Ingrid, because the susceptibility index of the *Mlo* overexpression (OX) construct is increased by a factor of 1.8 compared to the empty vector. In case of *mlo* mutants, a successful complementation is assumed if the susceptibility index is increased by a factor > 5 (Spies *et al.*, 2012). In this sense, the positive control Ingrid BC *mlo5* (enhanced susceptibility by factor > 30) and WB-352 (enhanced susceptibility by a factor > 10) are clearly complemented. The relative susceptibility index of WB-358 was increased only by a factor of 4.6. Spies *et al.* (2012) interpreted

such phenotype as partial complementation that is caused by partial functional *Mlo* alleles. In respect of this fact, WB-358 is a true *mlo* mutant. Because the complementation factor is near the threshold value, the corresponding *mlo* allele could be either partial or non-functional.

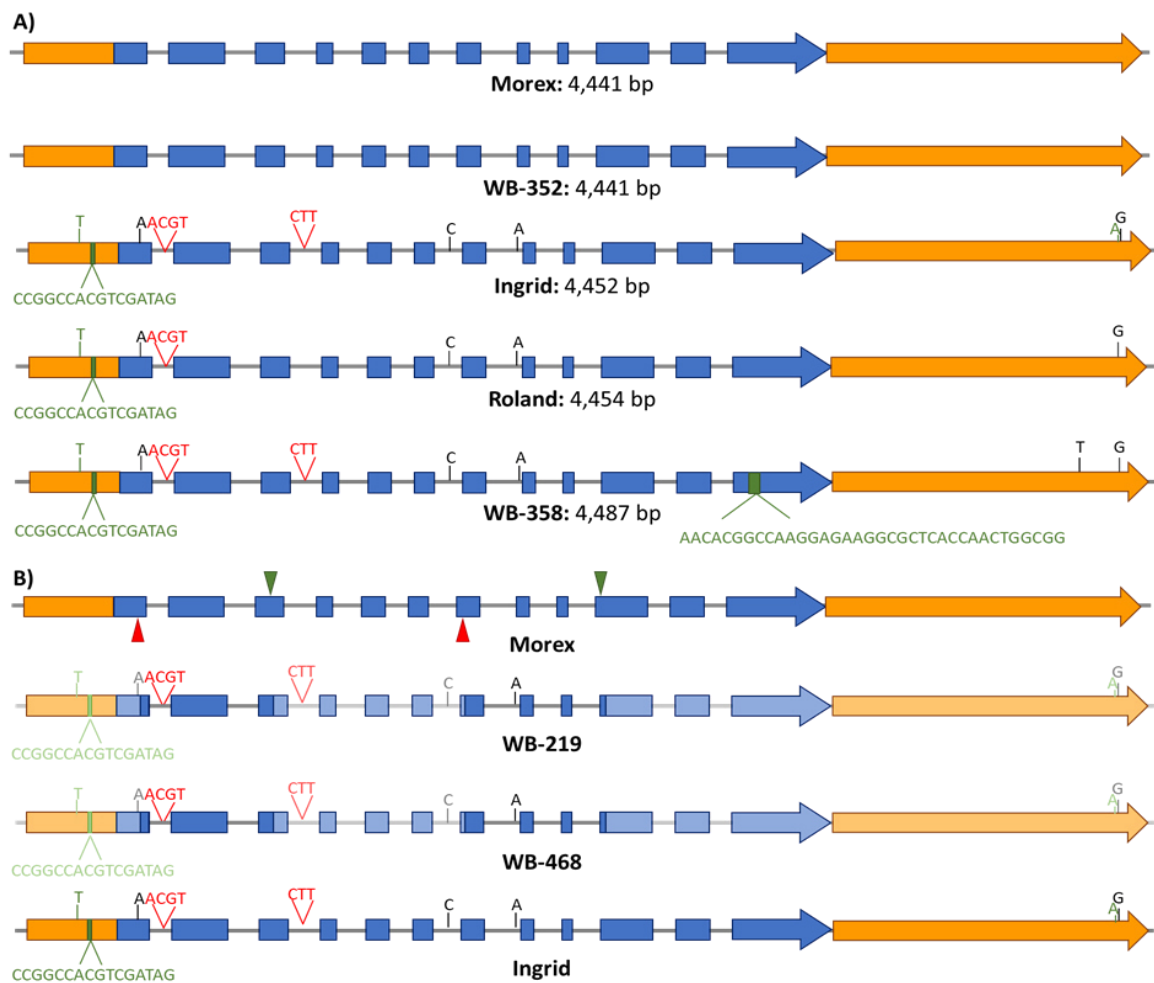


Figure R 8: Schematic representation of the *Mlo* Sanger sequencing results for the indicated genotypes

A) Sequencing results of the full-length alleles from overlapping PCR fragments (amplified from genomic DNA) with *Mlo* (*Mildew resistance locus o*) specific primers for the indicated genotypes. The sequence of the cultivar Ingrid was published before (GenBank: Y14573.1). The gene length per genotype is given in base pairs (bp). The Sanger sequencing results were represented as scheme, whereby Morex is used as reference and all indicated alterations refer to this allele. The arrow head indicate the orientation of the gene model (from 5' to 3' end). The orange box/arrow encodes for the 5' and 3' UTRs (untranslated regions); blue boxes for exons and the grey line for introns, respectively. The letters represent changed nucleotides and the following colour code was used: green – insertion, red – deletion and black – single nucleotide polymorphism (SNP).

B) The first scheme represents the reference sequence (Morex) where the binding positions of the used primer pairs are indicated as red (forward primers) and green triangles (reverse primers), respectively. The second and third scheme represent the assumed sequences of the *mlo-11* genotypes WB-219 and WB-468 in light colour shades (based on results of Piffanelli *et al.*, 2004) in comparison to the reference. The colour code is the same like indicated in **A**, and the dark shades represent the Sanger sequencing results of the present work. For a better comparability the Ingrid *Mlo* allele scheme is depicted below.

The genotypes WB-352 and WB-358 were both classified as traditional landraces with origin in Syria and Sudan, respectively. The only natural occurring *mlo* alleles are *mlo-11* and its variant

mlo-11 cnv2 (Jørgensen *et al.*, 1992; Ge *et al.*, 2016; Kusch & Panstruga, 2017). Because both landraces were tested negatively for these alleles, the presence of potential novel natural *mlo* alleles was hypothesized. To test this, the alleles from different genotypes were analysed via PCR amplification followed by Sanger sequencing. The *mlo-11* mutant was originally discovered in an Ethiopian landrace (Jørgensen *et al.*, 1976). Piffanelli *et al.* (2004) further characterized this mutation and relying on a phylogenetic tree that was based on a 25 kb long region harbouring the *Mlo* gene, they identified three distinct gene haplotypes (I-III) in cultivated accessions. The *mlo-11* genotypes were closely related to each other and form a sub-clade of haplotype I. In this respect, the cultivar Ingrid was selected for the sequencing approach because it was identified as member of the haplotype I clade and its gene coding as well as the genomic DNA sequences were available (Piffanelli *et al.*, 2004).

Additionally, to the landraces WB-352 and WB-358, the reference genotype Morex was chosen for the sequencing of the complete genomic alleles. Morex served as amplification control during the PCRs and based on the quality of the control sequence, it was possible to verify the detected polymorphisms. The Morex *Mlo* allele belongs to the haplotype III clade (Piffanelli *et al.*, 2004). It was expected that the Morex *Mlo* allele displays polymorphisms when compared to the Ingrid *Mlo* allele. Because the current reference genome is based on Morex, the genomic DNA sequence of the *Mlo* allele is public and was compared with the Morex sequence generated in the present investigation. Both sequences were identical and all changes depicted in the schemes in Figure R 8 were based on this allele (Figure R 8A, first scheme). For the second control, the cultivar Roland, no haplotype information was available. The *Mlo* allele of WB-352 is completely identical to the Morex allele (Figure R 8A, second scheme) and thus functional. In respect of the phylogenetic analysis from Piffanelli *et al.* (2004), both alleles belong to the haplotype III clade. This result confirms the negative outcome of the amplification test for the presence of the *mlo-11* allele, which belongs to the haplotype I clade. Nevertheless, the *mlo*-like phenotype of WB-352 cannot be explained by this result.

As expected, the sequence of the Ingrid *Mlo* allele displays several changes compared to the reference (Figure R 8A, third scheme). The analysis revealed that all sequence alterations occur in non-coding regions: in the 5' or 3' untranslated regions (UTRs) or in introns. The only exception was a silent single nucleotide polymorphism (SNP) in the first exon. Two SNPs were identified within intronic regions and one at 3' UTR end. In the 5' as well as in the 3' UTR, a single nucleotide insertion was detected. Additionally, 16 nucleotides were inserted in the 5' UTR while four and three nucleotides were deleted in the first and the third intron, respectively. The Roland *Mlo* allele is very similar to the Ingrid allele (Figure R 8A, fourth scheme). The former allele only lacks the three nucleotides long deletion in the third intron and the single nucleotide insertion in the

3' UTR. Based on the phylogenetic tree from Piffanelli *et al.* (2004), the Roland allele belongs to the haplotype clade I.

The *Mlo* allele of WB-358 is also highly similar to the Ingrid allele. An additional SNP in the 3' UTR and a 36 nucleotides long insertion in exon twelve were identified (Figure R 8A, fifth scheme). According to the literature, the C-terminal region encodes for a calmodulin binding motive (Kim *et al.*, 2002b). In order to prove if the insertion in exon twelve interrupts this functional domain, the predicted WB-358 protein was compared with the protein sequence from Morex via protein alignment. The detected insertion led to a non-frame shift mutation and the 12 amino acids were inserted behind residue 424. Kim *et al.* (2002b) described that the calmodulin binding motive is constituted by the residues 414-435 and thus, the insertion interrupts indeed the functional domain. Furthermore, Kim *et al.* (2002b) stated the importance of an intact calmodulin binding motive for the defensive function of *Mlo*. In respect of the partial *Mlo* complementation (Figure R 7), the corresponding aberrant WB-358 protein variant is rather less than non-functional. These results could explain also the weak *mlo* resistance phenotype (Table R 1).

Beside the full-length *Mlo* allele sequencing, a partial allele sequencing of WB-219 and WB-468 was performed (Figure R 8B). Both genotypes were positively tested for the *mlo-11* allele and based on the phylogenetic tree of Piffanelli *et al.* (2004), the corresponding alleles should be highly similar to the alleles of the haplotype I clade like Ingrid's *Mlo* allele. The two sequenced gene regions were selected because of the identified alterations in these regions in the Ingrid allele in comparison to the reference Morex. The binding positions of the used primers are indicated with red and green triangles in the first scheme of Figure R 8B. The sequencing of the first fragment of both *mlo-11* genotypes led to the identification of the same four-nucleotide long deletion that was detected in the Ingrid *Mlo* allele (Figure R 8B, second and third scheme). Moreover, the same SNP in the seventh intron, which was detected in the Ingrid *Mlo* allele, was found in both genotypes (Figure R 8B, second and third scheme). These findings support the positive results of the *mlo-11* test and are in line with the presumptions about the corresponding alleles.

The sequencing of the genomic *Mlo* alleles revealed that the presumed *mlo* mutant WB-352 harbours a functional allele, which is identical to the reference allele from Morex. This result did not explain the overserved phenotype and the complete *Mlo* complementation (Figure R 7 and Table R 1). To assess if an altered expression of the *Mlo* gene in WB-352 causes the *mlo*-like phenotype, a semi-quantitative PCR approach was performed. Besides the WB-352, the reference genotype Morex, WB-358 and Ingrid BC *mlo5* were selected for this approach based on cDNAs generated from total leaf RNA. The expression of *Mlo* and of *UBC* (*ubiquitin-conjugating enzyme 3*) of inoculated and non-inoculated samples was analysed 6 h post inoculation because

Piffanelli *et al.* (2002) described that the *Mlo* expression is highest at this time point. *UBC* is a house keeping gene with constitutive expression, which is not altered by the pathogen inoculation (Skov *et al.*, 2007).

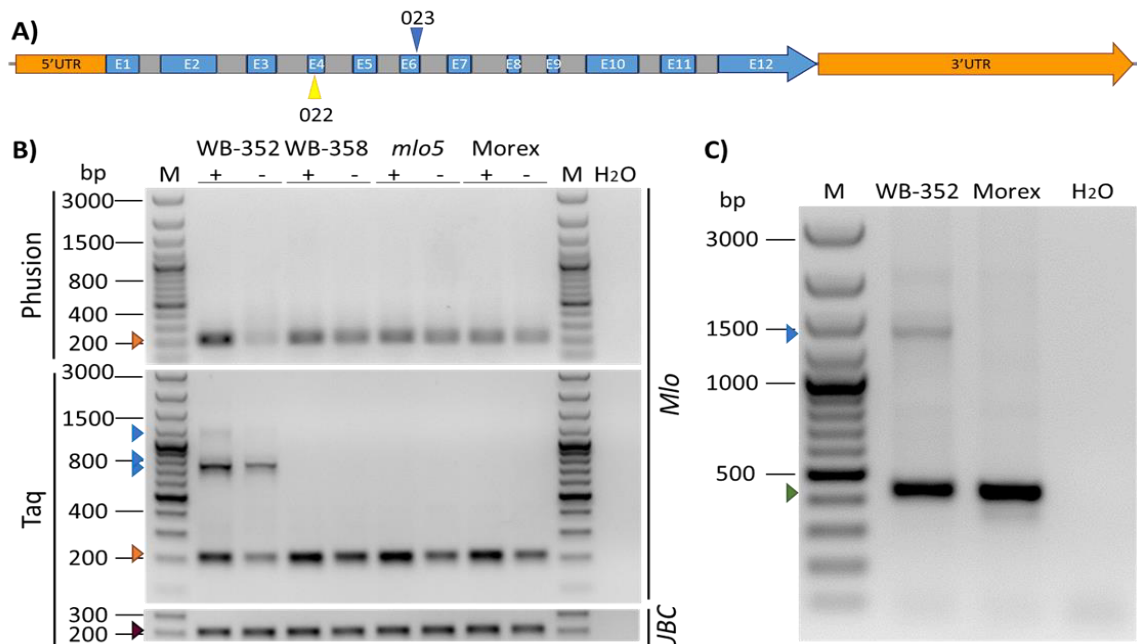


Figure R 9: Amplification of the indicated genotypes with *Mlo* or *UBC* specific primers

A) Schematic representation of the *Mlo* (*Mildew resistance locus o*) gene model. The binding positions of the selected primers (O22 and O23) are indicated with coloured triangles. The colour code is the same as in Figure R 6.

B) The cDNAs of powdery mildew inoculated (+) or non-inoculated (-) leaf samples from the four genotypes (WB-352, WB-358, Ingrid BC *mlo5* (*mlo5*) and Morex) were used for the PCR based amplification with the indicated polymerases (Phusion or Taq). The semi-quantitative PCRs were performed from three independent biological replicates with similar results and thus, a representative replicate was selected. Purified water was used as negative control during the amplification and the GeneRuler 100 bp Plus (M) was utilized as size standard. A 210 base pair (bp) long product was expected for the *Mlo* gene (orange arrow head). The amplification with the Taq-polymerase revealed three additional WB-352-specific products of the following sizes: ~750 bp, ~850 bp and ~1,200 bp (blue arrow heads). Additionally, the DNA samples were analysed for the amplification of the house keeping gene *UBC* (*ubiquitin-conjugating enzyme 3*). The expected product is 210 bp long (purple arrow head).

C) Taq-based amplification of the *Mlo* gene from genomic DNA of the genotypes WB-352 and Morex. The PCR was performed several times (>3) with similar results. Purified water was used as negative control during the amplification and the GeneRuler 100 bp Plus (M) was utilized as size standard. A 431 bp long product was expected (green arrow head). The amplification revealed one additional WB-352-specific product (~1,400 bp, blue arrow head).

In all four genotypes, the powdery mildew inoculation led to an increase of the *Mlo* transcript (Figure R 9B upper panel, comparison of the inoculated versus non-inoculated samples). In the following experiments, the same cDNA samples were examined but the cheaper Taq- instead of the Phusion-polymerase was used during amplification. This new amplification approach displayed the same *Mlo* transcript induction caused by the powdery mildew inoculation (Figure R 9B middle panel, for all genotypes). In contrast, the amplification of *UBC* revealed no changes of the transcript amounts between the inoculated and non-inoculated samples

(Figure R 9B lower panel). The altered expression patterns of *Mlo* were in accordance with the findings reported by Piffanelli *et al.* (2002). Nevertheless, *Mlo* seems to be not differentially expressed in WB-352 than in the other genotypes which still not explains its *mlo*-like phenotype. Nonetheless, the change of the polymerase resulted also in an unexpected finding. The PCRs with the Taq-polymerase led to the amplification of additional WB-352-specific fragments (Figure R 9B middle panel). The three unexpected products were much larger than the respective cDNA product of 210 base pairs (bp) or even than the genomic product of 431 bp. They were amplified in all biological replicates and their assumed sizes were: ~750 bp, ~850 bp and ~1,200 bp (blue arrow heads in Figure R 9B middle panel and B 2A).

Based on the differential product amplification of the two polymerases observed for the cDNA samples, genomic DNA samples of WB-352 and Morex were also used for a PCR with the Taq-polymerase (Figure R 9C). The Taq based amplification led, beside the expected genomic *Mlo* product of 431 bp (green arrow head), to the identification of a much larger WB-352-specific product (~ 1,400 bp, blue arrow head). In contrast to *Arabidopsis*, barley possesses only one *Mlo* gene (Kusch & Panstruga, 2017), but the current results indicate the presence of a (partial) duplicate of the *Mlo* gene in the genome of WB-352, which seems to be transcribed. These findings resemble the *mlo-11* mutation that is also characterized by the presence of a partial duplication in form of a repeat array (Piffanelli *et al.*, 2004). This repeat array seems to interfere with the transcription of the functional *Mlo* copy, which led to a reduced transcript level (Peterhänsel & Lahaye, 2005). Under the assumption, that the partial *Mlo* duplicate of WB-352 also interferes with the transcription of the functional *Mlo* copy, a further characterization of the presumed duplicate was performed.

The duplicate cannot be an exact gene copy because the amplified products were larger than the expected *Mlo* products. To determine the duplicate length, several PCRs with different primer combinations were performed (Figure R 10 and B 2A). The data suggest that a large part of the *Mlo* gene is duplicated in WB-352 because all primer combinations that were located between first and the eighth exon of the *Mlo* gene led to the amplification of the additional aberrant products. As example, four additional cDNA products (~1,300 bp, ~1,700 bp, ~2,400 bp and ~3,000 bp) were amplified with the primer combination 003b/008 and all products were larger than the expected one of 722 bp (Figure R 10B). Particularly, the ~ 1,300 bp product seems to be more abundant than the expected product. This could hint to an altered transcript level of the functional *Mlo* allele which was not recognized in the semi-quantitative PCR but could explain the *mlo*-like phenotype. Nevertheless, this apparent transcript reduction was observed only in part of the performed amplifications. The amplification of genomic WB-352 DNA with the primer combination 003b/008 led also to several products. Besides the expected product of 1,555 bp,

one larger product (~3,000 bp) and two much shorter products (~200 bp, ~350 bp) were generated (Figure R 10B).

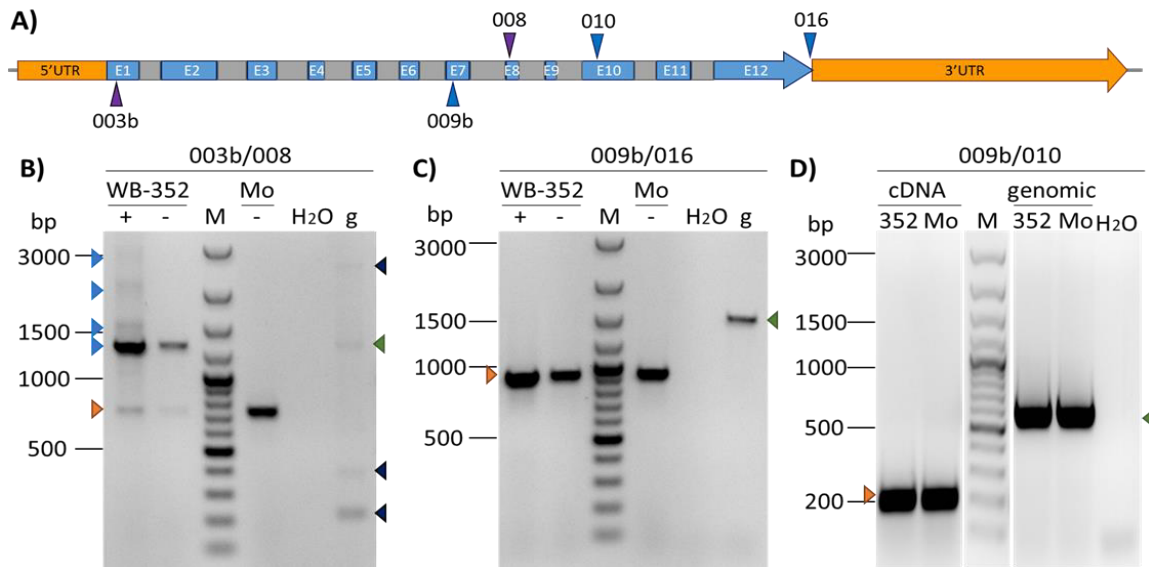


Figure R 10: Determination of the length of the presumed WB-352-specific *Mlo* duplicate

A) Schematic representation of the *Mlo* (*Mildew resistance locus o*) gene model. The binding positions of the selected primers (003b, 008, 009b, 010 and 016) are indicated with triangles. The colour code is the same as in Figure R 6.

B) The cDNAs of powdery mildew inoculated (+) or non-inoculated (-) leaf samples from WB-352 and Morex were used for the PCR based amplification (primer combination 003b/008) with the Taq polymerase. The PCRs (primer combinations 003b/008 and 009b/016) were performed from three independent biological replicates with similar results and thus, the gel pictures from one representative replicate were selected. Purified water was used as negative control during the amplification and the GeneRuler 100 bp Plus (M) was utilized as size standard. A 722 base pair (bp) long product was expected for the *Mlo* gene (orange arrow head). The amplification on cDNA of inoculated WB-352 leaves revealed four additional genotype-specific products of the following sizes: ~1,300 bp, ~1,700 bp, ~2,400 bp and ~3,000 bp (light blue arrow heads). In the non-inoculated sample only one additional fragment was amplified (~1,300 bp, light blue arrow heads). The amplification of genomic DNA of WB-352 revealed, beside the expected product (1,555 bp, green arrow head), three additional products (~200 bp, ~350 bp and ~3,000 bp, dark blue arrow heads).

C) The same cDNAs were used for a PCR with the primer combination 009b/016. In all samples only the expected products were amplified. The expected cDNA product is 915 bp long (orange arrow head) and the expected genomic product is 1,478 bp long (green arrow head).

D) The powdery mildew inoculated cDNA samples of WB-352 (352) and Morex (Mo), as well as the genomic DNAs of the two genotypes were used for a PCR with the primer combination 009b/010. Purified water was used as negative control during the amplification and the GeneRuler 100 bp Plus (M) was utilized as size standard. In all samples only the expected products were amplified. The expected cDNA product is 213 bp long (orange arrow head) and the expected genomic product is 588 bp long (green arrow head).

Because the 5'UTR length varied over time for the different annotated *Mlo* gene models, primers located at the 5'UTR were presumably unsuited to determine the begin of the predicted duplicate, in particular for the amplification on cDNA. In contrast, the end of the aberrant products was narrowed down. The PCRs with the primer combination 009b/016 and 009b/010 led to no amplification of additional WB-352-specific products neither on cDNA samples nor on genomic

DNA (Figure R 10C-D). It is possible that the duplicate is constituted by the repeated sequence of the first eight exons alone or in addition to the unchanged sequence for the rest of the gene. So far, this hypothesis was not addressed because it is not possible to amplify the full-length genomic *Mlo* gene with the Taq-polymerase. The generated product would be too long (> 4,000 bp). Nonetheless, a change of the polymerase could be problematic. In regard of the presented differential amplification of the Phusion- and the Taq-polymerase, it would be necessary to test several enzymes, which was not done so far.

In all performed PCRs with primers located between the first and the eighth exon, several products were amplified. These amplified products have variable sizes and such pattern indicates that the primer sequences were repeated several times and that the intermediate sequences varied in their length. To prove this hypothesis, the most prominent aberrant WB-352-specific products were gel purified and used for Sanger sequencing. In this respect, sequences from the additional genomic product generated with the primer combination 022/023 (~1,400 bp) and from the cDNA products generated with the primer combinations 022/023 (~750 bp) and 003b/008 (~1,300 bp), were obtained, respectively. In the first step, the purified PCR products were sequenced with the two primers that were used for the amplification and based on the attained results, the products generated with the primer combination 022/023 were re-sequenced with the primers 005 and 004. All obtained sequences were used for the attempt to determine the underlying structure of the presumed repeat array (Figure R 11).

The annotated *Mlo* gene model and the binding positions of important primers (coloured triangles) are represented as scheme (Figure R 11A). The sequencing results of the genomic fragment revealed that the WB-352-specific product was indeed amplified from a second *Mlo*-like gene structure. Furthermore, the obtained sequences imply the presence of two highly similar PCR products with an expected length of 1,336 bp and 1,338 bp, which corresponds to the assumed size of the gel-purified PCR product (~1,400 bp). These products differ from each other only in a variable region of about 180 nucleotides. In the first hypothetical version (Figure R 11A, lower left scheme), the sequence of primer 006 is incomplete and directly followed by the last 59 nucleotides of the first *Mlo* intron. The remaining product sequence displayed the annotated *Mlo* intron-exon structure. In case of the second hypothetical version (Figure R 11A, lower right scheme), the primer sequence 006 is complete and followed by the expected sequence of the fifth intron. The primer 023 is located at the end of the sixth exon and its sequence could be also detected completely. Nevertheless, based on the sequencing results, the product did not end at this point. Instead, the 023 sequence is directly followed by the last 96 nucleotides of the second *Mlo* exon. The remaining product sequence displayed again the annotated *Mlo* intron-exon

structure. These results support the hypothesized (partial) duplication of the *Mlo* gene and also the presumed repeat array structure of that duplication.

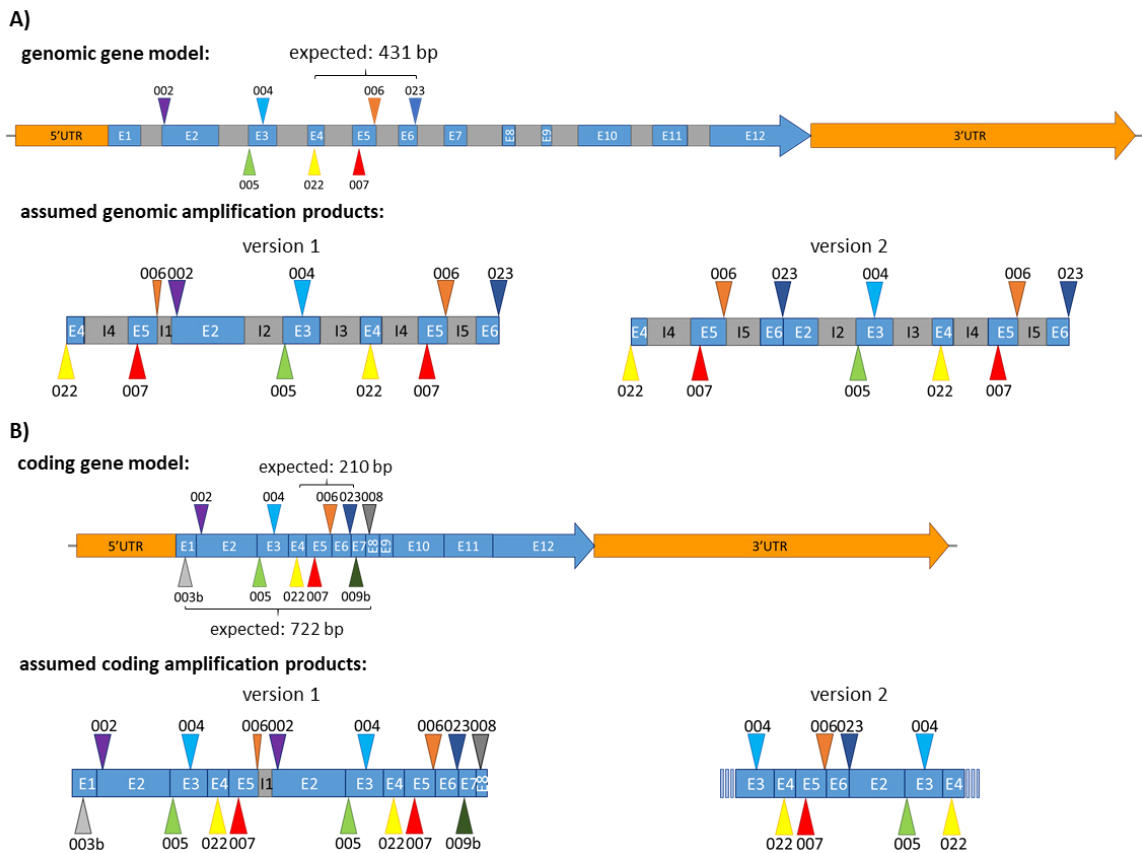


Figure R 11: Schematic representation of the Sanger sequencing results of the WB-352-specific *Mlo* amplification products

A) The upper scheme represents the genomic gene model of *Mlo* (*Mildew resistance locus o*). The binding positions of important primers are indicated by the coloured triangles. The expected product of the primer combination 022/023 is 431 base pairs (bp) long and it is indicated by the bracket. The lower two schemes denote the genomic amplification products that were hypothesized on the basis of the sequencing results of the primers 004, 005, 022 and 023. The blue boxes represent the exons and the grey boxes the introns with the indicated numbers, respectively.

B) The upper scheme represents the coding gene model of *Mlo* and the lower schemes of the hypothesized cDNA amplification products. The expected amplification products of the primer combination 022/023 (210 bp) and 003b/008 (722 bp) were indicated by brackets. Otherwise, the used labelling is the same as described in **A**). The primers 003b, 004, 005, 008, 022 and 023 were selected for the sequencing.

The sequences of the primers 022 and 023 that were used for the generation of the products were also sequenced within the aberrant fragments of WB-352. It was not possible to determine in which way the presumed products display distinct regions within the hypothesized duplicate or if they overlap in their identical sequence regions. For example, the end of version 1 and the begin of version 2 could represent the same region of the duplicate. This alternative product has an expected length of 2,243 nucleotides. Nonetheless, and despite several independent repetitions,

the current PCR results could not disentangle if this kind of product does actually exist or not (Figure R 9C).

As mentioned before, the present results indicate that the hypothesized *Mlo* duplicate in WB-352 is transcribed because aberrant products could be amplified on cDNA samples (Figure R 9B and 10B). The most prominent aberrant products were Sanger sequenced (Figure R 11B). The upper scheme represents the coding region of the *Mlo* gene and the binding positions of important primers as coloured triangles. The obtained sequences imply the presence of PCR products (Figure R 11B, lower left scheme) with an expected length of 1,256 bp (003b/008) and 744 bp (022/023), which corresponds to the presumed sizes of the gel-purified PCR products (~1,300 bp and ~750 bp, respectively). The obtained sequence corresponds to the spliced variant of version 1 from the genomic products, which was prolonged at the end by the expected *Mlo* sequences. The results indicate again a sequence, where the primer sequence 006 is incomplete and directly followed by the remaining 59 nucleotides of intron one of the *Mlo* gene. This part was the only sequence corresponding to an intronic region, otherwise the transcripts of the hypothesized *Mlo* duplicate seem to be correctly spliced. Additionally, the sequencing of the PCR product generated with the primer combination 022/023 hints to the presence of a second variant. Its sequence corresponds to the correctly spliced variant of the second genomic version (correct end of the sixth exon followed by the last 96 nucleotides of the second exon, Figure R 11B, lower right scheme). It was not possible to determine the complete product sequence (indicated by the light-coloured boxes Figure R 11B, lower right scheme). Only 640 bp of the expected ~750 bp fragment could be explained by the sequencing results.

In summary, the results of the *Mlo* complementation assay imply that WB-352 is actually a *mlo* mutant (Figure R 7). In particular, the reduced transcript level of the functional *Mlo* allele (Figure R 10B) could explain the mutant phenotype. It is possible that this reduced transcript level is related to the expression of the apparent (partial) duplication of the *Mlo* gene in WB-352. This hypothesis is based on similarities between the here present potential *mlo* mutant and the *mlo-11* mutant. In case of the *mlo-11* mutant, the transcription of the *mlo-11* specific repeat array upstream of the functional *Mlo* allele led to a reduction/abolishment of its functional *Mlo* transcript based transcriptional interference (Piffanelli *et al.*, 2004; Peterhänsel & Lahaye, 2005). To specify this hypothesis, the WB-352 specific *Mlo* duplicate/paralog was characterized in more detail. It is constituted by (at least) the first eight exons of the *Mlo* gene and in respect of the numerous PCR fragments with different sizes, these exons seem to be repeated several times, probably in varying order. It was assumed that two different 'junctions' of these repeats were sequenced because of the high identity of the obtained products that varied only in a region of about 180 nucleotides. The identical fragment regions could represent the same genomic region.

Furthermore, the results imply that the additional *Mlo* copy is expressed and that the transcripts were spliced. Based on the semi-quantitative PCRs with the primer combination 003b/008, the expected *Mlo* transcript is reduced and the amount of the aberrant *Mlo* transcript seems to be elevated (Figure R 10B). In particular, this observation could explain the *mlo*-like phenotype of WB-352 because the transcripts of the presumed repeat array should be less or non-functional. In case of the different primer combinations located within the first eight exons, this effect was not detected (for example 022/023, Figure R 9B). Nevertheless, the obtained sequencing results explain this circumstance because it is possible to amplify the expected as well as aberrant products from the hypothesized *Mlo* duplicate transcripts. If the WB-352 specific *Mlo* duplicate/paralog is actually causing the *mlo*-like phenotype by the same or a similar mechanism as described for the *mlo-11* mutant needs still further investigation. In particular, the location of the WB-352 duplicate/paralog could further illuminate the possible mechanism.

3.5. Identification of candidate genes involved in powdery mildew resistance based on a genome-wide-association study

To identify new race-nonspecific resistance genes or new alleles of known genes, a genome-wide-association study (GWAS) is a promising approach (Bartoli & Roux, 2017, Bengtsson *et al.*, 2017). The basis for the study's GWAS is built by the reported powdery mildew resistance data and the exome capture data (Bustos-Korts *et al.*, accepted) of 267 and 403 Whealbi genotypes, respectively. This led to an overlap of 220 lines, where phenotype as well as single nucleotide polymorphisms (SNPs) data were available. Because of the focus on race-nonspecific resistance, the 13 known *mlo* carriers and six genotypes identified as carrier of race-specific major *R*-genes/resistance specificities were excluded from the analysis to prevent the detection of the corresponding peaks. BLUEs and variance components for the two isolates were obtained using linear mixed models. Additionally, the repeatability and the heritability for the two isolate datasets were derived from the estimated variance components (Figure B 3). The repeatability of the 22 sub-experiments infected with the powdery mildew isolate D35/3 varied between 0.65-0.95 and the heritability was determined as 0.88. In case of powdery mildew isolate RiIII, the repeatability of the 15 sub-experiments varied between 0.70-0.93 and the heritability was determined as 0.87, respectively. The results indicate a high reproducibility of the phenotypic data and that a high percentage of the phenotypic variation was genetically determined. Moreover, the artificial maximal infection (*Max*) was determined *in silico* by the selection of the higher infection value from the two isolate data sets. Hereafter, *Max* refers always to the trait generated by the BLUE values. It was expected that the *Max* trait could reduce the detection of race-specific associations. The genotype data from the 201 lines were filtered again for a minor allele frequency of 5 % and the GWAS was performed using a linear mixed model approach that considers a kinship

matrix for the correction of population/family structure. According to the computed Rogers' distances, there is a small subpopulation of 28 genotypes (Table B 2) that are genetically closer to each other as compared to the rest of the genotypes in the whole population (Figure B 4). The majority (75 %) of the genotypes of this subpopulation originate from South East Asia. The average and the standard deviation of the infected leaf area of the subpopulation (46.0 ± 20.3 %) is almost identical to the average of the whole population (45.4 ± 19.4 %). In this sense, no difference on the powdery mildew resistance could be detected regarding the population structure. Additionally, the effect of the population structure on the GWAS power was assessed. The associations between the genetic distance matrix and the phenotypic distance matrices of the three traits (*Max* trait and the single isolates RiIII and D35/3) were calculated. On the basis of their small magnitudes ($r_{Max} = 0.19$, $r_{RiIII} = 0.15$, $r_{D35/3} = 0.13$) only a marginal impact is expected.

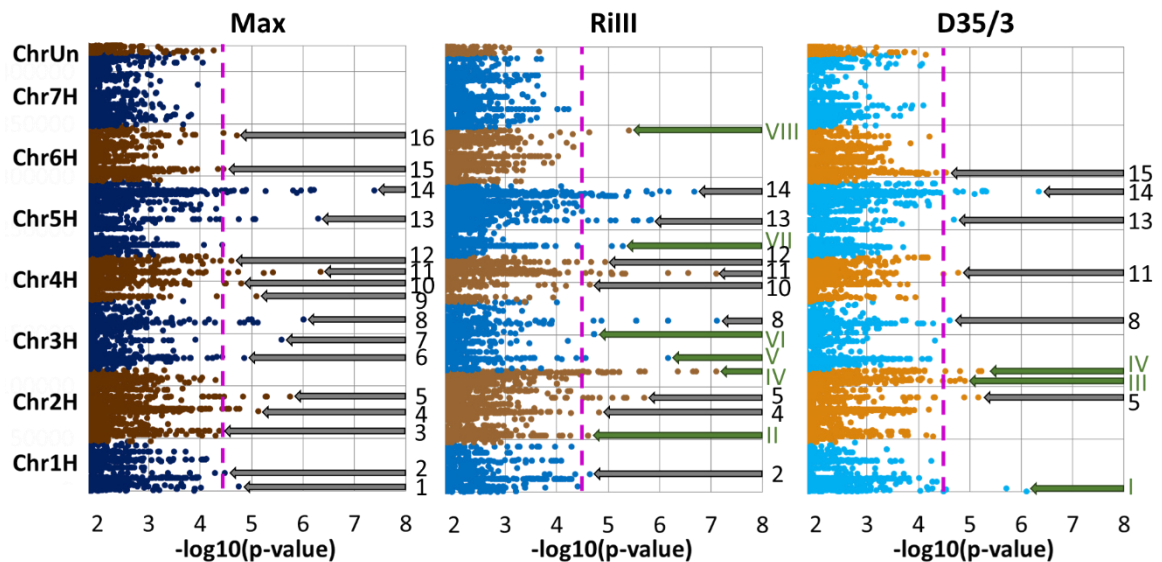


Figure R 12: Manhattan plots of the $-\log_{10}$ -transformed p-values for the three traits (*Max*, RiIII and D35/3)

Only the $-\log_{10}(\text{p-value}) > 2$ were displayed and the significance threshold of $-\log_{10}(\text{p-value}) = 4.45$ is depicted as pink dotted line. The sixteen hypothetical race-nonspecific loci were labelled with grey errors and numerical digits. The hypothetical race-specific loci were highlighted by green errors and Roman numerals. If a locus is present in more than one trait, the same digit is used.

The linear mixed model was fitted at each of the 424,567 selected SNP positions and the p-values of marker-trait associations are presented as Manhattan plots for each of the three traits (*Max*, RiIII and D35/3, Figure R 12). To control the genome-wide multiple-test Type I error, the significance threshold was estimated based on the effective number of independent tests ($n = 1,414$) for a significance level of 5 % according to Gao *et al.* (2008). In this respect, SNPs having a $-\log_{10}(\text{p-value}) \geq 4.45$ were considered as significant (Table B 5). The sixteen numbered loci from the *Max* trait were considered as race-nonspecific. They are distributed over the chromosomes 1H to 6H (Figure R 12, grey errors). In total, five of the 16 loci (5, 8, 11, 13 and 14) were present

in all three traits. The locus 15 is present in the *Max* and the D35/3 trait, but absent in the RiIII trait. In contrast, the loci 2, 4, 10, and 12 were present in the RiIII and the *Max* trait, but absent in the D35/3 trait. All SNPs that were only significant in the D35/3 or RiIII trait were treated as potential race-specific associations (Figure R 12, green errors). Three potential race-specific loci were identified for D35/3 whereas this number increased to six loci in case of RiIII. The locus IV on chromosome 2H has significant associations for D35/3 as well as RiIII, but has no significant effect in the *Max* trait. This fact indicates that the peak of D35/3 and of RiIII could be caused by a race-specific resistance gene and it supports the hypothesis that race-specific effects were reduced in the *Max* trait. Moreover, the previous identification of two candidates of a race-specific resistance gene that were located within locus IV (Hoseinzadeh *et al.*, 2019) also supports this hypothesis.

The reduced detection of already known resistance genes by means of the meta-analysis was evaluated. The analysis of the *Mlo* locus on chromosome 4H revealed that none of the 77 SNPs, which were located within or in proximity of the gene (2.6 kb up- or downstream of the gene), were significant. On the other hand, the analysis of the potential *Mla* locus (*RGH1bcd*) on chromosome 1H revealed that only 33 SNPs were located within or in the surrounding of the locus (20 kb downstream and 4 kb upstream of the gene). Nevertheless, none of the SNPs was significantly associated.

Table R 2: Overview of the 33 identified candidate genes

Candidate	Gene-ID ¹	Position ²	Chr ³	Numbers of SNPs		
				total	significant	Alleles ⁴
WB-CG_1	HORVU1Hr1G003530	7841384-7848784	1H	64	1	2
WB-CG_2	HORVU1Hr1G044590	324183366-324191923	1H	9	1	2
WB-CG_3	HORVU2Hr1G064440	437374076-437376773	2H	19	1	2
WB-CG_4	HORVU2Hr1G072510	520255665-520255964	2H	2	1	2
WB-CG_5	HORVU2Hr1G095410	669741409-669745252	2H	12	4	4
WB-CG_6*	HORVU3Hr1G013300	28687216-28698803	3H	37	1	2
WB-CG_7*	HORVU3Hr1G064390	491376493-491383553	3H	8	1	2
WB-CG_8*	HORVU3Hr1G088110	623728863-623759727	3H	26	3	2
WB-CG_9	HORVU3Hr1G088120	623761065-623762908	3H	18	1	2
WB-CG_10	HORVU3Hr1G092280	637688729-637689337	3H	12	1	2
WB-CG_11*	HORVU4Hr1G005530	12461885-12465023	4H	48	1	2
WB-CG_12	HORVU4Hr1G051290	420307747-420310209	4H	7	1	2
WB-CG_13*	HORVU4Hr1G070630	577036452-577041335	4H	17	1	2
WB-CG_14*	HORVU4Hr1G071250	580092261-580097067	4H	24	1	2
WB-CG_15	HORVU4Hr1G071290	580171165-580174500	4H	14	1	2
WB-CG_16	HORVU4Hr1G085960	633040947-633043196	4H	13	1	2
WB-CG_17*	HORVU5Hr1G078000	554454779-554457103	5H	16	1	2
WB-CG_18	HORVU5Hr1G078100	554458843-554463859	5H	79	2	2
WB-CG_19*	HORVU5Hr1G078330	554737443-554738375	5H	18	1	2
WB-CG_20*	HORVU5Hr1G114400	643787096-643795670	5H	13	1	2

Table R 2 (continued)

Candidate	Gene-ID ¹	Position ²	Chr ³	Numbers of SNPs		
				total	significant	Alleles ⁴
WB-CG_21	HORVU5Hr1G115160	645842910-645846424	5H	27	1	2
WB-CG_22	HORVU5Hr1G116810	649183282-649184450	5H	5	1	2
WB-CG_23*	HORVU5Hr1G116860	649208466-649212390	5H	18	1	2
WB-CG_24	HORVU5Hr1G116890	649379862-649380963	5H	15	1	2
WB-CG_25	HORVU5Hr1G117600	650944272-650946995	5H	17	3	2
WB-CG_26	HORVU5Hr1G117610	650950839-650956876	5H	44	1	2
WB-CG_27	HORVU5Hr1G117630	650970593-650971965	5H	11	1	2
WB-CG_28*	HORVU5Hr1G117650	650973514-650980482	5H	27	2	2
WB-CG_29	HORVU5Hr1G117670	650997747-650999529	5H	24	1	2
WB-CG_30	HORVU5Hr1G117690	651046705-651052934	5H	67	5	2
WB-CG_31*	HORVU5Hr1G117970	651513461-651520020	5H	54	5	2
WB-CG_32	HORVU6Hr1G086670	561925344-561927935	5H	9	1	2
WB-CG_33	HORVU6Hr1G089250	568471257-568476880	5H	31	1	2

¹ current annotation in Morex (2017)

² physical gene position in the reference genome

³ corresponding chromosome number

⁴ total number of defined alleles

* candidate genes with confirmed annotation and selected for allele amplification

Within the 16 identified loci, 70 SNPs were considered as significant and they were analysed for linkage disequilibrium (LD, measured as r^2) with free the software TASSEL 5 (Figure B 5). The significant SNPs that were located in the same locus, were usually in strong disequilibrium to each other ($r^2 \geq 0.7$). Causes for non-random associations among these markers could be a functional correlation, the close proximity (physical linkage) and the genetic relatedness of the genotypes. Furthermore, the analysis revealed that also the significant SNPs from different chromosomes are in disequilibrium to each other ($r^2 = 0.1-0.6$). In particular, the significant SNPs of the chromosomes 1H, 3H, 4H and 5H seem to be linked. Further possible causes for the observed non-random associations could be: genetic drift and co-selection of different loci.

The 70 significant SNPs of the *Max* trait were selected for the determination of candidate genes. In total, 50 SNPs were located within 33 annotated gene models of the current reference genome (Mascher *et al.*, 2017, Table R 2).

3.6. Evaluation of the identified candidate genes involved in powdery mildew resistance based on *in silico* and *in vitro* analyses

3.6.1. *In silico* determination of alleles of the identified candidate genes

Valuable information about candidate gene functions can be provided by the assessment of different alleles. In this respect, the allele status of the 33 candidates was determined. The used barley collection was assembled to represent the most relevant genetic diversity for European agriculture (<https://www.wheatbi.eu/plant-diversity/key-facts/>) and it was hypothesized that the candidate genes occurred in different alleles. All significant SNPs of the *Max* trait that were

located within the respective annotated gene model, were selected to define the alleles because SNPs can be inherited in specific clusters due to genetic linkage (Flint-Garcia *et al.*, 2003, Table R 2 and B 7). In the majority of the candidate genes, only one SNP was determined as significant and because of this, only two alleles were possible (Table R 2). In seven candidates more than one significant SNP was detected, but with the exception of WB-CG_5, they also defined only two alleles. The LD plot (Figure B 5) revealed that these significant SNPs were in complete LD with each other ($r^2 = 1$). In case of WB-CG_5, four alleles could be defined (Table R 2). Nevertheless, two of these alleles were rare alleles (Table B 7). The allele 2 was detected only in WB-042, WB-048, WB-130 and WB-133. All four moderately susceptible genotypes belong to the detected Asian sub-population. Additionally, this allele was present in the susceptible genotype WB-327. The allele 3 was present only in WB-501 (a susceptible member of the sub-population). These four significant SNPs were in strong LD to each other ($r^2 = 0.8-0.9$, Figure B 5).

An analysis of the abundance of the alleles revealed that one allele was always predominant in the population, which is hereafter usually referred as major allele. In analogy, the less abundant allele is referred as minor allele. In the majority of the candidate gene, the minor allele was observed in 5-14 % of the genotypes. The candidates WB-CG_401, WB-CG_404, WB-CG_405 and WB-CG_504 build an exception because their minor alleles were present in 20-40 % of the genotypes.

For the further work, it was necessary to confirm the annotated gene models. The 'blastn' analysis identified at least one related gene in *Aegilops tauschii* subsp. *tauschii* or *Brachypodium distachyon* for 31 of the candidate genes. The sequences of these predicted genes (Table B 6) were compared with the annotated gene models. This allowed the confirmation of important gene structure features such as the start and stop codons of the candidates. Moreover, cDNA clones and expressed sequence tags (ESTs) from barley (Table B 6), that correlate with the curated gene models presented here, were searched in order to minimize the risks of the detection of pseudogenes. Twelve candidate genes fulfilled these criteria (Table R 2).

3.6.2. Expression and amplification of the defined candidate alleles in various genotypes

To functionally validate the most promising candidates, they should be either transiently silenced or overexpressed. For the overexpression approach, the genomic full-length alleles were used to capture the significant SNPs that were mainly located in non-coding regions (introns or UTRs). For the twelve candidates, which were selected for the allele amplification, two alleles were defined (Table R 2). For the amplification of the major allele of all candidates, the reference genotype Morex was used because the primer design was based on its sequence and it is susceptible against powdery mildew. To amplify the minor allele, several (resistant) genotypes were tested, but only

one representative variety per candidate gene was selected (Figure B 6A). Because full-length alleles were the target, it was not possible to design primers that were unique for the respective candidate gene. In order to maximize the chance to amplify the candidate in various genotypes, conserved regions were specifically selected for the primer design. Nevertheless, this approach led to the amplification of related sequences of all candidates, except WB-CG_28. In case of six candidates (WB-CG_8, WB-CG_11, WB-CG_17, WB-CG_19, WB-CG_23 and WB-CG_28), a product of the expected size was amplified for both alleles (Figure B 6A, red asterisk). In contrast, none of the expected products was amplified under various conditions for the remaining six candidate genes, not even in the reference genotype Morex (Figure B 6A).

In respect of the planned silencing approach, it was necessary to determine if the six selected candidate genes were expressed. To design specific primers, the si-Fi21 tool was used to predict the gene regions with the highest production of efficient siRNAs (small interfering RNAs), but without potential off-targets. The transcript amplification of cDNA samples of inoculated and non-inoculated leaf samples from Morex and Ingrid BC *mlo5* were analysed. From all candidates, except WB-CG_8, it was possible to amplify one product of the expected size (Figure B 6B). These results support the hypothesized specificity of the primers. The four genes from chromosome 5H (WB-CG_17, WB-CG_19, WB-CG_23 and WB-CG_28) were the most promising candidates because the corresponding peaks on chromosome 5H were significant in all three traits and they seem to co-localize with a previously mapped seedling resistance QTL (Aghnoum *et al.*, 2010). *Rbgq15* was identified in the mapping populations Vada/SusPtrit and L94/Vada and the *lipoxygenase 2* (GenBank: L37358.1) was proposed as potential casual gene. Nonetheless, functional validation data are missing (Aghnoum *et al.*, 2010). Based on a blast analysis, three lipoxygenases (HORVU5Hr1G093700, HORVU5Hr1G093770 and HORVU5Hr1G117110) on chromosome 5H were possible candidates for *lipoxygenase 2*. HORVU5Hr1G093700 and HORVU5Hr1G093770 were located close to loci 13 and HORVU5Hr1G117110 is located within locus 14. Nevertheless, none of the SNPs in these three genes was significantly associated in either of the three traits. This result emphasizes the necessity to further analyze the candidate genes.

In the following, the expression patterns of the four selected candidates in a susceptible (Morex) and a resistant genotype (WB-052) were assessed. This analysis was performed as quantitative PCRs of cDNAs generated from inoculated and non-inoculated leaf samples. The transcript level of WB-CG_17 and WB-CG_23 was quantified relative to the endogenous control *UBC* and the non-inoculated samples (0 h post inoculation, Figure R 13). In case of WB-CG_19 and WB-CG_28, the relative transcript quantification was not reliable because the measured Cq (quantification cycle)-values were above the recommended threshold. Nevertheless, previous analyses revealed a clear product amplification of both genes on cDNA samples (Figure B 6B). Therefore, this effect is

probably caused by competitive amplification of the test and control transcript in the same reaction. It is possible that the amplification of the endogenous control gene is favoured, due to a higher amplification efficacy of the primer pair and/or the higher copy number of the house keeping gene.

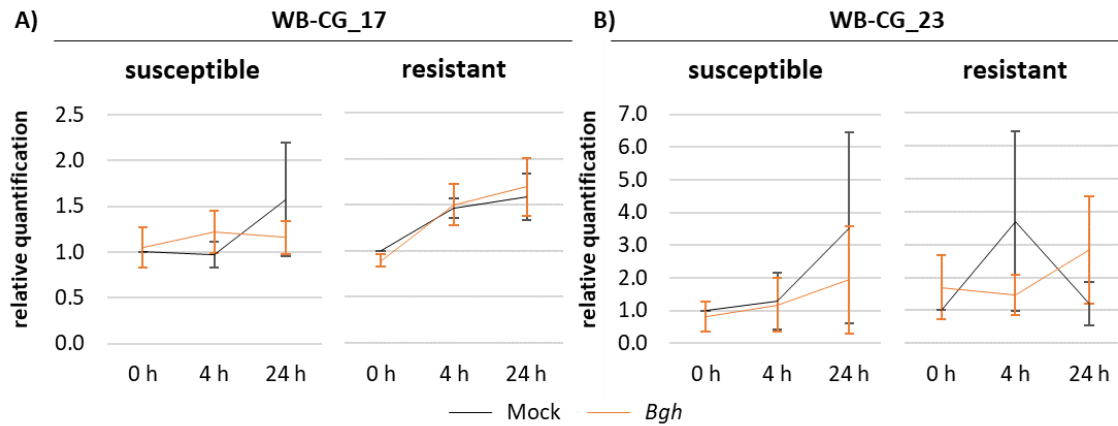


Figure R 13: Relative quantification of the transcripts of WB-CG_17 and WB-CG_23

The expression of WB-CG_17 (A) and WB-CG_23 (B) was quantified relative to the endogenous control *UBC* (*ubiquitin-conjugating enzyme 3*) for three different time points (0 h, 4 h and 24 h post inoculation [p. i.]) in a susceptible (Morex) and a resistant (WB-052) genotype. As template, cDNAs of powdery mildew inoculated (*Bgh*: *Blumeria graminis* f. sp. *hordei*) and non-inoculated (control) total leaf samples were used. The mean values and standard deviations from three biological replicates were calculated and significant differences between control and inoculated samples are determined by unpaired two-tailed t-test with GraphPad Prism 7.01. ‘*’ p-value ≤ 0.05

The relative quantification of WB-CG_23 was possible, but the high standard deviations did not allow any conclusion (Figure R 13B), especially not about the response of the gene to the powdery mildew inoculation. In contrast, the relative quantification of the minor allele of WB-CG_17 (resistant genotype) indicates a general transcript induction over time (Figure R 13A). Nonetheless, this effect is not detected for the major allele (susceptible genotype, Figure R 13A). The relative quantification values from the inoculated and the non-inoculated samples were very similar and it suggests that the expression of WB-CG_17 is not altered after powdery mildew attack.

All in all, the results of the quantitative PCR were rather inconclusive, probably because of dilutional effects. The cDNAs were generated from total leaf RNA, but only the epidermis cells were attacked by the pathogen. It is possible that the candidate transcript level is altered only in attacked cells. To investigate this hypothesis, microarray data of inoculated and non-inoculated barley epidermis peels (cultivar Vada) that were published by Delventhal *et al.* (2017), were re-analysed. The transcript level is represented by the mean signal intensities with standard deviations of the four candidate genes for the non-inoculated controls, the samples inoculated with the adapted fungus *Blumeria graminis* f. sp. *hordei* (*Bgh*, Figure R 14) or the non-adapted

fungus *Blumeria graminis* f. sp. *tritici* (*Bgt*, Figure R 14). The data were provided for four different time points (6 h, 12 h, 24 h and 74 h post inoculation).

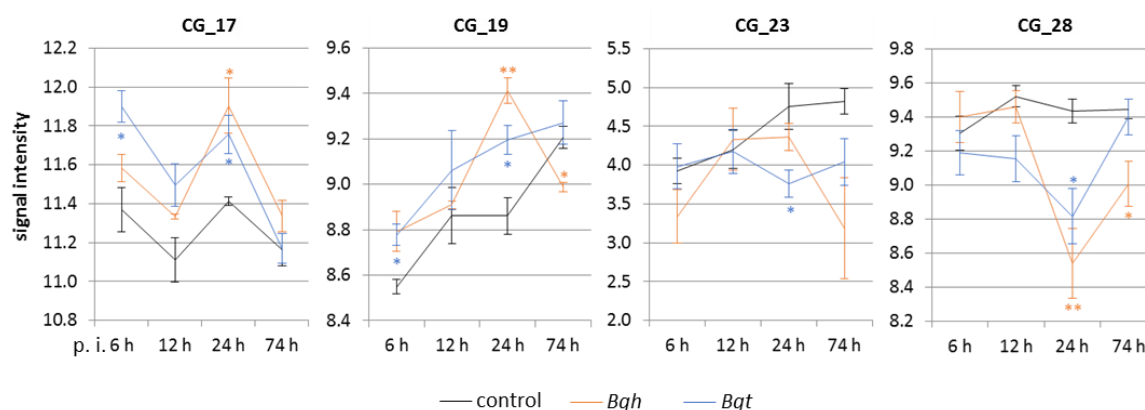


Figure R 14: Relative expression of the four candidate genes as mean signal intensities of microarray data

The quantile-normalized signal intensities represent the relative expression of WB-CG_17, WB-CG_19, WB-CG_23 and WB-CG_28 based on microarray data (Delventhal *et al.*, 2017). The mean values and standard deviations of three biological replicates were calculated from powdery mildew inoculated and non-inoculated (control) barley epidermis peels. The samples were either inoculated with the adapted fungus *Blumeria graminis* f. sp. *hordei* (*Bgh*) or the non-adapted fungus *Blumeria graminis* f. sp. *tritici* (*Bgt*). Four different time points (6 h, 12 h, 24 h and 74 h) post inoculation (p. i.) were analysed and significant differences between control and inoculated samples are determined by unpaired two-tailed t-test with GraphPad Prism 7.01. '*' p-value ≤ 0.05 ; '**' p-value ≤ 0.005

The measured signal intensities of WB-CG_17 indicate a rhythmic pattern in the control as well as in the inoculated samples (Figure R 14, first column). The transcript level is higher 6 h and 24 h post inoculation as compared to 12 h and 74 h post inoculation, respectively. This result is in accordance with the detected transcript increase of the minor allele in the quantitative PCR (Figure R 13A). Wang *et al.* (2011) reported a similar pattern for defence related genes regulated by the circadian clock in the absence of a major *R*-gene in infected *Arabidopsis* plants. This observation supports the presumed clock regulation of the candidate gene. Moreover, the measured signal intensities of WB-CG_17 are altered significantly by the pathogen inoculation, although the rhythmic pattern is preserved. The transcript is significantly induced 6 h and 24 h after attack of the non-adapted powdery mildew fungus (Figure R 14). In case of the adapted fungus, only the induction 24 h post inoculation is significant (Figure R 14). Nevertheless, the data indicate also an increased transcript level 6 h post inoculation. The results were in accordance with the detected alterations in the product amplification of the inoculated samples of Morex and Ingrid BC *mlo5* 6 h post inoculation (Figure B 6B). Moreover, the results support the hypothesis that the transcript level is only altered in attacked epidermis cells, because the data of the quantitative PCR indicate that the overall transcript level in the leaf is not changed by powdery mildew inoculation (Figure R 13A). All in all, WB-CG_17 seems to be regulated by the circadian clock and the expression is altered by powdery mildew inoculation in attacked tissue.

A general increase of the transcript level of WB-CG_19 is indicated by the mean signal intensities of the control samples (Figure R 14, second column). Besides this, the transcript is significantly induced 24 h post inoculation. This induction is observed after attack of the adapted as well as the non-adapted fungus. The measured signal intensities of the samples inoculated with *Blumeria graminis* f. sp. *tritici* (*Bgt*) display the same general trend as the control samples, but the overall transcript level is elevated in this last case (Figure R 14). This effect is also detected for the samples inoculated with *Bgh* (Figure R 14) and the results correlate with increased product amount of the inoculated samples of Morex and Ingrid BC *mlo5* (Figure B 6B). Nonetheless, only the mean signal intensities of the samples inoculated with *Bgh* drop significantly after the 24 h peak.

The mean signal intensities of WB-CG_23 were in general lower as for the other three candidates (Figure R 14, third column). Besides the low transcript level, also the reduction of the transcript level after pathogen inoculation (Figure B 6B) was observed in the previous quantitative PCR approach. This trend is also visible by the measured signal intensities of the samples inoculated with the adapted fungus (6 h post inoculation, Figure R 14), but not in case of the non-adapted fungus (Figure R 14). In contrast, the powdery mildew inoculation with both fungi led to decreased signal intensities in the 24 h and 74 h samples. Nevertheless, the standard deviations were high and thus, the reliability of the interpretation is decreased.

A similar effect was observed for the mean signal intensities of WB-CG_28 (Figure R 14, last column). The inoculation with both fungi (time point 24 h post inoculation) resulted in a significant reduction of the values. This effect is stronger and lasts longer after inoculation with the adapted fungus (Figure R 14) compared to the samples inoculated with the non-adapted fungus (Figure R 14).

The analyses revealed that all four candidate genes were expressed and the data indicate that their transcription is altered by powdery mildew inoculation. These alterations were observed after attack of the adapted as well as of the non-adapted powdery mildew fungus. The results imply that the candidates probably participate in host and nonhost resistance.

3.6.3. Determination of the allele effect on powdery mildew resistance

The effects of the different candidate alleles were assessed. In the first approach, the average infected leaf area of the different alleles was calculated (Figure R 15 and Table B 8) and in the second approach, the proportion of variation on the infected leaf area that is explained by the single SNPs or attributed by the defined alleles is compared with each other. With the exception of WB-CG_28, this proportion is identical because the alleles of the other three candidates were determined by one significant SNP (Table R 2). To estimate the effects of a single candidate gene, separate models for the different genes were fitted.

The minor allele (A1) of WB-CG_17 is present in 14 genotypes (frequency of 6.9 %). The average infected leaf area of these 14 genotypes was $22.9 \% \pm 3.28 \%$ (mean \pm standard error of the mean, Figure R 15 and Table B 8). In contrast, the average infected leaf area of the 185 genotypes carrying the major allele (A2) was $51.4 \% \pm 0.97 \%$ (Figure R 15 and Table B 8). The minor allele of WB-CG_19 was present in 21 genotypes (10.4 %). In this respect, the observation frequency was slightly higher in comparison to WB-CG_17. The average infected leaf area of the minor allele carriers of WB-CG_19 ($n = 21$) was $24.8 \% \pm 2.48 \%$ and of the major allele carriers ($n = 179$) $51.9 \% \pm 0.94 \%$, respectively (Figure R 15 and Table B 8). Similar observation frequencies of the minor alleles were detected for WB-CG_23 (20 genotypes, 9.9 %) and WB-CG_28 (18 genotypes, 8.9 %). In addition, also the average infected leaf areas of the minor allele carriers of WB-CG_23 ($28.4 \% \pm 3.48 \%$) and WB-CG_28 ($24.2 \% \pm 3.09 \%$) as well as of the major allele carriers of WB-CG_23 (179 genotypes, $51.5 \% \pm 0.98 \%$) and WB-CG_28 (181 genotypes, $51.5 \% \pm 0.95 \%$) were almost identical, respectively (Figure R 15 and Table B 8). In regard of these results, all minor alleles displayed a strong effect on the powdery mildew resistance (Figure R 15). These effects were significant. Nonetheless, it has to be considered that the significant SNPs were in high LD to each other (Figure B 5). The number of genotypes, where the minor alleles were detected, might represent this aspect. In the majority of the genotypes (19 out of 29 varieties) more than one minor allele was determined. For example, in the six genotypes WB-052, WB-056, WB-074, WB-137, WB-401 and WB-472 all four minor alleles were annotated and four of these genotypes (WB-052, WB-056, WB-074 and WB-401) originate in Ethiopia which could hint to a higher relatedness of these genotypes (in the respective genomic regions). It cannot be excluded that the observed resistance of the varieties is independent of the proposed candidate genes. Instead the resistance could be caused by race-specific resistance genes like it is the case for WB-052.

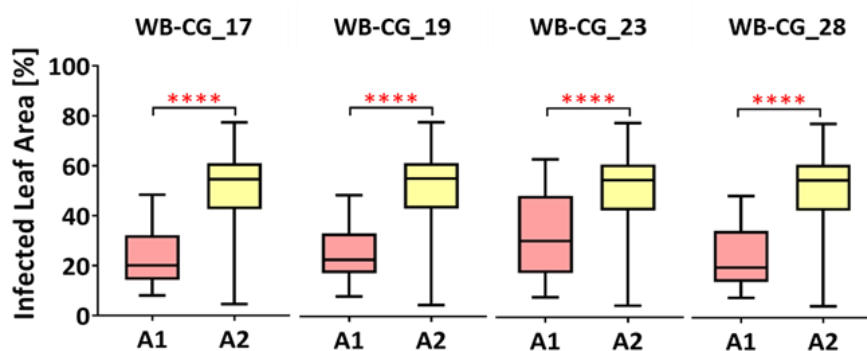


Figure R 15: Box plots of the average infected leaf area for the defined alleles

The significant SNPs of WB-CG_17, WB-CG_19, WB-CG_23, WB-CG_28 were used to define the allele status and the average infected leaf area from the BLUEs (in %) were calculated for the two possible alleles (A1 and A2). The error bars represent the minimal and maximal values. The significance was determined by unpaired, two-tailed t-test with GraphPad Prism 7.01. '****' p-value < 0.0001

The R^2 of the fitted linear model for WB-CG_17 indicates that 23.4 % of phenotypic variation is explained by the significant SNP. The explained variation of the significant SNP of WB-CG_19 was determined as 31 %. In contrast, only 16.7 % of the phenotypic variation is explained by the significant SNP of WB-CG_23. In case of WB-CG_28, two SNPs were significantly associated and for both SNPs, separate linear models were fitted (SNP650973939chr5H: $R^2 = 24.5$ % and SNP650976700chr5H: $R^2 = 27.3$ %). In addition, a third model was fitted for WB-CG_28. This model should determine the phenotypic variation, which is attributed by the defined alleles. The allele model did not provide any advantage over the SNP models, which is reflected in the identical R^2 values of these models. It is likely that this circumstance is caused by the complete LD between the two significant SNPs (Figure B 5). The proportion of the phenotypic variance that is explained by the *Rbgq15* QTL ranged from 6.2-24.8 % (Aghnoum *et al.*, 2010). These results imply a similar effect size of the present loci and the *Rbgq15* QTL.

3.7. Functional assessments of the four most promising candidate genes

3.7.1. Functional analysis of selected candidates based on *in silico* data

Beside the phenotypic evaluations, the candidate genes were analysed in regard of their putative functions (Table R 3). The closest protein homologs (Table B 6) of Arabidopsis, rice and the related species *Aegilops tauschii* subsp. *tauschii* or *Brachypodium distachyon* were identified. Additionally, the predicted off-targets in barley were taken into account as potential candidate homologs (Table B 6). All protein sequences were selected for multiple alignments and conserved domains were predicted with the 'Pfam 32.0 sequence search' tool (Figure B 7 to B 10).

For WB-CG_17 no function was annotated (Table R 3) and the potential off-targets (HORVU5Hr1G078020 and HORVU7Hr1G063660) were not further considered because they overlap only partially with the candidate sequence. The top candidates of the NCBI blast revealed two proteins annotated as 'UPF0664 stress-induced protein C29B12.11c' in *A. tauschii* and *B. distachyon* (Table R 3). The protein sequences of *A. tauschii* and *B. distachyon* display a sequence identity of 98.0 % and 91.2 % to the candidate sequence, respectively. A similar high sequence identity (90.8 %) was determined for the closest rice homolog: an arabinogalactan protein (AGP). In addition, the Arabidopsis homolog was annotated as classical AGP as well (Table R 3). This type of proteins is supposed to play an important role as cell surface regulator and in defence responses (Ellis *et al.*, 2010; Nguema-Ona *et al.*, 2014). The sequence identity between the candidate protein sequence and the Arabidopsis protein (73.9 %) is lower as for the monocot homologs (91-98 %). In the protein homolog of Arabidopsis as well as in the proteins of *A. tauschii* and *B. distachyon*, a PH-GRAM_WBP2 (Pleckstrin Homology-Glucosyltransferases, Rab-like GTPase activators and Myotubularins_WW binding protein 2) domain was annotated according

to the NCBI descriptions (domain family: cd13214, Figure B 7A). GRAM domains were usually found in membrane-associated proteins (Doerks *et al.*, 2000). Interestingly, the Arabidopsis homolog was detected in a screening for plasma membrane bound proteins (Marmagne *et al.*, 2004). Nevertheless, the 'Pfam 32.0 sequence search' tool predicted no conserved domain in any of the protein sequences. The high sequence identities between the annotated PH-GRAM_WBP2 domains and the respective regions in the present candidate and the rice homolog indicate that also these two proteins contain a PH-GRAM_WBP2 domain (Figure B 7B). In consideration of the results, it is likely that WB-CG_17 is a membrane-associated protein which is presumably glycosylated.

Table R 3: Summary of the predicted functions of potential candidate homologs

Candidates	Annotated ¹	Barley ²	Related species ³	Arabidopsis ⁴	Rice ⁵
CG_17	unknown	-	UPF0664 stress-induced protein C29B12.11c	classical AGP	AGP
CG_19	DPMT subunit	DPMT-related	DPMT subunit 3-like	DPMS3	unknown
CG_23	BTB/POZ/Kelch-associated protein	BTB/POZ/Kelch-associated protein	BTB/POZ domain-containing protein At2g46260-like	LRB1 & 2	E1-BTB1 & 2
CG_28	FEN1-B	FEN1-A	FEN1-B	FEN1	FEN1-B & A

¹ function of the candidate gene

² function of potential barley homolog predicted as candidate off-target by the si-FI21 tool

³ functions of potential homologs in the related species *A. tauschii* or *B. distachyon*) identified in the 'NCBI blastn' analysis

⁴ function of potential Arabidopsis homolog(s) identified via 'blastp' analysis against the TAIR server

⁵ function of potential rice (*Oryza sativa ssp japonica cv. Nipponbare*) homolog(s) identified via 'blastp' analysis against the rice genome annotation project server

The following abbreviations were used: AGP – arabinogalactan protein; DPMT – dolichol-phosphate mannosyltransferase; DPMS – dolichol phosphate mannose synthase; BTB/POZ – Brica-Brac/-Tramtrack/-Broad Complex & Poxvirus and Zinc finger; LRB – Light-Response BTB; FEN – flap endonuclease

WB-CG_19 was annotated as 'dolichol-phosphate mannosyltransferase subunit' (Table R 3). A similar function was predicted for the putative barley and *A. tauschii* homologs. The barley homolog displays a sequence identity of only 37.1 % because the C-terminal part of the homologous protein is missing (42 amino acids, Figure B 8A). In contrast, the *A. tauschii* homolog is almost identical to the here presented candidate sequences (98.8 %). For the rice and Arabidopsis homologs an identity of 67.2 % and 68.5 % was determined, respectively. In case of the rice homolog, no function was annotated (Table R 3). In contrast to this, the annotated

function of the Arabidopsis homolog as 'dolichol phosphate mannose synthase 3' (DPMS3) was functionally confirmed (Jadid *et al.*, 2011). In accordance with the annotated functions, a 'dolichol-phosphate mannosyltransferase subunit 3' (DPM3) domain was predicted by the 'Pfam 32.0 sequence search' tool in all protein sequences, except the truncated barley homolog (Figure B 8A). As expected, the identities of the sequences of the predicted domain are even higher as for the complete protein sequence, especially for the rice homolog (Figure B 8B). All results indicate, that WB-CG_19 acts as potential barley homolog of AtDPMS3, which is important for the production of dolichol-phosphate mannose in Arabidopsis (Jadid *et al.*, 2011).

The functions of WB-CG_23 and its' barley homolog are annotated as 'BTB/POZ/Kelch-associated protein' (Table R 3). The 'Bric-a-Brac/-Tramtrack/-Broad Complex (BTB)/-POXvirus and Zinc finger (POZ) motif is a common protein-protein interaction motif and members of this family participate in diverse biological processes (Stogios *et al.*, 2005). The sequence identity of the two barley proteins was determined as 72.2 %. In contrast, the sequence identity of the closest homolog of *B. distachyon* to the here presented candidate was only 53.3 %. Nevertheless, the protein function was annotated as 'BTB/POZ domain-containing protein At2g46260-like' (Table R 3). At2g46260 is, beside At3g61600, one of the two protein homologs that were identified in Arabidopsis. These two proteins share 88 % sequence identity to each other and they were annotated as Light-Response BTB1 (LRB1) and LRB2 (Christians *et al.*, 2012). The proteins constitute Cullin3-based E3 ubiquitin ligases, which were involved in the regulation of flowering and light signalling in Arabidopsis (Shu & Yang, 2017). Additionally, there are indications that the proteins act as negative regulator of the jasmonate mediated defence against pathogens (Qu *et al.*, 2010). The sequence identity to the here presented candidate genes was determined as 41.4 % and 41.1 %, respectively. In contrast, the two protein homologs identified in rice were annotated as 'BTB with E1 subfamily conserved sequence' instead as a E3 ligase (Table R 3). Nevertheless, ubiquitin-activating E1 enzymes participate also in protein degradation (Shu & Yang, 2017). The two rice homologs share a similar proportion of sequences identity among each other and also compared to the candidate gene (E1-BTB1 & E1-BTB2: 63.8 % identity, E1-BTB1 & WB-CG_23: 60.3 %; E1-BTB2 & WB-CG_23: 52.1 %), respectively. The 'Pfam 32.0 sequence search' tool predicts in all protein sequences a BTB (BTB/POZ domain) and a BACK (BTB And C-terminal Kelch) domain (Figure B 9A). Christians *et al.* (2012) reported also a nuclear localization signal (NLS) in LRB1 and LRB2. Based on the prediction of the 'NLS Mapper', this motif is not present in E1-BTB1 of rice and the two barley protein sequences (Figure B 9A). The identities of the sequences of the predicted BTB and BACK domains are higher as compared to those of the complete protein sequence (up to 20 %), especially for the BTB domain in the rice and the *B. distachyon* homolog (Figure B 9B). As expected, the C-terminal regions of the protein sequences were no functional domain was

annotated, were less related to each other (44-65 %, Figure B 9B). All together, these results suggest that WB-CG_23 participate in protein degradation and that the annotated 'BTB/POZ' domain is essential for that function.

WB-CG_28 is annotated as 'flap endonuclease (FEN) 1-B' and the barley homolog as FEN1-A (Table R 3). The sequence identity of the two proteins was determined as 55.8 %. This proportion is similar to the one reported for the two rice homologs (60.0 %, Kimura *et al.*, 2003). Nevertheless, the sequence identity of two FEN1-B homologs (WB-CG_28 & rice FEN1-B) among each other was much higher (76.9 %) and between the two FEN1-A homologs, too (79.5 %). Even higher were the identities that were determined between the *A. tauschii* 'flap endonuclease 1-B-like' homolog and the candidate sequence (98.1 %) and the *B. distachyon* FEN1-B homolog (88.9 %), respectively (Table R 3). In contrast, Arabidopsis expresses only one FEN1 protein, which is related to the FEN1-A type (Kimura *et al.*, 2003, Schultz *et al.*, 2007). The determined sequence identity (55.0 %) was almost identical to the one calculated between the candidate sequence and the other FEN1-A homologs in barley and rice (55.8 % and 56.8 %, respectively). The 'Pfam 32.0 sequence search' tool predicts in all protein sequences a XPG (Xeroderma Pigmentosum Complementation Group G) N-terminal domain and a XPG Internal-region (Figure B 10A). The annotation of the I-domains of the two rice homologs was slightly longer (Kimura *et al.*, 2003). The analysis of the N- and I-domain sequences revealed a high sequences identity (> 74 %) of all flap endonucleases to the candidate sequence (Figure B 10B). Also, the C-terminal regions of the FEN1-B homologs display a high sequence identity (> 59 %) to each other. In accordance with the literature (Kimura *et al.*, 2003), only a low sequence identity (30-33 %) of the C-terminal candidate region to the FEN1-A homologs was detected (Figure B 10B). In consideration of the results, WB-CB_28 is a flap endonuclease 1 type-B protein. Nonetheless, the function of this protein type remains elusive because it seems that it displays a distinct function to the FEN1-A type proteins (Kimura *et al.*, 2003).

Beside the general view on the annotated candidate functions, the effect of the different alleles was addressed. In all four selected candidate genes two alleles were defined based on the significant SNPs (*Max* trait). The major as well as the minor alleles per candidate were present in several genotypes and to provide a better comparability of the results, the respective alleles were always cloned from the same two varieties (Figure B 6A). The major allele was cloned from the susceptible genotype Morex and the minor allele from the resistant genotype WB-052, respectively. Because Morex was selected for cloning, the corresponding protein sequences represent the annotated reference sequences of the candidates that were also used in the multiple sequence alignments of the potential candidate homologs (Figure B 7 to B 10). The majority of the annotated SNPs as well as the detected changes, based on the sequencing results

of the cloned alleles were located in non-coding regions (introns, 3' and 5' UTRs). The same phenomenon was reported before in other monocot species (Huang & Han, 2014; Barker & Edwards, 2009). The generated coding sequences of the different alleles were translated *in silico* into proteins and the putative protein sequences were compared with each other.

These data indicate five SNPs in the coding sequence of WB-CG_17' minor allele in comparison to the major allele. Four of the five SNPs did not alter the protein sequence due to synonymous amino acid exchanges (Figure B 7A). The last amino acid exchange (Ile⁶⁴Val) occurs in the putative PH-GRAM_WBP2 domain and it restores the conserved amino acid (Figure B 7A). In contrast, the significant SNP554456783chr5H is located in the beginning of the annotated 3' UTR and thus, the region was included in the cloned candidate allele.

In the coding sequence of WB-CG_19, only one SNP was detected between the two alleles. It causes a synonymous exchange in a conserved amino acid of the predicted DPM3 domain (Figure B 8A). The significant SNP554738172chr5H is also located in a non-coding region, in the first intron.

In case of WB-CG_23, nine SNPs were detected in the coding sequences of the two alleles and three of these SNPs led to synonymous amino acid exchanges (Figure B 9A). Five of the SNPs were located outside of predicted domains. Because the two exchanges Val⁴⁶Leu and Arg³⁰⁴His were conservative replacements in low conserved regions, it is presumed that the alterations have a low effect on the function of the putative proteins. The two alterations Gly⁹Ala and Leu¹⁸⁰Val display also conservative replacements, but of conserved amino acids. The exchange of Proline³⁷⁰ to Leucine denote a radical amino acid exchange, which causes probably a stronger effect on the protein function. In contrast, the exchange of Glutamic acid⁵¹ to Aspartic acid represents again a conservative replacement. The exchange is located in the mutated NLS of the candidate protein (Figure B 9A). Nevertheless, none of these SNPs were determined as significant and the significant SNP649211044chr5H is located once more in an intronic region (begin of the fourth intron).

For WB-CG_28, two SNPs were identified as significant. SNP650976700chr5H is also annotated in an intronic region (end of the eleventh intron), but SNP650973939chr5H is located in the begin of the seventeenth exon. It causes the exchange of a, in FEN1-B type proteins, conserved amino acid (Ala³⁷³Thr) and thus, from a hydrophobic to a polar uncharged amino acid (Figure B 10A). Moreover, it is expected that the protein corresponding to the minor allele is 51 amino acids longer, because SNP650980476chr5H creates a new start codon in the annotated 5'UTR (Figure B 10A). Nonetheless, the effects of this alteration could not be analysed, because it was not possible to obtain an *Escherichia (E.) coli* clone expressing the full-length version of any allele.

3.7.2. Functional validation of selected candidates based on transient silencing and overexpression

Beside the *in silico* analyses to assess the putative functions of the selected candidate genes, they should be also functionally validated *in planta* (Table A 14) via transient induced-gene silencing (TIGS) and transient overexpression (OX). Both methods rely on particle bombardment to transiently transform epidermis cells and the presence of a reporter allow the evaluation of the (penetration) resistance in response to powdery mildew infection. This technique has been successfully used during the last 20 years to validate candidate genes in this particular pathosystem (Panstruga, 2004).

As first approach, the candidate genes were transiently silenced (Table R 4). It is assumed that the generated hairpin constructs form double stranded RNA molecules, which were processed into small interfering RNAs (Douchkov *et al.*, 2005). These siRNAs led than to a degradation of the candidate transcripts based on RNA interference. None of the transiently silenced candidate genes display a significant effect on the susceptibility against powdery mildew neither in the resistant genotype nor in the susceptible one (Table R 4). Nonetheless, the positive control (*Mlo*) indicates the success of the experimental series because its silencing significantly enhances the powdery mildew resistance in both varieties. The negative result can be caused by several factors. For example, the candidate regions, were selected in respect of an *in silico* prediction but there is no actual prove of the production or the efficiency of the generated siRNAs. Other reasons could be functional redundancy among the potential homologous proteins or the small effect size of the genes.

Table R 4: Effect of the transient silencing of the candidate genes on the resistance of a resistant and a susceptible genotype against powdery mildew isolate CH4.8

Construct ¹	WB-052 (resistant)		Morex (susceptible)	
	Relative SI (\log_2) ²	p-value (t-test) ³	Relative SI (\log_2)	p-value (t-test)
WB-CG_17	0.10 ± 0.34 ⁴	0.7756	0.00 ± 0.14	> 0.9999
WB-CG_19	0.08 ± 0.48	0.8720	-0.12 ± 0.21	0.5887
WB-CG_23	0.00 ± 0.22	> 0.9999	0.02 ± 0.14	0.8864
WB-CG_28	0.40 ± 0.30	0.2237	0.12 ± 0.14	0.4021
<i>Mlo</i> ⁵	-1.72 ± 0.29	0.0003	-2.80 ± 0.20	< 0.0001

¹ indicate the bombarded (candidate) gene

² \log_2 -transformed susceptibility index (SI) relative to the empty vector control (pIPKTA30N)

³ significance was assessed by unpaired two-tailed t-test against the hypothetical value '0' with GraphPad Prism 7.01

⁴ mean values and the standard errors of the mean from five independent bombardment experiments

⁵ transient silencing of target gene (pIPKTA36: *Mildew resistance locus o*) decreases significantly the susceptibility to powdery mildew and served as positive control (Douchkov *et al.*, 2005)

Statistically significant results were highlighted in bold. p-value ≤ 0.05

In the second approach, the effect of the transient overexpression of the different candidate alleles on the (penetration) resistance against powdery mildew was determined (Table R 5). The genomic full-length alleles were constitutively expressed under control of the Cauliflower mosaic virus (CaMV) 35S promoter and it is assumed that the allele transcripts were overexpressed and processed correctly in the transformed cells.

The positive control (wheat *Prx103*) indicates the success of the experimental series because its overexpression significantly enhances the powdery mildew resistance in both varieties. In contrast, neither the overexpression of the minor allele nor of the major allele from WB-CG_19 results in a significant effect on the resistance against powdery mildew in the resistant or the susceptible genotype. In case of WB-CG_17, the overexpression of the minor allele, but not of the major allele, enhances significantly the susceptibility in both genotypes against powdery mildew. In contrast, the significantly enhanced susceptibility caused by the overexpression of the major allele of WB-CG_23 is only detected for the resistant variety. According to the functional validation via overexpression, at least WB-CG_17 and WB-CG_23 seem to be involved in the resistance response against the adapted powdery mildew fungus and the detected effects are allele and genotype dependent (Table R 5).

Table R 5: Effect of the transient overexpression of the candidate genes on resistance of a resistant and a susceptible genotype against powdery mildew isolate CH4.8

Construct ¹	WB-052 (resistant)		Morex (susceptible)	
	Relative SI (log ₂) ²	p-value (t-test) ³	Relative SI (log ₂)	p-value (t-test)
WB-CG_17 minor	1.28 ± 0.27⁴	0.0034	0.25 ± 0.09	0.0278
WB-CG_17 major	0.35 ± 0.36	0.3706	0.25 ± 0.21	0.2791
WB-CG_19 minor	0.58 ± 0.25	0.0608	0.25 ± 0.19	0.2347
WB-CG_19 major	-0.68 ± 0.54	0.2583	0.18 ± 0.19	0.3896
WB-CG_23 minor	0.28 ± 0.28	0.3559	0.13 ± 0.10	0.2708
WB-CG_23 major	0.90 ± 0.20	0.0037	0.23 ± 0.17	0.2343
<i>Prx103</i> ⁵	-1.15 ± 0.21	0.0014	-0.40 ± 0.12	0.0171

¹ indicate the bombarded (candidate) gene allele

² log₂-transformed susceptibility index (SI) relative to the empty vector control (pIPKTA9)

³ significance was assessed by unpaired two-tailed t-test against the hypothetical value '0' with GraphPad Prism 7.01

⁴ mean values and the standard errors of the mean from four independent bombardment experiments

⁵ transient overexpression of target gene (pJP01: *Class III peroxidase* from wheat) decreases significantly the susceptibility to powdery mildew and served as positive control (Altpeter *et al.*, 2005)

Statistically significant results were highlighted in bold. p-value ≤ 0.05

The minor allele of WB-CG_17 enhances the susceptibility in a compatible as well as in an incompatible resistance reaction. In contrast, the results suggest that the major allele of WB-CG_23 enhances the susceptibility only in the incompatible resistance response. It is possible

that the identified candidate genes act either as disease susceptibility genes (a gene which makes susceptible to a certain pathogen), as susceptibility factors (necessary factor for the growth of the pathogen *in planta*) or as negative regulator of resistance pathways (Fan & Doerner, 2012).

3.8. Selection of the best promoter_GUS construct for transient validation assays

The last part of this study, focused on the question of the selection of a suitable reporter construct for transient bombardment assays. The correct selection of a reporter construct, is an essential part of the experimental design. For transient assays in the pathosystem *Triticeae-Blumeria graminis*, the green fluorescent protein (GFP) as well as the β -glucuronidase (GUS) proved to be appropriate reporters (Schweizer *et al.*, 1999b). In the present study, a glucuronidase assay was performed during the functional validations of the candidate genes (Table A 14). The method is based on the conversion of an indigogenic substrate to a blue product by the GUS protein, which is encoded by the *uidA* gene of *E. coli* (Jefferson *et al.*, 1987; Panstruga, 2004). The expression of the *uidA* (respectively *GUS*) gene was controlled by the constitutive maize *ubiquitin* (*Ubi*) promoter. This construct is referred hereafter as pUbiGUS (Schweizer *et al.*, 1999b). Over the time various promoter_GUS constructs were generated and used as reporter in transient assays, but their efficiency was never evaluated under comparable conditions like it is reported here (Table A 14). The four the constructs (pIPKb002_GUS-pIPKb005_GUS) were described by Himmelbach *et al.* (2007) and pV668 by Schweizer *et al.* (1999a & 1999b). In a first approach the total number of GUS stained cells was analysed in relation to the pUbiGUS construct and in response to powdery mildew inoculation (Table R 6). As normalization construct pBC17 was selected, because it expresses the two genes that were necessary for the anthocyanin production (Leduc *et al.*, 1994). The effect of the different promoter_GUS constructs was assessed as ratio of the total number of GUS stained cells to the total number of anthocyanin stained cells (GUS/pBC17, Table R 6). Positive GUS/pBC17 ratios represent more GUS than anthocyanin stained cells and vice versa. In case of the inoculated samples, none of the five promoter constructs displayed a significant effect in comparison to pUbiGUS. It is likely that this is related to the high variance of the pUbiGUS samples. For the constructs pIPKb003_GUS and pV668 significantly lower GUS/pBC17 ratios were determined in the non-inoculated samples when compared to pUbiGUS. Nevertheless, the same tendencies of the different constructs were obtained in the inoculated and non-inoculated samples, which indicates that the inoculation per se has no effect. In general, it seems that the total GUS cell number is decreased in the constructs pV668, pIPKb004_GUS and pIPKb005_GUS. Because of the weak effects of the different constructs, a second approach was designed (Table A 14).

Table R 6: Effect of the different promoter_GUS constructs on the total number of GUS stained cells

Construct	Promoter ²	Inoculated ¹		Non-inoculated	
		GUS/pBC17 (log ₂) ³	p-value (t-test) ⁴	GUS/pBC17 (log ₂)	p-value (t-test)
pUbiGUS	<i>Ubi</i>	0.37 ± 0.38 ⁵	-	0.58 ± 0.07	-
pIPKb002_GUS	<i>Ubi</i>	0.37 ± 0.12	0.9987	0.36 ± 0.07	0.0719
pIPKb003_GUS	<i>Act</i>	0.46 ± 0.18	0.8434	0.33 ± 0.05	0.0348
pV668	35S	-0.07 ± 0.24	0.3767	-0.32 ± 0.17	0.0077
pIPKb004_GUS	d35S	0.01 ± 0.21	0.4462	0.08 ± 0.31	0.1874
pIPKb005_GUS	<i>GstA1</i>	-0.40 ± 0.21	0.1453	-0.16 ± 0.30	0.0761

¹ inoculation with the powdery mildew isolate CH4.8

² indicate the promoters used in the different constructs: *Ubi* – maize *ubiquitin* promoter, *Act* – rice *actin* promoter, 35S – Cauliflower mosaic virus (CaMV) 35S promoter, d35s – enhanced CaMV 35S promoter, *GstA1* –wheat *glutathione S-transferase A1* promoter

³ log₂-transformed ratio of the total number of GUS (β-glucuronidase) stained cell relative to the normalization construct (pBC17)

⁴ significance was assessed by unpaired two-tailed t-test against pUbiGUS with GraphPad Prism 7.01

⁵ mean values and the standard errors of the mean from three independent bombardment experiments

Statistically significant results were highlighted in bold. p-value ≤ 0.05

In this approach, the staining/colour intensity of the GUS-stained cells was evaluated with a tool that was able to detect automatically GUS-stained cells from microscopic pictures and calculated the cell hue of them. The average background intensities of the pictures and the total number of anthocyanin-stained cells were used for the normalization. The bombardment of each promoter_GUS constructs was repeated three times. Later, one experiment was excluded from the analysis because of an apparent overexposure during the picture taking (different background intensity). The effect of the six different promoter_GUS constructs on the staining/colour intensity of GUS stained cells was assessed as normalized cell hue for the indicated total cell number per construct (Table R 7). All five promoter_GUS constructs displayed a significant decrease of the staining/colour intensity (cell hue) when compared to pUbiGUS. Although, it is possible that the lower number of cells per test construct used for the evaluation, led to an overestimation of the effect. Particularly, this could be the case for pIPKb003_GUS and pIPKb005_GUS. Nevertheless, the determined effects of the different constructs were in accordance with the observed trends in the previous approach (Table R 6).

The results of both approaches indicate that first of all, pUbiGUS is the most efficient promoter_GUS construct. It yielded in the highest average total GUS cell number and reached the darkest staining intensity of the cells. The average total GUS cell numbers of the constructs pIPKb002_GUS, pIPKb003_GUS were in a similar range to pUbiGUS, but the staining intensity was determined about 50 % lower. In contrast, the average total GUS cell numbers and the staining intensity of the constructs pV668, pIPKb004_GUS and pIPKb005_GUS were strongly reduced

when compared to pUbiGUS. These results indicate a lower efficiency as reporter construct. The observed effects were in accordance with the literature, except for pIPKb005_GUS (Himmelbach *et al.*, 2007). It was reported that the expression of the epidermis specific *GstA1* promoter is higher in the evaluated tissue (Himmelbach *et al.*, 2007). Both versions of the 35S promoter were much less efficient than the *ubiquitin* promoter in the two approaches (Table R 6 and R 7). These results confirm the data of McElroy *et al.* (1991), which have described the low expression of this constitutive promoter in monocots. All in all, the pUbiGUS construct was confirmed as best reporter construct for transient assays based on particle bombardment.

Table R 7: Effect of the different promoters_GUS constructs on the staining/colour intensity of GUS stained cells

Construct	Promoter ¹	Normalized cell hue ²	p-value (t-test) ³	n ⁴
pUbiGUS	<i>Ubi</i>	23.80 ± 0.45 ⁵	-	133
pIPKb002_GUS	<i>Ubi</i>	14.07 ± 0.34	< 0.0001	85
pIPKb003_GUS	<i>Act</i>	12.42 ± 1.08	< 0.0001	12
pV668	35S	6.25 ± 0.20	< 0.0001	67
pIPKb004_GUS	d35S	9.75 ± 0.25	< 0.0001	84
pIPKb005_GUS	<i>GstA1</i>	3.90 ± 0.25	< 0.0001	4

¹ indicate the promoters used in the different constructs: *Ubi* – maize *ubiquitin* promoter, *Act* – rice *actin* promoter, 35S – Cauliflower mosaic virus (CaMV) 35S promoter, d35s – enhanced CaMV 35S promoter, *GstA1* –wheat *glutathione S-transferase A1* promoter

² cell hue values of selected cells were multiplied with the normalization factor (ratio of the total number of GUS (β -glucuronidase) stained cells to the total number of anthocyanin stained cells) to correct for the different shooting efficiencies of the constructs.

³ significance was assessed by unpaired two-tailed t-test against pUbiGUS with GraphPad Prism 7.01

⁴ total number of GUS stained cells selected for the analysis

⁵ mean values and the standard errors of the mean from the selected cells

Statistically significant results were highlighted in bold. p-value \leq 0.05

4. Discussion

4.1. Evaluation of the observed powdery mildew resistance

4.1.1. A critical view on the phenotyping approach

During the last decades, the importance of the research on natural diversity of modern crops achieved increasing attention because domestication and subsequent breeding led to a large reduction of the genetic diversity within the modern gene pool (McCouch *et al.*, 2013; Schmid *et al.*, 2018; Kilian *et al.*, 2006). The access to the genetic diversity increased constantly regarding high through-put and next-generation sequencing approaches (Cobb *et al.*, 2013). In the near future, not the genotyping will be the most limiting factor, instead it will be the time-consuming phenotyping procedures (Cobb *et al.*, 2013). In particular, the accuracy, the precision and the through-put of phenotyping approaches are a highly discussed topics (Rouphael *et al.*, 2018; Kumar *et al.*, 2015). The phenotyping is usually performed under field or controlled conditions (Cobb *et al.*, 2013). Both environmental set ups provide advantages and disadvantages. Cobb *et al.* (2013) summarized several factors that has to be considered in this context. Major advantages of controlled conditions, for examples greenhouse experiments, are the increased heritability, the maximized information with a minimum of replicates and the relatively easy implementation of automation and standardization approaches (Cobb *et al.*, 2013). Usually, most accurate and precise results within a reasonable limit to the cost were provided by controlled conditions (Cobb *et al.*, 2013). These parameters were from great importance for the application in high-resolution approaches like genome-wide-association (GWA) studies (Cobb *et al.*, 2013; Burghardt *et al.*, 2017). In this regard, it was decided to perform the phenotyping for the association study under controlled conditions (Figure R 2 and R 3 as well as Table B 1 and B 2).

The relevance of results generated under controlled conditions is controversially discussed in science. The minimized environmental variation that is investigated under these conditions, is advantage and disadvantage in the same moment in consideration of the precision and the relevance of the results for breeders and farmers, respectively (Cobb *et al.*, 2013; Kumar *et al.*, 2015). In field conditions, genotype X environment (GxE) interactions can be characterized in a wide range of environmental conditions to evaluate effects over time and space (Cobb *et al.*, 2013).

Another factor which has to be taken into account for the evaluation of resistance data is the developmental stage. In greenhouse experiments usually seedling phenotypes were analysed that was also the case in the present study (Figure R 2 and R 3 as well as Table B 1 and B 2). In contrast to field trials, where the phenotyping is frequently performed over the whole growing season. Besides the higher costs for field trials, also the time management has to be considered. In a greenhouse, experiments can be performed the whole year with minimal biological noise to

generate biological replicates (Cobb *et al.*, 2013). In contrast to field trials, where biological replicates were either generated at the same location over different years or at different locations in one year (Figure R 4 and Table B 3). For example, barley seedling powdery mildew assays need under controlled conditions approximately 2-3 weeks from sowing until scoring of the final disease symptoms. In a field trial with natural infection, the scoring can be performed after approximately 10 weeks. This scoring is performed at the adult plant stage because the natural infection of seedlings is usually low regarding the environmental conditions in early spring. This circumstance highlights, why seedling powdery mildew resistance is often considered as unimportant. Nevertheless, achieved insights about resistance mechanisms might be also important for the understanding of adult plant resistance. This is, for example, the case for *mlo* alleles, where negative pleiotropic effects were mainly observed in the adult plant but not in the seedling stage (Kusch & Panstruga, 2017).

Controlled conditions are often favoured to impose a specific stress. In particular, when plants should be inoculated with specific pathogen strains to achieve a higher precision (Cobb *et al.*, 2013). A careful consideration of the possible (epidemic) spread of these usually high virulent strains in the environment is necessary. Another important factor that is often ignored, is the interplay with other microorganisms (Panstruga & Kuhn, 2019). Under greenhouse conditions, the influence of pests as well as beneficial microorganisms is limited which might further increase the accuracy and precision of the results.

In the present study, the majority of the phenotyping was performed under controlled conditions in greenhouse experiments in consideration of the above stated advantages. In regard of the planned application of the phenotype data in a genome-wide-association study (GWAS), a high repeatability and heritability should be achieved. Therefore, the phenotyping was performed under standardized conditions on detached seedling leaves with specific powdery mildew isolates (Figure A 1). This set up is commonly used to analyse (mainly) race-specific powdery mildew resistance (Silvar *et al.*, 2011; Šurlan-Momirović *et al.*, 2016; Dreiseitl, 2017). Nevertheless, it was also successfully used in an association study to identify race-nonspecific resistance genes (Spies *et al.*, 2012). The method creates an artificial environment where the susceptibility of the investigated material is usually higher as in comparison to whole plants. This effect is partially caused by the horizontal position of the leaves which increased the accessible space for the fungal spores. Additionally, the cutting of the leaves could trigger wound responses probably altering the resistance. In case of race-specific resistances, these factors were usually less important based on the large and specific effects of the analysed genes. Regarding the small effects caused by polygenic resistance, which is highly dependent on the environment (Niks *et al.*, 2015, Aghnoum *et al.*, 2010), they have to be taken into consideration. In view of the indications that several

defence-related genes/proteins are involved in wound responses (van Loon *et al.*, 2006), it is possible that the wounding lead to enhanced or decreased powdery mildew resistance responses. This effect might be observed in general or in dependence of the genetic background. To minimize this effect, all leaf segments were processed in the same way in the present study. Additionally, the ends of the leaf segments were not inoculated and taken into the scoring area regarding the Teflon frames, which were positioned on top of the leaves (Figure A 1).

The enhanced susceptibility caused by the detached leaf assay per se was considered as advantage of the method. In general, the selected screening procedure aimed for the highest possible infection. To differentiated the resistance responses of the population poly-virulent isolates were selected. These isolates were virulent against many commonly used major resistance genes/specificities (Table M 2). Additionally, the basal part of the leaf was chosen for the inoculation because the younger areas are more susceptible (Figure A 1). In the sense of the highest possible infection, also an artificial maximal infection (*Max* trait) was generated *in silico* to better distinguish the (race-nonspecific) resistance responses (Figure R 3B). The initial characterization of the powdery mildew resistance responses of the 459 genotypes was performed with the German isolate D35/3 (Figure R 2 and Table B 1). This isolate display a high virulence regarding the virulence pattern on a commonly used differential set of barley. According to the data, which were provided by the JKI Kleinmachnow, the isolate is virulent against 12 major resistance genes/specificities commonly present in European material (Table M 2). The high virulence of the isolate seems to be represented in the results (Figure R 2 and Table B 1). More than 75 % of the material were classified as moderately susceptible or susceptible and only 8.1 % of the material was resistant (Figure R 2 and Table B 1). Nevertheless, the results have to be seen critically. This is necessary because the experiment was performed only in one biological replicate. The decision, to not repeat this experimental series, was made because the screening should provide only a rough overview about the variation of the powdery mildew resistance within the whole panel. In this sense, the obtained information was useful to guide the further selection of a smaller representative genotype panel. This panel was constituted by 267 genotypes and it was analysed in detail for the powdery mildew resistance of seedlings (Figure R 3 and Table B 2). In regard of the success of a similar approach (Spies *et al.*, 2012), two isolates were selected for the complete screening. The same isolate as for the initial test (D35/3) and additionally the Danish isolate RiIII was selected. Both isolates display distinct, complementing virulence patterns (Table M 2). Together, they were virulent against 22 commonly used major *R*-genes/resistance specificities based on the differential set. The presented results indicate that the two isolates were able to differentiate the responses for most genotypes (Figure R 3). To better evaluate the resistance responses, four resistance classes were defined (Table M 3). According to these classes,

more than 83 % of the material is either susceptible or moderately susceptible regarding the *Max* trait (Figure R 3). This result is in accordance with the initial screening and the high infection, which was aimed for. Additionally, the high virulence of the isolates could be represented by it. Nevertheless, the classification has to be considered carefully because the experiment was performed in several sub-experiments (Figure B 3), which makes a normalization necessary. The normalization depends on the variance of the resistance response of the control genotype. In this regard, it has an effect on the average of the test genotypes and thus on their classification. In the present study, the susceptible genotype Morex was used for the normalization. The overall standard deviation of the infected leaf area from all Morex values was 9.0 % and 9.4 % for D35/3 and RiIII, respectively. Nevertheless, the standard deviation of the mean values of the different sub-experiments, which were used for the normalization, was 5.7 % for the D35/3 and 3.5 % for the RiIII. These low values highlight that the genotype was similar susceptibility in all sub-experiments. The high repeatability presented here (Figure B 3) indicate that the analysed traits were reproducible under the selected conditions. Nonetheless, it has to be considered that the disease scoring was performed manually. In respect of the advanced development of image-based phenotyping systems (Awada *et al.*, 2018; Lee *et al.*, 2018; Nguyen *et al.*, 2018), probably a higher repeatability could be achieved nowadays. Additionally, the through-put could be increased with automated phenotyping systems. The low through-put was the major reason for the selection of a smaller genotype panel in the present study. The automation of phenotyping systems has improved through the recent progress in machine-learning (Lee *et al.*, 2018). Such automated phenotyping platforms allow a more precise quantification of the trait of interest. For example, in the majority of the published studies (including this work), powdery mildew is scored in rather poorly defined parameters like 'infected leaf area' (Panstruga & Kuhn, 2019). The semi-automated phenotyping platform, which is now available for the disease scoring of powdery mildew on detached cereal leaves (based on personal communication with S. Lück and D. Douchkov), increase the accuracy and precision of the phenotyping. In this regard, such system would have been beneficial in consideration of the application of the phenotype data in a GWAS. Nevertheless, also this automated system relies on detached leaves.

Non-invasive phenotyping methods, which could be used under field conditions were from higher interest for breeders and farmers (Awada *et al.*, 2018). Since such systems were not commonly available so far, Cobb *et al.* (2013) recommended the use of controlled conditions for the generation of hypotheses, which could be tested under field conditions with a reduced genotype panel. A similar set up was selected in the present study. A subset of 102 genotypes was assessed for the powdery mildew resistance under field conditions (Figure R 4 and Table B 3). In particular, this analysis was included in the study because of the focus on race-nonspecific resistance. This

type of resistance was described by different terms in the past. Examples are 'quantitative', 'field' and 'adult plant' resistance (Niks *et al.*, 2015; Chen, 2013; Jørgensen & Wolfe, 1994). Such classifications are not absolute because several different aspects were used to define them. Adult plant resistance usually describes the resistance conferred by several minor effect genes only active in the adult plant stage (Li *et al.*, 2014a). In this regard, the plants were susceptible in the seedling stage (Chen, 2013). This resistance type was studied for example in wheat against powdery mildew and leaf rust (Li *et al.*, 2014a) and in barley against powdery mildew (Gupta *et al.*, 2015). Probably the more interesting resistance type is the one which is independent of the developmental stage (Chen, 2013). Nevertheless, seedling as well as adult plant experiments were necessary for the confirmation of both resistance types. Field resistance is often described as resistance, which cannot be detected in greenhouse (seedling) assays (Chen, 2013). Nonetheless, these definitions/aspects have to be evaluated in respect of the dependence of resistance responses to sample size, environmental conditions and/or developmental stage (Niks *et al.*, 2015). Subtle changes in the resistance can be better observed in field trials regarding their polycyclic character and the sheer number of individuals that were analysed at the same time and place (Niks *et al.*, 2015). The high dependence of resistance responses on environmental factors is long known, but the understanding of its regulation is still limited. Resistance responses were influenced by light, temperature, the circadian clock and the overall cellular redox state (Roden & Ingle, 2009, Mazza & Ballaré, 2015; Hua, 2013). In this regard, the high temperature fluctuation, particularly during the night, can change observed resistance responses (Niks *et al.*, 2015). Probably, also seedling screenings might reveal so-called adult plant resistance genes under low temperature conditions (Niks *et al.*, 2015). Additionally, general developmental stage-dependent gene expression alterations have to be considered (Niks *et al.*, 2015).

Also in the present study, the association between the seedling and the adult plant resistance should be assessed. Additionally, it was tried to evaluate if the cultivars that were resistant in the seedling stage were also resistant in the adult plant stage. In this context, it has to be kept in mind that the seedling data were generated under controlled conditions and the adult plant resistance under field conditions (Figure R 4 and Table B 3). Thus, not only the developmental stage, but also the environment changed dramatically. The field trials were performed at two locations with natural powdery mildew infection (Figure R 4A). In contrast to a previous study (Spies *et al.*, 2012), only a moderate association ($r = 0.45$) was found between the greenhouse and field resistance data (Figure R 4B). QTLs with effective resistance against barley powdery mildew are highly depended on the developmental stage (Aghnoum *et al.*, 2010). The different growth rates of the tested genotypes led to a range of developmental stages present to the time point of scoring. Additionally, the planting in Bergen/Wohlde was performed one week earlier as in Gatersleben.

In this regard, not even within the field data the same developmental stage was analysed. In the present study this effect was not further investigated. In general, it is an advantage of seedling assays that different growth rates can be mostly neglected.

In what extent the observed association is influenced by the change of the developmental stage (within the data and between adult versus seedling resistance) cannot be really assessed with the selected approach. Particularly, because resistance is also highly dependent on the environmental conditions and the pathogen race (isolate) composition (Aghnoum *et al.*, 2010; Niks *et al.*, 2015). In respect of the natural infection, no information about the virulence of the infecting isolates is known. It would have been necessary to collect the field isolates and to test them on a differential set to achieve this detailed information. Although the high correlation coefficient ($r = 0.81$) between both field data sets indicate that the field isolates might had similar virulence patterns. Additionally, the high heritability (0.87) of the field data indicate that the observed resistance variation is mainly determined genetically. In regard of the presumed race-specific resistance responses of most genotypes and the observed shift of 55 % of the genotypes in their resistance classification, the isolate composition could be a major reason for the lower association as previously reported (Spies *et al.*, 2012). Additionally, the environmental conditions of both fields have to be considered (Figure A 2) because the basal as well as the *R*-gene mediated defences are regulated by light and temperature in mono- as well as in dicot plants (Wang *et al.*, 2009b; Xie *et al.*, 2011). Regarding the relative air humidity and average temperature, the conditions at both locations were similar to each other, but nearly twice as much rainfall was recorded in Bergen/Wohlde (Figure A 2). The recorded data in Bergen/Wohlde were similar to the general average conditions in Germany (<http://www.beste-reisezeit.org/pages/europa/deutschland.php>). In case of Gatersleben, the rainfall was too low, which indicate that the plant might have suffered under drought conditions. In general, drastically different conditions were detected on the fields regarding the well-watering conditions and stable temperatures in the greenhouse experiments. Temperature and rainfall can both influence the resistance responses. The effectiveness of R proteins is either up- or down regulated by high temperatures (Hua, 2013). Two weeks prior scoring (end of May), elevated temperatures were recorded at both locations (Figure A 2). During this time period, the upper soil was dried out, which could trigger drought stress responses in the plants. In the next two weeks more than 50 mm rainfall was recorded in Bergen/Wohlde, but only 13 mm in Gatersleben. This higher rainfall at Bergen/Wohlde might be responsible for the higher infection at this location (Figure R 4A). This presumption is based on the results of Barker *et al.* 1998, who detected a partial breakdown of the *mlo* resistance after sudden relief of drought stress. This breakdown is independent of the *mlo* allele but dependent on the genetic background (Barker *et al.*, (1998). The influence of other factors like the infection

pressure (based on higher spore density) and the interplay with other microorganisms was not evaluated so far. In sense of the sensible regulation of resistance responses, the moderate association (Figure R 4B) between the different phenotyping approaches could have been caused by several factors alone or in combination.

In respect of the discussed factors influencing the resistance (Aghnoum *et al.*, 2010; Niks *et al.*, 2015) and the achieved results, it was presumed that the controlled conditions provided precise resistance phenotype data. In recommendation of Cobb *et al.* (2013), the observed seedling resistance under controlled conditions was used to generate hypotheses, which were further validated under field conditions. In this sense, four genotypes were selected for a further characterization because of the high resistance at both field locations as well as in the seedling screenings. The additional analyses could mostly clarify the underlying resistance mechanisms (Figure R 5) and thus confirm the importance of the initial seedling resistance phenotyping.

4.1.2. Confirmation and postulation of resistance genes and their importance for barley breeding

Sustainable disease management in plants is a highly discussed topic of society. In particular, the provision of resistant cultivars is demanded to decrease the application of plant protection agents. In respect of the reduced genetic diversity in modern crops, plant genetic resources were more and more exploited (McCouch *et al.*, 2013; Schmid *et al.*, 2018; Kilian *et al.*, 2006). Wild relatives and locally adapted landraces provide a good source for new, sometimes superior, alleles (Zhang *et al.*, 2017; McCouch *et al.*, 2013; Kilian *et al.*, 2006). The access to such alleles offers a great chance for future sustainable plant breeding. In the context of disease resistance genes, the introgression of alleles from wild relatives and landraces proved to be beneficial since several decades (Jørgensen & Wolfe, 1994; Schmalenbach *et al.*, 2008; Friedt *et al.*, 2011).

The analysed genotype panel was highly diverse in respect of the biological/cultivation status and the growth habit (Figure R 1). Only one quarter of the material represents typical modern elite material (Figure R 1C). The remaining material is constituted mainly by landraces, traditional cultivars and wild barleys. In regard of the seedling resistance screenings, over 80 % of the material was moderately susceptible or susceptible (Figure R 3). This result has to be seen under the point that the highest possible powdery mildew infection should be achieved as discussed in the previous section. Interestingly, the majority of the elite material (88 %) was (moderately) susceptible under the tested conditions. In contrast to this, more than half of wild barleys were moderately resistant or resistant. This observation is in accordance with the literature because most of the important race-specific resistance genes were found initially in wild barleys or landraces (Jørgensen & Wolfe, 1994; Czembor *et al.*, 2000-2002). Furthermore, the powdery mildew screenings revealed several resistant genotypes which were analysed in more detail. This

step was included because interesting (new) alleles of known resistance genes might be hidden in the material. Additionally, race-specific resistant genotypes should be excluded from the GWAS panel to focus on the identification of race-nonspecific resistance loci. In the seedling screenings, more than 20 genotypes per isolate were considered as completely resistant (Figure R 3). Almost 30 % of this material is constituted by landraces (Figure R 3 and Table B 2). Furthermore, the four genotypes moderately resistant in the field and the greenhouse assays, were traditional or wild material (Figure R 4 and Table B 3). Nevertheless, the majority of the tested landraces (84 %) were moderately susceptible or susceptible in the greenhouse experiments (Figure R 3 and Table B 2). A similar distribution of phenotypes was described by Dreiseitl (2017) in a population of wild barleys.

The complete absence of disease symptoms observed in the seedling assays could be caused by race-specific resistance genes (Niks *et al.*, 2015). In this respect, the resistant genotypes were analysed regarding the race-specificity of their resistance responses. The comparison of the scored data from both isolates confirmed the race-specificity for nine lines. A possibility to further examine the race-specificity of the resistance would have been the analysis if the responses were accompanied by the development of intense brown spots or blotches. These symptoms can accompany hypersensitive responses (HR) which end with the death of the infected cells (Morel & Dangl, 1997). The resistance which is conferred by *Mildew resistance locus a* (*Mla*) alleles depends on HR reactions (Morel & Dangl, 1997) and it was reported that particularly these symptoms can be macroscopically visible (Lu *et al.*, 2016). Nevertheless, a classification of race-specificity based on phenotypic observations is rather unsure because unrelated general stress responses can also lead to similar phenotypes. Another approach to assess the race-specificity of the resistance is to determine if mutant *Mildew resistance locus o* (*Mlo*) alleles were present in the genotype panel (Figure R 6). Recessive mutations in the *Mlo* gene confer HR independent, broad-spectrum and race-nonspecific resistance against *Bgh* based on the formation of cell wall appositions (Jørgensen, 1992). The prevalent *mlo* alleles are the chemical induced *mlo-9* allele and the natural occurring *mlo-11* allele (Kusch & Panstruga, 2017; Reinstädler *et al.*, 2010). In respect of the diverse panel and the high percentage of landraces, it was hypothesized that several resistances could be caused by this natural allele. Six of the eleven identified *mlo-11* carriers were classified as landraces and wild barleys, four as breeding material and one as traditional cultivar, respectively (Figure R 6 and Table A 1). In the latter five genotypes the *mlo-11* was introduced specifically into the gene pool. The other six genotypes might had been interesting for breeders, but in view that the resistance causing allele is already widely used, they were not valuable anymore. This prior knowledge about the underlying resistance source probably saved resources regarding the high cost for the development of new varieties.

To further characterize the resistance of the remaining ten genotypes, tests with seven additional powdery mildew isolates were performed (Table R 1). The assessment of a population with various isolates allows the postulation of underlying resistance genes/alleles in dependence of the resistance complexity (Šurlan-Momirović *et al.*, 2016; Silvar *et al.*, 2011; Dreiseitl, 2017). For instance, Šurlan-Momirović *et al.* (2016) reported that nine isolates were sufficient to distinguish the major resistance spectra of the 'Serbian GenBank' barley collection. In total, the resistance spectra of the ten resistant and the two control genotypes were determined in response to nine powdery mildew isolates (Figure R 6, Table B 2 and R 1). Morex was included to control the inoculation efficiency because no resistance specificity has been reported so far in this particular genotype. A comparison of the resistance spectra of Roland (Table R 1) and the differential barley accession P08B revealed a high similarity between both susceptibility patterns. This observation confirms the potential of the approach because the presence of the *Mla9* specificity was reported in both lines (Hovmøller *et al.*, 2000). WB-043, WB-065, WB-226 and WB-385 displayed very similar resistance spectra among each other (Table R 1) and to the differential accession P01. In this differential genotype, the *Mla1* specificity is present which is also referred as *MI(AI2)* (Jørgensen & Wolfe, 1994). WB-043 represents the cultivar Algerian that is the main donor of the *Mla1* specificity (Jørgensen & Wolfe, 1994; Wiberg, 1974). Additionally, it is an ancestor of the cultivar Tyra (WB-226, <https://www.lfl.bayern.de/mam/cms07/ipz/dateien/abstgerste.pdf>), for which the same specificity was annotated (Hovmøller *et al.*, 2000). Wiberg (1974) stated the presence of *Mla1* also in MAROCAINE O79 (WB-065). In respect of these characterizations, the resistance observed in the Algerian cultivar/landrace ALGER 48 (WB-385) is also considered as *Mla1* based. The resistance spectra of WB-307 (W 23833/2196 11) and WB-499 (HID144) were nearly identical (Table R 1). Both spectra display similarities to the resistance spectrum of SI-3. WB-499 is an Iranian wild barley and WB-307 is classified as Israeli advanced/improved cultivar. The lack of a more distinct resistance spectra could be related to the European origin of the isolates. It was reported that the absence of isolates coming from the same region as the resistant genotypes could result in missing compatible (susceptible) reactions in wild barleys (Dreiseitl & Dinooor, 2004). Additional tests with isolates better adapted to Mediterranean resistance genes could confirm this hypothesis. Similar results were achieved for the Israeli cultivar MR 3/51 (WB-305, Table R 1). Also for this genotype, it was not possible to postulate a resistance gene/specificity because none of spectra of the differential panel was comparable. Nevertheless, the observed resistance spectra of all three genotypes indicate the presence of race-specific resistance genes. These probably uncharacterized genes might be valuable for breeders, particularly because all three genotypes were only susceptible against one of the nine tested powdery mildew isolates (Table R 1).

Besides the identification of these seven genotypes with clear race-specific resistances, the presence of three *mlo* mutants was presumed (Table R 1). The *mlo-9* allele was introduced in the German cultivar Barke (WB-510, Silvar *et al.*, 2009). In case of the landraces WB-352 (IG 32742) and WB-358 (Soggio Soudan (B) S.G. 147/49), the subsequent analyses supported this presumption, too (Figure R 7 to R 11). The observed resistance of both genotypes is abolished by the transient complementation with a functional *Mlo* allele (Figure R 7). This effect was reported in the past for other *mlo* mutants (Spies *et al.*, 2012; Ge *et al.*, 2016). In case of WB-358, the sequencing of the allele revealed an insertion interrupting the C-terminal calmodulin binding motive (Figure R 8A). It was assumed that this mutation led to aberrant Mlo proteins causing the resistance. In general, calcium signalling plays an important role in the regulation of plant defence responses (Stael *et al.*, 2015; Poovaiah *et al.*, 2013). Additionally, it is important for the Mlo function and the *mlo* conferred resistance (Kusch & Panstruga, 2017; Freymark *et al.*, 2007; Kim *et al.*, 2002a). A dysfunctional calmodulin binding motive, halves the Mlo ability to negatively regulate defence responses but did not suppress it completely (Kim *et al.*, 2002b). The presented data are in accordance with this finding because the resistance observed in WB-358 was only partial (Table R 1). Similar observations were reported for the *mlo-12* and *mlo-28* mutants (Piffanelli *et al.*, 2002).

The sequencing of the WB-352 allele revealed a functional *Mlo* copy which is identical to the Morex allele (Figure R 8A). The following analyses indicated the presence of a (at least) partial *Mlo* copy/paralog (Figure R 9 to R 11). This copy seems to constitute a repeat array of the first eight exons and introns. Nevertheless, the complete structure could not be determined so far (Figure R 11). The presence of a repeat array and the detected reduced transcript level of the functional *Mlo* allele in WB-352 resemble the features described for the *mlo-11* mutant (Piffanelli *et al.*, 2004). It was proposed that the functional *Mlo* transcript is downregulated in this mutant because of transcriptional interference (Peterhänsel & Lahaye, 2005). Nonetheless, whether or not a similar mechanism is causing the *mlo*-like phenotype in WB-352 is still an open question. Besides transcriptional interference, also homology-dependent gene silencing or chromatin remodelling activities could cause the observed transcript reduction (Figure R 10). The presented results suggest that the events leading to the *mlo-11* mutation and the WB-352 specific *mlo* duplication occurred independently from each other. The functional *Mlo* copies belong to different clades and the repeat array of *mlo-11* encompass only the first five (Piffanelli *et al.*, 2004) instead of the first eight exons and introns (Figure R 11).

Until now, 40 different *mlo* alleles were described (Reinstädler *et al.*, 2010). Nevertheless, only *mlo-11* and its variant *mlo-11 (cnv2)* are natural alleles and they were initially found in Ethiopian landraces (Jørgensen, 1992; Ge *et al.*, 2016). For every *mlo* mutant, pleiotropic negative trade-offs

were described which lead to yield penalties. It was speculated that these trade-offs are the reason why the natural alleles are absent in natural populations everywhere else except the country of origin (Brown, 2015). Despite this, it was possible to identify two novel natural *mlo* alleles in a Syrian (WB-352) and a Sudanese (WB-358) landrace (Figure R 9 to R 11). The results indicate that both new alleles are distinct mutations. This implies that *mlo* mutations occurred indeed several times independently from each other in nature. Because both novel alleles were not described before, it was presumed that they occur only in low frequencies in their countries of origin. Similar observations were state for the Ethiopian *mlo-11* mutation (Negassa, 1985). Until now, the question of the negative trade-offs in the here described mutants has not been addressed because the genetic background has to be considered. In landraces, unfavourable alleles are often present. In order to distinguish between the negative effects of the *mlo* alleles and the general response of the material, it would be preferable to introgress the alleles into modern high yielding material. It seems to exist a correlation between the conferred powdery mildew resistance level and the strength of the negative pleiotropic effects (Kusch & Panstruga, 2017). In particular for plant breeders this aspect is important. Regarding the presumption that the novel allele of WB-358 is a weak *mlo* allele, this genotype might hold value for further plant breeding approaches. Nonetheless, further tests were required to evaluate if the positive and negative effects of the *mlo* mutation were more in balance in WB-358 or WB-352.

As in the previous section discussed, four genotypes were moderately resistant/resistant at both field locations as well as in the seedling assays. An additional screening with 27 European powdery mildew isolates should assess the race-specificity of the observed resistance (Figure R 5 and Table B 4). All four genotypes provided a strong resistance for most of the isolates. Nevertheless, this effect could depend on the origins of the isolate set as it was stated before for wild barleys (Dreiseitl & Dinooor, 2004). The Ethiopian landraces HOR 2573 (WB-052) was resistant against all tested isolates (Figure R 5 and Table B 4). It was described that the resistance is HR dependent (Spies *et al.*, 2012). Recently, the genotype was published as donor of the *MILa-H* resistance (Hoseinzadeh *et al.*, 2019). Based on the reported data, it is expected that the responsible QTL provides protection against almost all European powdery mildew isolates. In sense that the QTL was not used in breeding approaches so far, the landrace WB-052 is a valuable resource. Probably no European isolate is currently adapted to the underlying resistance gene in regard of the low selection pressure.

A similar effect is observed for the Moroccan genotype WB-066 (MAROCCO) which is resistant against 26 isolates (Figure R 5 and Table B 4). Nonetheless, it is assumed that another set of (better adapted) isolates could break the resistance. The observed resistance spectrum was similar to the ones of the differential lines P20, SI-1 and Camilla. According to Dreiseitl (2015), the

resistances of SI-1 and Camilla were conferred by the *Ml(SI-1)* resistance gene/specificity. Until now, this resistance gene is not further characterized. In contrast, the resistance of P20 is conferred by *Mlat* (from Atlas, Jørgensen & Wolfe, 1994). The gene was mapped to chromosome 1H (Jørgensen & Wolfe, 1994), but the exact gene position is still unknown. In this regard, the genotype data could not provide further information. Nevertheless, *Mlat* is one of the prevalent resistance genes in landraces of Egypt and Morocco (Czembor, 2000; Czembor, 2002). Based on this information, it was assumed that the observed resistance of the traditional cultivar/landrace is also conferred by *Mlat*. The here presented data indicate that until now European powdery mildew isolates were not fully adapted to this resistance gene. In this sense, the gene could be valuable for breeders.

In case of the Turkish genotype WB-476, it was not possible to postulate a resistance gene because of the heterogeneous responses to nine isolates (Figure R 5 and Table B 4). Until now it could be not finally determined if the effect is caused by real heterogeneous responses of the material or if the used seed stock was contaminated. The morphological analysis of the genotype during the field experiments revealed also in this regard heterogenous phenotypes, in addition to the heterogenous resistance responses. This observation supports the presumed seed contamination with another genotype. Nevertheless, this did not exclude completely the possibility of real heterogeneous responses. The phenomenon of heterogeneity of powdery mildew resistance responses was addressed by Dreiseitl (2017). In a subset of the tested wild barley collection more than one resistance phenotype was observed in single seed descendants (Dreiseitl, 2017). Also the seed batch of WB-476 used in the present study, was generated from single seed descendants by cooperation partners. This method is expected to minimize the number of segregating (resistance) loci to a level which is ignorable in practice. Dreiseitl (2017) speculated that the heterogeneity observed in the wild barleys is caused by the open flowering nature of *Hordeum vulgare* subsp. *spontaneum*. Another possibility for the here presented heterogeneous responses is a meiotic instable mutation like proposed for the *mlo-11* allele (Piffanelli *et al.*, 2004). If *mlo-11* plants are self-fertilized, a low percentage of fully susceptible progenies is obtained (Piffanelli *et al.*, 2004). According to the published data (<https://urgi.versailles.inra.fr/gnpis-core/#accessionCard/id=aHR0cHM6Ly9kb2kub3JnLzEwLjE1NDUOL0NRWlILMg==>), WB-476 represents the genotype HOR 3270. It is classified as Turkish wild barley, which would support the hypothesis of true heterogenous responses as described by Dreiseitl (2017). In contrast, HOR 3270 is also annotated as Turkish Breeding line 'Svalöfs 53/510-44' in accordance to the GIBIS database (<https://gbis.ipk-gatersleben.de/gbis2i/faces/index.jsf>). Despite the biological status, Spies *et al.* (2012) reported an HR dependent resistance response of the genotype. This observation suggests

of the presence of a not further specified race-specific resistance gene, which might be interesting for plant breeders.

The Ethiopian landrace HOR 5428 (WB-400) displays a moderate susceptibility against all isolates (Figure R 5 and Table B 4). The prevalence of such a resistance response was observed in several landrace collections and it is usually interpreted as indicator for partial resistance (Silvar *et al.*, 2011; Šurlan-Momirović *et al.*, 2016). Over the time, partial resistance was described by many terms like ‘race-nonspecific’, ‘quantitative’ or ‘adult plant’ resistance (Jørgensen & Wolfe, 1994; Niks *et al.*, 2015). Although in the pure term of use, it is just a description of the incomplete resistance phenotype (Parlevliet, 1985; Jørgensen & Wolfe, 1994). As discussed in the previous section, the extent of resistance responses is influenced by many factors (Niks *et al.*, 2015). In this regard, polygenic as well as monogenic resistance genes could be causal for the observed resistance (Niks *et al.*, 2015; Kou & Wang, 2010). A further investigation of the genotype in biparental crosses or with additional isolates adapted to Mediterranean resistance genes might shed light on the underlying resistance mechanism. In context of the unclear resistance mechanism, monitoring of the extent of the observed moderate susceptibility and its durability could be from special interest for breeders.

The investigation of the diverse Whealbi population revealed different types of powdery mildew resistance responses (Figure R 2 to R 4). This information might be valuable for plant breeders. It was possible to confirm or to postulate 19 race-specific resistances of mainly previously identified resistance genes as well as 14 race-nonspecific *mlo* based resistances (Figure R 5 to R 11 and Table R 1). Additionally, two novel *mlo* alleles could be described (Figure R 6 to R 11). In this respect, one of the major aims of the study was achieved. In particular, eight genotypes were identified as potentially interesting material for plant breeders. These genotypes provide novel or less common genetic material which could be applied for the generation of new breeding material that can hopefully ends with the release of a new variety.

4.2. Population structure in diverse barley material

Natural diverse material holds a great potential for plant breeding (McCouch *et al.*, 2013). In wild relatives and locally adapted landraces new, sometimes superior, alleles can be found (Zhang *et al.*, 2017; McCouch *et al.*, 2013; Kilian *et al.*, 2006). Nonetheless, the unlocking of this potential can be quite difficult. GWA studies proved to be very versatile in this respect (Huang & Wang, 2014). With GWA studies it is possible to identify QTLs or causal genes involved in the trait of interest in large and diverse populations (Huang & Wang, 2014).

The Whealbi population encompasses material from several organizations/institutions and it was collected to provide access to the most relevant genetic diversity for European agriculture (<https://www.whealbi.eu/plant-diversity/key-facts/>). The collection encompasses typical modern

elite material as well as landraces, traditional cultivars and wild barleys. (Figure R 1A). This composition might have a strong influence on the success of the performed GWAS because a principle component analysis of the diverse barley material stored in the German federal ex situ genebank at IPK Gatersleben revealed a clear genetic differentiation of domesticated and wild material (Milner *et al.*, 2019). In this regard, a careful assessment of the genetic relatedness and the population structure is necessary in association studies (Burghardt *et al.*, 2017). When both aspects were not adequately corrected, synthetic associations can occur because genotypes share causal and noncausal markers (Price *et al.*, 2010; Vilhjálmsson & Nordberg, 2013; Korte & Farlow, 2013).

The diversity of the Whealbi collection is not restricted to the biological/cultivation status. In addition, the material is diverse in regard of the growth habit. Particularly, the wild material displays a spring like growth habit, which is also predominantly in the presented population (Figure R 1B). This observation is in contrast to the stated prevalence of the winter growth habit of wild material (Pourkheirandish & Komatsuda, 2007). The majority of the genotypes that show a winter annual growth habit in the present population, corresponded to breeder's material or advanced/improved cultivars (Table A 1). Another important diversity factor could be the row type. The present population includes two- as well as six-rowed barleys. Nevertheless, the influence of this diversity factor was not further addressed in the present study.

It was reported that barley populations display also a strong differentiation according to the origin of the material (Russell *et al.*, 2016; Schmid *et al.*, 2018). The here presented material originated worldwide (Figure B 1 and Table A 1). Nearly, a quarter of the material originated either in Europe or in the Middle East, respectively. Almost all genotypes, whose origins were annotated in Afrika, came from Ethiopia (36 %) or the northern regions (50 %). In more detail, these northern African origins corresponded to Egypt, Morocco and Libya. The Mediterranean region and Ethiopia are considered as second domestication origins based on the high diversity of landraces and wild barleys originating in these regions (Schmid *et al.*, 2018). A structuring of the population due to its origin may indicate local adaptations to specific environments (Russell *et al.*, 2016; Zhang *et al.*, 2017). In this regard, it was proposed to restrict diversity panels to genotypes belonging to the same genetic cluster, which often correlates with the geographical origin (Bartoli & Roux, 2017). In those panels, the resolution as well as the power might be increased because the probability of genetic and/or allelic heterogeneity is reduced (Brachi *et al.*, 2013; Bartoli & Roux, 2017). In general, heterogeneity influences strongly the detection of associated markers (Brachi *et al.*, 2011). Rajaraman *et al.* (2018) reported such an approach. They selected 76 landraces and 127 cultivars of the Whealbi collection, but analysed them in separate GWA studies to identify associations responsible for the powdery mildew adaptation of their candidate genes (Rajaraman

et al., 2018). With this approach they were able to identify associated single nucleotide polymorphisms (SNPs), which were distinct between the two groups (Rajaraman *et al.*, 2018). These results highlight that probably higher power and better resolution would have been achieved if the here present population were divided in different sub-populations regarding the specified biological status. It is possible that the effects of different markers negate each other because of opposing effects on the phenotype (Korte & Farlow, 2013). The advantage of the here present approach lay in the circumstance that with a high probability the identified associations were independent from effects of, for example, the biological status.

In respect of the phenotyping through-put, a reduced genotype panel was selected. The selection was based on the distribution of powdery mildew responses (Figure R 2) and not on genetic clusters as recommended by (Bartoli & Roux, 2017). The reduced panel represented the same characteristics as the complete population regarding biological status and growth habit (Figure R 1). The subsequent characterization of the powdery mildew resistant genotypes (Figure B 4 to B 11), led to the exclusion of 21 genotypes from the panel to focus on the identification of novel race-nonspecific associations. Further reduced was the panel because no exome capture data were provided for 47 genotypes (Bustos-Korts *et al.*, accepted). This led to a final set of 201 genotypes selected for the GWAS.

Besides the cultivation status and the geographical origin (Milner *et al.*, 2019; Spies *et al.*, 2012), other determinants for the structuring of a barley population can be the row type (Wang *et al.*, 2012; Bengtsson *et al.*, 2017) and the growth habit (Rostoks *et al.*, 2006). In some cases, also a combination of these factors is observed (Pasam *et al.*, 2012). Accordingly to the cited literature, the population structures were mainly estimated by a Bayesian approach implemented in the program STRUCTURE (Pritchard *et al.*, 2000) or by principle component analyses. In contrast, the GWAS of present work relayed solely on a genetic relatedness matrix (Figure B 4) based on the Rogers' distance (Rogers, 1972). It has been shown that the Rogers' distance (Rogers, 1972) is appropriated to uncover pedigree relationships between, for example, essentially derived varieties in plants (Reif *et al.*, 2005). The Rogers' distance matrix was used for the estimation of the population structure present in the dataset. In addition, the associations between the Rogers' and the phenotypic distances were calculated. Slight positive correlations between the phenotypic distances of the three traits (*Max*, *RiIII* and *D35/3*) and the genetic distance were observed. In respect of their small magnitudes ($r_{Max} = 0.19$, $r_{RiIII} = 0.15$, $r_{D35/3} = 0.13$), a marginal impact of population structure on the detection power of the GWAS is expected for the studied population. Based on the Rogers' distance, the selected panel of 201 genotypes is clearly divided in two groups (Figure B 4). A small deme of 28 genotypes was assumed to be present within the population. The sub-population is constituted mainly by traditional cultivars and

landraces from South East Asia (75 %) and wild material (18 %) from the Middle East. Landraces and wild barleys often display a distinct genetical pattern in regard of their geographical origin (Russell *et al.*, 2016; Poets *et al.*, 2015). This effect varies between different populations because the genetic architecture of cultivated barley is shaped by a mosaic-like pattern. This pattern is partly caused by the ancient unequal contributions of several wild source populations to the modern gene pool (Poets *et al.*, 2015). Additionally, the natural gene flow between wild and cultivated barleys in the same geographical regions contributes of this pattern (Schmid *et al.*, 2018). Furthermore, recent introgressions of wild alleles in the modern gene pool increased the admixture between ancient and cultivated material (Poets *et al.*, 2015). In this respect, the difference in the genetic background of the two subpopulations could be caused by the heterogeneous selection of the Asian material or by genetic drift as a result of complete or partial isolation of the Asian material (Papa, 2005).

As discussed in section 4.1.1., the diverse population spans the complete range of susceptibility against powdery mildew (Figure R 2 and R 3). Similar effects have been observed in different studies before (Spies *et al.*, 2012; Bengtsson *et al.*, 2017). In contrast to another study (Bengtsson *et al.*, 2017), the subpopulation displayed no effect regarding of the powdery mildew resistance. The average infected leaf area of the identified sub-population is 46.0 ± 20.3 %, which is almost identical to the average infected leaf area of the whole population (45.4 ± 19.4 %).

In the here presented study, a rather low structure of the population into two groups was presumed. Other studies reported a higher structuring of diverse barley material (Milner *et al.*, 2019; Spies *et al.*, 2012; Pasam *et al.*, 2012). The Rogers' distance of the present panel (Figure B 4) indicate also a further sub-clustering of the population. The genetic distance differences between these small clusters were less pronounced as for the selected two groups. Nevertheless, in respect of the approach proposed by Bartoli & Roux (2017) and the effects recently reported by Rajaraman *et al.* (2018), a further division in smaller clusters (Figure B 4) might have yielded in better resolution and power, when they had been analysed in separate association studies. To test this hypothesis, further investigation would be necessary.

4.3. Pitfalls of genome-wide-association studies

Association studies proved to be versatile in human, animal and plant science (Zhu *et al.*, 2008; Myles *et al.*, 2009). GWA studies are a common method since about 20 years and have earned special interest during the last decade (Burghardt *et al.*, 2017). In barley, candidate genes for various important agronomical traits (Wang *et al.*, 2012; Pasam *et al.*, 2012) as well as for disease resistance (Turuspekov *et al.*, 2016; Bengtsson *et al.*, 2017; Spies *et al.*, 2012) have been identified with this method.

The reliability of the genotype and the phenotype data are essential for the success of a GWAS (Burghardt *et al.*, 2017). For the provision of the genotype data, several types of marker were established overtime, but single nucleotide polymorphisms (SNPs) have distinct features which were advantageous for association studies (Nadeem *et al.*, 2018). Particularly, their abundance through the complete genome make them beneficial for GWA studies. In this respect, SNPs are versatile since a complete sequencing of highly repetitive genomes like the barley genome is still not affordable for large populations. As alternative, exome capture data were established (Warr *et al.*, 2015). Mascher *et al.* (2013) published an exome capture platform which reduces the complexity of the barley genome by 50-fold and the method was used successfully in association studies by Pankin *et al.* (2014) and Russell *et al.* (2016). Also, the present genotype data were generated according to this method (Bustos-Korts *et al.*, accepted). Normally, the exome represents 1-2 % of the genome (Warr *et al.*, 2015). In case of the method described by Mascher *et al.* (2013), 1.23 % of the barley genome is enriched with the platform. About 56 % of the captured exons correspond to high confidence and 27 % to low confidence genes (Mascher *et al.*, 2013). The remaining captured space (17 %) was not located in annotated exons (Mascher *et al.*, 2013). These regions could correspond to the origin of regulatory RNAs or non-coding sequences like 5' and 3' untranslated regions or promoter sequences. Additionally, they might correspond to genes, which were not present or annotated in Morex because also full-length cDNA sequences of the cultivar Haruna Nijo were included in the array design (Mascher *et al.*, 2013).

For the present GWAS (Figure R 12), a final set of 424,567 SNPs were selected on the basis of the described quality criteria (section 2.5.1). This leads to a SNP frequency of 6.89 SNPs/kb, in respect of the captured exome space of 61.6 mega base pairs (Mascher *et al.*, 2013). According to Barker & Edwards (2009), SNP frequencies in barley ranges from 5-12 SNPs/kb and the average SNP frequency was determined as 6.3 SNPs/kb. In this regard, it was presumed that the presented SNP density was suitable for a GWAS. In the present data set, no information about insertions, deletions or other structural variants were available. Nevertheless, a further investigation of these markers might be interesting because they can be causal markers (Hartmann *et al.*, 2017).

The principle of linkage disequilibrium (LD) plays an important role in association analyses and the LD within a population is influenced by several factors (Flint-Garcia *et al.*, 2003). Examples for such factors are the recombination frequency and the mating system (Flint-Garcia *et al.*, 2003). Cultivated barley is predominantly a selfing species, in contrast to wild barley which displays a high outcrossing rate (Brown *et al.*, 1978). In general, effective recombination rates are lower in selfing species (Flint-Garcia *et al.*, 2003). This leads to a higher extent of LD in cultivated barley. Moreover, the number of SNPs necessary for a GWAS is mainly determined by the LD and in consequence, a higher number of markers are necessary for outcrossing species (Flint-Garcia *et*

al., 2003). Besides this, the extent of LD determines also the resolution of a GWAS which is generally higher in studies with wild relatives (Flint-Garcia *et al.*, 2003). In regard of previous studies (Comadran *et al.*, 2009; Pasam *et al.*, 2012) and the mixed composition of the population where the percentage of landraces and wild material is increased (Figure R 1), a rather low LD can be expected. Nevertheless, a detailed analysis of the LD decay was not done until now. In frame of the determination of the significance threshold for marker-trait associations (Figure R 12), the number of independent tests (Gao *et al.*, 2008) was estimated as 1,414. This calculation was performed with chromosome wide computed LD matrices.

Besides the selection of suitable genotype data, the reliability of the phenotype data is also from essential importance for the success of a GWAS (Burghardt *et al.*, 2017). As discussed in section 4.1.1, the resistance against powdery mildew is strongly influenced by plant age, environmental conditions and the virulence of the used isolate (Aghnoum *et al.*, 2010). In regard that all three factors can be controlled in greenhouse experiments, the phenotype data were generated under controlled conditions to achieve more precise and accurate data. Nevertheless, also phenotype data scored in trials have been used successfully to identify resistance candidate genes/QTLs in the present pathosystem (Gupta *et al.*, 2018; Bengtsson *et al.*, 2017; Gupta *et al.*, 2015). The advantages and disadvantages of the selected phenotyping approaches are discussed in section 4.1.1. As measure of the quality, the heritability and repeatability of the phenotype data can be used (Piepho & Möhring, 2007). The here presented high repeatability (0.65-0.95) and heritability values (0.87-0.88) for both isolate data sets (Figure B 3) indicate that powdery mildew resistance is a reproducible trait and that a high percentage of the phenotypic variation is explained genetically. These results were in accordance with previous studies (Hoseinzadeh *et al.*, 2019; Bengtsson *et al.*, 2017). Nevertheless, in the present study only a part of the heritability is explained by the significant associations per candidate (Figure R 15 and Table B 8). The 'missing heritability problem' is reported for many GWA studies and can be caused by several factors (Brachi *et al.*, 2011, Gibson, 2012; Korte & Farlow, 2013). One of these factors is the occurrence of rare variants. In the present study, they were filtered out prior to model fitting. In this respect, markers having minor allele frequencies below to the predefined threshold of 5% were discarded from analyses.

The selection of a suitable statistical model is another important aspect. Many studies have been performed to determine the best option. Linear mixed models as proposed by Yu *et al.* (2006) are nowadays regularly used in plant science and provide often the most reliable results (Yu *et al.*, 2006; Stich *et al.*, 2008; Wang *et al.*, 2012). For this reason, a mixed model approach was also chosen in the present study. It was decided to fit the model for the single isolate data separately as well as for the *Max* trait (Figure R 12). Nevertheless, the determination of the candidate genes

relied only on the *Max* trait. This decision was based on the hypothesis that the corresponding peaks represent rather race-nonspecific associations because the *Max* trait combines the effects of both isolates. The detection of clear race-specific peaks in the single isolate sets support this hypothesis (Figure R 12 and Table B 5). As described in section 4.1., the selected phenotyping approach should identify race-specific resistances (Table R 1 and Figure R 5). Nevertheless, the approach led only to the identification of (race-specific) resistant genotypes when at least one isolate was virulent. For the GWAS panel, the genotypes, which were resistant against both isolates were excluded, but the small subgroup of genotypes, which were susceptible against only one isolate were included. In this regard, the selected approach was performed inconsequently. The decision was based on the assumption that the partial overcome of the responsible major *R*-gene(s) will not lead to a clear peak in the GWAS or that it will be possible to identify the corresponding GWAS peak(s). This seems to be the case (Figure R 12). Additionally, in view of the variance of resistance responses, it has to be considered that more genotypes might have been excluded from the panel. As alternative approach, the complete material could have been used and the race-specific peaks were identified afterwards. The clear identification of such peaks in the present data (Figure R 12) indicate that this alternative approach might have been superior. The significantly associated SNPs on chromosome 2H (Figure R 12 and Table B 5) co-localize with the potential causal genes of the *MILa-H* resistance (Hoseinzadeh *et al.*, 2019). The described donor of this resistance is WB-052 (HOR 2573), one of the partial resistant genotypes. Nonetheless, the significantly associated SNPs of the this peak in the RIII and D35/3 traits were not significant in the *Max* trait. This observation supports the presumption that the peaks in this trait correspond mainly to race-nonspecific associations. Additional supporting evidence in favour of the hypothesis is that none of the SNPs located in *Mlo* locus or near the *Mla* locus were significantly associated (Figure R 12 and Table B 5).

The 70 SNPs that were significantly associated with the *Max* trait cluster in 16 loci and were distributed over 6 chromosomes (Figure R 12 and Table B 5). The strong LD pattern among the SNPs located in one locus (Figure B 5) could be caused by physical linkage, a functional correlation of the SNPs or the genetic relatedness of the genotypes. Additionally, the analysis revealed further a moderate LD of the significant SNPs between different chromosomes (Figure B 5). This LD could be a result of genetic drift or a co-selection of different loci. Moreover, the genetic heterogeneity of the population has to be considered. Indirect associations as a result of a disequilibrium between multiple factors, epistasis and population structure, are statistically true, reproducible associations instead of false positives ones (Platt *et al.*, 2010). These associations are independent of sample size and marker density (Platt *et al.*, 2010). Additionally, the occurrence of more than one causal marker/gene has to be taken into account since genetically quantitative resistance is

conferred by several minor effect genes (polygenic). Also, pleiotropic effects have to be considered in regard that various defence-related genes are involved in several biotic and abiotic stress responses (van Loon *et al.*, 2006). If any of the identified SNP is such a synthetic association was not further investigated because only the most promising candidates were selected for the validations.

One of the studies aims was to assess if a GWAS is feasible in such diverse barley material. The achieved results highlight the success of the selected approach. It was possible to identify 214 SNPs which were significantly associated in at least one of the three analysed traits (Table B 5). Seventy of these significantly associated SNPs were regarded as potentially race-nonspecific associations. The diverse material provided at least two alleles per defined candidate gene (Table R 2) and the results indicate for the four most promising candidates a clear association with resistance (Figure R 15). These identified candidates could be validated in *in silico*, *in vitro* and *in planta* assays (discussed in section 4.4). In respect of these results, it can be stated that a GWAS in a highly diverse barley population is feasible.

4.4. Possible new players in the regulation of defence responses in the barley-powdery mildew pathosystem

4.4.1. Relevance of the identified candidate genes

To assess the effect of the 70 significant associated SNPs (Table B 5), it was analysed if they are located in annotated gene models (current reference genome, Mascher *et al.*, 2017). Fifty of the 70 significantly associated SNPs were located in 33 gene models (Table R 2 and Table B 6). According to their annotated functions, they are involved in various processes (Figure D 1).

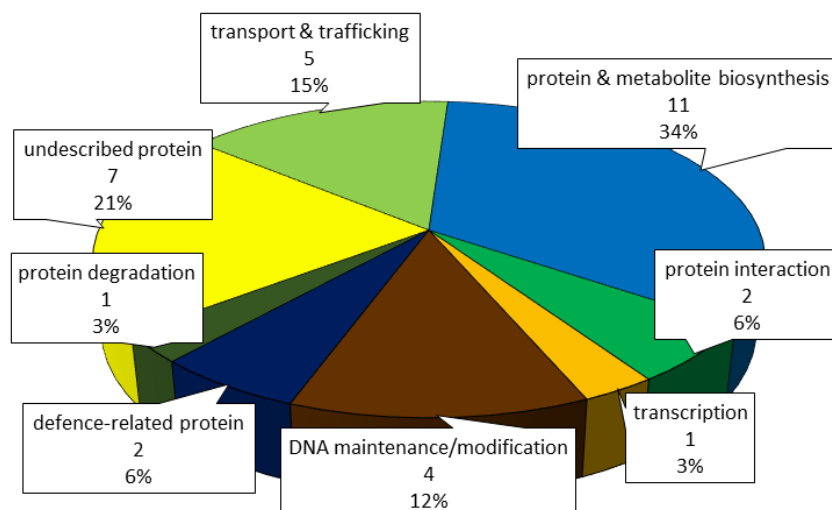


Figure D 1: Classification of the 33 candidate genes according to their annotated functions

The 33 candidates were summarized into eight groups in regard of their potential functions and the total number as well as the proportion of the candidates per group is depicted.

The functional annotations are based mostly on sequence homology to conserved domains which did not provide information about the real biological function of the candidates. As an example,

one protein was annotated according to a conserved protein- protein interaction domain involved in diverse processes like transcriptional regulation, cytoskeleton dynamics and ubiquitination (Stogios *et al.*, 2005). In addition, it has to be considered that these 33 candidate genes were clustered into 16 loci encompassing one to twelve genes (Figure R 12 and Table R 2). If several candidate genes form a locus it could be a result of a high LD between the corresponding markers or because more than one gene is involved in the trait of interest. The analysis of the LD between the significant SNPs (Figure B 5) indicates that maybe both factors apply. In respect of this circumstance, a further prioritizing of the candidates was necessary.

The first step in the prioritizing approach was the attempt to confirm the annotated gene models based on cDNA clones, expressed sequence tags (ESTs) and (predicted) genes in related species (Table B 6). Only from five out of twelve candidate genes with confirmed annotation it was possible to amplify full-length genomic as well as short cDNA products (Figure B 6). It was decided to focus on the four candidates of chromosome 5H because the peaks on chromosome 5H were more significant and loci 13 and 14 seem to co-localize with the previously mapped seedling resistance QTL *Rbgq15* (Aghnoum *et al.*, 2010). As causal gene, the *lipxygenase 2* (GenBank: L37358.1) was proposed (Aghnoum *et al.*, 2010). Nevertheless, the analysis revealed that none of the SNPs located in the three possible lipxygenases on chromosome 5H was significantly associated in either of the three traits. This result suggests that the proposal of Aghnoum *et al.* (2010) might be misleading. Nonetheless, it also has to be considered that causal markers are not always the most significant markers because of genetic heterogeneity (Platt *et al.*, 2010; Korte & Farlow, 2013). Another plausible explanation is that additional genes can be hidden in the genomic regions of the identified powdery mildew resistant varieties. In respect of the exome capture data, only genes annotated in the susceptible reference genotype Morex were considered in the presented analysis. This particular question could be answered by additional sequencing of the genomic regions in the resistant genotypes. Furthermore, it has to be taken into account that several genes within the corresponding genomic region might be involved in the seedling resistance responses against powdery mildew.

The identification of resistance QTLs or resistance genes is from high importance for the development of new resistant varieties. New technological possibilities lead to an adaptation and development of new plant breeding techniques. Marker-assisted selection and genomic prediction can accelerate the breeding progress (Lande & Thompson, 1990; Meuwissen *et al.*, 2001; Nadeem *et al.*, 2018; Zhu *et al.*, 2008). In regard of the higher resolution of GWA studies, the significantly associated SNPs and the identified candidates (Figure R 12, Table R 2 and B 5) of the present study, provide some value for plant breeders. Particularly, the flanking markers of the identified QTLs could be used for marker-assisted selection.

4.4.2. Are the four selected candidate genes casual genes?

Several *in silico*, *in vitro* and *in planta* analyses were performed to identify and to the most promising candidate genes. The presented results support the hypothesis that several of them were involved in the regulation of powdery mildew resistance responses and are in this sense resistance genes.

In respect of the annotated function and the functional *in silico* analysis (Table R 3 and Figure B 8), the candidate WB-CG_19 might correspond to the barley homolog of Arabidopsis' *dolichol phosphate mannose synthase 3 (DPMS3)*. DPMS3 is a binding partner of the DPMS2 and DPMS1 and it is required for the generation of isoprenyl-linked glycans (Jadid *et al.*, 2011). Glycans play an important role during infection with pathogens. As an example, human studies report that nearly all microbe and virus infections are linked to the binding of the pathogen to specific cell surface glycans (Hart & Copeland, 2010). In plants, it is proposed that glycans attached to plasma membrane recognition receptors are the initial contact site between cell and invading pathogen (Häweker *et al.*, 2010). DPMS3 seems to represent the binding module between DPMS1 and DPMS2 *in planta* (Jadid *et al.*, 2011). Additionally, yeast data revealed that DPMS3 tethers the protein complex to the endoplasmic reticulum membrane (Ashida *et al.*, 2006). The functional complex of all three subunits generates dolichol-phosphate mannose which is an important intermediate during the *N*-glycosylation of proteins (Jadid *et al.*, 2011). The correct attachment of *N*-glycans is essential for plant development and abiotic stress responses like salt stress (Kang *et al.*, 2008; von Schaewen *et al.*, 2008). Moreover, it was demonstrated that *N*-glycans are required for the plant innate immune responses of Arabidopsis (Saijo *et al.*, 2009; Häweker *et al.*, 2010). Particularly, these responses were mediated by pattern recognition receptors in dependence of the receptor quality control in the endoplasmic reticulum (Saijo *et al.*, 2009; Häweker *et al.*, 2010). These results suggest a crucial role of the candidate gene in respect of abiotic and biotic stress responses. Nevertheless, neither the transient overexpression nor the silencing of the tested alleles resulted in a significant alteration of the powdery mildew resistance (Table R 4 and R 5). In contrast to these negative results, the transcriptional analysis revealed that the gene is significantly upregulated by powdery mildew inoculation (Figure R 14). The transcript level spikes 24 h post inoculation corresponding to the time point when the haustorium is established in a compatible resistance interaction (Zhang *et al.*, 2005). Interestingly, the transcript level is significantly reduced afterwards in the samples inoculated with the adapted powdery mildew fungus but not in the samples inoculated with the non-adapted fungus (Figure R 14). This observation suggests that only the adapted fungus could be able to manipulate the candidate transcription to probably suppress an induced defence response. The results (Figure R 14) imply that the candidate gene is actually involved in the regulation of the defence or stress responses

after powdery mildew attack. Furthermore, the results suggest that the candidate is involved in the basal and/or nonhost resistance. These hypotheses are supported by the reported extensive modifications of the plant glycan structure that occur after fungal attack (Chaliha *et al.* 2018). It is possible that the negative results of the transient assays (Table R 4 and R 5) are explained by the identical protein sequences of both candidate alleles (Figure B 8). In this regard, it is a plausible explanation that the causal SNP was not captured in the used constructs. The specific downregulation of the candidate transcript by the adapted powdery mildew fungus (Figure R 14), which could be necessary to circumvent the innate immunity of barley, might explain the negative results, too. A repetition of the transient assays after inoculation with the non-adapted powdery mildew fungus could shed light on this particular question.

The *in silico* functional analysis of WB-CG_17 (Table R 3 and Figure B 7) revealed that the protein with unknown function could encode an arabinogalactan protein (AGP). AGPs form highly complex families and the diversity of the attached *O*-glycan chains is astonishing (Ellis *et al.*, 2010; Nguema-Ona *et al.* 2014). AGPs can be found in the plasma membrane, the cell wall, the apoplastic space, multivesicular bodies and in secretions like wound exudates (Ellis *et al.*, 2010; Mareri *et al.*, 2019). The functions of this protein class are still not fully understood, but they seem to be involved in various plant growth and developmental processes (Ellis *et al.*, 2010; Nguema-Ona *et al.* 2014). Additionally, AGPs were involved in several abiotic and biotic stress responses (Mareri *et al.*, 2019). The potential candidate homologs of the related grass species were classified as 'UPF0664 stress-induced protein C29B12.11c' (Table R 3) implying a general role in stress responses. This hypothesis is in accordance with previous observations that defence-related genes were involved in the regulation to various stresses like wounding and temperature stress (van Loon *et al.*, 2006; Hua, 2013). Nevertheless, no further information is available for this protein family. The PH-GRAM-WBP2 domain, which is annotated in the potential candidate homologous proteins (Table R 3 and Figure B 7), represents a conserved motif in eukaryotes (<https://www.ncbi.nlm.nih.gov/Structure/cdd/cddsrv.cgi?uid=275401>). In humans, this domain is associated with various relevant disease and signalling pathways (Chen *et al.*, 2017). In general, GRAM domain proteins are involved in plasma-membrane-associated processes like intracellular protein binding or lipid-binding signalling (Doerks *et al.*, 2000). These results indicate that WB-CG_17 could be associated with membrane processes. This is further supported by the detection of the potential *Arabidopsis* homolog during the screening for membrane associated proteins (Marmagne *et al.*, 2004 & 2007). Besides the regulatory functions named above, AGPs are also involved in the responses to microbes (Ellis *et al.*, 2010; Nguema-Ona *et al.* 2014). These plant-microbe interactions were mainly studied in the root (Mareri *et al.*, 2019). As an example, the production of extensins and AGPs is induced after pathogen attack probably to reinforce the

cell wall via extensive oxidative cross-linking (Nguema-Ona *et al.* 2014). Additionally, it was proposed that AGPs might be involved in the recognition or attachment of pathogens (Mareri *et al.*, 2019). Besides, there are indications that AGPs can form a 'biofilm' which show antimicrobial properties and that can act as physical barrier (Mareri *et al.*, 2019). Gaspar *et al.* (2004) presented evidence for the specific function of AGP17 of Arabidopsis in the regulation of the response to *Agrobacterium tumefaciens* infection. They suggested mechanisms on how AGP17 can act as susceptibility factor in this interaction. The here presented results of the transient overexpression of the minor allele of WB-CG_17 (Table R 5) indicated that also the candidate may act as susceptibility factor or disease susceptibility gene. The observed increased susceptibility in the resistant as well as in the susceptible background (Table R 5) supports the general importance of this protein in the interplay between *Bgh* and barley. Liang *et al.* (2018) reported the specific expression increase of a plasma membrane bound AGP epitope in rice after infection with the biotrophic fungus *Magnaporthe oryzae*. A similar upregulation of WB-CG_17 transcript was detected in powdery mildew inoculated epidermis peels (Figure R 14). These results imply that the candidate is more likely participating in the regulation of defence responses than being involved as recognition site for the fungus during attack. Nevertheless, further investigation is necessary to specify the function of the candidate. In general, it is unclear if the detected expression alterations of AGPs after abiotic and biotic stresses are an indirect/direct result of the cell responses or just part of cell damages (Mareri *et al.*, 2019). The transcriptional analysis of WB-CG_17 revealed further that the candidate could be regulated by the circadian clock (Figure R 14). The circadian clock is beside temperature, light and redox signalling one of the major regulators of defence responses to ensure the specific timing of the costly responses (Hua, 2013; Sharma & Bhatt, 2015; Lu *et al.*, 2017; Karapetyan & Dong, 2018). Wang *et al.* (2011) reported expression patterns of clock regulated defence genes after pathogen inoculation in Arabidopsis resembling the one of WB-CG_17 (Figure R 14). A further analysis of the candidate sequence, especially of the promoter region, for regulatory clock elements and a detailed assessment of the expression profile could shed light on the hypothesized circadian clock regulation. The observed transcription pattern of WB-CG_17 (Figure R 14) resembles in particular the pattern described for pathogen induced clock regulated defence genes in absence of a major *R*-gene (Wang *et al.*, 2011). This observation supports the hypothesized race-nonspecificity of the resistance response regulated by the candidate. Further supported is the hypothesis by the enhanced susceptibility mediated by the overexpression (Table R 5). This effect is achieved in the susceptible as well as in the resistant genotype. Particularly, this circumstance is interesting because the resistance is conferred in a race-specific manner (Figure R 5 and Table B 4, Hoseinzadeh *et al.*, 2019). Additionally, the altered expression of the potential Arabidopsis candidate homolog after

Geminivirus infection (Ascencio-Ibáñez *et al.*, 2008) could indicate a general upregulation of the candidate after pathogen attack.

The third tested candidate WB-CG_23 is annotated as 'Bric-a-Brac/-Tramtrack/-Broad Complex (BTB)/-POxvirus and Zinc finger (POZ)/ Kelch protein' and the *in silico* functional analysis (Table R 3) implies that the candidate may act as barley homolog of Arabidopsis' *Light-Response BTB (LRB) 1* or 2. LRB proteins seem to be conserved between mono- and dicot plants, although they cluster in specific clades (Christians *et al.*, 2012). In accordance with these results, the monocot LRB homologs of *Brachypodium distachyon* and rice show a higher sequence identity to the here presented barley homologs as compared to the dicot LRBs of *Arabidopsis thaliana* (*At*) (Figure B 9). In addition to *LRB1* and *LRB2*, a third *LRB* is annotated in Arabidopsis which is presumed to be a pseudogene and absent in most species (Christians *et al.*, 2012). The homologous proteins *LRB1* and *LRB2* were firstly described by Qu *et al.* (2010) as *POB1* (POZ/BTB Containing Protein1) and *POB2*, respectively. They seem to negatively regulate the jasmonate mediated pathogen defence in Arabidopsis (Qu *et al.*, 2010). *LRB1* and *LRB2* can homo- and dimerize to form together with Cullin3 ubiquitin E3 ligases (Christians *et al.*, 2012). The protein complexes are involved in the regulation of diverse processes. On the one hand, these E3 ligases target *FRIGIDA* (a major regulator of flowering in Arabidopsis) for proteasomal degradation during vernalization and thus initiate flowering (Hu *et al.*, 2014). On the other hand, they participate in the regulation of phytochromes (Christians *et al.*, 2012; Ni *et al.*, 2014). In Arabidopsis five phytochromes (*PhyA-PhyE*) have been annotated (Xu *et al.*, 2015). They perceive the ratio of red to far-red light and modulate plant growth, development and immune responses (Xu *et al.*, 2015; Ballaré, 2014). In particular, *phyB* in combination with other phytochromes regulates defence responses like the activation of lipoxygenases (Zhao *et al.*, 2014). This regulatory function of *PhyB* was demonstrated for different pathogens and the corresponding signalling pathways. As examples, the single *phyB* mutant of Arabidopsis is more susceptible against *Fusarium oxysporum* (Kazan & Manners, 2011) and *Botrytis cinerea* (Cerrudo *et al.*, 2017) while the double mutant *phyAphyB* displays reduced resistance responses after infection with *Pseudomonas syringae* pv. *tomato* (Genoud *et al.*, 2002; Griebel & Zeier, 2008). In respect of the attacking pathogen, either the salicylic acid or the jasmonate signalling pathway is induced but both are regulated in a light dependent manner (Ballaré, 2014). These regulations rely mainly on *PhyB* and the ultraviolet-B photoreceptor *UVR8* (Ballaré, 2014). Additionally to Arabidopsis, other plant species like rice display phytochrome regulated defence responses (Xie *et al.*, 2011). There are also indications for a light dependent regulation of resistance responses against powdery mildews (Wang *et al.*, 2010). The resistance of cucumber (*Cumunis sativus* L.) against *Sphaerotheca fuliginea* depends on salicylic acid and light quality (Wang *et al.*, 2010). The described Cullin3-LRB1/2 E3 ligases of

Arabidopsis promote the degradation of PhyB and PhyD in a light regulated manner (Christians *et al.*, 2012). Additionally, the degradation depends on the phosphorylation and degradation of Phytochrome Interacting Factor 3 (PIF3, Ni *et al.*, 2014). Moreover, the E3 ligases positively regulate the PhyA level (Christians *et al.*, 2012). In monocot plants, only three phytochromes (PhyA to PhyC) were found (Mathews & Sharrock, 1997) and the same holds true for barley (Szücs *et al.*, 2006). These results indicate a differentiated regulation of light signals in mono- and dicot plants. Nevertheless, the phytochrome dependent regulation mechanisms of salicylic acid and jasmonate dependent defence responses seem to be conserved. As an example, the rice *phyAphyBphyC* mutant displays enhanced susceptibility against *Magnaporthe oryza* (Xie *et al.*, 2011). If the here presented candidate is actually involved in the regulation of phytochromes in barley needs further investigation. Nonetheless, the hypothesized function of WB-CG_23 as LRB homolog is supported by the high sequence identity of the functional domains between the homologous proteins (Figure B 9). Christians *et al.* (2012) presumed that the regions surrounding the BTB domain are involved in the target recognition. Particularly, the sequence following the BTB domain is conserved between the candidate and its potential homologs (Figure B 9). This finding supports the presumed function of WB-CG_23 as phytochrome regulator. In addition, the same rice proteins were identified as WB-CG_23 and AtLRB homologs (Gingerich *et al.*, 2007; Christians *et al.*, 2012), although these rice proteins were annotated as 'BTB with E1 subfamily conserved sequence'. The transient overexpression of the major candidate allele resulted in enhanced susceptibility against powdery mildew (Table R 5). This effect supports a function of the candidate in the regulation of these particular defence responses. Nonetheless, the detected effect is only observed in the resistant background (Table R 5). In this respect, further investigation is necessary to clarify whether the candidate acts in dependence of the genetic background. A repeated transient overexpression of both alleles in a moderately resistant genotype under various light conditions could shed light on this particular idea especially in respect of the possible regulation of phytochromes. Nevertheless, it has to be taken into account that the candidate and its potential homolog (HORVU5Hr1G116800, Table R 3) could act redundantly like it was reported for AtLRB1 and AtLRB2 (Christians *et al.*, 2012). Nevertheless, none of the SNPs located in the barley homolog is significantly associated in the here reported GWAS (Table B 5). This could be related to genetic heterogeneity in the population or because the candidate WB-CG_23 acts specifically in the regulation of this particular defence responses. In comparison to the other candidate genes presented in this study, the expression of WB-CG_23 is rather low which complicates the results interpretation (Figure R 13, Figure R 14 and Figure B 6). Nevertheless, it seems that the transcript level of the candidate gene is altered after powdery mildew inoculation (Figure R 14). This observation supports a defence related function. In case of

AtLRB1/2, a broad expression in mainly all tissues and all developmental stages was reported by Christians *et al.* (2012). If the present candidate gene is also expressed in a wide variety of tissues or altered by different light conditions would need further investigation.

WB-CG_28 was the last candidate that was addressed in the functional validations. It was annotated as 'flap endonuclease (FEN) 1-B' which was confirmed by the *in silico* analysis (Table R 3 and Figure B 10). In general, FEN1 proteins form structure-specific endonucleases which are highly conserved among species (Balakrishnan & Bambara, 2013). They are essential for the processing of Okazaki fragments, long-patch base excision repair and telomere maintenance (Balakrishnan & Bambara, 2013). Most studies have been performed either in human, animal or yeast systems. Thus, the knowledge about plant FEN1 homologs is still limited. In Arabidopsis, *FEN1* is a single copy gene (Schultz *et al.*, 2007) which is essential for the maintenance of the genome stability and development (Zhang *et al.*, 2016b) as well as transcriptional gene silencing (Zhang *et al.*, 2016a). *fen1* mutant plants have shorter telomers and altered DNA methylation (Zhang *et al.*, 2016a). Additionally, their root apical meristem as well as the quiescent centre are defective (Zhang *et al.*, 2016b). In contrast to most species, two functional homologs, *FEN1-A* and *FEN1-B*, were described in rice. Both proteins seem to be required for cell proliferation (Kimura *et al.*, 2003). The here presented *in silico* analysis revealed further potential FEN1-B proteins in barley, *Aegilops tauschii* and *Brachypodium distachyon* (Table R 3 and Figure B 10). This circumstance could indicate that this protein type might be conserved in monocot plants. The further characterization of the rice FEN1-B led to the hypothesis that it fulfils distinct functions besides cell proliferation regulation. Firstly, only *OsFEN1-A* is able to complement the *FEN1* null mutant of yeast (*rad27*, Reagan *et al.*, 1995) whereas *OsFEN1-B* failed (Kimura *et al.*, 2003). Besides the expression of both homologs in proliferating tissue, *OsFEN1-B* seem to be specifically expressed in mature leaves (Kimura *et al.*, 2003). Similar results were presented here for the barley *FEN1-B* homolog (WB-CG_28). The candidate expression was detected in mature first leaves and also in epidermis peels (Figure R 14 and Figure B 6). Regarding the significant transcript reduction in response to the adapted as well as the non-adapted powdery mildew fungus (Figure R 14), an involvement of the candidate in regulation of defence responses is hypothesized. Unfortunately, it was not possible to retrieve an *Escherichia coli* clone expressing any of the full-length candidate alleles. In respect of the negative outcome of the transient silencing approach (Table R 4) and the missing results of the transient overexpression, it was not possible to further validate the candidate function regarding the powdery mildew resistance responses.

One aims of this study was the identification of race-nonspecific resistance genes (alleles) of barley involved in the response to powdery mildew. Several indications for the here presented candidates were discussed which allowed the hypothesis that the four selected candidates are

involved in the regulation of powdery mildew resistance responses. If these genes act as resistance or susceptibility genes could not be determined finally. A function of these candidates in resistance responses is supported by the literature. Nevertheless, none of the genes was described until now in the context of powdery mildew resistance (in barley). In this sense, new insights in the barley-powdery mildew interaction could be obtained.

The results presented here allow the hypothesis that all four candidate genes may act indeed in a race-nonspecific manner. The major facts supporting this hypothesis are: (1) the selected candidates were significant in all three GWAS traits (Figure R 12 and Table B 5); (2) the annotated functions of the genes imply that they are involved in basic regulatory processes (Table R 3); (3) the transcript levels of all candidates were altered after inoculation with the adapted as well as the non-adapted powdery mildew fungus (Figure R 14); and (4) at least two of the candidates alter significantly the susceptibility against powdery mildew when overexpressed (Table R 5). Furthermore, the obtained results indicate that these candidates act rather as susceptibility factor or disease susceptibility gene than as direct resistance genes.

The here presented approach was specifically designed to assess the differential effect of the candidate alleles on the powdery mildew response (Figure R 15, Table B 7 and B 8). The functional validations were performed as transient single cell transformations (Table R 4 and R 5). The assay design support further the race-nonspecific function of the candidates. As an example, a third powdery mildew isolate was selected for the evaluation of the allelic effects. Moreover, it has to be considered that the resistance of the resistant genotype selected for the functional validation is caused race-specifically by a major *R*-gene (Figure R 5 and Table B 4, Hoseinzadeh *et al.*, 2019). Nevertheless, this major *R*-gene may also mask the smaller effects of some of the candidate genes/alleles. The presumed small effects of the candidates could be one of the reasons why the transient silencing did not lead to clear results (Table R 4). In respect of the transient nature of the single cell analysis, it would be very difficult to assess if the generated hairpin structures of the constructs were actually processed to small interfering RNAs or how efficient they are. As alternative approach virus-induced gene silencing could be performed to analyse a knock-down of the candidates. Another factor which should be considered is a possible functional redundancy of the candidates and their potential homologous proteins. In case of the overexpression assay, it has to be taken into account that the natural candidate alleles were not knock-out prior the overexpression. In this regard, only dominant effects of the candidates could be observed. Furthermore, it has to be kept in mind that the alleles were overexpressed under control of the 35S promoter. This promoter is weaker expressed in monocot as in dicot plants (McElroy *et al.*, 1991), which was confirmed by the here presented analysis of different promoter_GUS constructs

(Table R 6 and R 7). Probably a stronger overexpression of the candidate alleles under control of another promoter could further differentiate the allelic effects.

In respect of the presented results, interesting candidate genes were identified which could be further investigated by the production of stable transformed plants or an additional screening for further alleles. If these candidates were really the causal genes for the loci 13 and 14 could not be answered finally, but the reported results support the function of them in the regulation of powdery mildew resistance responses. In addition, they might act as resistance or as susceptibility genes.

5. Summary

Powdery mildew is caused by the biotrophic fungus *Blumeria graminis* f. sp. *hordei* and it is one of the important foliar diseases of barley (*Hordeum vulgare* L.). Climate change and conscious consumers will push future sustainable disease management towards methods that mostly rely on genetic resistance of crop varieties. The major aims of this study were the assessment if a genome-wide-association study is feasible in a diverse barley population in respect of the identification of novel resistance genes or new alleles of known genes against the barley powdery mildew fungus and the validation of the most promising candidate alleles.

To achieve these aims, a natural diverse barley population was assessed in two approaches: (1) the seedling resistance responses against two poly-virulent powdery mildew isolates and (2) the adult plant resistance under natural occurring powdery mildew infection. The subsequent analyses of resistant genotypes led to the identification of two potential novel natural *mlo* mutants, the confirmation of previously annotated resistance genes and the postulation of known resistance genes in so far uncharacterized material. The genome-wide-association study in the diverse barley population resulted in the identification of 33 candidate genes distributed over six chromosomes clustered in 16 loci. The four most promising candidate genes were located in two loci which co-localize with the previously identified seedling powdery mildew resistance QTL *Rbgq15*. Afterwards, functional validations were performed using several *in silico*, *in vitro* and *in planta* approaches. The validation results indicate that all four candidates might be involved in the regulation of the powdery mildew resistance responses of barley seedlings. The four candidates were proposed to function in basic regulatory processes. This proposed candidate functions and the alterations of the transcript levels of all candidates after inoculation with the adapted as well as the non-adapted powdery mildew fungus support a race-nonspecific mode of action of the candidates. Further, the effects of different candidate alleles were addressed by transient transformation assays. The alleles of two candidates, a potential arabinogalactan protein and the hypothesized barley homolog of AtLRB1/2, displayed significant enhanced powdery mildew susceptibility after transient overexpression in leaf epidermis cells. Besides the four top candidates, eight additional candidate gene models could be confirmed by subsequent analyses. A further investigation of these candidates might provide new valuable insights in the regulation of powdery mildew responses of barley.

6. Zusammenfassung

Eine der wichtigen Krankheiten der Gerste (*Hordeum vulgare* L.) ist Mehltau. Diese Erkrankung der Blätter wird durch den biotroph wachsenden Pilz *Blumeria graminis* f. sp. *hordei* ausgelöst. Klimawandel und die zunehmende bewusste Ernährung der Bevölkerung machen es notwendig, dass eine nachhaltige Landwirtschaft sich in der Zukunft zunehmend auf die genetische Resistenz von Nutzpflanzen stützt. Die Hauptziele der vorliegenden Studie waren die Beurteilung der Realisierbarkeit einer genomweiten Assoziationsstudie in einer diversen Gerstenpopulation bezüglich der Identifizierung von neuen Resistenzgenen oder neuen Allelen von bekannten Genen gegenüber dem echten Gerstenmehltaupilz und die Validierung der vielversprechendsten Kandidatenallele.

Um diese Ziele zu erreichen, wurde eine natürliche Gerstenpopulation mittels zweier Ansätze untersucht: (1) die Keimlingsresistenz gegenüber von zwei poly-virulenten Mehltausisolaten und (2) die Resistenz der erwachsenen Pflanzen nach natürlicher Mehltauinfektion. Die nachfolgenden Analysen der resistenten Genotypen führte zur Identifizierung von zwei neuen natürlichen *mlo* Mutanten, der Bestätigung von zuvor annotierten Resistenzgenen und der Postulierung von bekannten Resistenzgenen in bisher nicht charakterisiertem Material. Die genomweite Assoziationsstudie der diversen Gerstenpopulation resultierte in der Identifizierung von 33 Kandidatengenen, welche auf sechs verschiedenen Chromosomen in 16 Loci verteilt sind. Die vier vielversprechendsten Kandidatengene sind in zwei Loci lokalisiert. Diese Loci kolokalisieren mit dem zuvor beschriebenen, im Keimlingsstadium wirksamen Mehltaresistenz QTL *Rbgq15*. Nachfolgende funktionelle Validierungen wurden mittels verschiedener *in silico*, *in vitro* und *in planta* Ansätzen durchgeführt. Die Validierungsergebnisse deuten an, dass alle vier Kandidaten in die Regulierung von Resistenzreaktionen von Gerstenkeimlingen gegen Mehltau involviert sind. Die vorgeschlagenen Funktionen der vier Kandidaten verweisen auf grundlegende regulatorische Prozesse. Diese vorgeschlagenen Funktionen und die Änderungen der Transkriptlevel aller Kandidaten nach der Inokulation mit dem angepasstem so dem nicht-angepasstem Mehltaupilz, unterstützen die angenommene rassen-unspezifische Handlungsweise der Kandidaten. Darüber hinaus wurden die Effekte der verschiedenen Kandidatenallele in transienten Transformationsassays untersucht. Die Allele von zwei Kandidaten, einem potentiell Arabinogalactanprotein und dem angenommenem Homolog von AtLRB1/2, zeigen signifikant erhöhte Mehltauanfälligkeit nach der transienten Überexpression in den Blattepidermiszellen. Neben diesen vier Topkandidaten, konnten nachfolgende Analysen die Genmodelle von acht zusätzlichen Kandidaten bestätigen. Eine weitere Untersuchung dieser Kandidaten führt möglicherweise zu neuen wertvollen Erkenntnissen bezüglich der Regulation der Reaktionen von Gerste auf Mehltau.

Appendices

References

- Acevedo-Gracia J., Kusch S., Panstruga R. (2014) *Magical research tour: MLO proteins in plant immunity and beyond*. *New Phytologist* 204: 273-281 DOI: 10.1111/nph.12889
- Aghnoum R., Marcel T. C., Johrde A., Pecchioni N., Schweizer P., Niks R. E. (2010) *Basal host resistance of barley to powdery mildew: connecting quantitative trait loci and candidate genes*. *Molecular Plant-Microbe Interaction Journal* 23: 91-102 DOI: 10.1094/mpmi-23-1-0091
- Agrawal N., Dasaradhi P. V. N., Mohmmmed A., Malhotra P., Bhatnagar R. K., Mukherjee S. K. (2003) *RNA interference: biology, mechanism, and applications*. *Microbiology and Molecular Biology Reviews* 67: 657-685 DOI: 10.1128/MMBR.67.4.657-685.2003
- Allaby R. G. (2015) *Barley domestication: the end of a central dogma*. *Genome Biology* 16:176 DOI: 10.1186/s13059-015-0743-9
- Altpeter F., Varshney A., Abderhalden O., Douchkov D., Sautter C., Kumlehn J., Dudler R., Schweizer P. (2005) *Stable expression of a defense-related gene in wheat epidermis under transcriptional control of a novel promoter confers pathogen resistance*. *Plant Molecular Biology* 57: 271-283 DOI: 10.1007/s11103-004-7564-7
- Andersen E. J., Ali S., Reese R. N., Yen Y., Neupane S., Nepal M. P. (2016) *Diversity and evolution of disease resistance genes*. *Evolutionary Bioinformatics* 12: 99-108 DOI: 10.4137/EBO.S38085
- Appiano M., Catalano D., Santillán Martínez M., Lotti C., Zheng Z., Visser R. G. F., Ricciardi L., Bai Y., Pavan S. (2015) *Monocot and dicot MLO powdery mildew susceptibility factors are functionally conserved in spite of the evolution of class-specific molecular features*. *BioMed Central Plant Biology* 15: 257-267 DOI: 10.1186/s12870-015-0639-6
- Ascencio-Ibáñez J. T., Sozzani R., Lee T.-J., Chu T.-M., Wolfinger R. D., Cella R., Hanley-Bowdoin L. (2008) *Global analysis of Arabidopsis gene expression uncovers a complex array of changes impacting pathogen response and cell cycle during geminivirus infection*. *Plant Physiology* 148: 436-454 DOI: 10.1104/pp.108.121038
- Ashida H., Maeda Y., Kinoshita T. (2006) *DPM1, the catalytic subunit of dolichol-phosphate mannose synthase, is tethered to and stabilized on the endoplasmic reticulum membrane by DPM3*. *The Journal of Biological Chemistry* 281: 896-904 DOI: 10.1074/jbc.M51311200
- Awada L., Phillips P. W. B., Smyth S. J. (2018) *The adaptation of automated phenotyping by plant breeders*. *Euphytica* 2014: 148 DOI: 10.1007/s10681-018-2226-z
- Azevedo C., Sadanandom A., Kitagawa K., Freialdenhoven A., Shirasu K., Schulze-Lefert P. (2002) *The RAR1 interactor SGT1, an essential component of R gene-triggered disease resistance*. *Science* 295: 2073-2076 DOI: 10.1126/science.1067554
- Balakrishnan L., Bambara R. A. (2013) *Flap endonuclease 1*. *Annual Review of Biochemistry* 82: 119-138 DOI: 10.1146/annurev-biochem-072511-122603
- Ballaré C. L. (2014) *Light regulation of plant defense*. *Annual Review of Plant Biology* 65: 335-363 DOI: 10.1146/annurev-arplant-050213-040145
- Baker S. J., Newton A. C., Crabb D., Guy D. C., Jefferies R. A., Mackerron D. K. L., Thomas W. T. B., Gurr S. J. (1998) *Temporary partial breakdown of mlo-resistance in spring barley by sudden relief of soil water-stress under field conditions: the effects of genetic background and mlo allele*. *Plant Pathology* 47: 401-410 DOI: 10.1046/j.1365-3059.1998.00261.x
- Barker G. L. A., Edwards K. J. (2009) *A genome-wide analysis of single polymorphism diversity in the world's major cereal crops*. *Plant Biotechnology Journal* 7: 318-325 DOI: 10.1111/j.1467-7652.2009.00412.x

- Bartoli C., Roux F. (2017) *Genome-wide association studies in plant pathosystems: toward an ecological genomics approach*. *Frontiers in Plant Science* 8: 763 DOI: 10.3389/fpls.2017.00763
- Baulcombe D. C. (2015) *VIGS, HIGS, FIGS: small RNA silencing in the interactions of viruses or filamentous organisms with their plant hosts*. *Current Opinion in Plant Biology* 26: 141-146 DOI: 10.1016/j.pbi.2015.06.007
- Bengtsson T., Åhman I., Manninen O., Reitan L., Christerson T., Due Jensen J., Krusell L., Jahoor A., Orabi J. (2017) *A novel QTL for powdery mildew resistance in nordic spring barley (*Hordeum vulgare* L. ssp. *vulgare*) revealed by genome-wide association study*. *Frontiers in Plant Science* 8: 1954 DOI: 10.3389/fpls.2017.01954
- Both M., Csukai M., Stumpf M. P. H., Spanu P. D. (2005) *Gene expression profiles of *Blumeria graminis* indicate dynamic changes to primary metabolism during development of an obligate biotrophic pathogen*. *The Plant Cell* 17: 2107-2122 DOI: 10.1105/tpc.105.032631
- Bourras S., McNally K. E., Ben-David R., Parlange F., Roffler S., Praz C. R., Oberhaensli S., Menardo F., Stirnweis D., Frenkel Z., Schaefer L. K., Flückiger S., Treier G., Herren G., Korol A. B., Wicker T., Keller B. (2015) *Multiple avirulence loci and allele-specific effector resistance of wheat to powdery mildew*. *The Plant Cell*. 27: 2991-3012 DOI: 10.1105/tpc.15.00171
- Brachi B., Morris G. P., Borevitz J. O. (2011) *Genome-wide association studies in plants: the missing heritability is in the field*. *Genome Biology* 12: 232 DOI: 10.1186/gb-2011-12-10-232
- Brachi B., Villoutreix R., Faure N., Hautèete N., Piquot Y., Pauwels M., Roby D., Cuguen J., Bergelson J., Roux F. (2013) *Investigation of the geographical scale of adaptive phenological variation and its underlying genetics in *Arabidopsis thaliana**. *Molecular Ecology* 22: 4222-4240 DOI: 10.1111/mec.12396
- Brenchley R., Spannagl M., Pfeifer M., Barker G. L. A., D'Amore R., Allen A. M., McKenzie N., Kramer M., Kerhornou A., Bolser D., Kay S., Waite D., Trick M., Bancroft I., Gu Y., Huo N., Luo M. C., Sehgal S., Gill B., Kianian S., Anderson O., Kersey P., Dvorak J., McCombie W. R., Hall A., Mayer K. F. X., Edwards K. J., Bevan M. W., Hall N. (2012) *Analysis of the bread wheat genome using whole-genome shotgun sequencing*. *Nature* 491: 705–710 DOI: 10.1038/nature11650
- Brown A. H. D., Zohary D., Nevo E. (1978) *Outcrossing rates and heterozygosity in natural populations of *Hordeum spontaneum* Koch in Israel*. *Heredity* 41: 49-62 DOI: 10.1038/hdy.1978.63
- Brown J. K. M. (2015) *Durable resistance of crops to disease: a Darwinian perspective*. *Annual Review of Phytopathology* 53: 513-539 DOI: 10.1146/annurev-phyto-102313-045914
- Burghardt L. T., Young N. D., Tiffin P. (2017) *A guide to genome-wide association mapping in plants*. *Current Protocols in Plant Biology* 2: 22-38 DOI: 10.1002/cppb.20041
- Busch W. S., Moore J. H. (2012) *Chapter 11: Genome-wide association studies*. *PLOS Computational Biology* 8: e1002822 DOI: 10.1371/journal.pcbi.1002822
- Büsches R., Hollrichter K., Panstruga R., Simons G., Wolter M., Frijters A., van Daelen R., van der Lee T., Diergaarde P., Groenendijk J., Töpsch S., Vos P., Salamini F., Schulze-Lefert P. (1997) *The barley Mlo Gene: a novel control element of plant pathogen resistance*. *Cell* 88: 695-705 DOI: 10.1016/S0092-8674(00)81912-1
- Bustin S. A., Benes V., Garson J. A., Hellemans J., Huggett J., Kubista M., Mueller R., Nolan T., Pfaffl M. W., Shipley G. L., Vandesompele J., Wittwer C. T. (2009) *The MIQE guidelines: minimum information for publication of quantification real-time PCR experiments*. *Clinical Chemistry* 55: 611-622 DOI: 10.1373/clinchem.2008.112797

- Bustos-Korts D., Russell J., Dawson I. K., Tondelli A., Trabanco N., Ferrandi C., Guerra D., Strozzi F., Nicolazzi E., Ozkan H., Çakır E., Yakışır E., Molnar-Lang M., Megyeri M., Miko P., Delbono S., Kyriakidis S., Booth A., Cammarano D., Cattivelli L. Rossini L., Stein N., Kilian B., Waugh R., van Eeuwijk F. A. (accepted) *Exome sequences and multi-environment field trials elucidate the genetic basis of adaptation in a diverse barley collection*. The Plant Journal (accepted)
- Butler D. G., Cullis B. R., Gilmour A. R. and Gogel B. J. (2009) *ASREML-R Reference Manual. Release 3.0*. Technical Report, Queensland Department of Primary Industries, Australia.
- Callis J. (2014) *The ubiquitination machinery of the ubiquitin system*. The Arabidopsis book 12: e0174. DOI:10.1199/tab.0174
- Camacho Villa T. C., Maxted N., Scholten M., Ford-Lloyd B. (2005) *Defining and identifying crop landraces*. Plant Genetic Resources 3: 373-384 DOI: 10/1079/PGR200591
- Campos M. L., Yoshida Y., Major I. T., de Oliveira Ferreira D., Weraduwage S. M., Froehlich J. E., Johnson B. F., Kramer D. M., Jander G., Sharkey T. D., Howe G. A. (2016) *Rewiring of jasmonate and phytochrome B signalling uncouples plant growth-defense tradeoffs*. Nature communications 7: 12570 DOI: 10.1038/ncomms12570
- Cantor R. M., Lange K., Sinsheimer J. S. (2010) *Prioritizing GWAS results: a review of statistical methods and recommendations for their application*. The American Journal of Human Genetics 86: 6-22 DOI: 10.1016/j.ajhg.2009.11.017
- Carver T. L. W., Kunoh H., Thomas B. J., Nicholson R. L. (1999) *Release and visualization of the extracellular matrix of conidia of Blumeria graminis*. Mycological Research 103: 547-560 DOI: 10.1017/S0953756298007400
- Cerrudo I., Caliri-Ortiz M. E., Keller M. M., Degano M. E., Demkura P. V., Ballaré C. L. (2017) *Exploring growth-defence trade-offs in Arabidopsis: phytochrome B inactivation requires JAZ10 to suppress plant immunity but not to trigger shade-avoidance responses*. Plant, Cell & Environment 40: 635-644 DOI: 10.1111/pce.12877
- Chaliha C., Rugen M. D., Field R. A., Kalita E. (2018) *Glycans as modulator of plant defense against filamentous pathogens*. Frontiers in Plant Science 9: 928 DOI: 10.3389/fpls.2018.00928
- Chen X. (2013) *High-temperature adult-plant resistance, key for sustainable control of stripe rust*. American Journal of Plant Sciences 4: 608-627 DOI: 10.4236/ajps.2016.43080
- Chen S., Wang H., Huang Y.-F., Li M.-L., Cheng J.-H., Hu P., Lu C.-H., Zhang Y., Tzeng C.-M., Zhang Z.-M. (2017) *WW domain-binding protein 2: an adaptor protein closely linked to the development of breast cancer*. Molecular Cancer 16: 128 DOI: 10.1186/s12943-017-0693-9
- Chowdhury J., Henderson M., Schweizer P., Burton R. A., Fincher G. B., Little A. (2014) *Differential accumulation of callose, arabinoxylan and cellulose in nonpenetrated versus penetrated papillae on leaves of barley infected with Blumeria graminis f. sp. hordei* New Phytologist 204: 650-660 DOI: 10.1111/nph.12974
- Chowdhury J., Schober M. S., Shirley N. J., Singh R. R., Jacobs A. K., Douchkov D., Schweizer P., Fincher G. B., Burton R. A., Little A. (2016) *Down-regulation of the glucan synthase-like 6 gene (HvGsl6) in barley leads to decreased callose accumulation and increased cell wall penetration by Blumeria graminis f. sp. hordei*. New Phytologist 212: 434-443 DOI: 10.1111/nph.14086
- Christians M. J., Gingerich D. J., Hua Z., Lauer T. D., Vierstra R. D. (2012) *The Light-Response BTB1 and BTB2 proteins assemble nuclear ubiquitin ligases that modify phytochrome B and D signaling in Arabidopsis*. Plant Physiology 160: 118-134 DOI: 10.1104/pp.112.199109

- Cobb J. N., DeClerck G., Greenberg A., Clark R., McCouch S. (2013) *Next-generation phenotyping: requirements and strategies for enhancing our understanding of genotype-phenotype relationships and its relevance to crop improvement*. Theoretical and Applied Genetics 126: 867-887 DOI: 10.1007/s00122-013-2066-0
- Collins N. C., Thordal-Christensen H., Lipka V., Bau S., Kombrink E., Qiu J.-L., Hükelhoven R., Stein M., Freialdenhoven A., Somerville S. C., Schulze-Lefert P. (2003) *SNARE-protein-mediated disease resistance at the plant cell wall*. Nature 425: 973-977 DOI: 10.1038/nature02076
- Colmsee C., Beier S., Himmelbach A., Schmutzer T., Stein N., Scholz U., Mascher M. (2015) *BARLEX – the barley draft genome explorer*. Molecular Plant 8: 964-966 DOI: 10.1016/j.molp.2015.03.009
- Comadran J., Thomas W. T.B., van Eeuwijk F. Á., Ceccarelli S., Grandó S., Stanca A. M., Pecchioni N., Akar T., Al-Yassin A., Benbelkacem A., Ouabbou H., Bort J., Romagosa I., Hackett C. A., Russell J. R. (2009) *Patterns of genetic diversity and linkage disequilibrium in a highly structured Hordeum vulgare association-mapping population for the Mediterranean basin*. Theoretical and Applied Genetics 119: 175-187 DOI: 10.1007/s00122-009-1027-0
- Conrath U. (2006) *Systemic acquired resistance*. Plant Signaling & Behavior 1: 179-184 DOI: 10.4161/psb.1.4.3221
- Craig A., Ewan R., Mesmar J., Gudipati V., Sadanandom A. (2009) *E3 ubiquitin ligases and plant innate immunity*. Journal of Experimental Botany 60: 1123-1132 DOI: 10.1093/lxb/erp059
- Czembor J. H. (2000) *Resistance to powdery mildew in barley (Hordeum vulgare L.) landraces from Egypt*. Plant Genetic Resources Newsletter 123: 52-60 ISSN: 1020-3362 Record Number: 20003025679
- Czembor J. H. (2001) *Resistance to powdery mildew in selections from barley landraces collected in Greece*. Agriculture and Food Science in Finland 10: 133-142 DOI: 10.23986/afsci.5681
- Czembor J. H. (2002) *Resistance to powdery mildew in selections from Moroccan barley landraces*. Euphytica 125: 397-409 DOI: 10.1023/A:1016061508160
- Dangl J. L., Jones J. D. G. (2001) *Plant pathogens and integrated defence response to infection*. Nature 441: 826-833 DOI: 10.1038/35081161
- Dangl J. L., Horvath D. M., Staskawicz B. J. (2013) *Pivoting the plant immune system from dissection to development*. Science 341: 746-751 DOI: 10.1126/science.1236011
- de Koning A. P. J., Gu W., Castoe T. A., Batzer M. A., Pollock D. D. (2011) *Repetitive elements may comprise over two-thirds of the human genome*. PLOS Genetics 7: e1002384 DOI: 10.1371/journal.pgen.1002384
- Delventhal R., Zellerhoff N., Schaffrath U. (2011) *Barley stripe mosaic virus-induced gene silencing (BSMV-IGS) as a tool for functional analysis of barley genes potentially involved in nonhost resistance*. Plant Signaling & Behavior 6: 867-869 DOI: 10.4161/psb.6.6.15240
- Delventhal R., Rajaraman J., Stefanato F., Rehman S., Aghnoum R., McGrann G. R. D., Bolger M., Usadel B., Hedley P. E., Boyd L., Nicks R. E., Schweizer P., Schaffrath U. (2017) *A comparative analysis of nonhost resistance across the two Triticeae crop species wheat and barley*. BMC Plant Biology 17: 232 DOI: 10.1186/s12870-017-1178-0
- Devoto A., Hartmann H. A., Piffanelli P., Elliott C., Simmons C., Taramino G., Goh C.-S., Cohen F. E., Emerson B. C., Schulze-Lefert P., Panstruga R. (2003) *Molecular phylogeny and evolution of the plant-specific seven-transmembrane MLO family*. Journal of Molecular evolution 56: 77-88 DOI: 10.1007/s00239-002-2382-5
- Dickson S. P., Wang K., Krantz I., Hakonarson H., Goldstein D. B. (2010) *Rare variants create synthetic genome-wide associations*. PLOS Biology 8: e1000294 DOI: 10.1371/journal.pbio.100294

- Doerks T., Strauss M., Brendel M., Bork P. (2000) *GRAM, a novel domain in glucosyltransferases, myotubularins and other putative membrane-associated proteins*. Trends in Biochemical Science: Protein Sequence Motifs 25: 483-485 DOI: 10.1016/S096-0004(00)01664-9
- Dong W., Nowara D., Schweizer P. (2006) *Protein polyubiquitination plays a role in basal host resistance of barley*. The Plant Cell 18: 3321-3331 DOI: 10.1105/tpc.106.046326
- Douchkov D., Nowara D., Zierold U., Schweizer P. (2005) *A high throughput gene-silencing system for the functional assessment of defense-related genes in barley epidermal cells*. Molecular Plant-Microbe Interaction Journal 18: 755-761 DOI: 10.1094/MPMI-18-0755
- Douchkov D., Lück S., Johrde A., Nowara D., Himmelbach A., Rajaraman J., Stein N., Sharma R., Kilian B., Schweizer P. (2014) *Discovery of genes affecting resistance of barley to adapted and non-adapted powdery mildew fungi*. Genome Biology 15:518 DOI: 10.1186/s13059-014-0518-8
- Douchkov D., Lueck S., Hensel G., Kumlehn J., Rajaraman J., Johrde A., Doblin M. S., Beahan C. T., Kopischke M., Fuchs R., Lipka V., Niks R. E., Bulone V., Chowdhury J., Little A., Burton R. A., Schober M. S., Bacic A., Fincher G. B., Schweizer P. (2016) *The barley (Hordeum vulgare) cellulose synthase-like D2 gene (HvCsID2) mediates penetration resistance to host-adapted and nonhost isolates of the powdery mildew fungus*. New Phytologist 212: 421-433 DOI: 10.1111/nph.14065
- Dreiseitl A. (2015) *Rare virulences of barley powdery mildew found in aerial populations in the Czech Republic from 2009 to 2014*. Czech Journal of Genetics and Plant Breeding 51: 1-8 DOI: 10.17221/254/201-CJGPB
- Dreiseitl A. (2017) *Heterogeneity of powdery mildew resistance revealed in accessions of the ICARDA wild barley collection*. Frontiers in Plant Science 8: 202 DOI: 10.3389/fpls.2017.00202
- Dreiseitl A., Dinooor A. (2004) *Phenotypic diversity of barley powdery mildew resistance sources*. Genetic Resources and Crop Evolution 51: 251-257 DOI: 10.1023/B:GRES.0000024010.12369.b3
- Eichmann R., Bischof M., Weis C., Shaw J., Lacomme C., Schweizer P., Douchkov D., Hensel G., Kumlehn J., Hüchelhoven R. (2010) *BAX INHIBITOR-1 is required for full susceptibility of barley to powdery mildew*. Molecular Plant-Microbe Interaction Journal 23: 1217-1227 DOI: 10.1094/MPMI-23-9-1217
- Elliott C., Zhou F., Spielmeier W., Panstruga R., Schulze-Lefert P. (2002) *Functional conservation of wheat and rice Mlo orthologs in defense modulation to the powdery mildew fungus*. Molecular Plant-Microbe Interactions 15: 1069-1077 DOI: 10.1094/MPMI.2002.15.10.1069
- Ellis M., Egelund J., Schultz C., Bacic A. (2010) *Arabinogalactan-proteins: kay regulators at the cell surface?* Plant Physiology 153: 403-419 DOI: 10.1104/pp.110.156000
- Falconer D. S., Mackay T. F. C (1996) *Introduction to quantitative genetics* (4th ed). Longman, Burnt Mill, England ISBN-10: 0582243025 ISBN-13: 978-05224302
- Fan J., Doerner P. (2012) *Genetic and molecular basis of nonhost disease resistance: complex, yes; silver bullet, no*. Current Opinion in Plant Biology 15: 400-406 DOI: 10.1016/j.pbi.2012.03.001
- FAO (2019) *FAOSTAT*.
URL: <http://www.fao.org/faostat/en/#data/QC/visualize> (Accessed on: 14.05.2019)
- Ferreira R. B., Monteiro S., Freitas R., Santos C. N., Chen Z., Batista L. M., Duarte J., Borges A., Teixeira A. R. (2006) *Fungal Pathogens: The battle for plant infection*. Critical Review of Plant Science 25: 505-524 DOI: 10.1080/07352680601054610

- Flint-Garcia S. A., Thornsberry J. M., Buckler E. S. (2003) *Structure of linkage disequilibrium in plants*. Annual Review of Plant Biology 54: 357-374 DOI: 10.1146/annurev.arplant.54.031902.134907
- Flor H. H. (1971) *Current status of the gene-for-gene concept*. Annual Review of Phytopathology 9: 275-296 DOI: 10.1146/annurev.py.09.090171.001423
- Frégeau-Reid J., Choo T.-M., Ho K.-M., Martin R. A., Konishi T. (2001) *Comparisons of two-row and six-row barley for chemical composition using doubled-haploid lines*. Crop Science 41: 1737-1743 DOI: 10.2135/cropsci2001.1737
- Freeman B. C., Beattie G. A. (2008) *An overview of plant defences against pathogens and herbivores*. The Plant Health Instructor DOI: 10.1094/PHI-I-2008-0226-01
URL: <https://www.apsnet.org/edcenter/disimpactmngmnt/topc/Pages/OverviewOfPlantDiseases.aspx> (Accessed on: 14.05.2019)
- Freialdenhoven A., Scherag B., Hollrichter K., Collinge D. B., Thordal-Christensen H., Schulze-Lefert P. (1994) *Nar-1 and Nar-2 two loci required for Mla12-specified race-specific resistance to powdery mildew in barley*. The Plant Cell 6: 983-994 DOI: 10.1105/tpc.6.7.983
- Freialdenhoven A., Peterhänsel C., Kurth J., Kreuzaler F., Schulze-Lefert P. (1996) *Identification of genes required for the function of the non-race-specific mlo resistance to powdery mildew in barley*. The Plant Cell 8: 5-14 DOI: <https://doi.org/10.1105/tpc.8.1.5>
- Freyark G., Diehl T., Miklis M., Romeis T., Panstruga R. (2007) *Antagonistic control of powdery mildew host cell entry by barley calcium-dependent protein kinases (CDPKs)*. Molecular Plant-Microbe Interaction Journal 20: 1213-1221 DOI: 10.1094/mpmi-20-10-1213
- Friedt W., Horsley R. D., Harvey B. L., Poulsen D. M., Lance R. C., Ceccarelli S., Grando S., Capettini F. (2011) *Chapter 8: Barley Breeding History, Progress, Objectives, and Technology*. In: S. E. Ullrich (Eds.). *Barley*. pp 160-220, Blackwell Publishing Ltd., Oxford DOI: 10.1002/9780470958636.ch8
- Frith M. C., Pheasant M., Mattick J. S. (2005) *The amazing complexity of the human transcriptome*. European Journal of Human Genetics 13: 894-897 DOI: 10.1038/sj.ejhg.5201459
- Gao X., Starmer J., Martin E. R. (2008) *A multiple testing correction method for genetic association studies using correlated single nucleotide polymorphisms*. Genetic Epidemiology 32: 361-369 DOI: 10.1002/gepi.20310
- Gao J., Bi W., Li H., Wu J., Liu D., Wang X. (2018) *WRKY transcription factors associated with NPR1-mediated acquired resistance in barley are potential resources to improve wheat resistance to Puccinia triticina*. Frontiers in Plant Science 9: 1486 DOI: 10.3389/fpls.2018.01486
- Gaspar Y. M., Nam J., Schultz C. J., Lee L.-Y., Gilson P. R., Gelvin S. B., Bacic A. (2004) *Characterization of the Arabidopsis lysine-rich arabinogalactan-protein AtAGP17 mutant (rat1) that results in a decreased efficiency of agrobacterium transformation*. Plant Physiology 135: 2162-2171 DOI: 10.1104/pp.104.045542
- Ge X., Deng W., Lee Z. Z., Lopez-Ruiz F. J., Schweizer P., Ellwood S. R. (2016) *Tempered mlo broad-spectrum resistance to barley powdery mildew in an Ethiopian landrace*. Scientific Reports 6: 1-10 DOI: 10.1038/srep29558
- Genissel A., Confais J., Lebrun M.-H., Gout L. (2017) *Association genetics in plants pathogens: minding the gap between the natural variation and the molecular function*. Frontiers in Plant Science 8: 1301 DOI: 10.3389/fpls.2017.01301
- Genomics platform from IRIC General Information on qPCR: [Understanding qPCR results](#)
URL: http://genomique.irc.ca/resources/files/Understanding_qPCR_results.pdf (Accessed on: 14.05.2019)

- Genoud T., Buchala A. J., Chua N.-H., Metraux J.-P. (2002) *Phytochrome signaling modulates the SA-perceptive pathway in Arabidopsis*. The Plant Journal 31: 87-95 DOI: 10.1046/j.1365-313X.2002.01338.x
- Gibson G. (2012) *Rare and common variants: twenty arguments*. Nature Reviews Genetics 13: 135-145 DOI: 10.1038/nrg3118
- Gingerich D. J., Hanada K., Shiu S.-H., Vierstra R. D. (2007) *Large-scale, lineage-specific expansion of a Bric-a-Brac/Tramtrack/Broad complex ubiquitin-ligase gene family*. The Plant Cell 19: 2329-2348 DOI: 10.1105/tpc.107.051300
- Glawe D. A. (2008) *The powdery mildews: a review of the world's most familiar (yet poorly known) plant pathogens*. Annual Review of Phytopathology 46: 27-51 DOI: 10.1146/annurev.phyto.46.0811407.104740
- González A. M., Marcel T. C., Kohutova Z., Stam P., van der Linden G. C., Niks R. E. (2010) *Peroxidase profiling reveals genetic linkage between peroxidase gene clusters and basal host and non-host resistance to rusts and mildew in barley*. PLOS ONE 5: e10495 DOI: 10.1371/journal.pone.0010495
- Görg R., Hollrichter K., Schulze-Lefert P. (1993) *Functional analysis and RFLP-mediated mapping of the Mlg resistance locus in barley*. The Plant Cell 3: 857-866 DOI: 10.1111/j.1365-313X.1993.00857.x
- Green J. R., Carver T. L. W. and Gurr S. J. (2002) *The formation and function of infection and feeding structures*. In: R. R. Bélanger, W. R. Bushnell, A. J. Dik, L. W. Carver (Eds.) *The powdery mildews-A comprehensive treatise*. pp 66-82, The American Phytopathological Society Press, St Paul, MN ISBN: 978-0-89054-291-0
- Griebel T., Zeier J. (2008) *Light regulation and daytime dependency of inducible plant defenses in Arabidopsis: phytochrome signaling controls systemic acquired resistance rather than local defense*. Plant Physiology 147: 790-801 DOI: 10.1104/pp.108.119503
- Gupta S., D'Antuono M., Bradley J., Li C., Loughman R. (2015) *Identification and expression of adult plant resistance in barley to powdery mildew (Blumeria graminis f. Sp. Hordei) in Australia*. Euphytica 203: 595-605 DOI: 10.1007/s10681-014-1280-4
- Gupta S., Vassos E., Sznajder B., Fox R., Khoo K. H. P., Loughman R., Chalmers K. J., Mather D. E. (2018) *A locus on barley chromosome 5H affects adult plant resistance to powdery mildew*. Molecular Breeding 38: 103 DOI: 10.1007/s/11032-018-0585-2
- Hart G. W., Copeland R. J. (2010) *Glycomics hits the big time*. Cell 143: 672-676 DOI: 10.1016/j.cell.2010.11.008
- Hartmann F. E., Sánchez-Vallet A., McDonald B. A., Croll D (2017). *A fungal wheat pathogen evolved host specialization by extensive chromosomal rearrangements*. The International Society for Microbial Ecology 11: 1189-1204 DOI: 10.1038/ismej.2016.196
- Harwood W. A. (2012) *Advances and remaining challenges in the transformation of barley and wheat*. Journal of Experimental Botany 63: 1791-1798 DOI: 10.1093/jxb/err380
- Häweker H., Rips S., Koiwa H., Salomon S., Saijo Y., Chinchilla D., Robatzek S., von Schaewen A. (2010) *Pattern recognition receptors require N-glycosylation to mediate plant immunity*. The Journal of Biological Chemistry 285: 4629-4636 DOI: 10.1074/jbcM109.063073
- Heffer V., Johnson K.B., Powelson M.L., Shishkoff N. (2006) *Identification of powdery mildew fungi anno 2006*. The Plant Health Instructor. DOI: 10.1094/PHI-I-2006-0706-01
URL: <https://www.apsnet.org/edcenter/disandpath/fungalasco/labexercises/Pages/PowderyMildew.aspx> (Accessed on: 14.05.2019)
- Henderson C. R. (1975) *Best linear unbiased estimation and prediction under a selection model*. Biometrics 31: 423-447 DOI: 10.2307/2529430

- Hermansen J. E., Torp U., Prahm L. P. (1978) *Studies of transport of live spores of cereal mildew and rust fungi across the North Sea*. Grana 17: 41-46 DOI: 10.1080/00173137809428851
- Himmelbach A., Zierold U., Hensel G., Riechen J., Douchkov D., Schweizer P., Kumlehn J. (2007) *A set of modular binary vectors for transformation of cereals*. Plant Physiology 145: 1192-1200 DOI: 10.1104/pp.107.111575
- Hirschhorn J. N., Daly M. J. (2005) *Genome-wide association studies for common diseases and complex traits*. Nature Reviews Genetics 6: 95-108 DOI: 10.1038/nrg1521
- Hoseinzadeh P. (2018) *High resolution genetic and physical mapping of a major powdery mildew resistance locus in barley*. Doctoral dissertation.
URL: <http://ediss.uni-goettingen.de/handle/11858/00-1735-0000-002E-E4B2-2?locale-attribute=en> (Accessed on: 14.05.2019)
- Hoseinzadeh P., Zhou R., Mascher M., Himmelbach A., Niks R. E., Schweizer P., Stein N. (2019) *High resolution genetic and physical mapping of a major powdery mildew resistance locus in barley*. Frontiers in Plant Science 10: 146 DOI: 10.3389/fpls.2019.00146
- Houston K., Tucker M. R., Chowdhury J., Shirley N., Little A. (2016) *The plant cell wall: a complex and dynamic structure as revealed by the responses of genes under stress conditions*. Frontiers in Plant Science 7: 984 DOI: 10.3389/fpls.2016.00984
- Hovmøller M. S., Caffier V., Jalli M., Andersen O., Besenhofer G., Czembor J. H., Dreiseitl A., Felsenstein F., Fleck A., Heinrics F., Jonsson R., Limpert E., Mercer P., Plesnik S., Rashal I., Skinnis H., Slater S., Vronska O. (2000) *The European barley powdery mildew virulence survey and disease nursery 1993-1999* Agronomie 20: 729-743 DOI: 10.1051/agro:2000172
- Hu X., Kong X., Wang C., Ma L., Zhao J., Wie J., Zhang X., Loake G. J., Zhang T., Huang J., Yang Y. (2014) *Proteasome-mediated degradation of FRIGIDA modulates flowering time in Arabidopsis during vernalization*. The Plant Cell 12: 4763-4781 DOI: 10.1105/tpc.114.132738
- Hua J. (2013) *Modulation of plant immunity by light, circadian rhythm, and temperature*. Current Opinion in Plant Biology 16: 406-413 DOI: 10.1016/j.pbi.2013.06.017
- Huang X., Han B. (2014) *Natural variations and genome-wide association studies in crop plants*. Annual Review of Plant Biology 65: 531-551 DOI: 10.1146/annurev-arplant-050213-035715
- Hückelhoven R. (2007) *Cell wall-associated mechanisms of disease resistance and susceptibility*. Annual Review of Phytopathology 45: 101-127 DOI: 10.1146/annurev.phyto.45.062806.094325
- Hückelhoven R., Panstruga R. (2011) *Cell biology of the plant-powdery mildew interaction*. Current Opinion in Plant Biology 14: 738-746 DOI: 10.1016/j.pbi.2011.08.002
- Hückelhoven R., Trujillo M., Kogel K.-H. (2000) *Mutations in Ror1 and Ror2 genes cause modification of hydrogen peroxide accumulation in mlo-barley under attack from the powdery mildew fungus*. Molecular Plant Pathogen 1: 587-292 DOI: 10.1046/j.1364-3703.2000.00032.x
- Humphry M., Conconi C., Panstruga R. (2006) *mlo-based powdery mildew immunity: silver bullet or simply non-host resistance?* Molecular Plant Pathology 7: 605-610 DOI: 10.1111/J.1364-3703.2006.00362.X
- Huq M. A., Akter S., Nou I. S., Kim H. T., Jung Y. J., Kang K. K. (2016) *Identification of functional SNPs in genes and their effects on plant phenotypes*. Journal of Plant Biotechnology 43: 1-11 DOI: 10.5010/JPB.2016.43.1.11
- Ioannidis J. P. A., Thomas G., Daly M. J. (2009) *Validating, augmenting and refining genome-wide association signals*. Nature Reviews Genetics 10: 318-328 DOI: 10.1038/nrg2544

- Jabbari M., Fakheri B. A., Aghnoum R., Mahdi Nezhad N., Ataei R. (2018) *GWAS analysis in spring barley (Hordeum vulgare L.) for morphological traits exposed to drought*. PLOS ONE 13: e0204952 DOI: 10.1371/journal.pone.0204952
- Jadid N., Mialoundama A. S., Heintz D., Ayoub D., Erhardt M., Mutterer J., Meyer D., Alioua A., Van Dorselaer A., Rahier A., Camara B., Bouvier F. (2011) *DOLICHOL PHOSPAHTE MANNOSE SYNTHASE1 mediates the biogenesis of the isoprenyl-linked glycans and influences development, stress response, and ammonium hypersensitivity in Arabidopsis*. The Plant Cell 23: 1985-2005 DOI: 10.1105/tpc.111.083634
- Jankowicz-Cieslak J., Till B. J. (2015) *Chapter 8: Forward and reverse genetics in crop breeding*. In: Al-Khayri J., Jain S., Johnson D. (Eds.) *Advances in plant breeding strategies: breeding, biotechnology and molecular tools*. pp 215-240 Springer, Cham DOI: 10.1007/978-3-319-22521-0_8
- Jefferson R. A., Kavanagh T. A., Bevan M. W. (1987) *GUS fusions: β -glucuronidase as a sensitive and versatile gene fusion marker in higher plants*. The EMBO journal 6: 3901-3907 DOI: 10.1002/j.1460-2075.1987.tb02730.x
- Johnson R. (1983) *Genetic Background of Durable Resistance*. In: F. Lamberti, J. M. Waller, N. A. Van der Graaff (Eds.) *Durable Resistance in Crops*. NATO Advanced Science Institutes Series (Series A: Life Sciences), vol 55., pp 2-26 Springer, Boston, MA, DOI: 10.1007/978-1-4615-9305-8_2
- Johrde A., Schweizer P. (2008) *A class III peroxidase specifically expressed in pathogen-attacked barley epidermis contributes to basal resistance*. Molecular Plant Pathology 9: 687-696 DOI: 10.1111/J.1364-3703.2008.00494.X
- Jones J. D. G. (2001) *Putting knowledge of plant disease resistance genes to work*. Current Opinion in Plant Biology 4: 281-287 DOI: 10.1016/S1369-5266(00)00174-6
- Jones J. D. G., Dangl J. L. (2006) *The plant immune system*. Nature 444: 323-329 DOI: 10.1038/nature05286
- Jørgensen J. H. (1976) *Identification of powdery mildew resistant barley mutants and their allelic relationship*. In: Barley Genetics III: Proceedings of the 3. International Barley Genetics Symposium, pp. 446-455, München: Verlag Karl Thiemeig
- Jørgensen J. H. (1992) *Discovery, characterization and exploitation of the Mlo powdery mildew resistance in barley*. Euphytica 63: 141-152 DOI: 10.1007/BF00023919
- Jørgensen J.H., Wolfe M. (1994) *Genetics of powdery mildew resistance in barley*. Critical Reviews in Plant Science: 13:1 97–119 DOI: 10.1080/07352689409701910
- Kang J. S., Frank J., Kang C. H., Kajiura H., Vikram M., Ueda A., Kim S., Bahk J. D., Triplett B., Fujiyama K., Lee S. Y., von Schaewen A., Koiwa H. (2008) *Salt tolerance of Arabidopsis thaliana requires maturation of N-glycosylated proteins in the Golgi apparatus*. Proceedings of the National Academy of Sciences 105: 5933-5938 DOI: 10.1073/pnas.0800237105
- Karapetyan S., Dong X. (2018) *Redox and the circadian clock in plant immunity: a balancing act*. Free Radical Biology and Medicine 119: 56-61 DOI: 10.1016/j.freeradbiomed.2017.12.024
- Kazan K., Manners J. M. (2011) *The interplay between light and jasmonate signalling during defence and development*. Journal of Experimental Botany 62: 4087-4100 DOI: 10.1093/jxb.err142
- Kilian B., Özkan H., Kohl J., von Haeseler A., Barale F., Deusch O., Brandolini A., Yucel C., Martin W., Salamini F. (2006) *Haplotype structure at seven barley genes: relevance to gene pool bottlenecks, phylogeny of ear type and site of barley domestication*. Molecular Genetics and Genomics 276: 230-241 DOI: 10.1007/s00438-006-0136-6
- Kim M. C., Lee S. H., Kim J. K., Chun H. J., Choi M. S., Chung W. S., Moon B. C., Kang C. H., Park C. Y., Yoo J. H., Kang Y. H., Koo S. C., Koo Y. D., Jung J. C., Kim S. T., Schulze-Lefert P., Lee S. Y., Cho M. J. (2002a) *Mlo, a modulator of plant defense and cell death, is a novel*

- calmodulin-binding protein*. The Journal of Biological Chemistry 277: 19304-19314 DOI: 10.1074/jbc.M108478200
- Kim M. C., Panstruga R., Elliott C., Müller J., Devoto A., Yoon H. W., Park H. C., Cho M. J., Schulze-Lefert P. (2002b) *Calmodulin interacts with MLO protein to regulate defence against mildew in barley*. Nature 416: 447-450 DOI: 10.1038/416447a
- Kimura S., Furukawa T., Kasai N., Mori Y., Kitamoto H. K., Sugawara F., Hashimoto J., Sakaguchi K. (2003) *Functional characterization of two flap endonuclease-1 homologues in rice*. Gene 18: 63-71 DOI: 10.1016/S0378-1119(03)00694-2
- Korte A., Farlow A. (2013) *The advantages and limitations of trait analysis with GWAS: a review*. Plant Methods 9: 29 DOI: 10.1186/1746-4811-9-29
- Kou Y., Wang S. (2010) *Broad-spectrum and durability: understanding of quantitative disease resistance*. Current Opinion in Plant Biology 13: 400-406 DOI: 10.1016/j.pbi.2009.12.010
- Kumar J., Pratap A., Kumar S. (2015) *Plant phenomics: an overview*. In: Kumar J., Pratap A., Kumar S. (Eds.) *Phenomics in crop plants: trends options and limitation*, 1-10, Springer, New Delhi DOI: 10.1007/978-81-322-2226-2_1
- Kusch S., Pesch L., Panstruga R. (2016) *Comprehensive phylogenetic analysis sheds light on the diversity and origin of the MLO family of integral membrane proteins*. Genome Biology Evolution 8: 878-895 DOI: 10.1093/gbe/evw036
- Kusch S., Panstruga R. (2017) *mlo-based resistance: an apparently universal “weapon” to defeat powdery mildew disease*. Molecular Plant-Microbe Interaction Journal 30: 179-189 DOI: 10.1094/mpmi-12-16-0255-CR
- Lande R., Thompson R. (1990) *Efficiency of marker-assisted selection in the improvement of quantitative traits*. Genetics 124: 743-756 PMID: 1968875; PMCID: PMC1203965
- Lawrenson T., Harwood W. A. (2019) *Creating targeted gene knockouts in barley using CRISPR/Cas9*. In: W. Harwood (Eds.) *Barley. Methods in Molecular Biology* vol 1900, pp 217-232 Humana Press, NY DOI: 10.1007/978-1-4939-8944-7_14
- Leduc, N., Iglesias, V.A., Bilang, R., Gisel, A., Potrykus, I. Sautter, C. (1994) *Gene-transfer to inflorescence and flower meristems using ballistic micro-targeting*. Sexual Plant Reproduction 7: 135-143 DOI: 10.1007/BF00230582
- Lee W.-S., Hammond-Kosack K. E., Kanyuka K. (2012) *Barley stripe mosaic virus-mediated tools for investigating gene function in cereal plants and their pathogens: virus-induced gene silencing, host-mediated gene silencing, and virus-mediated overexpression of heterologous protein*. Plant Physiology 160: 582-590 DOI: 10.1104/pp.112.203489
- Lee U., Chang S., Putra G. A., Kim H., Kim D. H. (2018) *An automated, high-throughput plant phenotyping system using machine learning-based plant segmentation and image analysis*. PLOS ONE 13: e0196615 DOI: 10.1371/journal.pone.0196615
- Legris M., Klose C., Burgie E. S., Costigliolo Rojas C., Neme M., Hiltbrummer A., Wigge P. A., Schäfer E., Vierstra R. D., Casal J. J. (2016) *Phytochrome B integrates light and temperature signals in Arabidopsis*. Science 35: 897-900 DOI: 10.1126/science.aaf5656
- Lenk M., Wenig M., Mengel F., Häußler F., Vlot A. C. (2018) *Arabidopsis thaliana immunity-related compounds modulated disease susceptibility in barley*. Agronomy 8: 142 DOI: 10.3390/agronomy8080142
- Li Z., Lan C., He Z., Singh R. P., Rosewarne G. M., Chen X., Xia X. (2014a) *Overview and application of QTL for adult plant resistance to leaf rust and powdery mildew in wheat*. Crop Science 54: 1907-1925 DOI: 10.2135/cropsci2014.02.0162
- Li M., Liu X., Bradbury P., Yu J., Zhang Y.-M., Todhunter R. J., Buckler E. S., Zhang Z. (2014b) *Enrichment of statistical power for genome-wide association studies*. BMC Biology 12: 73-82 DOI: 10.1186/s12915-014-0073-5

- Liang Y., Zhao J., Wang C., Jing Y., Chengyun L. (2018) *Infection with blast fungus (Magnaporthe oryzae) leads to increased expression of an arabinogalactan-protein in both susceptible and resistant rice cultivars*. *Physiological and Molecular Plant Pathology* 102: 136-143 DOI: 10.1016/j.pmpp.2018.01.002
- Lightfoot D. J., McGrann G. R. D., Able A. J. (2017) *The role of a cytosolic superoxide dismutase in barley-pathogen interactions*. *Molecular Plant Pathology* 18: 323-335 DOI: 10.1111/mp.12399
- Lindhout P. (2002) *The perspectives of polygenic resistance in breeding for durable disease resistance*. *Euphytica* 124: 217-226 DOI: 10.1023/A:1015686601404
- Liu J., Cheng X., Liu D., Xu W., Wise R., Shen Q.-H. (2016) *The miR9863 family regulates distinct Mla alleles in barley to attenuate NLR receptor-triggered disease resistance and cell-death signalling*. *PLOS Genetics* 10: e1004755 DOI: 10.1371/journal.pgen.1004755
- Lu X., Kracher B., Saur I. M. L., Bauer S., Ellwood S. R., Wise R., Yaeno T., Maekawa T., Schulze-Lefert P. (2016) *Allelic barley MLA immune receptors recognize sequence-unrelated avirulence effectors of the powdery mildew pathogen*. *Proceedings of the National Academy of Sciences* 113: E6486-E6495 DOI: 10.1073/pnas.1612947113
- Lu H., McClung R. C., Zhang C. (2017) *Tick Tock: circadian regulation of plant immunity*. *Annual Review of Phytopathology* 55: 12.1-12.25 DOI: 10.1146/annurev-phyto-080516-035451
- Malthus T. R. (1798) *An Essay on the Principle of Population, as it affects the future Improvement of Society, with Remarks on the Speculations of Mr. Godwin, M. Condorcet, and Other Writers*. 1st edition, J. Johnson, London
URL: <http://www.esp.org/books/malthus/population/malthus.pdf> (Accessed on: 14.05.2019)
- Mareri L., Romi M., Cai G. (2019) *Arabinogalactan proteins: actors or spectators during abiotic and biotic stress in plants?* *Plants Biosystems – An International Journal Dealing with all Aspects of Plant Biology* 153: 173-185 DOI: 10.1080/11263504.2018.1473525
- Marmagne A., Rouet M.-A., Ferro M., Rolland N., Alcon C., Joyard J., Garin J., Barbier-Brygoo H., Ephritikhine G. (2004) *Identification of new intrinsic proteins in Arabidopsis plasma membrane proteome*. *Molecular & Cellular Proteomics* 3.7: 675-691 DOI: 10.1074/mcp.M400001-MCP200
- Marmagne A., Ferro M., Meinel T., Bruley C., Kuhn L., Garin J., Barbier-Brygoo H., Ephritikhine G. (2007) *A high content in lipid-modified peripheral proteins and integral receptor kinases features in the Arabidopsis plasma membrane proteome*. *Molecular & Cellular Proteomics* 6.11: 1980-1996 DOI: 10.1074/mcp.M700099-MCP200
- Mascher M., Richmond T. A., Gerhardt D. J., Himmelbach A., Clissold L., Sampath D., Ayling S., Steuernagel B., Pfeifer M., D'Ascenzo M., Akhunov E. D., Hedley P. E., Gonzales A. M., Morrell P. L., Kilian B., Blattner F., Scholz U., Mayer K. F. X., Flavell A. J., Muehlbauer G. J., Waugh R., Jeddelloh J. A., Stein N. (2013) *Barley whole exome capture: a tool for genomic research in the genus Hordeum and beyond*. *The Plant Journal* 76: 494-505 DOI: 10.1111/tpj.12294
- Mascher M., Gundlach H., Himmelbach A., Beier S., Twardziok S. O., Wicker T., Radchuk V., Dockter C., Hedley P. E., Russell J., Bayer M., Ramsay L., Liu H., Haberer G., Zhang X.-Q., Zhang Q., Barrero R. A., Li L., Taudien S., Groth G., Felder M., Hastie A., Šimkova H., Staňkova H., Vrana J., Chan S., Munoz-Amatriain M., Ounit R., Wanamaker S., Bolser D., Colmsee C., Schmutzer T., Aliyeva-Schnorr L., Grasso S., Tanskanen J., Chailyan A., Sampath D., Heavens D., Clissold L., Cao S., Chapman B., Dai F., Han Y., Li H., Li X., Lin C., McCooke J. K., Tan C., Wang P., Wang S., Yin S., Zhou G., Poland J. A., Bellgard M., Borisjuk L., Houben A., Doležal J., Ayling S., Lonardi S., Kersey P., Langridge P., Muehlbauer G. J., Clark M. D., Caccamo M., Schulman A. H., Mayer K. F. X., Platzer M., Close T. J., Scholz U., Hansson M., Zhang G., Braumann I., Spannagl M., Li C., Waugh R.,

- Stein N. (2017) *A chromosome conformation capture ordered sequence of the barley genome*. *Nature* 544: 427-448 DOI: 10.1038/nature22043
- Mazza C. A., Ballaré C. L. (2015) *Photoreceptors UVR8 and phytochrome B cooperate to optimize plant growth and defense in patchy canopies*. *New Phytologist* 207: 4-9 DOI: 10.1111/nph.13332
- McCouch S., Baute G. J., Bradeen J., Bramel P., Bretting P. K., Buckler E., Burke J. M., Charest D., Cloutier S., Cole G., Dempewolf H., Dingkuhn M., Feuillet C., Gepts P., Grattapaglia D., Guarino L., Jackson S., Knapp S., Langridge P., Lawton-Rauh A., Lijua Q., Lusty C., Michael T., Myles S., Naito K., Nelson R. L., Pontarollo R., Richards C. M., Rieseberg L., Ross-Ibarra J., Rounsley S., Hamilton R. S., Schurr U., Stein N., Tomooka N., van der Knaap E., van Tassel D., Toll J., Valls J., Varshney R. K., Ward J., Waugh R., Wenzl P., Zamir D. (2013) *Feeding the future*. *Nature* 499: 23-24 DOI: 10.1038/499023a
- McDonald J. H. (2014) *Handbook of biological statistics: Multiple comparisons*. (3rd ed.) Sparrky House Publishing 254-260
URL: <http://www.biostathandbook.com/multiplecomparisons.html> (Accessed on: 14.05.2019)
- McElroy D., Blowers A. D., Jenes B., Wu R. (1991) *Construction of expression vectors based on the rice actin1 (Act1) 5' region for use in monocot transformation*. *Molecular and General Genetics* 231: 150–160 DOI: 10.1007/BF00293832
- Melchinger A., Messmer M., Lee M., Woodman W., Lamkey K. (1991) *Diversity and relationships among US maize inbreds revealed by restriction fragment length polymorphisms*. *Crop Science* 31: 669–678 DOI: 10.2135/cropsci1991.0011183X003100030025x
- Meuwissen T. H. E., Hayes B. J., Goddard M. E. (2001) *Prediction of total genetic value using genome-wide dense marker maps*. *Genetics* 157: 1819-1829 PMID: 11290733; PMCID: PMC1461589
- Milner S. G., Jost M., Taketa S., Rey Mazón E., Himmelbach A., Oppermann M., Weise S., Knüpffer H., Basterrechea M., König P., Schüler D., Sharma R., Pasam R. K., Rutten T., Guo G., Xu D., Zhang J., Herren G., Müller T., Krattinger S. G., Keller B., Jiang Y., González M. Y., Zhao Y., Habekuß A., Färber S., Ordon F., Lange M., Börner A., Graner A., Reif J. C., Scholz U., Mascher M., Stein N. (2019) *Genebank genomics highlights the diversity of a global barley collection*. *Nature Genetics* 51: 319-326 DOI: 10.1038/s41588-018-0266-x
- Moral J., Montilla-Bascón G., Canales F. J., Rubiales D., Prats E. (2017) *Cytoskeleton reorganization/disorganization is a key feature of induced inaccessibility for defence to successive pathogen attacks*. *Molecular Plant Pathology* 18: 662-671 DOI: 10.1111/mpp.12424
- Morel J.-B., Dangl J. L. (1997) *The hypersensitive response and the induction of cell death*. *Cell Death and Differentiation* 4: 671-683 DOI: 10.1038/sj.cdd.4400309
- Mulualem T., Bekeko Z. (2016) *Advances in quantitative trait loci, mapping and importance of markers assisted selection in plant breeding research*. *International Journal of Plant Breeding and Genetics* 10: 58-68 DOI: 10.3923/ijpbg.2016.58.68
- Mundt C. (2014) *Durable resistance: a key sustainable management of pathogens and pests*. *Infection, Genetics and Evolution* 27: 446-455 DOI: 10.1016/j.meegid.2014.01.011
- Myles S., Peiffer J., Brown P. J., Ersoz E. S., Zhang Z., Costich D. E., Buckler E. S. (2009) *Association mapping: critical considerations shift from genotyping to experimental design*. *The Plant Cell*: 21: 2194-2202 DOI: 10.1105/tpc.109.068437

- Nadeem M. A., Nawaz M. A., Shahid M. Q., Doğan Y., Comertpay G., Yildiz M., Hatipoğlu R., Ahmad F., Alsaleh A., Labhane N., Özkan H., Chung G., Baloch F. S. (2018) *DNA molecular markers in plant breeding: current status and recent advancements in genomic selection and genome editing*. *Biotechnology & Biotechnological Equipment* 32: 261-285 DOI: 10.1080/13102818.2017.1400401
- Mathews S., Sharrock R. A. (1997) *Phytochrome gene diversity*. *Plant, Cell and Environment* 20: 666-671 DOI: 10.1046/j.1365-3040.1997.d01-117.x
- National Center for Biotechnology Information (NCBI) (1988) Bethesda (MD): National Library of Medicine (US), National Center for Biotechnology Information.
URL: <https://www.ncbi.nlm.nih.gov/> (Accessed on: 14.05.2019)
URL: https://blast.ncbi.nlm.nih.gov/Blast.cgi?PAGE_TYPE=BlastSearch (Accessed on: 14.05.2019)
- Negassa M. (1985) *Geographic distribution and genotypic diversity of resistance to powdery mildew of barley in Ethiopia*. *Hereditas* 102: 113-121 DOI: 10.1111/j.1601-5223.1985.tb.00472.x
- Ni W., Xu S.-L., Tepperman J. M., Stanley D. J., Maltby D. A., Gross J. D., Burlingame A. L., Wang Z.-Y., Quail P. H. (2014) *A mutually assured destruction mechanism attenuates light signaling in Arabidopsis*. *Science* 344: 1160-1164 DOI: 10.1126/science.1250778
- Niks R. E., Marcel T. C. (2009) *Nonhost and basal resistance: how to explain specificity?* *New Phytologist* 182: 817-828 DOI: 10.1111/j.1469-8137-2009.02849.x
- Niks R. E., Qi X., Marcel T. C. (2015) *Quantitative resistance to biotrophic filamentous plant pathogens: concepts, misconceptions, and mechanisms*. *Annual Review of Phytopathology* 53: 445-470 DOI: 10.1146/annurev-phyto-080614-115928
- Niks R. E., Rubiales D. (2002) *Potentially durable resistance mechanisms in plants to specialised fungal pathogens*. *Euphytica* 124: 201-216 DOI: 10.1023/A:1015634617334
- Nguema-Ona E., Vicré-Gibouin M., Gotté M., Plancot B., Lerouge P., Bardor M., Driouich A. (2014) *Cell wall O-glycoproteins and N-glycoproteins: aspects of biosynthesis and function*. *Frontiers in Plant Science* 5: 499 DOI: 10.3389/fpls.2014.00499
- Nguyen G. N., Norton S. L., Rosewarne G. M., James L. E., Slater A. T. (2018) *Automated phenotyping for early vigour of field pea seedlings in controlled environment by colour imaging technology*. *PLOS ONE* 13: e0207788 DOI: 10.1371/journal.pone.0207788
- Opalski K. S., Schultheiss H., Kogel K.-H., Hüchelhoven R. (2005) *The receptor-like MLO protein and the RAC/ROP family G-protein RACB modulate actin reorganization in barley attacked by the biotrophic powdery mildew fungus Blumeria graminis f. sp. hordei*. *The Plant Journal* 41: 291-303 DOI: 10.1111/j.1365-313X.2004.02292.x
- Papa R. (2005) *Gene flow and introgression between domesticated crops and their wild relatives*. In: *Proceedings of the International Workshop on the Role of Biotechnology for the Characterization and Conservation of Crop, Forestry, Animal and Fishery Genetic Resources*. Turin, Italy.
URL: <http://www.fao.org/biotech/docs/papa.pdf> (Accessed on: 14.05.2019)
- Pankin A., Campoli C., Dong X., Kilian B., Sharma R., Himmelbach A., Saini R., Davis S. J., Stein N., Schneeberger K., von Korff M. (2014) *Mapping-by-sequencing identifies HvPHYTOCHROME C as candidate gene for the early maturity 5 locus modulating the circadian clock and photoperiodic flowering in barley*. *Genetics* 198: 383-396 DOI: 10.1534/genetics.114.165613
- Panstruga R. (2004) *A golden shot: how ballistic single cell transformation boosts the molecular analysis of cereal-mildew interactions*. *Molecular Plant Pathology* 5: 141-148 DOI: 10.1111/J.1364.3703.200.00280.X

- Panstruga R., Kuhn H. (2019) *Mutual interplay between phytopathogenic powdery mildew fungi and other microorganisms*. *Molecular Plant Pathology* 20: 463-470 DOI: 10.1111/mpp.12771
- Park E., Nedo A., Caplan J. L., Dinesh-Kumar S. P. (2018) *Plant-microbe interactions: organelles and the cytoskeleton in action*. *New Phytologist* 217: 1012-1028 DOI: 10.1111/nph.14959
- Parlevliet J. E. (1985) *16-Resistance of the non-race-specific type*. In: A. P. Roelfs, W. R. Bushnell (Eds.) *The Cereal Rusts*, Volume II: Diseases, Distribution, Epidemiology, and Control, pp 501-525, Academic Press DOI: 10.1016/B978-0-12-148402-6.50024-9
- Pasam R. K., Sharma R., Malosetti M., van Eeuwijk F. A., Haseneyer G., Kilian B., Graner A. (2012) *Genome-wide association studies for agronomical traits in a world wide spring barley collection*. *BMC Plant Biology* 12: 16 DOI: 10.1186/1471-2229-12-16
- Peterhänsel C., Lahaye T. (2005) *Be fruitful and multiply: gene amplification inducing pathogen resistance*. *Trends in Plant Science* 10: 257-260 DOI: 10.1016/j.tplants.2005.04.005
- Piepho H.P., Büchse A., Emrich K. (2003) *A hitchhiker's guide to mixed models for randomized experiments*. *Journal of Agronomy and Crop Science* 189:310–322 DOI: [10.1046/j.1439-037X.2003.00049.x](https://doi.org/10.1046/j.1439-037X.2003.00049.x)
- Piepho H.-P., Möhring J. (2007) *Computing heritability and selection response from unbalanced plant breeding trials*. *Genetics* 177: 1881-1888 DOI: 10.1534/genetics.107.074229
- Piffanelli P., Zhou F., Casais C., Orme J., Jarosh B., Schaffrath U., Collins N. C., Panstruga R., Schulze-Lefert P. (2002) *The barley MLO modulator of defense and cell death is responsive to biotic and abiotic stress stimuli*. *Plant Physiology* 123: 1076-1085 DOI: 10.1104/pp.010954
- Piffanelli P., Ramsay L., Waugh R., Benabdelmouna A., D'Hont A., Hollrichter K., Jørgensen J. H., Schulze-Lefert P., Panstruga R. (2004) *A barley cultivation-associated polymorphism conveys resistance to powdery mildew*. *Nature* 430: 887-891 DOI: 10.1038/nature02781
- Platt A., Vilhjálmsson B. J., Nordborg M. (2010) *Conditions under which genome-wide association studies will be positively misleading*. *Genetics* 186: 1045-1052 DOI: 10.1534/genetics.110.121665
- Poets A. M., Fang Z., Clegg M. T., Morrell P. L. (2015) *Barley landraces are characterized by geographically heterogeneous genomic origins*. *Genome Biology* 16: 173 DOI: 10.1186/s13059-015-0712-3
- Poovaiah B. W., Du L., Wang H., Yang T. (2013) *Recent advances in calcium/calmodulin-mediated signalling with an emphasis on plant-microbe interactions*. *Plant Physiology* 163: 531-542 DOI: 10.1104/pp.113.220780
- Pourkheirandish M., Komatsuda T. (2007) *The importance of barley genetics and domestication in a global perspective*. *Annals of Botany* 100: 999-1008 DOI: 10.1093/aob/mem139
- Praz C. R., Bourras S., Zeng F., Sánchez-Martín J., Menardo F., Xue M., Yang L., Roffler S., Böni R., Herren G., McNally K. E., Ben-David R., Parlange F., Oberhaensli S., Flückiger S., Schäfer L. K., Wicker T., Yu D., Keller B. (2017) *AvrPm2 encodes an RNase-like avirulence effector which is conserved in the two different specialized forms of wheat and rye powdery mildew fungus*. *New Phytologist* 213: 1301-1314 DOI: 10.1111/nph.14372
- Price A. L., Zaitlen N. A., Reich D., Patterson N. (2010) *New approaches to population stratification in genome-wide association studies*. *Nature Reviews Genetics* 11: 459-463 DOI: 10.1038/nrg2813
- Pritchard J. K., Stephens M., Donnelly P. (2000) *Inference of population structure using multilocus genotype data*. *Genetics* 155: 945-959 PMID: 10835412; PMCID: PMC1461096
- Pronobis M. I., Deutch N., Pfeifer M. (2016) *The Miraprep: a protocol that uses a miniprep kit and provides maxiprep yields*. *PLOS ONE* 11: 1-12 DOI: 10.1371/journal.pone.0160509

- Pryce-Jones E., Carver T., Gurr S. (1999) *The roles of cellulase enzymes and mechanical force in host penetration by Erysiphe graminis f.sp. hordei*. *Physiological and Molecular Plant Pathology* 55: 175-182 DOI: 10.1006pmpp.1999.02222
- Qu N., Gan W., Bi D., Xia S., Li X., Zhang Y. (2010) *Two BTB proteins function redundantly as negative regulators of defense against pathogens in Arabidopsis*. *Botany* 88: 953-960 DOI: 10.1139/B10-067
- Rafalski A. (2002) *Application of single nucleotide polymorphisms in crop genetics*. *Current Opinion in Plant Biology* 5: 94-100 DOI: 10.1016/s1369-5266(02)00240-6
- Rajaraman J., Douchkov D., Lück S., Hensel G., Nowara D., Pogoda M., Rutten T., Meitzel T., Höfle C., Hückelhoven R., Klinkenberg J., Trujillo M., Bauer E., Schnutzer T., Himmelbach A., Mascher M., Lazzari B., Stein N., Kumlehn J., Schweizer P. (2018) *Evolutionarily conserved partial gene duplication in the Triticeae tribe of grasses confers pathogen resistance*. *Genome Biology* 19: 116 DOI: 10.1186/s13059-018-1472-7
- R Development Core Team (2008). *R: A language and environment for statistical computing*. R Foundation for Statistical Computing, Vienna, Austria. ISBN 3-900051-07-0
URL: <https://www.r-project.org/> (Accessed on: 14.05.2019)
- Reagan M. S., Pittenger C., Siede W., Friedberg E. C. (1995) *Characterization of a mutant strain of Saccharomyces cerevisiae with a deletion of the RAD27 gene, a structural homolog of the RAD2 nucleotide excision repair gene*. *Journal of Bacteriology* 177: 364-371 DOI: 10.1128/jb.177.2.364-371.1995
- Reif J. C., Melchinger A. E., Frisch M. (2005) *Genetical and mathematical properties of similarity and dissimilarity coefficients applied in plant breeding and seed bank management*. *Crop Science* 45: 1-7 DOI: 10.2135/cropsci2005.0001
- Reiner T., Hoefle C., Hückelhoven R. (2016) *A barley SKP1-like protein controls abundance of the susceptibility factor RACB and influences in the interaction of barley with the barley powdery mildew fungus*. *Molecular Plant Pathology* 17: 184-195 DOI: 10.1111/mpp.12271
- Reinstädler A., Müller J., Czembor, Piffanelli P., Panstruga R. (2010) *Novel induced mlo mutant alleles in combination with site-directed mutagenesis reveal functionally important domains in the heptahelica barley Mlo protein*. *BMC (BioMed Central) Plant Biology* 10: 31 DOI: 10.1186/1471-2229-10-31
- Roden L. C., Ingle R. A. (2009) *Lights, rhythms, infection: the role of light and the circadian clock in determining the outcome of plant-pathogen interactions*. *The Plant Cell* 21: 2546-2552 DOI: 10.1105/tpc.109.069922
- Rogers J. S. (1972) *Measures of genetic similarity and genetic distance*. In: Wheeler M. R. (Eds.) *Studies in genetics*, VII. Publ. 7213., pp 145-153 Univ. of Texas
URL: <https://repositories.lib.utexas.edu/handle/2152/27775> (Accessed on: 14.05.2019)
- Romero C. C. T., Vemeulen J. P., Vels A., Himmelbach A., Mascher M., Niks R. E. (2018) *Mapping resistance to powdery mildew in barley reveals a large-effect nonhost resistance QTL*. *Theoretical and Applied Genetics* 131: 1031-1045 DOI: 10.1007/s00122-018-3055-0
- Rostoks N., Ramsay L., MacKenzie K., Cardle L., Bhat P. R., Roose M. L., Svensson J. T., Stein N., Varshney R. K., Marshall D. F., Graner A., Close T. J., Waugh R. (2006) *Recent history of artificial outcrossing facilitates whole-genome association mapping in elite inbred crop varieties*. *Proceedings of the National Academy of Sciences* 103: 18656-18661 DOI: 10.1073/pnas.0606133103
- Rouphael Y., Spíchal L., Panzarová K., Casa R., Colla G. (2018) *High-throughput plant phenotyping for developing novel biostimulants: from lab to field or from field to lab?* *Frontiers in Plant Science* 9: 1197 DOI: 10.3389/fpls.2018.01197

- Rutledge K., McDaniel M., Boudreau D., Ramroop T., Teng S., Sprout E., Costa H., Hall H., Hunt J. (2011) *Food staple*. National Geographic
URL: <https://www.nationalgeographic.org/encyclopedia/food-staple/> (Accessed on: 14.05.2019)
- Russell J., Mascher M., Dawson I. K., Kysiakidis S., Calixto C., Freund F., Bayer M., Milne I., Marshall-Griffiths T., Heinen S., Hofstad A., Sharma R., Himmelbach A., Knauff M., van Zonneveld M., Brwon J. W. S., Schmid K., Kilian B., Muehlbauer G. J., Stein N., Waugh R. (2016) *Exome sequencing of geographically diverse barley landraces and wild relative gives insight into environmental adaptation*. *Nature Genetics* 48: 1024–1030 DOI: 10.1038/ng.3612
- Saijo Y., Tintor N., Lu X., Rauf P., Pajerowska-Mukhtar K., Häweker H., Dong X., Robatzek S., Schulze-Lefert P. (2009) *Receptor quality control in the endoplasmic reticulum for plant innate immunity*. *The European Molecular Biology Organization Journal* 28: 3439–3449 DOI: 10.1038/emboj.2009.263
- Saur I. M. L., Bauer S., Kracher B., Lu X., Franzeskakis L., Müller M. C., Sabelleck B., Kümmel F., Panstruga R., Maekawa T., Schulze-Lefert P. (2019) *Multiple pairs of allelic MLA immune receptor-powdery mildew AVRAs effectors argue for a direct recognition mechanism*. *eLIFE* 8: e44471 DOI: 10.7554/eLife.44471
- Savary S., Ficke A., Aubertot J.-N., Hollier C. (2012) *Crop losses due to diseases and their implications for global food production losses and food security*. *Food Security* 4: 519–537 DOI: 10.1007/s12571-012-0200-5
- Schmalenbach I., Körber N., Pillen K. (2008) *Selecting a set of wild introgression lines and verification of QTL effects for resistance to powdery mildew and leaf rust*. *Theoretical and Applied Genetics* 117: 1093–11106 DOI: 10.1007/s00122-008-0847-7
- Schmid K., Kilian B., Russell J. (2018) *Barley domestication, adaptation and population genomics*. In: N. Stein and G. J. Muehlbauer (Eds.) *The Barley Genome*, Compendium of Plant Genomes, pp 317–336, Springer, Cham DOI: 10.1007/978-3-319-92528-8_17
- Schultz R. W., Tatineni V. M., Hanley-Bowdoin L., Thompson W. F. (2007) *Genome-wide analysis of the core DNA replication machinery in the higher plants Arabidopsis and rice*. *Plant Physiology* 144: 1697–1714 DOI: 10.1104/pp.107.101105
- Schulze-Lefert P. (2004) *Knocking on the heaven's wall: pathogenesis of and resistance to biotrophic fungi at the cell wall*. *Current Opinion in Plant Biology* 7: 377–383 DOI: 10.1016/j.pbi.2004.05.004
- Schulze-Lefert P., Vogel J. (2000) *Closing the ranks to attack by powdery mildew*. *Trends in Plants Science* 5: 343–348 DOI: 10.1016/S1360-1385(00)01683-6
- Schweizer P. (2007) *Nonhost resistance of plants to powdery mildew—New opportunities to unravel the mystery*. *Physiological and Molecular Plant Pathology* 70: 3–7 DOI: 10.1016/j.pmpp.2007.07.004
- Schweizer P., Christoffel A., Dudler R. (1999a) *Transient expression of members of the germinal-like gene family in epidermal cells of wheat confers disease resistance*. *The Plant Journal* 20: 541–552 DOI: [10.1046/j.1365-3113.1999.00624.x](https://doi.org/10.1046/j.1365-3113.1999.00624.x)
- Schweizer P., Pokorný J., Abderhalden O., Dudler R. (1999b) *A transient assay system for the functional assessment of defense-related genes in wheat*. *Molecular Plant-Microbe Interaction Journal* 12: 647–654 DOI: [10.1094/MPMI.1999.12.8.647](https://doi.org/10.1094/MPMI.1999.12.8.647)
- Seeholzer S., Tsuchimatsu T., Jordan T., Bieri S., Pajonk S., Yang W., Jahoor A., Shimizu K. K., Keller B., Schulze-Lefert P. (2010) *Diversity at the Mla powdery mildew resistance locus from cultivated barley reveals sites of positive selection*. *Molecular Plant-Microbe Interaction Journal* 23: 497–509 DOI: 10.1094/MPMI-23-0497

- Sehgal D., Singh R., Rajpal V. R. (2016) *Quantitative trait loci mapping in plants: concepts and approaches*. In: Rajpal V., Rao S., Raina S. (Eds.) *Molecular breeding for sustainable crop improvement. Sustainable Development and Biodiversity*, vol 11, pp 31-59 Springer, Cham DOI: 10.1007/978-3-319-27090-6_2
- Sharma M., Bhatt D. (2015) *The circadian clock and defence signaling in plants*. *Molecular Plant Pathology* 16: 210-218 DOI: 10.1111/mpp.12178
- Shu K., Yang W. (2017) *E3 ubiquitin ligases: ubiquitous actors in plant development and abiotic stress responses*. *Plant & Cell Physiology* 58: 1461-1476 DOI: 10.1093/pcp/pcx071
- Silvar C., Casas A. M., Kopahnke D., Habekuß A., Schweizer G., Gracia M. P., Lasa J. M., Ciudad F. J., Molina-Cano J. L., Igartua E., Ordon F. (2009) *Screening the Spanish barley core collection for disease resistance*. *Plant Breeding* 129: 45-52 DOI: 10.1111/j.1439-0523.2009.01700.x
- Silvar C., Flath K., Kopahnke D., Gracia M. P., Lasa J. M., Casas A. M., Igartua E., Ordon F. (2011) *Analysis of powdery mildew resistance in the Spanish barley core collection*. *Plant Breeding* 130: 195-202 DOI: 10.1111/j.1439-0523.2010.01843.x
- Skou J. P., Jørgensen J. H., Lilholt U. (1984) *Comparative studies on callose formation in powdery mildew compatible and incompatible barley*. *Journal of Phytopathology* 109: 147-168 DOI: 10.1111/j.1439-0434.1984.tb00702.x
- Skov J., Hagedorn P., Lyngkjaer M. (2007) *qPCR reference genes for barley*. Paper presented at 3. International qPCR symposium, Freising, Germany.
URL: <https://www.gene-quantification.de/qpcr2007/publications/P087-qPCR-2007.pdf>
Accessed on: 14.05.2019)
- Smith H. C., Smith M. (1974) *Surveys of powdery mildew in wheat and an estimate of national yield losses*. *New Zealand Journal of Experimental Agriculture* 2: 441-445 DOI: 10.1080/03015521.1974.10427711
- Spies A., Korzun V., Bayles R., Rajaraman J., Himmelbach A., Hedley P. E., Schweizer P. (2012) *Allele mining in barley genetic resources reveals genes of race-non-specific powdery mildew resistance*. *Frontiers in Plant Science* 2: 1-22 DOI: 10.3389/fpls.2011.00113
- Stael S., Kmieciak P., Willems P., Van Der Kelen K., Coll N. S., Teige M., Van Breusegem F. (2015) *Plant innate immunity-sunny side up?* *Trends in Plant Science* 20: 3-11 DOI: 10.1016/j.tplants.2014.10.002
- St. Clair D. A. (2010) *Quantitative disease resistance and quantitative resistance loci in breeding*. *Annual Review of Phytopathology* 48: 247-268 DOI: 10.1146/annurev-phyto-080508-081904
- Stich B., Möhring J., Piepho H.-P., Heckenberger M., Buckler E., S., Melchinger A. E. (2008) *Comparison of mixed-model approaches for association mapping*. *Genetics* 178: 1745-1754 DOI: 10.1534/genetics.107.079707
- Stogios P. J., Downs G. S., Jauhal J. J. S., Nandra S. K., Privé G. G. (2005) *Sequence and structural analysis of BTB domain proteins*. *Genome Biology* 6: R82 DOI: 10.1186/gb-2005-6-10-r82
- Šurlan-Momirović G., Flath K., Silvar C., Branković G., Kopahnke D., Knežević D., Schliephake E., Ordon F., Perović D. (2016) *Exploring the Serbian GenBank barley (Hordeum vulgare L. ssp. vulgare) collection for powdery mildew resistance*. *Genetic Resources and Crop Evolution* 63: 275-287 DOI: 10.1007/s10722-015-0246-2
- Szücs P., Karsai I., von Zitzewitz J., Mészáros K., Cooper L. L. D., Gu Y. Q., Chen T. H. H., Hayes P. M., Skinner J. S. (2006) *Positional relationships between photoperiod response QTL and photoreceptor and vernalization genes in barley*. 112: 1277-1285 DOI: 10.1007/s00122-006-0229-y

- Tsuba M., Katagiri C., Takeuchi Y., Takada Y., Yamaoka N. (2002) *Chemical factors of the leaf surface involved in the morphogenesis of Blumeria graminis*. *Physiological and Molecular Plant Pathology* 60: 51-57 DOI: 10.1006/pmpp.2002.0376
- Turuspekov Y., Ormanbekova D., Rsaliev A., Abugalieva S. (2016) *Genome-wide association study on stem rust resistance in Kazakh spring barley lines*. *BMC Plant Biology* 16: 6 DOI: 10.1186/s12870-015-0686-z
- Unité de Recherche Génomique Info (URGI)
URL: <https://urgi.versailles.inra.fr/siregal/siregal/card.do?id=126&dbName=siregal&class Name=genres.collection.CollectionsImpl> (Accessed on: 14.05.2019)
- van Loon L. C., Rep M., Pieterse C. M. J. (2006) *Significance of inducible defense-related proteins in infected plants*. *Annual Review of Phytopathology* 44: 135-162 DOI: 10.1146/annurev.phyto.44.070505.143425
- Vilhjálmsón B. J., Nordberg M. (2013) *The nature of confounding in genome-wide association studies*. *Nature Reviews Genetics* 14: 1-2 DOI: 10.1038/nrg3382
- von Schaewen A., Frank J., Koiwa H. (2008) *Role of complex N-glycans in plant stress tolerance*. *Plant Signalling & Behavior* 3: 871-873 DOI: 10.1073/pnas.0800237105
- Wang W., Wen Y., Berkey R., Xiao S. (2009a) *Specific targeting of the Arabidopsis resistance protein RPW8.2 to the interfacial membrane encasing the fungal haustorium renders broad-spectrum resistance to powdery mildew*. *The Plant Cell* 21: 2989-2913 DOI: 10.1105/tpc.109.067587
- Wang Y., Bao Z., Zhu Y., Hua J. (2009b) *Analysis of temperature modulation of plant defense against biotrophic microbes*. *Molecular Plant-Microbe Interaction Journal* 22: 498-506 DOI: 10.1094/MPMI-22-5-0498
- Wang H., Jiang Y. P., Yu H. J., Xia X. J., Shi K., Zhou Y. H., Yu J. Q. (2010) *Light quality affects incidence of powdery mildew, expression of defence-related genes and associated metabolism in cucumber plants*. *European Journal of Plant Pathology* 127: 125-135 DOI: 10.1007/s10658-009-9577-1
- Wang W., Barnaby J. Y., Tada Y., Li H., Tör M., Caldelari D., Lee D.-u., Fu X.-D., Dong X. (2011) *Timing of plant immune responses by a central circadian regulator*. *Nature* 470: 110-115 DOI: 10.1038/nature09766
- Wang M., Jiang N., Jia T., Leach L., Cockram J., Waugh R., Ramsay L., Thomas B., Luo Z. (2012) *Genome-wide association mapping of agronomic and morphologic traits in highly structured populations of barley cultivars*. *Theoretical and Applied Genetics* 124: 233-246 DOI: 10.1007/s00122-011-1697-2
- Warr A., Robert C., Hume D., Archibald A., Deeb N., Watson M. (2015) *Exome sequencing: current and future perspectives*. *G3: Genetics, Genomes, Genetics* 5: 1543-1550 DOI: 10.1534/g3.115.018564
- Wei F., Gobelmann-Werner K., Morroll S. M., Kurth J., Mao L., Wing R., Leister D., Schulze-Lefert P., Wise R. P. (1999) *The Mla (powdery mildew) resistance cluster is associated with three NBS-LRR gene families and suppressed recombination within a 240-kb DNA interval on chromosome 5S (1HS) of barley*. *Genetics* 153: 1929-1948 PMID: 10581297; PMCID: PMC1460856
- Wei F., Wing R. A., Wise R. P. (2002) *Genome dynamics and evolution of the Mla (powdery mildew) resistance locus in barley*. *The Plant Cell* 14: 1903-1917 DOI: 10.1105/tpc.002238
- Weir B. S., Anderson A. D., Hepler A. B. (2006) *Genetic relatedness analysis: modern data and new challenges*. *Nature Reviews Genetics* 7: 771-780 DOI: 10.1038/nrg1960
- Whealbi.eu
URL: <https://www.whealbi.eu/plant-diversity/key-facts/> (Accessed on: 14.05.2019)

- Wiberg A. (1974) *Sources of resistance to powdery mildew in barley*. Hereditas 78: 1-40 DOI: 10.1111/j.1601-5223.1974.tb01426.x
- Wyand R. A., Brown J. K. M. (2003) *Genetic and forma specialis diversity in Blumeria graminis of cereals and its implications for host-pathogen co-evolution*. Molecular Plant Pathology 4: 187-198 DOI: 10.1046/j.1364-3703.2003.00167.x
- Xiao S., Ellwood S., Calis O., Patrick E., Li T., Coleman M., Turner J. G. (2001) *Broad-spectrum mildew resistance in Arabidopsis thaliana mediated by RPW8*. Science 291: 118-120 DOI: 10.1126/science.291.5501.118
- Xie X.-Z., Xue Y.-J., Zhou J.-J., Zhang B., Chang H., Takano M. (2011) *Phytochromes regulate SA and JA signaling pathways in rice and are required for developmentally controlled resistance to Magnaporthe grisea*. Molecular Plant 4: 688-696 DOI: 10.1093/mp/ssr005
- Xu W., Meng Y., Wise R. P. (2014) *Mla- and Rom1-mediated control of microRNA398 and chloroplast copper/zinc superoxide dismutase regulates cell death in response to the barley powdery mildew fungus*. New Phytologist 201: 1396-1412 DOI: 10.1111/nph.12598
- Xu X., Paik I., Zhu L., Huq E. (2015) *Illuminating progress in phytochrome-mediated light signaling pathways*. Trends in Plant Science 20: 641-650 DOI: 10.1016/j.tplants.2015.06.010
- Yamaoka N., Matsumoto I., Nishiguchi M. (2006) *The role of primary germ tubes (PGT) in the life cycle of Blumeria graminis: The stopping of PGT elongation is necessary for the triggering of appressorial germ tube (AGT) emergence*. Physiological and Molecular Plant Pathology 69: 153-159 DOI: 10.1016/j.pmpp.2007.04.003
- Yu J., Pressoir G., Briggs W. H., Vroh Bi I., Yamasaki M., Doebley J. F., McMullen M. D., Gaunt B. S., Nielsen D. M., Holland J. B., Kresovich S., Buckler E. S. (2006) *A unified mixed-model method for association mapping that accounts for multiple levels of relatedness*. Nature Genetics 38: 203-207 DOI: 10.1038/ng1702
- Zadok J. C., Chang T. T., Konzak C. F. (1974) *A decimal code for the growth of cereals*. Weed Research 14: 415-421 DOI: 10.1111/i.1365-3180.1974.tb01084.x
- Zhang Z., Henderson C., Perfect E., Carver T. L. W., Thomas B. J., Skamnioti P., Gurr S. J. (2005) *Of genes and genomes, needles and haystacks: Blumeria graminis and functionality*. Molecular Plant Pathology 6: 561-575 DOI:10.1111/j.1364-3703.2005.00303.x
- Zhang J., Xie S., Zhu J.-K., Gong Z. (2016a) *Requirement for flap endonuclease 1 (FEN1) to maintain genomic stability and transcriptional gene silencing in Arabidopsis*. The Plant Journal 87: 629-640 DOI: 10.1111/tpj.13224
- Zhang Y., Wen C., Liu S., Zheng L., Shen B., Tao Y. (2016b) *Shade avoidance 6 encodes an Arabidopsis flap endonuclease required for maintenance of genome integrity and development*. Nucleic Acids Research 44: 1271-1284 DOI: 10.1093/nar/gkv1474
- Zhang H., Mittal N., Leamy L., Barazani O., Song B.-H. (2017) *Back into the wild- apply untapped genetic diversity of wild relatives for crop improvement*. (Evolutionary Applications 10: 5-24 DOI: 10.1111/eva.12434
- Zhao Q., Dixon R. A. (2014) *Altering the cell wall and its impact on plant disease: from forage to bioenergy*. Annual review of Phytopathology 52: 69-91 DOI: 10.1146/annurev-phyto-082712-102237
- Zhao Y., Zhou J., Xing D. (2014) *Phytochrome B-mediated activation of lipoxygenase modulates an excess red light-induced defence response in Arabidopsis*. Journal of Experimental Botany 65: 4907-4918 DOI: 10.1093/jxb/eru247
- Zhou M. X. (2010) *Barley production and consumption*. In: G. Zhang and C. Li (Eds.) *Genetics and improvement of barley malt, Advanced Topics in Science and Technology in China* (ATSTC), pp 1-17, Springer, Berlin, Heidelberg DOI: 10.1007/978-3-642-01279-2_1

- Zhou G., Broughton S., Zhang X.-Q., Ma Y., Zhou M., Li C. (2016) *Genome-wide association mapping of acid soil resistance in barley (Hordeum vulgare L.)*. *Frontiers in Plant Science* 7: 406 DOI: 10.3389/fpls.2016.00406
- Zhu C., Gore M., Buckler E. S., Yu J. (2008) *Status and prospects of association mapping in plants*. *The Plant Genome* 1: 5-20 DOI: 10.3835/plantgenome2008.02.0089
- Zhu J., Zhou Y., Shang Y., Hua W., Wang J., Jia Q., Liu M., Yang J. (2016) *Genetic evidence of local adaptation and long distance migration in Blumeria graminis f. sp. hordei population from China*. *Journal of Genetic Plant Pathology* 82: 69-81 DOI: 10.1007/s10327-016-0643-1
- Zierold U., Scholz U., Schweizer P. (2005) *Transcriptome analysis of mlo-mediated resistance in the epidermis of barley*. *Molecular Plant Pathology* 6: 139-151 DOI: 10.1111/J.1364.3703.2005.00271.X
- Zimmermann G., Bäumlein H., Mock H.-P., Himmelbach A., Schweizer P. (2006) *The multigen family encoding Germin-Like proteins of barley. Regulation and function in basal host resistance*. *Plant Physiology* 142: 181-192 DOI: 10.1104/pp.106.083824
- Zohary D., Hopf M., Weiss E. (2012) *Chapter1: Current stat of the art*. In: *Domestication of plants in the Old World: the origin and spread of domesticated plants in Southwest Asia, Europe, and the Mediterranean Basin* (4th edition) Oxford University Press, Oxford ISBN: 0199549060 (hbk.), 9780199549061 (hbk.)

Appendix A: additional material and methods

a) Important equipment and consumables

Item	Manufactured by
4-well plates	Greiner Bio-One
5.0 ml freestanding mailing tubes with cap	VWR
7900HT Fast Real-Time PCR System with 384-Well Block Module	Applied Biosystems
Axioplan 2 imaging	Carl Zeiss AG
Axio Scan Z.1	Carl Zeiss AG
Axio Scope.A1	Carl Zeiss AG
Big square plates (23.2 cm x 23.2 cm)	Schütt, Göttingen
Biolistic® PDS-1000/He Particle Delivery System	BIO RAD
Biomedical MLR-350	SANYO
Biometra Tadvanced	Analytic Jena
Centrifuge 5415 R	Eppendorf
Colibri Microvolume Spectrometer	Titertek Berthold
Custom designed polytetrafluoroethylene (PTFE) frames (Teflon frames)	eMachineShop
HERA safe	HERAEUS
HV-F20SCL	Hitachi
INTAS Geldoc	INTAS
Macrocarriers for PDS-1000/He and Hepta systems	BIO RAD
Steel beads (3.175 mm, DIN 5401)	Hecht
Microcarriers, 1.0 µm gold	BIO RAD
MLR-352H-PE Plant Growth Chamber	Panasonic
Objective EC Plan-Neofluar 5x/0.16 (440320-9902-000)	Carl Zeiss AG
Objektiv EC Plan-Neofluar 10x/0,3 Ph1 (440331-9902-000)	Carl Zeiss AG
Objective EC Plan-Neofluar 10x/0.3 M27 (420340-9901-000)	Carl Zeiss AG
Objective Fluar 5x/0.25 M27 (420130-9900-000)	Carl Zeiss AG
Petri dishes	Greiner Bio-One
Primer (unmodified DNA Oligos, salt free)	eurofins genomics
Riplate® SW (10mL) deep well plate	Ritter
Rupture Disks 900 psi	BIO RAD
Stopping Screen	BIO RAD
TissueLyser®	Qiagen
Thermomixer Compact	Eppendorf
Vacuum pump	ILMVAC
Vortex – Genie 2	Scientific Industries

b) Important chemicals

Substance	Manufactured by
Agarose	Biozym
Ammonium acetate	Carl Roth
Ampicillin Sodium Salt	Carl Roth
β -Mercaptoethanol	Sigma-Aldrich
Benzimidazole	Fluka
5-Bromo-4-chloro-3-indolyl- β -D-glucuronic acid (X-Gluc)	Biosynth
Calcium chloride	Carl Roth
Calcium nitrate tetra hydrate	Carl Roth
Chloroform	Carl Roth
dNTP Mix [10 mM each]	Thermo Scientific™
Ethanol (96 %)	Carl Roth
Ethidium bromide [10g/l]	Carl Roth
Ethylenediaminetetraacetic acid disodium salt dihydrate (EDTA)	Carl Roth
Glucose	Carl Roth
Glycerol	Carl Roth
Hexadecyltrimethylammonium bromide (CTAB)	Carl Roth
Isoamyl alcohol (99.9 %)	Carl Roth
Kanamycin	Carl Roth
Magnesium chloride hexahydrate	Merck
Manganese (II) chloride	Riedel-de Hën
Methanol	Carl Roth
Microagar	Duchefa
3-(<i>N</i> -morpholino) propanesulfonic acid (MOPS)	Carl Roth
Oligo(dT) ₁₈ primer	Thermo Scientific™
Phytoagar	Duchefa
Polyvinylpyrrolidone K30 (PVP)	Carl Roth
Polyethylene glycol (PEG) 4000	Thermo Scientific™
Potassium acetate	Carl Roth
Potassium chloride	Carl Roth
Potassium ferricyanide	Carl Roth
Potassium hexacyanoferrate (II) trihydrate	Carl Roth
Rubidium chloride	Sigma-Aldrich
Silver nitrate	Carl Roth
Sodium acetate	Carl Roth
Sodium chloride	Carl Roth
Sodium dihydrogen phosphate	Carl Roth
Sodium hydrogen phosphate	Carl Roth
Spectinomycin dihydrochloride pentahydrate	Sigma-Aldrich
Tris(hydroxymethyl)aminomethane	Carl Roth
Triton X-100	Carl Roth
Tryptone	Otto Nordwald
Tween-20	Sigma
Yeast extract	Duchefa

c) Marker and proteins

Substance	Ordering number	Manufactured by
Apal [10 U/ μ l]	ER1411	Thermo Scientific™
DNase I, RNase-free [1 U/ μ l]	EN0521	Thermo Scientific™
GeneRuler 100 bp Plus DNA Ladder, ready-to-use	SM0324	Thermo Scientific™
GeneRuler 1 kb Plus DNA Ladder, ready-to-use	SM1334	Thermo Scientific™
GoTaq® Probe qPCR Master Mix	A6101	Promega
Phusion High-Fidelity DNA Polymerase [2 U/ μ l]	F530L	Thermo Scientific™
RevertAid First Strand cDNASynthesis Kit	K1621	Thermo Scientific™
Ribolock [40 U/ μ l]	EO0381	Thermo Scientific™
RNase A [10 U/ml]	-	Fermentas
SmaI [10 U/ μ l]	ER0661	Thermo Scientific™
SmartLadder	MW-1700-10	Eurogentec
SmI (Swal) [10 U/ μ l]	ER1241	Thermo Scientific™
T4 DNA Ligase [5 Weiss U/ μ L]	EL0014	Thermo Scientific™
Taq PCR Mastermix Kit	Cat No./ID: 201443	Qiagen

d) Kits

Substance	Ordering number	Manufactured by
DNeasy® Plant Mini Kit	Cat No./ID: 69104	Qiagen
Gateway LR Clonase™ II Enzyme mix	11791020	Invitrogen™
GeneJET PCR purification Kit	K0702	Thermo Scientific™
GoTaq® Probe qPCR Master Mix	A6101	Promega
JETSTAR MIDI Kit	-	GENOMED
PureLink™ HiPure Plasmid DNA Purification Kit	K210005	Invitrogen™
QIAprep® Spin Miniprep	Cat No./ID: 27104	Qiagen
RNeasy® Plant Mini Kit	Cat No./ID: 74903	Qiagen

e) Solutions

Solution	Composition
Benzimidazole	<ul style="list-style-type: none"> • 40 mg/ml benzimidazole in 96 % ethanol
Calcium nitrate	<ul style="list-style-type: none"> • 1 M Ca(NO₃)₂ pH 10.0
CTAB buffer for DNA extraction	<ul style="list-style-type: none"> • 2 % CTAB • 200 mM Tris-HCl pH 8.0 • 20 mM EDTA pH 8 • 1.4 M NaCl • 1 % PVP • 0.28 M β-mercaptoethanol (freshly added)
DNA Loading Dye	<ul style="list-style-type: none"> • 10 % (v/v) glycerol • 0.01 % (w/v) bromophenol blue in TAE
EDTA	<ul style="list-style-type: none"> • 0.5 M EDTA (pH 8.0)
GUS-staining solution (1.4 M)	<ul style="list-style-type: none"> • 20 % (v/v) Methanol • 0.1 % (w/v) X-Gluc • 20 % (v/v) phosphate buffer • 10 mM EDTA • 0.001 % Triton-X • 1.4 mM K₄Fe(CN)₆ x3H₂O • 1.4 mM K₃Fe(CN)₆ pH 6.8-7.2
GUS-staining solution (3 M)	<ul style="list-style-type: none"> • 20 % (v/v) Methanol • 0.1 % (w/v) X-Gluc • 20 % (v/v) phosphate buffer • 10 mM EDTA • 0.001 % Triton-X • 3 mM K₄Fe(CN)₆ x3H₂O • 3 mM K₃Fe(CN)₆ pH 6.8-7.2
Phosphate buffer for GUS-solution	<ul style="list-style-type: none"> • 250 mM Na₂HPO₄ • 250 mM NaH₂PO₄ pH 6.5
Phytoagar solution for 4-well plates (not autoclaved)	<ul style="list-style-type: none"> • 1 % (m/v) Phytoagar • 20 mg/l benzimidazole
Phytoagar solution for big shooting plates	<ul style="list-style-type: none"> • 1 % (m/v) Phytoagar • 20 mg/l benzimidazole

Appendix A

Solution	Composition
Phytoagar solution for maintenance	<ul style="list-style-type: none"> • 1 % (m/v) Phytoagar • 35 mg/l benzimidazole • 1 mg/l AgNO₃
Phytoagar solution for small shooting plates	<ul style="list-style-type: none"> • 0.5 % (m/v) Phytoagar • 10 mg/l benzimidazole
Silver nitrate	<ul style="list-style-type: none"> • 1 M AgNO₃ in H₂O
TAE (1x)	<ul style="list-style-type: none"> • 40 mM Tris-HCl (pH 8.4) • 20 mM acetic acid • 1 mM EDTA
TAE (50x)	<ul style="list-style-type: none"> • 2 M Tris-HCl (pH 8.4) • 1 M acetic acid • 50 mM EDTA
TE buffer (10x)	<ul style="list-style-type: none"> • 0.1 M Tris-HCl • 10 mM EDTA
TE buffer (1x)	<ul style="list-style-type: none"> • 10 mM Tris-HCl • 1 mM EDTA
Transformation buffer I (for the preparation of chemical competent cells)	<ul style="list-style-type: none"> • 0.03 M potassium acetate • 0.1 M RbCl • 0.05 M MnCl • 0.01 M CaCl₂ <p style="margin-left: 20px;">pH 5.8 The solution was sterile filtered.</p>
Transformation buffer II (for the preparation of chemical competent cells)	<ul style="list-style-type: none"> • 0.01 M MOPS • 0.01 M RbCl • 0.075 M CaCl₂ • 15 % w/v glycerol <p style="margin-left: 20px;">pH 7.0 The solution was sterile filtered.</p>
Tris-HCl	<ul style="list-style-type: none"> • 1 M Tris-HCl pH 8.0
Wash buffer I for DNA extraction	<ul style="list-style-type: none"> • 76 % Ethanol • 200 mM sodium acetate
Wash buffer II for DNA extraction	<ul style="list-style-type: none"> • 76 % Ethanol • 10 mM ammonium acetate

f) Culture media

Medium	Composition
LB media (liquid)	<ul style="list-style-type: none"> • 10 g/l Tryptone • 5 g/l Yeast extract • 5 g/l NaCl pH 7.4
LB media (solid)	<ul style="list-style-type: none"> • 10 g/l Tryptone • 5 g/l Yeast extract • 5 g/l NaCl • 1.5 % (w/v) microagar pH 7.4
LB media (for chemical competent cells)	<ul style="list-style-type: none"> • 10 g/l Tryptone • 5 g/l Yeast extract • 5 g/l NaCl • 2.5 mM Mg SO₄ (sterile filtered) • 2.5 mM MgCl (sterile filtered) pH 7.4
SOC medium	<ul style="list-style-type: none"> • 10 g/l Tryptone • 5 g/l Yeast extract • 5 g/l NaCl • 0.19 g/l KCl • 2.03 g/l MgCl₂ • 3.6 g/l glucose pH 7.0

The bacterial culture media were prepared and if necessary supplemented with the indicated antibiotics.

Medium	Concentration
Ampicillin	100 mg/l
Kanamycin	50 mg/l
Spectinomycin	100 mg/l

g) Software and databases

Software/Database	Developer/Accessed through
ASReml-R	https://www.vsnr.co.uk/software/asreml-r/
BARLEX	http://apex.ipk-gatersleben.de/apex/f?p=284:10
Clustal Omega	https://www.ebi.ac.uk/Tools/msa/clustalo/
EMBOS Needle (nucleotide alignment)	https://www.ebi.ac.uk/Tools/psa/emboss_needle/nucleotide.html
EMBOS Needle (protein alignment)	https://www.ebi.ac.uk/Tools/psa/emboss_needle/
ExpASy -Translate tool	https://web.expasy.org/translate/
Galaxy	http://galaxy.ipk-gatersleben.de/
GIBIS	https://gbis.ipk-gatersleben.de/gbis2i/faces/index.jsf
HarVEST barley	https://harvest.ucr.edu/
INTAS GelDoc	INTAS
IPK Barley BLAST server	https://webblast.ipk-gatersleben.de/barley_ibsc/
Microsoft Office 2010 &2016	Microsoft
NCBI megablast	https://blast.ncbi.nlm.nih.gov/Blast.cgi?PAGE_TYPE=BlastSearch
NCBI blastp	https://blast.ncbi.nlm.nih.gov/Blast.cgi?PROGRAM=blastp&PAGE_TYPE=BlastSearch&LINK_LOC=blasthome
NLS prediction	http://nls-mapper.iab.keio.ac.jp/cgi-bin/NLS_Mapper_form.cgi
Oligo Calc: Oligonucleotide Properties Calculator	http://biotools.nubic.northwestern.edu/OligoCalc.html
Pfam 32.0 sequence search	http://pfam.xfam.org/
Prism7.01	GraphPad Software, La Jolla California USA; www.graphpad.com
qPCR Primer & Probe Design Tool by eurofins Genomics	https://www.eurofinsgenomics.eu/de/ecom/tools/qpcr-assay-design/
R (v2.15; v3.4.3; v3.5.1)	https://www.r-project.org/

Appendix A

Software/Database	Developer/Accessed through
Rice genome annotation project	http://rice.plantbiology.msu.edu/analyses_search_blast.shtml
RQ manager 1.2.1	Applied Biosystems™
SDS 2.4.1 software	Applied Biosystems™
si-Fi21	http://www.snowformatics.com/si-fi.html
TAIR	https://www.arabidopsis.org/
TAIR10 protein blastp	https://www.arabidopsis.org/Blast/index.jsp
TASSEL 5 (version 20180111)	https://www.maizegenetics.net/tassel
T _m calculator	https://www.thermofisher.com/us/en/home/brands/thermo-scientific/molecular-biology/molecular-biology-learning-center/molecular-biology-resource-library/thermo-scientific-web-tools/tm-calculator.html
URGI	https://urgi.versailles.inra.fr/siregal/siregal/accessionAction.do?collectionId=126

h) Vectors

The following previously generated plasmids were used.

pBC17

This plasmid was described by Leduc *et al.* (1994) and it harbours the maize (*Zea mays* L.) genes necessary for the anthocyanin production (*B-Peru* and *C1*) under the control of the constitutive Cauliflower mosaic virus (CaMV) 35S promoter and the *Agrobacterium Nopaline Synthase* (*Nos*) terminator. It confers ampicillin resistance. The construct was used for the normalization of the shooting efficiency by the promoter_GUS tests.

pUbiGUS

The vector was described by Schweizer *et al.* (1999b). The backbone of this construct, is reconstituted by the pUC19 plasmid and it confers ampicillin resistance. The multiple cloning site of the vector was used to insert the constitutive maize *ubiquitin* (*Ubi*) promoter (~820 bp), a part of a maize *Ubi* intron (~1,000 bp), the *uidA* (*GUS*) gene of *E. coli* strain 12 and the CaMV 35S terminator (~160 bp).

pIPKb002_GUS

The plasmid was described by Himmelbach *et al.* (2007) as binary destination vector for the Gateway cloning system (by Invitrogen; GenBank: EU161568). The vector overexpresses the *GUS* gene under control of the constitutive maize *Ubi* promoter and confers spectinomycin and streptomycin resistance.

pIPKb003_GUS

This construct was also generated by Himmelbach *et al.* (2007) in the same way as described for pIPKb002_GUS. It overexpresses the *GUS* gene under control of the constitutive rice (*Oryza sativa* L.) *actin1* (*Act1*) promoter (GenBank: EU161569).

pIPKb004_GUS

This construct was also described by Himmelbach *et al.* (2007). It overexpresses the *GUS* gene under control of an enhanced CaMV 35S (d35S) promoter (GenBank: EU161570).

pIPKb005_GUS

This construct was also generated by Himmelbach *et al.* (2007). It overexpresses the *GUS* gene under control of the epidermis-specific wheat (*Triticum aestivum* L.) *glutathione S-transferase A1* (*GstA1*) promoter (GenBank: EU161571).

pV668

This vector was described by Schweizer *et al.* (1999a & 1999b) and it is also referred as pNcoGUS. The plasmid is based on the pDH51 backbone and confers ampicillin resistance. The *GUS* gene is overexpressed under control of the constitutive CaMV 35S promoter and terminator.

pIPKTA9

This plasmid was described by Zimmermann *et al.* (2006) as overexpression (OX) construct, which confers ampicillin resistance. The vector is based on a pUC18 backbone and the CaMV 35S promoter and terminator enclosing a multiple cloning site. The plasmid was used for the generation of the OX constructs and utilized as empty vector control in the OX and the *Mildew resistance locus o* (*Mlo*) complementation assays.

pIPKTA9_Mlo

This construct is based on pIPKTA9 and was generated by D. Nowara (unpublished). The functional *Mlo* allele of Ingrid that was extracted from the BAC F15 clone described by Büschges *et al.*, 1997. The construct was used for the *Mlo* complementation assay.

pIPKTA30N

The vector was generated by Douchkov *et al.* (2005) as final destination vector for the Gateway cloning system. The vector is based on a pUC18 backbone. It contains the CaMV 35S promoter and terminator, two Gateway cassettes, attR sites and the *ccdB* gene. The two cassettes are oriented in opposite directions and are separated by the second intron of the wheat *RGA2* gene (GenBank: AF326781). The plasmid confers ampicillin and chloramphenicol resistance and allows a single-step transfer of two copies of the PCR fragment cloned in pIPKTA38 by using the Gateway LR clonase mix (Invitrogen™). The plasmid was used for the generation of the RNAi (RNA interference) constructs and as empty vector control for the transient-induced gene silencing (TIGS).

pIPKTA36

The RNAi construct was also generated by Douchkov *et al.* (2005) and because of the silencing of the *Mlo* gene (HORVU4Hr1G082710.2), it phenocopies the *mlo*-mediated resistance. The vector is used as control for the silencing.

pIPKTA38

The vector was also described by Douchkov *et al.* (2005) and it confers kanamycin resistance. It was used as Gateway Entry vector (GenBank: EF622216) and it is a derivative of the pENTR1a vector with a new multiple cloning site and excised *ccdB* gene.

pJP01

This plasmid was described before (Schultheiss *et al.*, 2014; Altpeter *et al.*, 2005) and it expresses a cDNA sequence of a wheat class III peroxidase (*Prx103*) under the control of the CaMV 35S promoter and terminator. The construct was referred before as p35S_TaPERO or pWIR3 (Schweizer *et al.*, 1999a; Schweizer *et al.*, 1999b) and was used as positive control for the OX assays.

i) Additional figures

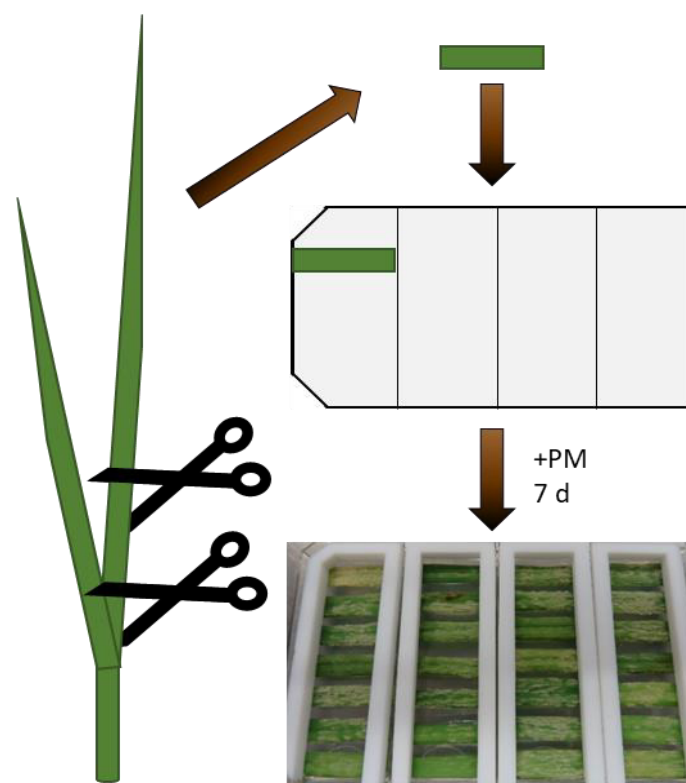


Figure A 1: Scheme of the experimental procedure of a detached leaf assay

The second leaves of 12 d old seedlings were cut at the basal end of the leaf and the segments were mounted with the adaxial surface up on 4-well plates filled with 1 % Phytoagar solution supplemented with bezimidazole [20 mg/l]. In total, up to five leaves per genotype were distributed on five different plates per sub-experiment and the leaf segments per genotype were placed at variable column and row positions per plate. The leaves of the control genotypes Morex and Roland were mounted on fixed plate positions between the test genotypes. After a plate was filled completely, custom designed polytetrafluoroethylene (PTFE) frames (Teflon frames) were placed on top of the leaves to fix the leaf segments in their position and to ensure that they stay flat. For the inoculation with the pathogen, all plates of a sub-experiment were placed within a settling tower and the spores of the selected powdery mildew isolate were blown into it from infected leaves. After the spores settled, the spore density was controlled via the glass slide that was placed within the settling tower. The average number of spores per mm² was calculated based on the microscopically determined spore numbers of at least three different sections on the glass slide. The spore density per experimental series was kept constant. The inoculated plates were incubated for 7 d under long-day conditions (16 h light / 8 h dark at 20 °C, 1 LS) in a MLR-352H-PE Plant Growth Chamber (Panasonic). The photograph within the scheme depicts a representative plate and the macroscopical disease symptoms were scored manually via estimation of the area of the leaf segment that was covered with the fungal mycelium (infected leaf area).

The detached leaf assay was used for different experimental approaches. For the first phenotypic screening, 459 Whealbi accessions were analysed in eight sub-experiments and inoculated with the powdery mildew isolate D35/3. In case of the complete phenotypic screening, 267 genotypes were inoculated with each powdery mildew isolate (D35/3 or RiIII) in 16 sub-experiments. The same leaf was halved horizontally and the most basal part was used for the inoculation with D35/3 spores. For the isolate test, three independent sub-experiments were performed and each leaf was cut horizontally into two to three segments. The plates were inoculated with spores of one of the following powdery mildew isolates: CH4.8, D2/4, D4/6, D35/2, MH21, Ro93a and Si1.

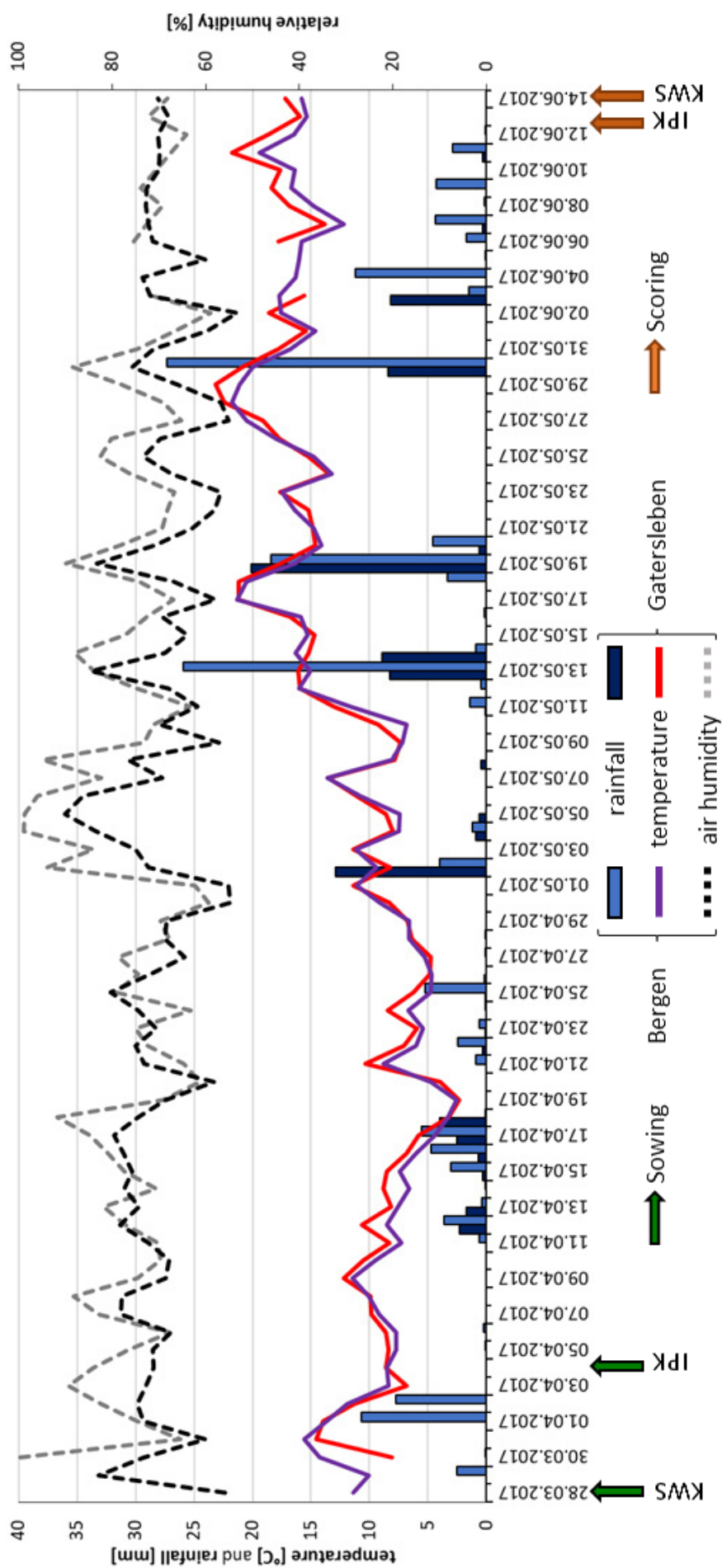


Figure A 2: Recorded weather data during the growth period of the field trials at both locations
 The average air temperature per day [°C], the relative air humidity [%] and the rainfall [mm] in Gatersleben and Bergen/Wohlde were recorded during the growth period of the field trials. Additionally, the sowing date (green arrow) and the scoring date (orange arrow) were indicated.

j) Additional tables

Table A 1: Specifications of the 459 used barley Whealbi genotypes

Whealbi ¹	Genebank ²	Genotype name	Growth ³	Bio. status ⁴	Origin ⁵
WB-001*	n. sp. ⁶	Manas	W	AC/IC	UKR
WB-002*	BCC1307	Igri	W	AC/IC	DEU
WB-003*	n. sp.	KW Cassia	W	BM	n. sp.
WB-004	n. sp.	KW Glacier	W	BM	n. sp.
WB-005	n. sp.	KW Tower	W	BM	n. sp.
WB-006	n. sp.	KW Capella	W	BM	n. sp.
WB-007*	n. sp.	Saffron	W	BM	n. sp.
WB-008*	n. sp.	Joy	W	BM	n. sp.
WB-009*	n. sp.	Wintmalt	W	BM	n. sp.
WB-010*	n. sp.	Meridian	W	BM	n. sp.
WB-011*	n. sp.	Escadre	W	BM	n. sp.
WB-012*	n. sp.	Lomerit	W	BM	n. sp.
WB-013*	n. sp.	Tenor	W	BM	n. sp.
WB-014*	n. sp.	Tonic	W	BM	n. sp.
WB-015	n. sp.	Keeper	W	BM	n. sp.
WB-016*	n. sp.	Irina	S	BM	n. sp.
WB-017*	n. sp.	Aurelia	S	BM	n. sp.
WB-018*	n. sp.	Orphelia	S	BM	n. sp.
WB-019*	n. sp.	Asta	S	BM	n. sp.
WB-020*	n. sp.	Aldebaran	W	AC/IC	ITA
WB-021	HOR10509	Athene	W	TL	ETH
WB-022*	n. sp.	Dea	W	TC	DEU
WB-023*	n. sp.	Fridericus	W	AC/IC	DEU
WB-024*	9367	HATIF DE GRIGNON	A	TC/L	FRA
WB-025	n. sp.	Ketos	W	AC/IC	FRA
WB-026*	n. sp.	Ponente	W	AC/IC	ITA
WB-027*	HOR10200 & 9557	ROBUR	W	AC/IC	FRA
WB-028*	n. sp.	Nure	W	AC/IC	ITA
WB-029	n. sp.	Tremois	S	AC/IC	FRA
WB-030	n. sp.	Tiffany	W	AC/IC	DEU
WB-031*	n. sp.	Tarm92	F	AC/IC	TUR
WB-032	HOR452	Pamina	F	TL	TUR
WB-037	n. sp.	Amillis	W	AC/IC	FRA
WB-038	n. sp.	Aquarelle	W	AC/IC	DEU
WB-039*	n. sp.	Istos	W	AC/IC	ITA
WB-040*#	n. sp.	Tibet-A4	F/W	TL	CHN
WB-042*##	HOR214	n. sp.	S	TL	JPN
WB-043*+	HOR261	Algerian	S	AC/IC	USA
WB-044	HOR303	Exedra	S	AC/IC	USA
WB-045*	HOR683	n. sp.	S	TL	GRC
WB-046	HOR728	n. sp.	S	TL	GRC
WB-047*	HOR736	n. sp.	S	TL	ALB
WB-048*#	HOR804	Arlington Awnless	S	AC/IC	USA

Table A 1 (continued)

Wheatbi ¹	Genebank ²	Genotype name	Growth ³	Bio. status ⁴	Origin ⁵
WB-049* ^{+#}	HOR842	n. sp.	S	TL	CHN
WB-050	HOR1036	n. sp.	S	TL	GRC
WB-051*	HOR1873	n. sp.	S	TL	GRC
WB-052 ^{7*+}	HOR2573	n. sp.	S	TL	ETH
WB-053	HOR2591	Psaknon	S	AC/IC	NZL
WB-054* ⁺	HOR2551	n. sp.	S	TL	ETH
WB-055* ⁺	HOR2932	n. sp.	S	TL	ETH
WB-056*	HOR3075	n. sp.	S	TL	ETH
WB-057	HOR3271	Ciro	S	AC/IC	DEU
WB-058* ⁺	HOR3275	Fong-tien	S	AC/IC	CHN
WB-059	HOR3726	Nigrate	S	AC/IC	USA
WB-060* [#]	HOR3988	n. sp.	S	TL	IND
WB-061* [#]	HOR4031	n. sp.	S	TL	IND
WB-062	HOR4060	Palestine 10	S	AC/IC	ISR
WB-063*	HOR4400	n. sp.	S	AC/IC	ERI
WB-065* ⁺	11193	MAROCAINE O79	S	TC/L	MAR
WB-066 ^{7*+}	11194	MAROCCO	S	TC/L	MAR
WB-067	11496	OM21	S	TC/L	MAR
WB-068*	11506	OSIRIS~US RHYN	S	TC/L	DZA
WB-069* ⁺	11563	RABAT	S	TC/L	MAR
WB-070* ⁺	11678	TUNISIE 1451	S	BM	TUN
WB-071	11679	TUNISIE 1458	S	BM	TUN
WB-072*	11680	TUNISIE 4A	S	BM	TUN
WB-073*	HOR5188	n. sp.	S	TL	ETH
WB-074* ⁺	HOR5342	n. sp.	S	TL	ETH
WB-075*	HOR5593	n. sp.	S	TL	ETH
WB-076*	HOR5865	No. 103	S	TL	ETH
WB-077	HOR3292	n. sp.	S	TL	ETH
WB-078	HOR3294	n. sp.	S	TL	ETH
WB-079*	HOR6253	n. sp.	S	TL	ETH
WB-081	HOR3536	n. sp.	S	TL	ETH
WB-082*	HOR10310	n. sp.	S	TL	ETH
WB-083	HOR10508	n. sp.	S	TL	ETH
WB-085*	HOR8658	n. sp.	S	TL	ETH
WB-086*	HOR3592	n. sp.	S	TL	ETH
WB-087*	HOR3600	n. sp.	S	TL	ETH
WB-088	HOR10761	n. sp.	S	TL	ETH
WB-089	HOR10162	n. sp.	S	TL	n. sp.
WB-090	HOR10169	n. sp.	S	TL	LBY
WB-091*	HOR10280	n. sp.	S	AC/IC	LBY
WB-092*	HOR4463	n. sp.	S	Wi	RUS
WB-093*	HOR4288	n. sp.	S	AC/IC	ETH
WB-094* ⁺	HOR1683	n. sp.	S	AC/IC	MAR
WB-095	HOR7326	n. sp.	S	AC/IC	MAR
WB-097	HOR7328	n. sp.	S	AC/IC	MAR

Table A 1 (continued)

Wheat ¹	Genebank ²	Genotype name	Growth ³	Bio. status ⁴	Origin ⁵
WB-098	HOR7329	n. sp.	S	AC/IC	MAR
WB-099*	HOR4450	n. sp.	S	AC/IC	ETH
WB-101**	n. sp.	Morex IPK (Seq)	S	TL	n. sp.
WB-102**	n. sp.	Beatrix-gebeizt	S	TL	n. sp.
WB-103	n. sp.	Djamila-gebeizt	S	TL	n. sp.
WB-104	n. sp.	Eunova-gebeizt	S	TL	n. sp.
WB-105*	n. sp.	Streif-gebeizt	S	TL	n. sp.
WB-106*	n. sp.	Ursa-gebeizt	S	TL	n. sp.
WB-107*	n. sp.	Victoriana-gebeizt	S	TL	n. sp.
WB-108	n. sp.	Tadmor-IPK	S	TL	n. sp.
WB-109	n. sp.	Arta-IPK	S	TL	n. sp.
WB-110*	BCC3	IG 128089	S	TL	AFG
WB-111*	BCC93	IQ 70061	F	TL	IRQ
WB-112*	BCC118	IG 128216	F (?)	TL	LBY
WB-113**	BCC126	IG 31903	F (?)	TL	MAR
WB-114*	BCC129	IG 31925	F (?)	TL	MAR
WB-115	BCC149	IG 32019	W	TC	MAR
WB-116*	BCC161	IG 32086	F (?)	TC	MAR
WB-117	BCC167	Shayir IG 32973	F (?)	BM/RM	OMN
WB-119*	BCC190	IG 31424	F (?)	TC	SYR
WB-120*	BCC192	IG 31444	F (?)	TC	SYR
WB-121*	BCC195	IG 31513	F (?)	TC	SYR
WB-123*	BCC219	K-10628	F (?)	TC	TJK
WB-124	BCC421	Xin Mai 1 Hao	S	TC	CHN
WB-125	BCC423	Gang Tuo Qing Ke 1 hao	S	TC	CHN
WB-126*	BCC427	E Dong 85-1	S	BM/RM	CHN
WB-127	BCC432	Fu 8	S	BM/RM	CHN
WB-128*	BCC436	Vladivostok	S	TC	CHN
WB-129	BCC438	Manchuria Native 1	S	TC	CHN
WB-130**	BCC439	Fengtien Black	S	TC	CHN
WB-131*	BCC446	Harbin Native	S	TC	CHN
WB-133**	BCC502	Itu Native	S	TC	CHN
WB-135**	BCC526	C-138	S	TC	IND
WB-136*	BCC527	BHS169	S	TC	IND
WB-137**	BCC532	Ratna	S	TC	IND
WB-138**	BCC533	Lakhan	S	TC	IND
WB-139	BCC535	PL 172	S	TC	IND
WB-140	BCC538	Rewari	S	TC	IND
WB-141	BCC551	Churtanchan 1	S	TC	IND
WB-142**	BCC577	Pandukeshwar 2	S	TC	IND
WB-143**	BCC579	Bijoria	S	TC	IND
WB-144**	BCC581	Bana	S	TC	IND
WB-145	BCC625	Dairokkaku	S	TC	JPN
WB-146	BCC642	Nigatsuko	S	TC	JPN
WB-147**	BCC666	Buhobori	S	TL	KOR

Table A 1 (continued)

Whealbi ¹	Genebank ²	Genotype name	Growth ³	Bio. status ⁴	Origin ⁵
WB-148*#	BCC667	Namhaebori	S	TL	KOR
WB-149**	BCC675	Hyanmaeg	S	TC	KOR
WB-150	BCC695	Tongyeong Covered 1	S	TC	KOR
WB-151**	BCC718	Sariweon Yugmobori 1	S	TC	KOR
WB-152**#	BCC729	Gupo Covered 2	S	TC	KOR
WB-153**#	BCC732	Gho 4	S	TC	NPL
WB-154*#	BCC745	Macha Khola 1	S	TC	NPL
WB-155	BCC759	Kagbeni 2	S	AC/IC	NPL
WB-156**#	BCC766	Ulleri 10	S	TC	NPL
WB-157**#	BCC768	Ulleri 20	S	AC/IC	NPL
WB-158**	BCC776	TKN24b	S	BM/RM	NPL
WB-159*	BCC801	AC Oxbow	S	TC	CAN
WB-160*	BCC806	Aliso	S	AC/IC	MEX
WB-161**	BCC812	Arupo	S	TC	MEX
WB-162*	BCC817	Beecher	S	TC	USA
WB-163	BCC818	Belford	S	W	USA
WB-164	BCC844	Chia	S	TC	COL
WB-165**	BCC847	Compana	S	TC	USA
WB-166**	BCC852	Diamond	S	TC	CAN
WB-167*	BCC860	FNC 1	S	TC	URY
WB-168**	BCC869	Gobernadora	S	TC	MEX
WB-169**	BCC875	Hazen	S	TL	USA
WB-170**	BCC881	Husky	S	TC	CAN
WB-171	BCC892	Kolla	S	AC/IC	BOL
WB-173	BCC899	Libra	S	TC	CHL
WB-174	BCC903	Manley	S	TC	CAN
WB-175*	BCC907	Munsing	S	TC	USA
WB-176	BCC927	Sacasco 1	S	AC/IC	PER
WB-177*	BCC929	Sanalta	S	AC/IC	CAN
WB-178	HOR930	n. sp.	S	TC	TUR
WB-179	BCC942	Unitan	S	AC/IC	USA
WB-181**	BCC1368	Aramier	S	AC/IC	NLD
WB-182*	BCC1370	Beatrice	S	AC/IC	FRA
WB-183**	BCC1371	Beka	S	AC/IC	FRA
WB-184	BCC1372	Bielik	S	TC	POL
WB-185*	BCC1373	Blenheim	S	AC/IC	GBR
WB-186**	BCC1374	Gambrinus	S	AC/IC	NLD
WB-187**	BCC1376	Carlsberg II	S	AC/IC	DNK
WB-188**	BCC1377	Ceres	S	TC	FRA
WB-189*	BCC1378	Claret	S	AC/IC	GBR
WB-190*	BCC1379	Diamant	S	AC/IC	CZE
WB-191*	n. sp.	Sixtine	n. sp.	TL	ITA
WB-192*	BCC1381	Georgie	S	TC	GBR
WB-193**	BCC1382	Golden Promise	S	TC	GBR
WB-194*	BCC1383	Golf	S	TC	GBR

Table A 1 (continued)

Whealbi ¹	Genebank ²	Genotype name	Growth ³	Bio. status ⁴	Origin ⁵
WB-195*	BCC1384	Grit	S	AC/IC	DEU
WB-196* ⁺	BCC1385	Gryf	S	AC/IC	POL
WB-197	BCC1386	Haisa II	S	TC	DEU
WB-198	BCC1387	Hebe	S	BM/RM	NLD
WB-199*	BCC1389	Hunter	S	AC/IC	IRL
WB-200*	HOR7531	n. sp.	S	AC/IC	POL
WB-201* ⁺	BCC1391	Isaria	S	AC/IC	DEU
WB-202	BCC1392	Kenia	S	AC/IC	DNK
WB-203* ⁺	BCC1394	Mansholt, zweizeilig	S	AC/IC	NLD
WB-204*	BCC1395	Menuet	S	BM/RM	NLD
WB-205	BCC1396	Mette	S	TC	SWE
WB-206* ⁺	BCC1397	MFB 104	S	AC/IC	HUN
WB-207	BCC1398	MK 42	S	TC	HUN
WB-208*	BCC1399	Nancy	S	AC/IC	SWE
WB-209	BCC1400	Natasha	S	TC	FRA
WB-210* ⁺	BCC1401	Ortolan	S	AC/IC	DEU
WB-211* ⁺	BCC1402	Pallas	S	AC/IC	SWE
WB-212	BCC1403	Perun	S	AC/IC	DEU
WB-213	n. sp.	Fior 6814	n. sp.	AC/IC	ITA
WB-214*	BCC1405	Plumage Archer	W	TC	ITA
WB-215	BCC1407	Probstdorfer Adorra	W	AC/IC	ITA
WB-216	BCC1408	Proctor	S	AC/IC	GBR
WB-217*	BCC1409	Quantum	S	AC/IC	AUS
WB-218*	BCC1410	Rika	S	TC	SWE
WB-219*	BCC1411	Salome	S	TC	DEU
WB-220* ⁺	BCC1412	Sörlla	S	TC	SWE
WB-221	BCC1413	Sissy	S	AC/IC	DEU
WB-222* ⁺	BCC1414	Spartan	S	AC/IC	CZE
WB-223	BCC1415	Spratt Archer	S	TC	GBR
WB-224* ⁺	BCC1416	Tellus	S	TC	SWE
WB-225	BCC1417	Trumpf (Triumph)	S	TC	DEU
WB-226* ⁺	BCC1418	Tyra	S	TC	DNK
WB-227* ⁺	BCC1419	Union	S	TC	DEU
WB-228*	BCC1420	Vada	S	TC	NLD
WB-229*	BCC1421	Valticky	S	TC	CZE
WB-230	BCC1422	Varunda	S	TC	NLD
WB-232* ⁺	BCC1424	Volla	S	TC	DEU
WB-233	BCC1425	Wisa	S	TC	DEU
WB-234	BCC1428	Archer	S	TC	GBR
WB-235	BCC1430	Chevallier	S	TC	FRA
WB-236* ⁺	BCC1431	Goldfoil	n. sp.	TC	AUS
WB-237*	BCC1432	Hana	S	TC	CZE
WB-238	BCC1433	Heils Franken	S	AC/IC	DEU
WB-239	BCC1439	Kwassitzer Hanna	S	AC/IC	CZE
WB-240	BCC1440	Pammers Hohenauer Vollkorn	S	TC	AUS

Table A 1 (continued)

Whealbi ¹	Genebank ²	Genotype name	Growth ³	Bio. status ⁴	Origin ⁵
WB-241* ⁺	BCC1441	Pflugs Intensiv	S	TC	DEU
WB-242* [#]	BCC1442	Plumage	S	TC	GBR
WB-243	BCC1443	Probsteiner Landgerste	S	TC	DEU
WB-244*	BCC1444	Slovensky 802	S	TC	CZE
WB-245	BCC1445	Souche 142 Strotzheim	S	TC	FRA
WB-246	BCC1447	Turquoise	S	TC	FRA
WB-247*	BCC1448	Agneta	S	TC	FIN
WB-248	BCC1450	Pomo	S	TC	FIN
WB-249*	BCC1452	Bigo	S	TC	NLD
WB-250* ⁺	BCC1453	Olli	S	TC	FIN
WB-252*	BCC1455	Belogorskij	S	TC	RUS
WB-253* ⁺	BCC1456	Viking	S	TC	RUS
WB-256	BCC1461	Omskij 80	S	TC	RUS
WB-258* ⁺	BCC1465	Doneckij 650	S	TC	UKR
WB-259* ⁺	BCC1466	Odesskij 100	S	TL	UKR
WB-260*	BCC1467	Zhodinskij 5	S	TL	BEL
WB-261* ⁺	BCC1468	Tselinij 213	S	TL	KAZ
WB-262*	BCC1469	Granal	n. sp.	TC	KAZ
WB-263* ⁺	BCC1470	Unumli-Arpa	W	TL	UZB
WB-264	BCC1471	Nutans 115	W	TL	ARM
WB-265	BCC1472	Auksinjai	S	TC	LTU
WB-266	BCC1474	Klepeninskij	S	TL	UKR
WB-267	BCC1476	Afrasiab	S	BM/RM	UZB
WB-269* ⁺	BCC1480	K 16411	S	TC	RUS
WB-270* ⁺	BCC1481	K 3222	S	TL	RUS
WB-271	BCC1482	Vjatich	S	TL	RUS
WB-272	BCC1483	K 4511	S	TL	RUS
WB-273*	BCC1484	K 9511	S	TL	RUS
WB-274* ⁺	BCC1485	Pallidum 45	S	TC	RUS
WB-275	BCC1487	K 21820	S	TC	RUS
WB-276*	BCC1490	Tulunskii 23/11	S	TC	RUS
WB-277*	BCC1491	K 10693	S	TC	RUS
WB-279* ⁺	BCC1497	K 11749	S	TC	KGZ
WB-280* ⁺	BCC1498	K 17227	S	TC	UZB
WB-281* ⁺	BCC1500	K 10628	S	TL	TJK
WB-282* ⁺	BCC1503	K 10877	S	TL	TKM
WB-283	BCC1504	Agul 2	S	TL	RUS
WB-284	BCC1505	Pallidum 4	S	TL	UKR
WB-285	BCC1506	Odesskij 36	S	TL	UKR
WB-286	BCC1524	Bavaria (Ackermanns Bavaria)	S	TL	DEU
WB-287* ⁺	BCC1529	Pumper	S	TL	AUS
WB-288	BCC1541	Novosadski 294 (NS 294)	S	TL	MKD
WB-289	BCC1548	Athenais	S	TL	CYP
WB-290* ⁺	BCC1561	HOR 383	S	TL	BGR
WB-291	BCC1565	HOR 750	S	TL	ALB

Table A 1 (continued)

Whealbi ¹	Genebank ²	Genotype name	Growth ³	Bio. status ⁴	Origin ⁵
WB-292	BCC1566	HOR 753	S	TL	GRC
WB-293	BCC1589	HOR 10555	S	TL	ITA
WB-294	HOR2800	FAO 3413	S	TL	IRN
WB-295	HOR2828	FAO 3443	S	BM/RM	IRN
WB-297*	HOR2835	FAO 3450	S	BM/RM	IRN
WB-298	HOR4727	n. sp.	S	BM/RM	TUR
WB-299*	HOR7985	n. sp.	S	BM/RM	TUR
WB-300*+	HOR8006	HOR 806	S	TL	TUR
WB-301*	HOR8050	HOR 8050	S	TL	TUR
WB-302*+	HOR8113	HOR 8113	S	TL	TUR
WB-303	HOR8160	HOR 8160	S	TC	TUR
WB-305*+	HOR11371	MR 3/51	S	TC	ISR
WB-306*	HOR11372	W 23833/8108	S	AC/IC	ISR
WB-307*+	HOR11373	W 23833/2196 11	S	AC/IC	ISR
WB-308*	HOR11374	W 23829/8039 11	S	TC	ISR
WB-309	HOR12830	n. sp.	n. sp.	TC	SYR
WB-310	HOR10879	n. sp.	S	TC	GEO
WB-311*+	HOR1962	Schwarze Gemeine Dreizack	S	TC	n. sp.
WB-312*	n. sp.	Gull	S	AC/IC	SWE
WB-313*	n. sp.	Binder	S	TL	DNK
WB-314*	n. sp.	Bonus	S	TL	SWE
WB-315*+	HOR11514	Anni	S	TL	EST
WB-316*	n. sp.	Optic	S	TL	GBR
WB-317*	n. sp.	Asplund	S	TL	SWE
WB-318	n. sp.	Jadar	S	TL	NOR
WB-319*+	HOR1528	Maskin	S	TL	n. sp.
WB-320*+	BCC1537	Vairogs	S	TL	LVA
WB-321*#	HOR4697	Jukag gedbori	W	TL	PRK
WB-322	BCC33	IG 33029	S/F (?)	TL	DZA
WB-323	BCC50	Baladi IG 32469	S/F (?)	TL	EGY
WB-324*	BCC53	IG 32498	S/F (?)	TL	EGY
WB-325*+	BCC56	IG 32812	S/F (?)	TL	EGY
WB-326	BCC57	K 10014	S/F (?)	TL	EGY
WB-327*	BCC97	IG 128193	S/F (?)	TL	JOR
WB-328	BCC98	IG 128194	S/F (?)	TL	JOR
WB-329*	BCC99	IG 128195	S/F (?)	TL	JOR
WB-330*	BCC100	IG 128196	S/F (?)	TL	JOR
WB-331	BCC101	IG 128197	S/F (?)	TL	JOR
WB-332	BCC102	IG 128198	S/F (?)	TL	JOR
WB-333*	BCC104	IG 128200	S/F (?)	TL	JOR
WB-334	BCC109	IG 110862	S/F (?)	TL	LBN
WB-335	BCC163	Shayri	S/F (?)	TL	OMN
WB-336	BCC164	Shayri IG 32826	S/F (?)	TL	OMN
WB-337	BCC165	Shayri IG 32962	S/F (?)	TL	OMN
WB-338	BCC166	Shayri IG 32971	S/F (?)	TL	OMN

Table A 1 (continued)

Whealbi ¹	Genebank ²	Genotype name	Growth ³	Bio. status ⁴	Origin ⁵
WB-340*	BCC187	IG 31406	S/F (?)	AC/IC	SYR
WB-341	BCC188	IG 31410	S/F (?)	TL	SYR
WB-342	BCC189	IG 31416	S/F (?)	TL	SYR
WB-343	BCC191	IG 31436	S/F (?)	TL	SYR
WB-344	BCC193	IG 31484	S/F (?)	TL	SYR
WB-345	BCC194	IG 31510	S/F (?)	TL	SYR
WB-346* ⁺	BCC196	IG 31518	S/F (?)	TL	SYR
WB-347	BCC198	Arabi Aswad IG 32575	S/F (?)	TL	SYR
WB-348	BCC199	Baladi IG 32596	S/F (?)	AC/IC	SYR
WB-349*	BCC20	Black Egyptian	S/F (?)	TL	ARE
WB-350*	BCC201	IG 32708	S/F (?)	AC/IC	SYR
WB-351*	BCC203	IG 32729	S/F (?)	TL	SYR
WB-352* ⁺	BCC205	IG 32742	S/F (?)	TL	SYR
WB-353	BCC209	Baladi IG 32801	S/F (?)	TL	SYR
WB-354	BCC212	Arabi Aswad IG 33094	S/F (?)	TL	SYR
WB-355* ⁺	BCC214	IG 128167	S/F (?)	BM/RM	SYR
WB-356*	BCC216	IG 128173	S/F (?)	TL	SYR
WB-357*	HOR2589	Sudan	S/F (?)	TL	SDN
WB-358* ⁺	HOR3045	Soggio Soudan (B) S.G. 147/49	S/F (?)	TL	SDN
WB-359	HOR4354	Acre Earliest	S/F (?)	TL	ISR
WB-360*	HOR449	n. sp.	S	TL	TUR
WB-361	HOR6957	n. sp.	S/F (?)	TL	YEM
WB-363*	HOR8212	Beduienengerste	S/F (?)	TL	EGY
WB-364	HOR10727	Bahatmi	S/F (?)	TL	SDN
WB-365* [#]	HOR4008	n. sp.	W (?)	TL	CHN
WB-366	HOR7051	n. sp.	W (?)	TL	NPL
WB-367	HOR10255	n. sp.	W (?)	TL	PAK
WB-368	HOR1751	n. sp.	S	TL	AFG
WB-369* ⁺	HOR572	n. sp.	S	TL	TUR
WB-370*	HOR3983	Peruvian Sel.1	S	TL	USA
WB-371	9598	TRIPOLITAINE	W	TC/L	LBY
WB-372*	HOR7939	n. sp.	S	TL	ETH
WB-374*	HOR10463	n. sp.	S	BM/RM	GEO
WB-375	HOR725	n. sp.	S	TL	GRC
WB-376* ⁺	HOR2833	n. sp.	S	TL	IRN
WB-377* ⁺	HOR10651	n. sp.	S	TL	IRQ
WB-378*	10116	ORGE SUD-MAROC	W	TC/L	MAR
WB-379	HOR11123	n. sp.	S	TL	ITA
WB-380	HOR9880	n. sp.	S	TL	LBY
WB-381	HOR9727	n. sp.	S	TL	LBY
WB-382	HOR7537	n. sp.	S	TL	POL
WB-383	HOR8832	Spiski (Lubicki)	S	TL	POL
WB-384	HOR9450	n. sp.	S	TL	ROU
WB-385*	10599	ALGER 48	S	TC/L	DZA
WB-386	n. sp.	Fior 8199	n. sp.	TL	ITA

Table A 1 (continued)

Whealbi ¹	Genebank ²	Genotype name	Growth ³	Bio. status ⁴	Origin ⁵
WB-387	HOR8638	n. sp.	S	TL	SVK
WB-388*	HOR1178	n. sp.	S	TL	TUR
WB-390	HOR1415	n. sp.	S	TL	TUR
WB-391*	HOR1740	n. sp.	S	TL	TUR
WB-392*	HOR8158	n. sp.	S	TL	TUR
WB-393	HOR4017	n. sp.	S	TL	MKD
WB-394	HOR1522	n. sp.	S	TL	AFG
WB-395	HOR1838	n. sp.	S	TL	AFG
WB-396	HOR4146	n. sp.	S	TL	DZA
WB-397*	HOR3961	n. sp.	S	TL	AUS
WB-398	HOR386	n. sp.	S	BM/RM	BGR
WB-399	HOR819	n. sp.	S	TL	EGY
WB-400 ^{7*+}	HOR5428	n. sp.	S	TL	ETH
WB-401*	HOR5939	H-2207	S	TL	ETH
WB-402	HOR10307	n. sp.	S	TL	ETH
WB-403	HOR10058	n. sp.	S	TL	FRA
WB-404	HOR9614	n. sp.	S	TL	GEO
WB-405	HOR771	n. sp.	S	TL	GRC
WB-406*	HOR940	n. sp.	S	TL	GRC
WB-407	HOR1860	n. sp.	S	TL	GRC
WB-408	HOR6954	n. sp.	S	TL	GRC
WB-409	HOR2815	n. sp.	S	TL	IRN
WB-410	n. sp.	Fior 10035	n. sp.	TL	ITA
WB-411*	HOR4261	n. sp.	S	TL	IRN
WB-413*	HOR4264	n. sp.	S	TL	IRN
WB-414	HOR4265	n. sp.	S	TL	IRN
WB-415*	HOR10477	n. sp.	S	TL	IRQ
WB-416	HOR10482	n. sp.	S	TL	IRQ
WB-417	HOR10607	n. sp.	S	TL	IRQ
WB-418	HOR10619	n. sp.	S	TL	IRQ
WB-419*	HOR10768	n. sp.	S	TL	IRQ
WB-420	HOR2002	n. sp.	S	TL	ITA
WB-421	HOR9702	n. sp.	S	TL	ITA
WB-422	HOR9882	n. sp.	S	TL	LBY
WB-423*	HOR9883	n. sp.	S	TL	LBY
WB-424 ^{*+}	HOR9842	n. sp.	S	TL	LBY
WB-425*	HOR10170	n. sp.	S	TL	LBY
WB-426	HOR1943	n. sp.	S	TL	GRC
WB-427*	HOR10136	n. sp.	S	TL	LBY
WB-428*	HOR10105	n. sp.	S	TL	LBY
WB-429*	HOR10111	n. sp.	S	TL	LBY
WB-430*	HOR10121	n. sp.	S	TL	LBY
WB-431	HOR10279	n. sp.	S	TL	LBY
WB-432	HOR10112	n. sp.	S	TL	LBY
WB-433*	HOR800	Ragusa 415	W	TL	MKD

Table A 1 (continued)

Whealbi ¹	Genebank ²	Genotype name	Growth ³	Bio. status ⁴	Origin ⁵
WB-434	HOR10138	n. sp.	S	TL	LBY
WB-435*	HOR10283	n. sp.	S	TL	LBY
WB-437	HOR9834	n. sp.	S	TL	LBY
WB-438	HOR10116	n. sp.	S	TL	LBY
WB-439	HOR10134	n. sp.	S	TL	LBY
WB-440*	HOR10126	n. sp.	S	TL	LBY
WB-441	HOR13438	n. sp.	S	TL	MAR
WB-442*	HOR1159	n. sp.	S	TL	GRC
WB-443	HOR13436	n. sp.	S	TL	MAR
WB-444	HOR1379	n. sp.	S	TL	GRC
WB-445	HOR3700	Mediascher Land	S	TL	ROU
WB-446*	BCC1576	n. sp.	S	TL	ESP
WB-447	HOR4072	n. sp.	S	TL	ESP
WB-448	HOR13887	ZARAGOZA	S	TL	ESP
WB-449* ⁺	HOR13932	LOS RODEOS	S	TL	ESP
WB-450* ⁺	HOR13928	VALLE DE SANTA INES	S	TL	ESP
WB-451	HOR420	n. sp.	S	TL	TUR
WB-452	HOR435	n. sp.	S	TL	TUR
WB-453	HOR4469	n. sp.	S	AC/IC	TUR
WB-454* ⁺	HOR4514	n. sp.	S/F (?)	TL	YEM
WB-455	HOR544	n. sp.	S	TL	TUR
WB-456* ⁺	HOR889	n. sp.	S	TL	TUR
WB-457* ⁺	HOR194	n. sp.	S	TL	UKR
WB-458* ⁺	HOR1466	n. sp.	S	TL	TUR
WB-459	HOR751	n. sp.	S	TL	MKD
WB-460* ⁺	HOR5895	H-2165	S	TL	ETH
WB-461*	HOR1468	Lyallpur 3647	S	TL	IND
WB-462*	HOR10334	n. sp.	S	TL	ETH
WB-463	HOR6514	n. sp.	S	TL	ETH
WB-464	HOR10958	n. sp.	S	TL	DZA
WB-465*	HOR5918	H-2188	S	TL	ETH
WB-466*	HOR5929	H-2197	S	TL	ETH
WB-467*	HOR11435	n. sp.	S	Wi	ETH
WB-468*	HOR10484	n. sp.	S	Wi	IRQ
WB-469* ⁺⁺	HOR2779	n. sp.	S	Wi	IRN
WB-470	HOR8813	n. sp.	S	Wi	POL
WB-472* ⁺⁺	HOR1464	n. sp.	S	Wi	AFG
WB-473* [#]	HOR7321	n. sp.	S	Wi	AFG
WB-474*	HOR5961	H-2230	S	Wi	ETH
WB-475	HOR10364	n. sp.	S	Wi	ITL
WB-476 ^{7*+}	HOR3270	(Svalöfs 53/510-44)	S	Wi (BM)	TUR
WB-477	HOR3941	Israeli 46	S	Wi	ISR
WB-478* ⁺	HOR9929	n. sp.	S	Wi	LBY
WB-483* [#]	FT269	n. sp.	F/W	Wi	JOR
WB-485	HID03	n. sp.	n. sp.	Wi	IRQ

Table A 1 (continued)

Whealbi ¹	Genebank ²	Genotype name	Growth ³	Bio. status ⁴	Origin ⁵
WB-486*	HID04	n. sp.	W	Wi	IRQ
WB-490*	HID69	n. sp.	n. sp.	TL	TUR
WB-497	HID138	n. sp.	F	Wi	IRN
WB-498	HID140	n. sp.	W	AC/IC	IRQ
WB-499* ⁺	HID144	n. sp.	F	Wi	IRN
WB-500	HID219	n. sp.	n. sp.	TC	AFG
WB-501* [#]	HID249	n. sp.	W	Wi	IRN
WB-505	HID357	n. sp.	W	Wi	TUR
WB-506	HID358	n. sp.	n. sp.	Wi	TUR
WB-510*	HOR13170	Barke	S	AC/IC	DEU
WB-512	HOR13169	Scarlett	S	BM	DEU

¹ official Whealbi number

² official genebank identifier

³ growth habit: A: alternative-intermediate; F: facultative; F/W: facultative/winter; S: spring; S/F: spring/facultative; W: winter

⁴ biological status: AC/IC: advanced/improved cultivar; BM: breeder's material; BM/RM: breeding/research material; TC: traditional cultivar; TC/L: traditional cultivar/landrace; TL: traditional landrace; Wi: wild material

⁵ country of origin indicated by the NATO Codification System Country Codes

⁶ n. sp.: not specified

⁷ selected lines for the large isolate test

* selected lines for the detached leaf assay with two powdery mildew isolates

+ selected lines for the field experiments

member of the subpopulation

The information which were summarized in this table were published on the URGI website (<https://urgi.versailles.inra.fr/siregal/siregal/accessionAction.do?collectionId=126>) and they were complemented according the GIBIS database (<https://gbis.ipk-gatersleben.de/gbis2i/faces/index.jsf>)

Table A 2: Virulence spectra of the seven powdery mildew isolates used for the small isolate test on a differential set of 33 barley lines

Accession	Gene ²	Code	Powdery mildew isolates ¹														
			CH4.8	D2/4	D4/6	D35/2	MH21	Ro93a	Si1	CHE	DEU	DNK	DEU	DNK	DEU	DNK	DEU
Alexis	<i>mlo9</i>	Mlo	0	0(P)	0	0(P)	0	0	0(P)	0	0(P)	0	0	0(P)	0	0(P)	0
Antalja (WI/7)	<i>MI(WI-7)</i>	WI-7	2	2	2	2	2	2	2	2	2	2	2	2	2	2	2
Borwina	<i>MI(Bw)</i>	Bw	2-3	2-3	2-3	3	2-3	3	2-3	2	2	2	2	2	2	2	2
Camilla	<i>U³</i>	U	1	0	2	2	2	2	2	0	0	2	2	0	0	3	3
Kredit	<i>MI(Kr)</i>	Kr	3	2-3	2-3	3	2-3	3	2-3	3	3	2-3	3	3	3	3	3
Laverda (U)	<i>MI(Lv)</i>	Lv	0	1	3	0	1	0	0	0	0	0	0	0	0	0	0
Lotta	<i>MI(Ab)</i>	Ab	3	2-3	2-3	2-3	2-3	2-3	2-3	3	3	2-3	3	3	3	2-3	2-3
P01	<i>Mla1</i>	Al	0	0	3	3	3	3	3	1	3	3	3	1	3	3	3
P02	<i>Mla3</i>	Ri	1	1	1	3	1	3	1	1-2	3	1	1-2	3	3	3	3
P03	<i>Mla6, (Mla14)</i>	Sp	3	3	3	3	3	3	0	3	3	0	3	3	0	0	0
P04B	<i>Mla7, Mlu</i>	Ly,u	3	2-3	3	3	2-3	3	1	3	3	1	3	3	3	3	3
P06	<i>Mla7, (Mik)</i>	Ly	3	2-3	3	3	2-3	3	0	3	3	0	3	3	3	3	3
P08B	<i>Mla9</i>	MC	0	0	0	3	0	3	0	0	3	0	0	3	0	0	0
P10	<i>Mla12</i>	Ar	3	3	3	3	3	3	2	3	3	2	3	3	3	3	3
P11	<i>Mla13, MI(Ru3)</i>	Ru	3	2-3	0	0	2-3	0	0	0	0	0	0	3	0	0	0
P12	<i>Mla22</i>	Ra	3	1	3	3	1	3	3	0	3	3	0	3	3	3	3
P14	<i>Mla</i>	Ra	3	2-3	3	3	2-3	3	3	3	3	3	3	3	3	3	3
P17	<i>Mik</i>	Kw	1-2	1	1-2	2-	1	1-2	1	3	1	1	3	3	1	1	1
P20	<i>Mlat</i>	At	2	2	2	2	2	2	2	2	2	2	2	2	2	2	2-3
P21	<i>Mlg, (MI(CP))</i>	We	3	2-3	3	3	2-3	3	0	2-3	3	0	2-3	2-3	2-3	2-3	2-3
P22	<i>mlo5</i>	Mlo	0	0(P)	0(P)	0(P)	0(P)	0(P)	2	0(P)	0(P)	2	0(P)	0(P)	0(P)	0(P)	0(P)
P23	<i>Mla</i>	La	2	2-3	2-3	3	2-3	2-3	2	3	2	2	3	3	2-3	2-3	2-3
P24	<i>Mlh</i>	Ha	3	3	3-4	3	3-4	3	0(P)	3	3	0(P)	3	3	3	3	3
SI-1 (RS1-12)	<i>MI(SI-1)</i>	SI-1	1	1	1	1	1	1	0	1	1	0	1	1	1	1	2-3
SI-2	<i>MI(SI-2)</i>	SI-2	2	1	1-2	2	1-2	2	0	1-2	2	0	1-2	1-2	1	1	1
SI-3	<i>MI(SI-3)</i>	SI-3	1	2-3	0	0/2	0	0	0	0	0	0	1	1	0	0	0
SI-4 (1-B-87)	<i>MI(SI-4)</i>	SI-4	0	0	0	3	0	0	0	0	3	0	1	1	0	0	0
SI-5	<i>MI(SI-5)</i>	SI-5	0	0	1	3	0	0	0	0	3	0	3	3	0	0	0

Table A 2 (continued)

Accession	Gene ²	Code	Powdery mildew isolates ¹												
			CH4-8	D2/4	D4/6	D35/2	MH21	Ro93a	Si1	247	227	240	233	125	78
			CHE	DEU	DEU	DEU	DEU	DNK	DNK	DEU	DEU	DNK	DNK	DNK	DEU
SI-6	<i>Mlf, mlt</i>	SI-6	1	0	1	2-3	0	0	2-3	1	2-3	0	2-3	1	1
SI-7	<i>Ml(SI-7)</i>	SI-7	1	1	0	2-3	0	0	2-3	0	2-3	0	2-3	1	1
Steffi	<i>Ml(St)</i>	St	2-3	3	2-3	3	0	0	3	0	3	0	2	2-3	2-3
WI-1 (RS142-29)	<i>Ml(WI-1)</i>	WI-1	0	1	0	0	1	1	0	0	0	1	1	1	1
Hanna	-	-	3-4	3	3	3	3	3	3	3	3	3	3	3	3

¹ represented by the work names, the official JKI numbers and the country of origin on the basis of the NATO Codification System Country Codes

² annotated resistance genes

³ until now unknown resistance gene

The infection types and the information about the resistance genes of the differential were provided by the JKI Kleinmachnow and the infection types were scored on a scale from 0-4 (0= resistant; 4=highly susceptible). The additional symbol 0(P) was included for a *mlo*-like phenotype.

Table A 3: Virulence spectra of the additional 18 powdery mildew isolates used for the comprehensive isolate test on a differential set of 33 barley lines

Accession	Gene ²	Code	Powdery mildew isolates ¹																																				
			114	116	122	167	168	170	176	212	225	229	231	232	234	235	237	239	241	245	114	116	122	167	168	170	176	212	225	229	231	232	234	235	237	239	241	245	
Alexis	<i>mlo9</i>	Mlo	0	0	0	2	2	0	1	2	0(P)	0	0(P)	0(P)	2	2-3	0(P)	0	0	0(P)	0(P)	0	0	0(P)	0(P)	0(P)	0(P)	0(P)	2	2-3	0(P)	0	0	0	0				
Antalia (WI/7)	<i>MI(WI-7)</i>	WI-7	2	1-2	0(P)	1-2	2	2	2	2	1-2	2	2	1-2	1	2	2	2	2	2	1-2	2	2	2	2	2	1-2	1	2	2	2	2	2	2	2	2			
Borwina	<i>MI(Bw)</i>	Bw	1-2	1	1	2-3	3	2-3	3	2-3	2-3	3	2-3	2-3	2	2-3	3	3	2-3	2	2-3	2	2-3	2-3	2-3	2	2-3	2-3	3	3	3	3	2-3	2-3	2-3	2-3			
Camilla	<i>U³</i>	U	0	0	0	0	1	1	1	0	2-3	0	0	2-3	0	1	1	1	1	1	1	1	0	0	1	1	1	1	0	2	2	1	1	1	1	1			
Kredit	<i>MI(Kr)</i>	Kr	2	2	2	2	2-3	3	3	3	2-3	3	3	2-3	3	3	3	3	3	3	3	3	3	3	3	3	3	3	3	3	3	3	3	3	3	2-3	2		
Laverda (U)	<i>MI(Lv)</i>	Lv	0	0	0	0	0	0	0	1	0	0	0	0	0	2-3	0	0	0	0	0	0	0	0	0	0	0	2-3	0	0	0	0	0	0	0	0	0		
Lotta	<i>MI(Ab)</i>	Ab	2	2	1	2	2-3	2	3	3	3	3	3	3	3	3	3	3	3	3	2-3	3	3	3	3	3	3	3	3	3	3	3	3	2	2	2	2		
P01	<i>Mla1</i>	Al	0	0	1	0	2-3	0	1	0	3	0	0	3	0	0	4	0	1	3	2-3	4	0	0	0	0	4	0	1	3	2-3	3	2	2	3	3			
P02	<i>Mla3</i>	Ri	1	1-2	1	1-2	2	3	3	1-2	3	1	1-2	3	1	1-2	3	1	1-2	2	3	3	1	1-2	2	3	3	1	1-2	3	1	1-2	3	1	1	1-2	1-2		
P03	<i>Mla6, (Mla14)</i>	Sp	2	2-3	0	3	3	3	2-3	3	3	3	3	3	3	3	3	3	3	3	3	3	3	3	3	3	3	3	3	3	3	3	3	3	3	3	3		
P04 B	<i>Mla7, Mlu</i>	Ly,u	2-3	2	2	3	2-3	3	3	3	3	3	3	3	3	2-3	3	3	3	3	3	3	3	3	3	3	2-3	3	3	3	3	3	3	3	2-3	2-3	2-3		
P06	<i>Mla7, (Mik)</i>	Ly	1-2	1	1	3	2-3	3	3	3	2-3	3	3	2-3	3	2	3	2	3	2	3	2	3	2	3	2	3	2	3	3	3	3	3	2	3	2	2		
P08B	<i>Mla9</i>	MC	0	0	3	0	0	0	3	0	0	3	0	3	0	0	0	0	3	0	3	0	0	3	0	0	0	0	0	0	0	0	0	0	0	1	3	3	
P10	<i>Mla12</i>	Ar	1-2	1	3	3	2	1	2-3	3	3	3	3	2-3	3	3	3	3	2-3	3	3	3	3	3	3	3	2	2	3	3	3	3	3	3	3	1-2	3	3	
P11	<i>Mla13, MI(Ru3)</i>	Ru	1	0	1	0	2-3	0	1	3	0	2-3	3	0	0	3	0	0	3	0	3	0	3	0	0	0	0	0	3	3	3	3	3	3	3	3	1	1	
P12	<i>Mla22</i>	-	3	2-3	3	3	1	3	1	2-3	0	0	3	0	0	3	3-4	0	3	3-4	0	3	3	3	3	3	0	3	3	3	3	3	3	3	3	2-3	0	0	
P14	<i>Mla</i>	Ra	3	2-3	1	3	2-3	3	3	3	3	3	3	2-3	3	3	3	3	3	3	3	3	3	3	3	3	3	3	3	3	3	3	3	3	3	2-3	3	2-3	
P17	<i>Mik</i>	Kw	3	1-2	3	1-2	2-3	1-2	3	3	3	2-3	2	2	2	2	2	2	2	2	2	2	2	2	2	2	2	2	2	2	2	2	2	2	2	2	1-2	1-2	
P20	<i>Mlat</i>	At	2	1	1	2	2	1	2	1	2	2	2	2	2	2	2	2	2	2	2	2	2	2	2	2	2	2	2	2	2	2	2	2	2	2	1	2	
P21	<i>Mlg, (MI(CP))</i>	We	0	3	0	0	0	3	2-3	2-3	3	3	3	2-3	3	3	3	3	3	3	3	3	3	3	3	3	3	3	3	3	3	3	3	3	3	0	2-3	2-3	
P22	<i>mlo5</i>	Mlo	0	1	0	0(P)	0(P)	0	1	0(P)	0(P)	0(P)	0(P)	0(P)	0	0(P)	0	0	0(P)	0	0(P)	0	0	0(P)	0(P)	0(P)	0	0(P)	0(P)	0(P)	0(P)	0(P)	0(P)	0(P)	0	0	0(P)	0(P)	
P23	<i>MlLa</i>	La	2	2	2-3	2	2	2	2-3	2	3	2	2-3	3	2	3	2	2-3	3	2-3	3	2-3	2-3	2-3	2-3	2-3	2-3	2-3	2-3	2-3	2-3	2-3	2-3	2-3	2-3	2-3	2	2	
P24	<i>Mlh</i>	Ha	2	2-3	2-3	3	2-3	3	2-3	3	3	3	3	3	3	3	3	3	3	3	3	3	3	3	3	3	3	3	3	3	3	3	3	3	3	3	2-3	2-3	
SI-1 (RS1-12)	<i>MI(SI-1)</i>	SI-1	0	1	1	1	0	0	0	1	3	1	0	0	0	1	3	1	0	0	0	0	0	0	0	0	0	1	0	1-2	0	1-2	0	0	0	0	0		
SI-2	<i>MI(SI-2)</i>	SI-2	0	1	0	0	0	3	0	1	1/3	2	0	2	2	1-2	2	2	2	2	2	2	2	2	2	2	2	2	2	2	2	2	2	2	2	1-2	0	1-2	
SI-3	<i>MI(SI-3)</i>	SI-3	0	0	1	0	1	0	1	0	0	1	0	3	2	1	1	0	1	0	3	2	1	0	3	2	1	1	1	1	1	1	1	1	0	1/3	1	1	
SI-4 (1-B-87)	<i>MI(SI-4)</i>	SI-4	0	0	0	0	0	0	0	0	0	0	0	0	0	0	0	0	0	0	0	0	0	0	0	0	0	0	0	0	0	0	0	0	0	0	0	0	
SI-5	<i>MI(SI-5)</i>	SI-5	1	0	0	0	1	1	3	0	1	2-3	0	3	0	0	1	2-3	0	3	0	0	0	0	3	0	0	0	0	0	0	0	0	0	0	0	0	0	3
SI-6	<i>Mlf, mlt</i>	SI-6	1	0	2	0	1	1	2	1	1	1-2	1	1	1	1	1	1-2	1	2	1	1	1	1	1	1	1	1	1	1	1	1	1	1	1	1	1	2	2

Table A 3 (continued)

		Powdery mildew isolates ¹																			
Accession	Gene ²	Code	114	116	122	167	168	170	176	212	225	229	231	232	234	235	237	239	241	245	
			DNK	DNK	DNK	DEU	DEU	DEU	DEU	SWE	DEU	DEU	DEU	DEU	GBR	CZE	POL	POL	DEU	FRA	
SI-7	MI(SI-7)	SI-7	0	0	2	1	0	1	2-3	0	1	1-2	1	2	1	0	1	0	1	2	
Steffi	MI(St)	St	0	0	0	0	2	3	2-3	3	2-3	2	2-3	4	1-2	2-3	3	3-4	2	0	
WI-1 (RS142-29)	MI(WI-1)	WI-1	0	0	1	0	0	0	0	0	0	0	0	0	0	0	0	0	0	1	
Hanna	-	-	3	3	3	2-3	2-3	3	2-3	3	3	3	3	3	3	3	2-3	3	2-3	2-3	

¹ represented by the official JKI numbers and the country of origin on the basis of the NATO Codification System Country Codes

² annotated resistance genes

³ until now unknown resistance gene

The infection types and the information about the resistance genes of the differential were provided by the JKI Kleinmachnow and the infection types were scored on a scale from 0-4 (0= resistant; 4=highly susceptible). The additional symbol 0(P) was included for a *m/o*-like phenotype.

Table A 4: Spore densities and age of the spores for the three different biological replicates of the small isolate test

Powdery mildew isolate ¹	Spore density	Age of spores			
		Replicate 1	Replicate 2	Replicate 3	
CH4.8	247	7-8 spores/mm ²	9 d	8 d	11 d
D2/4	227	5-6 spores/ mm ²	7 d	9 d	11 d
D4/6	240	4-7 spores/ mm ²	8 d	10 d	12 d
D35/2	233	8-9 spores/ mm ²	8 d	10 d	12 d
MH21	125	7-9 spores/ mm ²	8 d	10 d	12 d
Ro93a	78	7-8 spores/ mm ²	7 d	9 d	11 d
Si1	224	7-8 spores/ mm ²	8 d	10 d	12 d

¹ represented by the work names and the official JKI numbers

Table A 5: Chemicals applied during the field trials**i) Gatersleben field**

Chemical	Concentration	Timepoint after sowing
Basagran® DP ¹	[3 l/ha]	4 weeks
Biathlon® 4D ¹	[70g/ha]	6 weeks
Dash® E.C. ¹	[1 l/ha]	6 weeks

ii) Bergen/Wohlde field

Chemical	Concentration	Timepoint after sowing
40er Korn-Kali ²	[80 kg/ha]	2 weeks
Calcium ammonium nitrate	[60 kg/ha]	3 weeks
Concert® sx ³	[100 g/ha]	6 weeks
2-methyl-4-chlorophenoxyacetic acid (MCPA)	[1 l/ha]	6 weeks
Duplosan® DP ⁴	[1 l/ha]	6 weeks
Calcium ammonium nitrate	[20 kg/ha]	7 weeks
Biscaya® ⁵	[0.3 l/ha]	11 weeks
Magnesium sulfate	[15 kg/ha]	11 weeks

¹ chemical produced by BASF

² chemical produced by K+S

³ chemical produced by Cheminova Deutschland GmbH & Co. KG

⁴ chemical produced by Dehner Agrar

⁵ chemical produced by Bayer CropScience Deutschland GmbH

Table A 6: Primers used for the determination of the *mlo-11* status and the semi-quantitative PCR

Name	Gene	Sequence	T _m ¹	Program ²	T _a ³	Length
65 AJ	HVGAPDH f ⁴	5'-CTAGCAGCCCTTCCACCTCTCCA-3'	66.0 °C	3-step	59.4 °C ⁵	322 bp ⁶
66 AJ	HVGAPDH r ⁴	5'-CAATGCTAGCTGACCACCAACTG-3'	64.4 °C			
69 AJ	ADUP7 <i>mlo11</i>	5'-CTCAAGCTTGCCACCATGTCGGACAAAAAAGGGG-3'	71.9 °C	3-step	50.9 °C ⁵	~1,200 bp ⁶
70 AJ	<i>Mlo6 mlo11</i>	5'-CATCTACTACTAGCATGTACC-3'	55.9 °C			

ii) Primers used for the semi-quantitative PCR

Name	Gene	Sequence	T _m ¹	Program ²	T _a ³	Length
022_MP	HvMlo f ⁴	5'-GGAAGAAATGGGAGACAGAGAC-3'	60.3 °C	3-step	51.8 °C ⁵	210 bp ⁶
023_MP	HvMlo r ⁴	5'-TGATGAAGCCTGCCCTCAAG-3'	59.4 °C		63.3 °C ⁷	431 bp ⁸
025_MP	HvUBC f ⁴	5'-ACTCCGAAGCAGCCAGAATG-3'	59.4 °C	3-step	52.9 °C ⁵	210 bp ^{6,8}
026_MP	HvUBC r ⁴	5'-GATCAAGCACAGGGGACACAAC-3'	59.8 °C			

¹ T_m: melting temperature based on the provided data sheet of the company

² cycling program selected based on the annealing temperature

⁴ f: forward primer; r: reverse primer

⁵ T_a: annealing temperature for Taq-Mastermix (Qiagen)-based PCR

⁶ product length of genomic DNA product

⁷ T_a: annealing temperature for Phusion- based PCR

⁸ product length of cDNA product

Table A 7: General composition of the Taq-Mastermix for one reaction and the general Taq-PCR cycling program**i) Overview of the Mastermix composition**

Compound	Volume (V=10 µl)
Taq PCR Mastermix (Qiagen)	5.0 µl
Primer forward [10 µM]	0.5 µl
Primer reverse [10 µM]	0.5 µl
DNA or cDNA	1.0 µl
Water	3.0 µl

ii) Overview of the PCR cycling program

Temperature	Time	Cycle
94 °C	3 min	1x
94 °C	1 min	30x
Ta ¹	30 sec	
72 °C	1 min/kb ²	
72 °C	10 min	1x
20 °C	∞	

¹Ta: annealing temperatures were indicated in the Tables A 6, A 8 and A 11

²velocity of the enzyme, the extension time was adjusted considering the length of the expected PCR product

The set up was used for the *mlo-11* screening, the semi-quantitative PCRs, the conformation of the WB-352-specific *Mlo* fragments and the generation of the functional validation constructs.

Table A 8: Primers used for *Mlo* sequencingi) Primers used for the full-length amplification of the *Mlo*-gene

Name	Position ¹	Sequence	T _m ²	Program ³	T _a ⁴	Length
001_MP	5'UTR f ⁵	5'-CGCGCATCAGCTGTGGTG-3'	63.1 °C	2-step	-	607 bp ⁶
002_MP	Exon 2 r ⁵	5'-CTTGTGCCGGTGTGGAACC-3'	63.5 °C			
003b_MP	Exon 1 f	5'-CCGCCATGGTCTCGT-3'	60.0 °C	2-step	70.5 °C	528 bp
004b_MP	Exon 3 r	5'-GGTGCAAGCTGCCCGTGG-3'	62.8 °C			
003_MP*	Exon 1 f	5'-CACGGCCCTCCACAAGCTCG-3'	63.1 °C	2-step	-	524 bp
004_MP*	Exon 3 r	5'-GCGAGCACGAAAGATGAAGACG-3'	61.8 °C			
005_MP	Exon 3 f	5'-GCAAGGTGGCGCTCATGTCC-3'	63.5 °C	2-step	-	513 bp
006_MP	Exon 5 r	5'-CACCCATCTGATGCCAGGGG-3'	63.5 °C			
007_MP	Exon 5 f	5'-CTGCACGGTCCGGTTCACG-3'	63.5 °C	2-step	-	633 bp
008_MP	Exon 8 r	5'-CACACCCACAGCGGAGG-3'	65.3 °C			
009b_MP*	Exon 7 f	5'-GCGCATTGTGCAAAACAGC-3'	59.8 °C	2-step	-	588 bp
010_MP*	Exon 10 r	5'-CATCTCCAGCTTGGTTCCAACAC-3'	62.4 °C			
011_MP	Exon 9 f	5'-GGGTGGCAGCGCTCATCTGG-3'	63.5 °C	2-step	-	526 bp
012_MP	Exon 11 r	5'-GCCCCACCACCCTTCATG-3'	63.5 °C			
013b_MP	Exon 11 f	5'-GCTACCACACGCAGATCGGG-3'	63.5 °C	3-step	67.8 °C	481 bp
014_MP	Exon 12 r	5'-CCGGGTACATGCCCTAGCC-3'	63.5 °C			
015_MP	Exon 12 f	5'-CCGTGCACCTGCTTCACAAGG-3'	63.7 °C	3-step	67.0 °C	489 bp
017_MP	3'UTR r	5'-GTCTATGTACTGGTGCCTCCAG-3'	62.4 °C			
018_MP	3'UTR f	5'-CCAAACGGCAATCAGTCTCATAAC-3'	61.0 °C	3-step	65.1 °C	619 bp
019_MP	3'UTR r	5'-GTCTGATGCTGTTGGAAGTAGTC-3'	60.6 °C			
020_MP	3'UTR f	5'-GTGCTGCTAAATATCCCTCTGTAC-3'	61.3 °C	3-step	65.1 °C	639 bp
021_MP	3'UTR r	5'-GTTCCAGCAGCATGTGCTTTGG-3'	62.4 °C			

Table A 8 (continued)ii) Primers used for the conformation of WB-352-specific *Mlo* fragment

Name	Position ¹	Sequence	T _m ²	Program ³	T _a ⁴	Length
003b_MP ⁺	Exon 1 f ⁵	5'-CCGCCATGGTGTCTCGTG-3'	60.0 °C	3-step	55.1 °C	722 bp ⁷
008_MP ⁺	Exon 8 r ⁵	5'-CACACCCACACGCGGGAGG-3'	65.3 °C			1,555 bp ⁶
009b_MP	Exon 7 f	5'-GCGCATTGTCCGAAAACAGC-3'	59.8 °C	3-step	55.1 °C	213 bp
010_MP	Exon 10 r	5'-CATCTCCAGCTTGGTTCCAACAC-3'	62.4 °C			588 bp
009b_MP	Exon 7 f	5'-GCGCATTGTCCGAAAACAGC-3'	59.8 °C	3-step	54.2 °C	915 bp
016_MP	Exon 12 r	5'-TCATCCCTGGCT GAAGGAAAAATC-3'	61.0 °C			1,478 bp
022_MP ⁺	Exon 4 f	5'-GGAAAGAAATGGGAGACAGAGAC-3'	60.3 °C	3-step	51.8 °C ⁸	210 bp
023_MP ⁺	Exon 6 r	5'-TGATGAAGCCTGCCCTCAAG-3'	59.4 °C		54.0 °C ⁴	431 bp

¹ Position: binding position within the annotated gene model (HORVU4Hr1G082710.2)² T_m: theoretical melting temperature based on the provided data sheet of the manufacturer cycling program selected based on the annealing temperature³ Program: annealing temperature for Phusion- based PCR⁴ T_a: annealing temperature for Phusion- based PCR⁵ f: forward primer; r: reverse primer⁶ product length of genomic DNA product⁷ product length of cDNA product⁸ T_a: annealing temperature for Taq-Mastermix (Qiagen)-based PCR*The two primer combinations used for the amplification from the *mlo-11* carriers WB-219 & WB-468.

+ Products purified and used for sequencing

Table A 9: General Phusion-Mastermix for one reaction

Compound	Volume (V=10 μ l) ¹	Volume (V=20 μ l) ²	Volume (V=50 μ l) ³
5xHF buffer	2.0 μ l	4.0 μ l	10.0 μ l
dNTPs [10mM each]	0.2 μ l	0.4 μ l	1.0 μ l
Primer forward [10 μ M]	0.5 μ l	1 μ l	2.5 μ l
Primer reverse [10 μ M]	0.5 μ l	1 μ l	2.5 μ l
Phusion DNA polymerase (2U/ μ l)	0.1 μ l	0.2 μ l	0.5 μ l
DNA or cDNA	1 μ l	1 μ l	5.0 μ l
Water	5.7 μ l	12.4 μ l	28.5 μ l

¹ semi-quantitative PCRs, the allele amplification and the expression analysis of the candidates.

² allele amplification and the expression analysis of the candidates

³ full-length *Mlo* sequencing

Table A 10: General Phusion-PCR cycling program

i) 2-step program used for the full-length *Mlo* sequencing, the allele amplification and the expression analysis of the candidates

Temperature	Time	Cycle
98 °C	30 sec	1x
98 °C	20-30 sec	30x
72 °C	15-30 sec/kb ¹	
72 °C	10 min	1x
20 °C	∞	

ii) 3-step program used for the full-length *Mlo* sequencing

Temperature	Time	Cycle
98 °C	30 sec	1x
98 °C	30 sec	30x
T _a ² °C	35 sec	
72 °C	15-30 sec/kb	
72 °C	10 min	1x
20 °C	∞	

iii) 3-step program used for the semi-quantitative PCR

Temperature	Time	Cycle
98 °C	30 sec	1x
98 °C	30 sec	30x
T _a ² °C	35 sec	
72 °C	15-30 sec/kb	
72 °C	10 min	1x
20 °C	∞	

iv) 3-step program used for the allele amplification, expression analysis of the candidates and the generation of the functional validation constructs

Temperature	Time	Cycle
98 °C	30-35 sec	1x
98 °C	10-20 sec	30-35x
T _a ² °C	30-35 sec	
72 °C	15-30 sec/kb	
72 °C	10 min	1x
20 °C	∞	

¹velocity of the enzyme, the extension time was adjusted considering the length of the expected PCR product

²T_a: annealing temperature indicated in Table A 6, A 8, A 11 and A 15

Table A 11: Primers used for functional validation assays

i) Primers used for the full-length allele amplification of the candidate genes and the generation of the constructs for the transient overexpression

Name	Gene ¹	Sequence	T _m ²	Program ³	T _a ⁴	Length
028_MP	WB-CG_17 f ⁵	5'-ATGGCGGAGAACCC-3'	46.0 °C	3-step	61 °C	1,961 bp ⁶
093_MP	WB-CG_17 r ⁵	5'-CAACTATACGACGAGATCAGCAAC-3'	61.0 °C			
031_MP	WB-CG_19 r	5'-TCAATCAGAGCTCACATCAAC-3'	55.9 °C	3-step	59 °C	751 bp
032_MP	WB-CG_19 f	5'-ATGAAGCACATATCAAGATC-3'	52.0 °C			
042_MP	WB-CG_20 f	5'-ATGGACGCGGGTTCG-3'	56.9 °C	3-step	66 °C	8613 bp
043_MP	WB-CG_20 r	5'-TCAAGTAGCAGTCTCGTCATCC-3'	60.3 °C			
048_MP	WB-CG_23 f	5'-ATGGACCCCGCCTCTC-3'	60.0 °C	3-step	68.5 °C	3,448 bp
049_MP	WB-CG_23 r	5'-TCAGGTTTGTACTCCAGGCTGC-3'	62.1 °C			
052_MP	WB-CG_28 r	5'-TTAAATGAAAGAAAAGGTGGGAGGC-3'	59.7 °C	3-step	66.5 °C	6,649 bp
053_MP	WB-CG_28 f	5'-CCGTGCTCTCCTCTCCTAAGG-3'	64.0 °C			
056_MP	WB-CG_31 f	5'-ATGGCCAGCTCCGGCA-3'	56.9 °C	3-step	67.8 °C	5,911 bp
057_MP	WB-CG_31 r	5'-TCACGAGACTGGGAATCATC-3'	59.8 °C			
060_MP	WB-CG_14 f	5'-ATGGAGTCGTCGTCC-3'	50.6 °C	3-step	52.9 °C	4,445 bp
061_MP	WB-CG_14 r	5'-GAGTGAGTATAGTCACAAAAAG-3'	54.7 °C			
064_MP	WB-CG_13 f	5'-CATAGAGAAGAAAATCCCTTC-3'	54.0 °C	3-step	57.3 °C	4,404 bp
065_MP	WB-CG_13 r	5'-AAAATTAACAAAAGGATGTATCATT-3'	51.5 °C			
068_MP	WB-CG_11 f	5'-ATGATGATTGGGTAGAAAC-3'	53.2 °C	3-step	55.2 °C	3,140 bp
069_MP	WB-CG_11 r	5'-CCTAAAAGTGAGGGGAAGTAC-3'	57.3 °C			
072_MP	WB-CG_8 r	5'-ATGGCGGAGGACGG-3'	48.0 °C	3-step	55.2 °C	1,944 bp
073_MP	WB-CG_8 f	5'-TCATTTCCCAATTCCTTC-3'	49.1 °C			
075_MP	WB-CG_7 f	5'-ATGCCGCTCCTCCAC-3'	53.3 °C	3-step	60.2 °C	6,801 bp
076_MP	WB-CG_7 r	5'-CGTTTGGTCAATACAGACATG-3'	55.9 °C			
079_MP	WB-CG_6 f	5'-ATGGCCGGGATCGACG-3'	56.9 °C	3-step	60.2 °C	10,931 bp
080_MP	WB-CG_6 r	5'-CGAGGCTGAAGCAGCG-3'	57.6 °C			

Table A 11 (continued)

ii) Primers used for the expression test of the candidate genes and the generation of the constructs for the transient silencing

Name	Gene ¹	Sequence	T _m ²	Program ³	T _a ⁴	Length
029_MP	WB-CG_17 r ⁵	5'-TCAGTACGTGTTGTCAGC-3'	53.7 °C	3-step	55 °C	422 bp ⁷
030_MP	WB-CG_17 f ⁶	5'-GGAATTTCTTGCCTTCG-3'	51.4 °C			
031_MP	WB-CG_19 r	5'-TCAATCAGAGCTCACATCAAC-3'	55.9 °C	3-step	55 °C	193 bp
033_MP	WB-CG_19 f	5'-CGTACCTCGCAGTTATACTTG-3'	57.9 °C			
050_MP	WB-CG_23 f	5'-CAATGAGGAAACAACGAAGCG-3'	57.9 °C	3-step	62 °C	492 bp
051_MP	WB-CG_23 r	5'-GGAACCCCAAAAAGATCAC-3'	57.3 °C			
054_MP	WB-CG_28 r	5'-ATGCCAGGAAATTCACAAGG-3'	55.3 °C	3-step	62 °C	461 bp
055_MP	WB-CG_28 f	5'-AGGTGAGGCAGAAAGCACAGT-3'	59.4 °C			
070_MP	WB-CG_11 f	5'-ACCCTAATTGCCGTGTCAAG-3'	57.3 °C	3-step	55.2 °C	463 bp
071_MP	WB-CG_11 r	5'-GTGAACGTGTGTGAGCTGGT-3'	59.4 °C			
073_MP	WB-CG_8 r	5'-TCAATTCCTTC-3'	49.1 °C	3-step	55.2 °C	486 bp
074_MP	WB-CG_8 f	5'-ATATACAGGGACCCGCCACT-3'	59.4 °C			

¹ candidate gene² T_m: theoretical melting temperature based on the provided data sheet of the manufacturer³ cycling program selected based on the annealing temperature⁴ T_a: annealing temperature for Phusion- based PCR⁵ f: forward primer; r: reverse primer⁶ product length of genomic DNA product⁷ product length of cDNA product

Table A 12: General qPCR-Mastermix for one reaction and the general qPCR cycling program**i) Overview of the Mastermix composition**

Compound	Volume (V=10 µl)
2x GoTaq® qPCR Master mix ¹	7.5 µl
Primer forward [10 µM]	1.31 µl
Primer reverse [10 µM]	1.31 µl
Primer UBC forward [10 µM]	1.31 µl
Primer UBC reverse [10 µM]	1.31 µl
Probe [10 µM]	0.375 µl
Probe UBC [10 µM]	0.375 µl
cDNA	1 µl ² or 1.5 µl ³
Water	0.5 µl ² or 0 µl ³

ii) Overview of the PCR cycling program

Temperature	Time	Cycle
95 °C	10 min	1x
95 °C	15 sec	40x
58 °C	30 sec	
72 °C	30 sec	

¹ Master mix supplemented with carboxy-X-rhodamine (CXR) reference dye to a final concentration of 510 nM

² WB-CG_119 & WB-CG_128

³ WB-CG_121 & WB-CG_409

Table A 13: Primers and probes used for the qPCR

Name	Gene	Sequence	T _m ¹
025_MP	HvUBC f ²	5'-ACTCCGAAGCAGCCAGAATG-3'	59.4 °C
026_MP	HvUBC r ²	5'-GATCAAGCACAGGGACACAAC-3'	59.8 °C
027_MP	HvUBC p ²	FAM ^{TM3} 5'-GAGAACAAGCGGAGTACAACCGCAAGGT-3' BHQ ^{®-14}	
102_MP	WB-CG_17 f	5'-TCGATCCACATGATCCTACC-3'	57.3 °C
103_MP	WB-CG_17 r	5'-TCACCAGAATGACACCAAAAC-3'	55.3 °C
104_MP	WB-CG_17 p	JOE TM 5'-CTGACAACACGTACTGATGCTTTGGCCTGAT-3' BHQ ^{®-1}	
105_MP	WB-CG_19 f	5'-CGCTCCTTGAAACCTCAAC-3'	56.7 °C
106_MP	WB-CG_19 r	5'-TTCCTTTGCCTCCACAATATC-3'	55.9 °C
107_MP	WB-CG_19 p	JOE TM 5'-CCCAACTGCCCTCAAGAAGCAGTGTTA-3' BHQ ^{®-1}	
108_MP	WB-CG_23 f	5'-TGAAATGGAGGACGAGCAG-3'	56.7 °C
109_MP	WB-CG_23 r	5'-CGGAACCCCAAAAAGATCAC-3'	57.3 °C
110_MP	WB-CG_23 p	JOE TM 5'-CCGGAGGGCTCGACATGCCTGAC-3' BHQ ^{®-1}	
111_MP	WB-CG_28 f	5'-TCTTCGCCATGTAACCTGACC-3'	57.3 °C
112_MP	WB-CG_28 r	5'-GCACAACCTCTTCTATGCAACC-3'	58.4 °C
113_MP	WB-CG_28 p	JOE TM 5'-ACTCACAATGGATCAGTTCATCGACTTATGTATCCTT-3' BHQ ^{®-1}	

¹ T_m: theoretical melting temperature based on the provided data sheet of the manufacturer

² f: forward primer; r: reverse primer; p: probe

³ fluorescein

⁴ Black Hole Quencher^{®-1}

Table A 14: Overview of the shooting experiments

i) Mlo complementation assay						
Construct 1 ¹	Construct 2 ²	Experiments ³	Genotype ⁴	Inoculation ⁵	Spore density	
pipkTA9	pUbiGUS	2	Ingrid, Ingrid BC mlo5, WB-352, WB-358	CH4.8	150-200 spores/mm ²	
pipkTA9_Mlo	pUbiGUS	2	Ingrid, Ingrid BC mlo5, WB-352, WB-358	CH4.8	150-200 spores/mm ²	
ii) Transient-induced gene silencing of the selected candidate genes						
Construct 1 ¹	Construct 2 ²	Experiments ³	Genotype ⁴	Inoculation ⁵	Spore density	
pipkTA30N	pUbiGUS	5	WB-052, Morex	CH4.8	450-530 spores/mm ²	
pipkTA36	pUbiGUS	5	WB-052, Morex	CH4.8	450-530 spores/mm ²	
pipkTA30N_WB-CG_17	pUbiGUS	5	WB-052, Morex	CH4.8	450-530 spores/mm ²	
pipkTA30N_WB-CG_19	pUbiGUS	5	WB-052, Morex	CH4.8	450-530 spores/mm ²	
pipkTA30N_WB-CG_23	pUbiGUS	5	WB-052, Morex	CH4.8	450-530 spores/mm ²	
pipkTA30N_WB-CG_28	pUbiGUS	5	WB-052, Morex	CH4.8	450-530 spores/mm ²	
iii) Transient overexpression of the selected candidate genes						
Construct 1 ¹	Construct 2 ²	Experiments ³	Genotype ⁴	Inoculation ⁵	Spore density	
pipkTA9	pUbiGUS	5	WB-052, Morex	CH4.8	150-250 spores/mm ²	
pJP01	pUbiGUS	5	WB-052, Morex	CH4.8	150-250 spores/mm ²	
pipkTA9_WB-CG_17	pUbiGUS	5	WB-052, Morex	CH4.8	150-250 spores/mm ²	
pipkTA9_WB-CG_19	pUbiGUS	5	WB-052, Morex	CH4.8	150-250 spores/mm ²	
pipkTA9_WB-CG_23	pUbiGUS	5	WB-052, Morex	CH4.8	150-250 spores/mm ²	

Table A 14 (continued)

iv) Total number of GUS stained cells of promoter_GUS constructs

Construct 1 ¹	Construct 2 ²	Experiments ³	Genotype ⁴	Inoculation ⁵	Spore density
pUbiGUS	pBC17	3	Ingrid	no	-
pV668	pBC17	3	Ingrid	no	-
pipKb002_GUS	pBC17	3	Ingrid	no	-
pipKb003_GUS	pBC17	3	Ingrid	no	-
pipKb004_GUS	pBC17	3	Ingrid	no	-
pipKb005_GUS	pBC17	3	Ingrid	no	-
pUbiGUS	pBC17	3	Ingrid	CH4.8	150-200 spores/mm ²
pV668	pBC17	3	Ingrid	CH4.8	150-200 spores/mm ²
pipKb002_GUS	pBC17	3	Ingrid	CH4.8	150-200 spores/mm ²
pipKb003_GUS	pBC17	3	Ingrid	CH4.8	150-200 spores/mm ²
pipKb004_GUS	pBC17	3	Ingrid	CH4.8	150-200 spores/mm ²
pipKb005_GUS	pBC17	3	Ingrid	CH4.8	150-200 spores/mm ²

v) Staining/colour intensity of GUS stained cells of promoter_GUS constructs

Construct 1 ¹	Construct 2 ²	Experiments ³	Genotype ⁴	Inoculation ⁵	Spore density
pUbiGUS	pBC17	3	Ingrid	no	-
pV668	pBC17	3	Ingrid	no	-
pipKb002_GUS	pBC17	3	Ingrid	no	-
pipKb003_GUS	pBC17	3	Ingrid	no	-
pipKb004_GUS	pBC17	3	Ingrid	no	-
pipKb005_GUS	pBC17	3	Ingrid	no	-

¹ test construct² reporter construct and/or normalization³ total number of experiments⁴ selected genotypes⁵ performed inoculation and corresponding powdery mildew isolate

Table A 15: Primers used for the colony PCR

i) Primers used for the colony PCRs of the overexpression constructs

Name	Region ¹	Sequence	T _m ²	T _a ³	Length
213_MP	35S promoter f ⁴	5'-ACGCACAAATCCCACTATCCTTC-3'	60.3 °C	61.1 °C	830 bp
031_MP	WB-CG_19 r ⁴	5'-TCAAATCAGAGCTCACATCAAC-3'	61.0 °C		
213_MP	35S promoter f	5'-ACGCACAAATCCCACTATCCTTC-3'	60.3 °C	64 °C	3,527 bp
049_MP	WB-CG_23 r	5'-TCAGGTTTGTACTCCAGGCTGC-3'	62.1 °C		
213_MP	35S promoter f	5'-ACGCACAAATCCCACTATCCTTC-3'	60.3 °C	64 °C	2,040 bp
093_MP	WB-CG_17 r	5'-CAACTATACGACGAGATCAGCAAC-3'	61.0 °C		

ii) Primers used for the colony PCRs of silencing constructs

Name	Region ¹	Sequence	T _m ²	T _a ³	Length
212_DN	35S terminator r ⁴	5'-ATGAGCGAAACCCTATAAGAACCCTA-3'	61.6 °C	47.1 °C	1,852 bp ⁵ , 700 bp ⁶ , 472 bp ⁷ , 770 bp ⁸ , 739 bp ⁹
215_MP	pipkTA30N intron f ⁴	5'-GGATAGCCCTCATAGATAGAGTAACTAA-3'	64.2 °C		
213_MP	35S promoter f	5'-ACGCACAAATCCCACTATCCTTC-3'	60.3 °C	47.1 °C	1,899 bp ⁵ , 724 bp ⁶ , 495 bp ⁷ , 794 bp ⁸ , 763 bp ⁹
214_MP	pipkTA30N intron r	5'-TCAAATTAACAATAATGCAGTATGAAGA-3'	55.9 °C		

¹ binding position in the generated construct² T_m: theoretical melting temperature based on the provided data sheet of the manufacturer³ T_a: annealing temperature⁴ f: forward primer; r: reverse primer⁵ product length of pipkTA30N⁶ product length of WB-CG_17⁷ product length of WB-CG_19⁸ product length of WB-CG_23⁹ product length of WB-CG_28

Table A 16: Primers used for the sequencing of the generated constructs**i) Primers used for sequencing of the overexpression constructs**

Name	Region¹	Sequence
212_DN	35S terminator	5'-ATGAGCGAAACCCTATAAGAACCCTA-3'
213_MP	35S promoter	5'-ACGCACAATCCCACTATCCTTC-3'
031_MP	WB-CG_19	5'-TCAATCAGAGCTCACATCAAC-3'
033_MP	WB-CG_19	5'-CGTACCTCGCAGTTATACTTG-3'
092_MP	WB-CG_17	5'-CAATCAGTTTGAAGCCCAGC-3'
093_MP	WB-CG_17	5'-CAACTATACGACGAGATCAGCAAC-3'
095_MP	WB-CG_23	5'-CCGATAAATTTGAGGTTCTTGC-3'
096_MP	WB-CG_23	5'-GGAGTAAACGAGAACTCCATATCTTG-3'

ii) Primers used for sequencing of the silencing constructs

Name	Region¹	Sequence
214_MP	pIPKTA30N intron	5'-TCAAATTAACAATGCAGTATGAAGA-3'
215_MP	pIPKTA30N intron	5'-GGATAGCCCTCATAGATAGAGTACTAACTAA-3'
029_MP	WB-CG_17	5'-TCAGTACGTGTTGTCAGC-3'
033_MP	WB-CG_19	5'-CGTACCTCGCAGTTATACTTG-3'
050_MP	WB-CG_23	5'-CAATGAGGAAACAACGAAGCG-3'
055_MP	WB-CG_28	5'-AGGTGAGGCAGAAGCACAGT-3'

¹ binding position in the generated construct

Appendix B: additional results

a) Additional figures

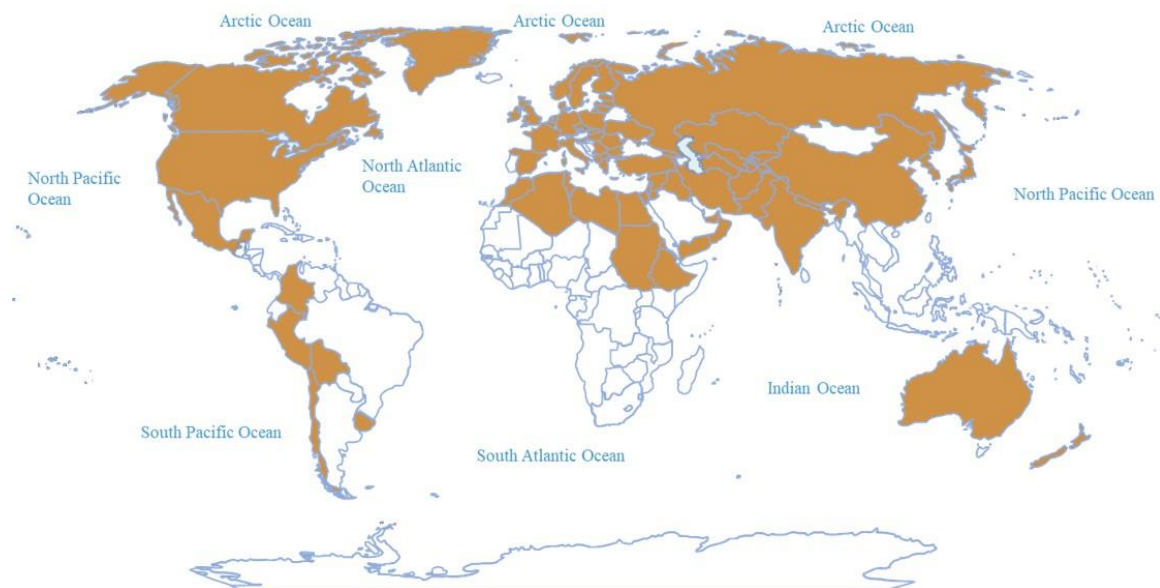


Figure B 1: Countries of origin of the 459 barley genotypes of the Whealbi collection
The 71 countries, where the selected varieties originate, were highlighted in brown.

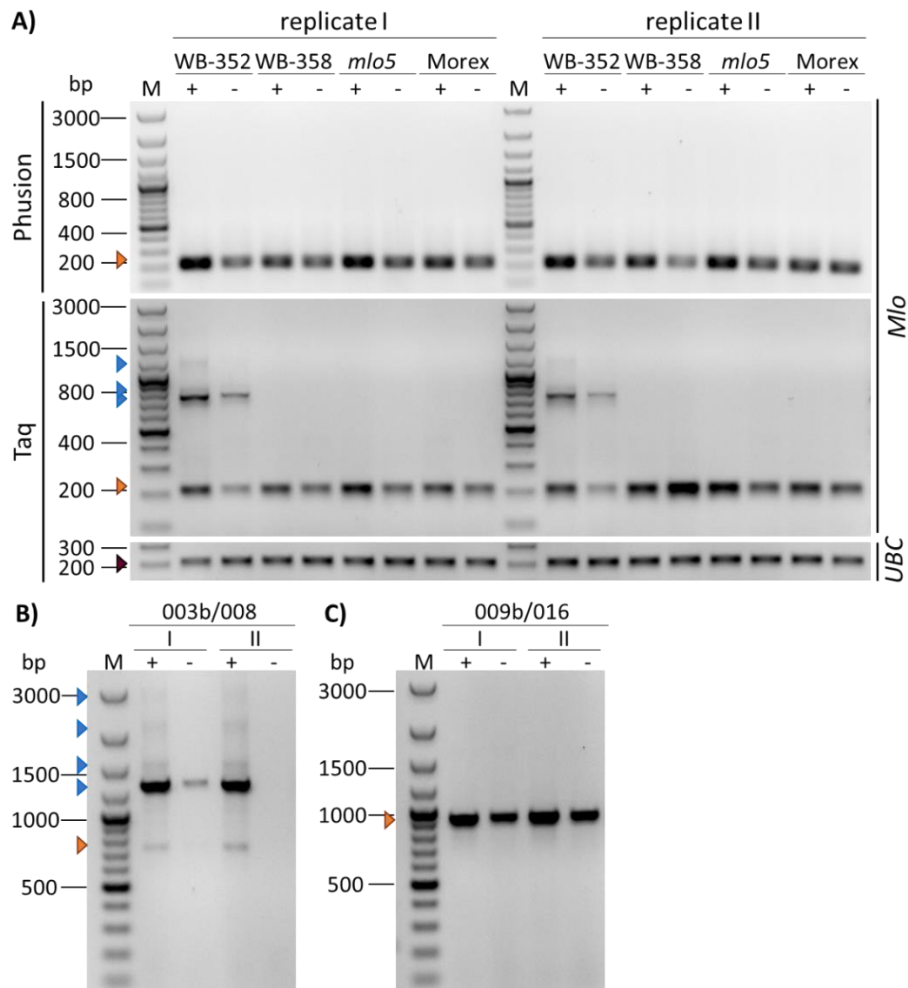


Figure B 2: Amplification of the indicated genotypes with *Mlo* or *UBC* specific primers for the remaining two biological replicates

A) The cDNAs of powdery mildew inoculated (+) or non-inoculated (-) leaf samples from the four genotypes (WB-352, WB-358, Ingrid BC *mlo5* (*mlo5*) and Morex) were used for the PCR based amplification with the indicated polymerases (Phusion or Taq). The gel pictures of the semi-quantitative PCRs from remaining two biological replicates (I & II) were depicted. The GeneRuler 100 bp Plus (M) was utilized as size standard. A 210 base pair (bp) long product was expected for the *Mlo* (*Mildew resistance locus o*) gene (orange arrow head). The amplification with the Taq polymerase revealed three additional WB-352-specific products of the following sizes: ~750 bp, ~850 bp and ~1,200 bp (blue arrow head). Additionally, the DNA samples were analysed for the amplification of the house keeping gene *UBC* (*ubiquitin-conjugating enzyme 3*). The expected product size is 210 bp (purple arrow head).

B) The cDNAs of powdery mildew inoculated (+) or non-inoculated (-) leaf samples from WB-352 were used for the PCR based amplification (primer combination 003b/008) with the Taq polymerase (two biological replicates I & II) were depicted. The GeneRuler 100 bp Plus (M) was utilized as size standard. A 722 base pair (bp) long product was expected for the *Mlo* gene (orange arrow head). The amplification on cDNA of inoculated WB-352 leaves revealed four additional specific products of the following sizes: ~1,300 bp, ~1,700 bp, ~2,400 bp and ~3,000 bp (blue arrow head). In the non-inoculated sample only one additional fragment was amplified ~1,300 bp (blue arrow head).

C) The same cDNAs were used for a PCR with the primer combination 009b/016. In all samples only the expected product (915 bp) were amplified (orange arrow head).

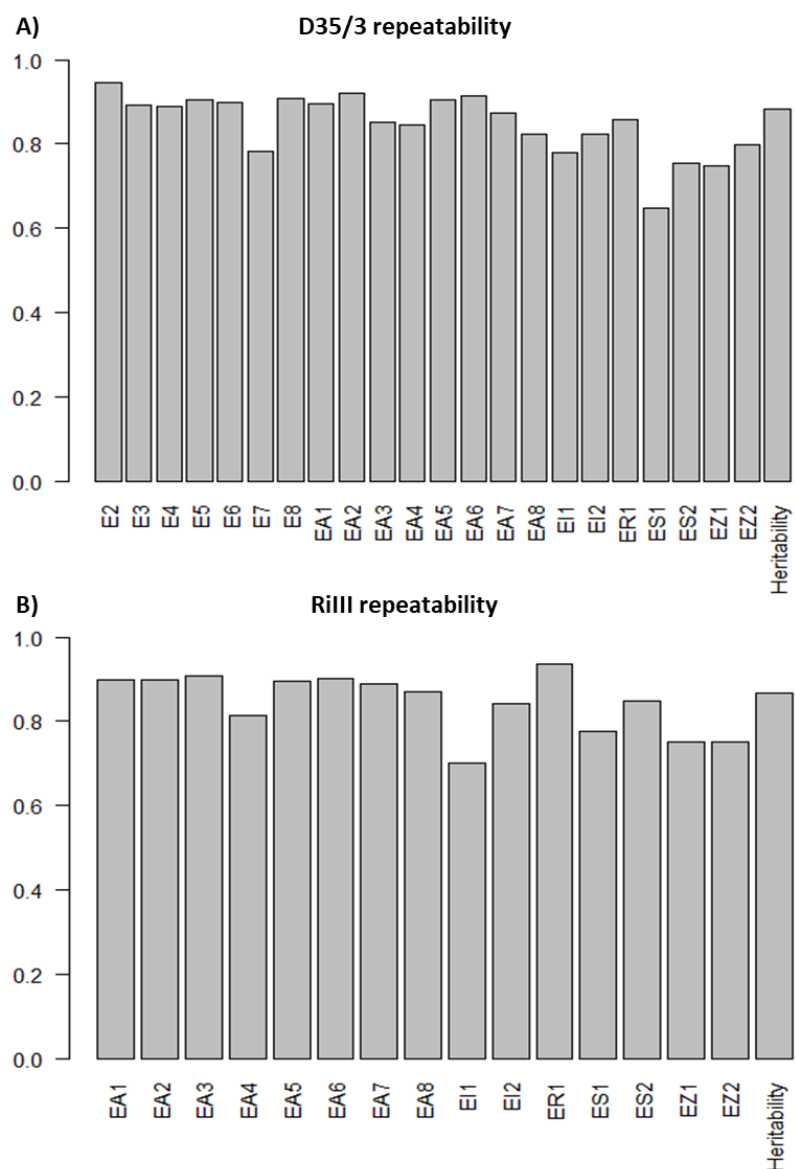


Figure B 3: Overview of the repeatability and the heritability of the phenotypic data

The repeatability of the different sub-experiments and the heritability were calculated for the phenotype data. **A)** represents the data for the inoculation with the powdery mildew isolate D35/3 and **B)** the data for the RiIII inoculation.

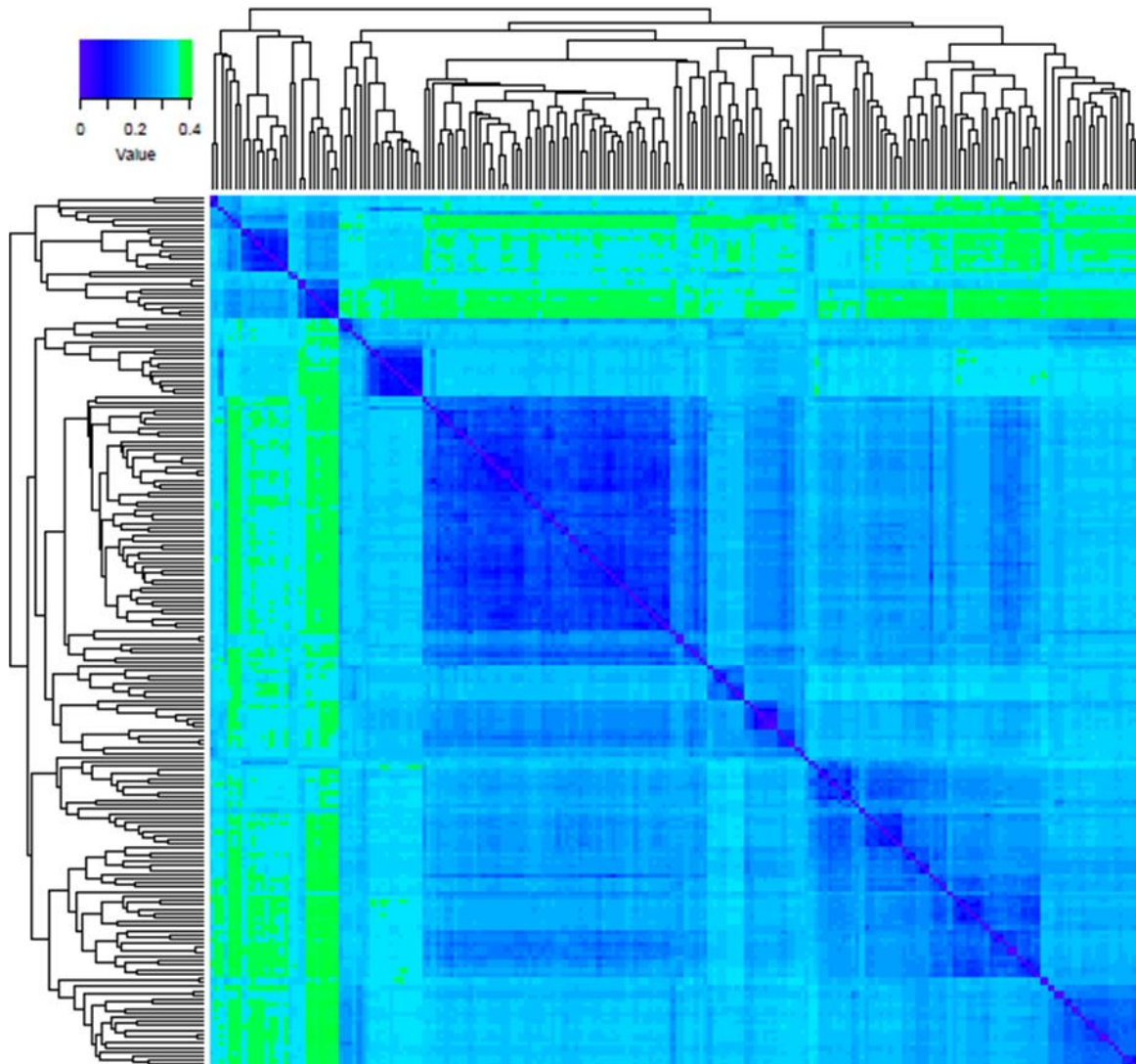


Figure B 4: Heat map of the calculated Rogers' distance from 201 genotypes

The Rogers' distance was calculated to estimate the dissimilarity of the 201 genotypes selected for the GWAS. A subpopulation of 28 genotypes were identified (indicated in Table A 1 and B 2)

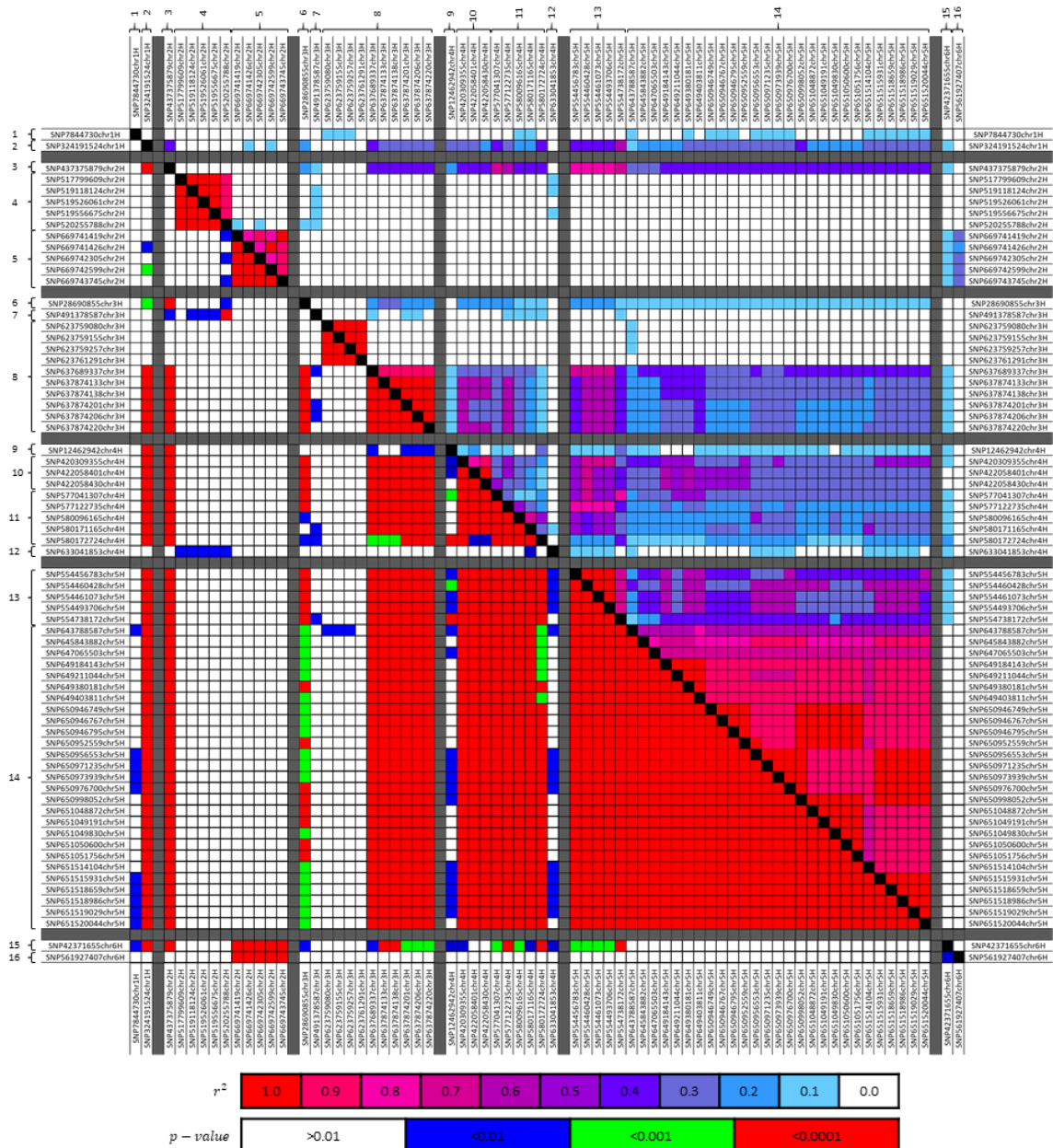


Figure B 5: Linkage disequilibrium plot for the significant SNPs of the *Max* trait
 Calculations of the pairwise linkage disequilibrium (LD) as sliding window (window size 50). Above the diagonal, r^2 values are displayed and the corresponding p -values for the two-sided Fisher's exact test displayed below the diagonal. Coloration of the corresponding p -values or r^2 values is indicated in the bars below. The numbered brackets represent the defined loci.

Appendix B

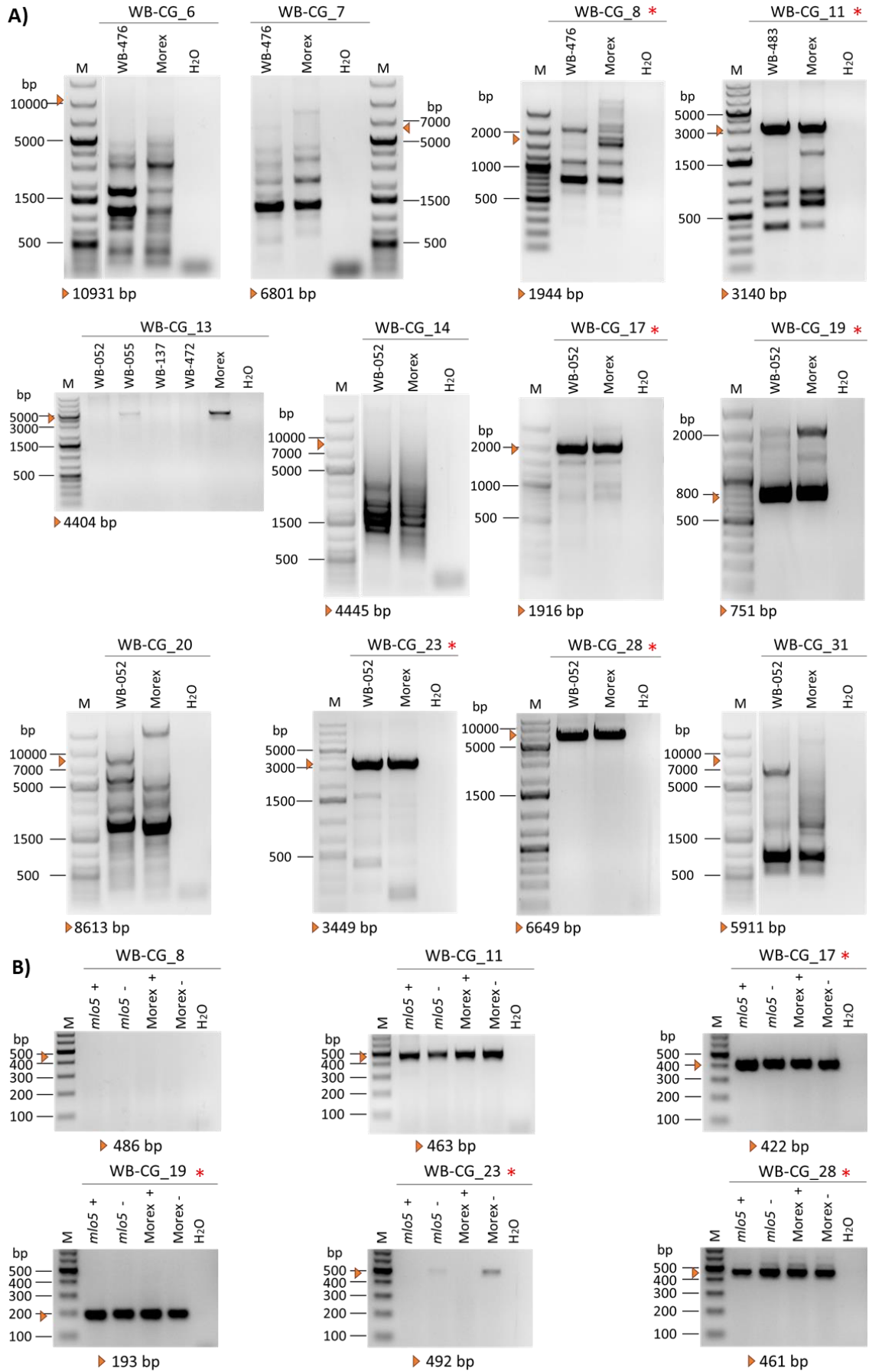


Figure B 6: Results of the allele amplification and the expression analysis of selected candidates

A) The gel pictures present the results of the full-length allele amplification. DNA of the indicated genotypes were used as template in the PCR reactions for the twelve candidate genes with confirmed annotation. The major allele 2 is always amplified from Morex and the minor allele 1 from the indicated Whealbi genotype, respectively. The orange arrow head indicates the expected product size, which exact size is given below the respective picture in base pairs (bp). Purified water was used as negative control during the amplification and either the GeneRuler 100 bp Plus or the GeneRuler 1 kb Plus was utilized as size standard (M). The red asterisk highlights the six candidates selected for the expression analysis.

B) The gel pictures present the results of the expression analysis of the six selected candidates. As template, cDNAs of powdery mildew inoculated (+) or not inoculated (-) leaf samples harvested 6 h post inoculation from Ingrid BC *mlo5* (*mlo5*) and Morex were used for the PCR based amplification. The orange arrow head indicates the expected product size, which exact size is given below the respective picture in base pairs (bp). Purified water was used as negative control during the amplification and the GeneRuler 100 bp Plus was utilized as size standard (M). The red asterisk highlights the four most promising candidate genes

Appendix B

A)

		Gly ³ Ala ^{syn}	
WB-CG_23	-----MDPGLSRGG--GLPSFEFAFNSENFSDRVLRLVVA	TDGVAGG	41
Barley	MAGGEGAAAAGVPTQAE	MDPGLSRGG--GLPSFEFAFNSENFSDRVLRLVVA	SDSVAGG 58
Brachypodium	MAGRGES-----	AMPEAAAEEVETKLECFDLAFN-SEFSDRLLRIEIVVPGDDVAEG	49
Arabidopsis_LRB1	MRG--TTENTDLDFDKTQMDP	DFTRHGSSSDGDFGFAFNDSNFSDRLLRIEIMGGFSDS--	57
Arabidopsis_LRB1	MRG--SNNTDLDFDKTE	MDSNFSRHGSSSEGDFGFAFNDSNFSDRLLRIEILGGFSDS--	56
Oryza_BT1	-----	-----	0
Oryza_BT2	-----	MDEDFSA--SRGPSFAFAFNSENFSDRVLRIEIVAGDDAAGA	41
		Val ⁴⁶ Leu Glu ⁵¹ Asp	
WB-CG_23	-----PLPDLVLRHREDLRH-----	-----	56
Barley	-----PLPDLVLRHREDLRH-----	-----	73
Brachypodium	-----SLTDCARHRKVKQEKRRQ-----	-----	67
Arabidopsis_LRB1	-RSDAEGCTSIADWARHRKR	RRREDNKKDNGV-AISDIVACAEQILTENNQPMDDAPEG	114
Arabidopsis_LRB1	-RSEVEGCTSIADWARHRKR	RREDIKKESGV-TISDIVACPEEQILT-EQPMDGCGPG	114
Oryza_BT1	-----	-----	0
Oryza_BT2	KGAAGEGCSLADWAHQ	RRRREELRREKESGKYTDLETCKVEAECDTYE-----	92
		KEEADGQTI	
WB-CG_23	-----KEEADGQTI	DSSWTMA-ATPVLRVKTIIYISSVLAANSPP	95
Barley	-----KEEADGKIIDSSCTMV-SAPVLRVKTIVINSVLAANSPP	-----	112
Brachypodium	-----IDSSPTMA-DTPALRVKTLHISSVILAARSAP	-----	98
Arabidopsis_LRB1	DNLDE-GEAMVEEAL---	SGDDD-ASSEPNWGLD-CSTVVRVKELHISSPILAAKSPP	167
Arabidopsis_LRB1	ENPDDEGGGEAMVEEAL---	SGDEEETSSEPNWGLD-CSTVVRVKELHISSPILAAKSPP	169
Oryza_BT1	-----	MDSFWSGGVSTPVLRVKNIIYISSAIIAASPP	32
Oryza_BT2	-E-NNEEPVAMIEESPP	DIGQDGDGDSWSME-CTQVLRVKSIIYISSAIIAASPP	149
		syn	
WB-CG_23	FLKLFNSGMKESDQRHLTQ	ADSGKVEVMMELLRMYTGKLAATEPNLLDILTAADK	155
Barley	FRKIFNSGMKESDQRHITLQ	ADSGTEETVIMELLSFMYTGKLSSTEPNLLDILMAADK	172
Brachypodium	FLKLFNSGMKESDQHTTIR	ISDS--EENAFMELLSFMYIGKLTTESTLLDILMAADK	156
Arabidopsis_LRB1	FYKLFNSGMRESEQRHVTL	RIASQ--EEGALMELLNFMYSNLSVTTAPALLDVLMAADK	225
Arabidopsis_LRB1	FYKLFNSGMRESEQRHVTL	RINAS--EAAALMELLNFMYSNAVSVTTAPALLDVLMAADK	227
Oryza_BT1	FFKLFNSGMKESDERQATL	RITDS--EENALMELLSFMYSGKLTSTDPITLLDILMAADK	90
Oryza_BT2	FYKLFNSGMKESDQRHATL	RITAS--EENALMELLSFMYSGKLTNQPITLLDILMAADK	207
		Leu ¹⁸⁰ Val	
WB-CG_23	FEVLACMRRCSQLLNLP	MTRTETALLYLDYPCSTSVAAEIQHLDAAKEFLANKYKVF	215
Barley	FEVLACMRHCNQLLNLP	MTRRESALLYLYPCSTSVAAEIRHLTNAKEFLASKYKVLAK	232
Brachypodium	FEVPSCMRHCSQLLISL	EMTIESALLYLEHGCSISQAAEVQCVIGAAKQFLAKYETDFDK	216
Arabidopsis_LRB1	FEVASCMRYCSRLLRN	MPMTPDSALLYLELPSSVIMAEAVQPLTDAARQFLASRKYKDTK	285
Arabidopsis_LRB1	FEVASCMRYCSRLLRN	MPMTPESALLYLELPSSVIMAKAVQPLTDAARQFLAARYKDTK	287
Oryza_BT1	FEVISCMRYCSQLLISL	MTMTESALLYLDLPCSTSMAAAVQPLTDAARQFLSNKYKDLTK	150
Oryza_BT2	FEVVSVMRHCSQLLISL	EMTIESALLYLDLPCSTSMAAAVQPLTDAARQFLANKYKDLTK	267
		syn	
WB-CG_23	FPHELMDFLAGIEAIFSS	SDLQIPSEDAIYTFLLKRWCEQYLQTEDRHKIWSRLLPLL	275
Barley	FSDELMDFLAGIEAIFSS	TDLQTRSEDTVYSFLEWACKQYEPETERHKIWSRLLPLV	292
Brachypodium	FCDEAMNLSLAGIEAIF	SSTDIHVISEEHVFKFLLHWARTRYLPEERRKHWSSHLPLV	276
Arabidopsis_LRB1	FHDEVMLFLAGIEAIL	SSDQLQIASEDAVYDFVFKWARGQYSLEDREILGSRLLYI	345
Arabidopsis_LRB1	FHEEVMSLFLAGIEAIL	SSDELQIASEDAVYDFILKWARAQYPCLEERREILGSRLLYSI	347
Oryza_BT1	FQDEVMNFLAGIEAIL	SSNDLQVASEDAIYDFLIRWARAQYKSEERREILSRLLPLV	210
Oryza_BT2	LQDEAMNFLAGIEAIL	WSNDLQVASEDAIYDFVFKWARSQYKLEERREILGSRLLPLV	327
		Arg ³⁰⁴ His	
WB-CG_23	RFNHMSWKQLHEVLTC	SDDA--IDNEETTKRITDALLHKAYPAHEQCALAVDTA--TCWQ	331
Barley	RFSHMTWSKLHEVLTC	GDDG--VDREQTKKLITDALLHKAYPAHEQGTEDT--NCWQ	348
Brachypodium	RFSHMTGTTLQAI	LACTDVTVIDLHEELTKRVTEVLLRKYRAQLEGSIA-----AVTT	330
Arabidopsis_LRB1	RFPYMTCKRKLKVLTC	SD--FEHEVASQVLEALFFKAEAPHQRILAAEGSDSMNRR	401
Arabidopsis_LRB1	RFPYMTCKRKLKVLTC	SD--FEHEIASKLVLEALFFKAEAPHQRSLAEEASLNRR	403
Oryza_BT1	RFSHMTCKRKLKVLIC	TD---LDHEQATKCVTEALLYKADAPHQRALAADVT--TCQK	264
Oryza_BT2	RFCHMTCKRKLKVLAC	ND---LDHEQATKCVTEALLYKADAPHQRQLAADVL--TCRK	381
		Pro ³⁷⁰ Leu	
WB-CG_23	VPORAYIQKPLKVV	EFDPRPQVIVYLDLTHEECSRLFPGEFFSOLFHLAGHNFYIMPT	391
Barley	VPORAYRLKPKIVV	EFDPRCPQVIVYLDLTRECSRLFPGEHISTHFLHLAGQDFRIMAV	408
Brachypodium	TAERAYVIKPMKV	VAFDQPCQVVVYDLTRQCSRIFFSGEIIISHPHLAGQRFSLMVY	390
Arabidopsis_LRB1	FIERAYKYRPLKVV	EPELPRPQCVYLDLKRKRECGGLFPPSGRVYSQAFHLLGGQGFLLSAH	461
Arabidopsis_LRB1	LIERAYKYRPLKVV	EPELPRPQCVYLDLKRKRECGGLFPPSGRVYSQAFHLLGGQGFLLSAH	463
Oryza_BT1	FAERAYKYRPLKVV	EFDPRPYQCIAYLDLKRKRECSRLFPPSGRMYSQAFHLLGGQGFLLSAH	324
Oryza_BT2	YAERAYKYRPLKVV	EFDPRPYQCIAYLDLKRKRECSRLFPPSGRIYSQAFHLLGGQGFLLSAH	441
		CEMEDQRKLYS	
WB-CG_23	CEMEDQRKLYS	FGLWLGIDHDKPEGSTCLTFNFEFAARTKS-SGEFVLKLRDEVI	FTGDC 450
Barley	CEMD-EQDKAYS	FGLFIATAKMRGPTCLTVDFEFAARTKS-SGKFVTRWENK	YTFGGDW 466
Brachypodium	CRME-EQDEI	HISFAVLLGIHGNPRGSTMVDFEFAARTGL-SGKFVSHFGRKHT	FTTDDP 448
Arabidopsis_LRB1	CNMD-QQSFHCFGLF	LGMQ--ERGAVSFGVDYEFFAARDKSTKEEYVSKYKGNV	FTFGGK 518
Arabidopsis_LRB1	CNMD-QQSFHCFGLF	LGMQ--ERGSVVSFGVDYEFARSKE-AEDFISKYKGNV	FTFGGK 519
Oryza_BT1	CNME-QQSTFYCFGLF	LGMQ--ERGSMSVTVDYEFFAARTRE-SGEFVSKYKGNV	FTFGGK 380
Oryza_BT2	CNMD-QQSAFHCFLF	LGMQ--ERGSTSVTVDYEFFAARTRE-SGEFVSKYKGYT	FTFGGK 497
		MOGCGDLF	
WB-CG_23	MOGCGDLF	GVPWSTFLADDS-LFIDGLLHLRAALTL-VEQFGVQT	493
Barley	MLGCSDLF	VEVPWSTFIANDN-LFIDDLVHLRADLRALVAPPGLQA	510
Brachypodium	AISECEVLF	RAPWSSFIADNS-HFIDGVLHLRADITV-VEQFAVQS	491
Arabidopsis_LRB1	AVGYRNLF	GIPTWSTFIAEDSQHFINGILHLRAELTI-KRSSDLH-	561
Arabidopsis_LRB1	AVGYRNLF	GIPTWSTFIAEDSQYFINGILHLRAELTI-KRSTDP--	561
Oryza_BT1	AVGYRNLF	AIPTWSTFMADDSLFIFLDGVLHLRAELTI-KQPTV--	421
Oryza_BT2	AVGYRNLF	AIPTWSTFMADDSLFIFEGVLHLRAELTI-KQP----	536

Appendix B

B)

BTB	WB-CG_23	Barley	Brachypodium	Arabidopsis_LRB1	Arabidopsis_LRB2	Oryza_BT1
Barley	81.0 %					
Brachypodium	71.0 %	68.0 %				
Arabidopsis_LRB1	58.0 %	56.0 %	63.3 %			
Arabidopsis_LRB2	57.0 %	55.0 %	63.3 %	93.9 %		
Oryza_BT1	71.0 %	69.0 %	74.5 %	67.7 %	67.7 %	
Oryza_BT2	68.3 %	65.3 %	74.7 %	67.7 %	68.7 %	81.8 %

BACK	WB-CG_23	Barley	Brachypodium	Arabidopsis_LRB1	Arabidopsis_LRB2	Oryza_BT1
Barley	74.8 %					
Brachypodium	50.0 %	55.1 %				
Arabidopsis_LRB1	55.1 %	54.1 %	46.9 %			
Arabidopsis_LRB2	53.1 %	53.1 %	45.9 %	87.8 %		
Oryza_BT1	60.2 %	63.3 %	54.1 %	70.4 %	71.4 %	
Oryza_BT2	56.1 %	57.1 %	50.0 %	71.4 %	70.4 %	85.7 %

C-terminal region	WB-CG_23	Barley	Brachypodium	Arabidopsis_LRB1	Arabidopsis_LRB2	Oryza_BT1
Barley	65.5 %					
Brachypodium	53.6 %	50.2 %				
Arabidopsis_LRB1	44.0 %	39.6 %	41.0 %			
Arabidopsis_LRB2	43.8 %	41.2 %	40.3 %	88.7 %		
Oryza_BT1	55.3 %	51.0 %	50.7 %	69.5 %	69.2 %	
Oryza_BT2	53.9 %	51.5 %	51.2 %	71.1 %	70.6 %	91.4 %

Figure B 9: Multiple sequence alignment of the WB-CG_23 homologs

A) The complete protein sequences, that were identified as candidate homologs of the indicated plant species, were aligned using the online tool ‘Clustal Omega’ with default settings. In case of Arabidopsis, the two homologs were labelled in accordance with the literature (Christians *et al.*, 2012). The composite alignment underwent minor hand editing and the conserved amino acids were coloured in grey. Dashes denote gaps. The predicted nuclear localization signals (NLS), the ‘Bric-a-Brac/-Tramtrack/-Broad Complex (BTB) and the BACK (BTB And C-terminal Kelch) domains were indicated by a violet, red and green frame, respectively. The corresponding gene names/functions were summarized in Table R 4. The blue coloured triangles represent the presence of the indicated amino acid exchanges in allele 1 compared to allele 2 and the grey triangles the presence of a synonymous (syn) amino acid exchanges.

B) The protein sequences of the predicted BTB and BACK domains as well as of the C-terminal regions were aligned with the online tool ‘EMBOSS Needle – protein alignment’ to determine the sequences identities between the indicated homologs.

Appendix B

A)

	MYSSRRLLPRLRKKKERGPQPRSVLSTSPAGKGCWTGSGGSGDGRLLAADA	
WB-CG_28	MGIKGLTKLLAEHAPRAAAQRVEDYRGRVIAIDASLSIQFLVWVGRKGTVEVLTNEAGE	60
Aegilops	MGIKGLTKLLAEHAPRAAVQRVEDYRGRVIAIDASLSIQFLVWVGRKGTVEVLTNEAGE	60
Brachypodium	MGIKGLTKLLAEHAPRAAAQRVEDYRGRVIAIDASLSIQFLVWVGRKGTVEVLTNEAGE	60
Oryza_FEN1-B	MGIKGLTKLLAEHAPGAAVRRVEDYRGRVVAIDTSLSIQFLIVVGRKGTVEVLTNEAGE	60
Barley	MGVKGTLKLLADNAPKSMREQKFESYFGRRIAVDASMSIQFLIVVGRGTGEMTLTNEAGE	60
Arabidopsis	MGIKGLTKLLADNAPSCMKEQKFESYFGRKIAVDASMSIQFLIVVGRGTGEMTLTNEAGE	60
Oryza_FEN1-A	MGIKGLTKLLADNAPKAMKEQKFESYFGRRIAVDASMSIQFLIVVGRGTGEMTLTNEAGE	60
	**:	
WB-CG_28	VTSHLQGM LNRTVRLLEAGIKPVFVFDGEPD LKKELAKRSLKRDDAS KDLHSAIEVGD	120
Aegilops	VTSHLQGM LNRTVRLLEAGIKPVFVFDGEP PALKKELAKRSLKRDDAS KDLHSAIEIGD	120
Brachypodium	VTSHLQGM LNRTVRLLEAGIKPVFVFDGEPD LKKRELAKRSLRRDDASE DLNRAIEVGD	120
Oryza_FEN1-B	VTSHLQGM LNRTVRILEAGIKPVFVFDGEPD MKKELAKRSLKRDDG SSDLNRAIEVGD	120
Barley	VTSHLQGM FSRITRLLEAGIKPVYVFDGK PPEMKDEL LKRHAKRNEATELTKAVEAGD	120
Arabidopsis	VTSHLQGM FNRITRLLEAGIKPVYVFDGK PPELKRQELAKRYSKRADATADLTGAIEAGN	120
Oryza_FEN1-A	VTSHLQGM FNRITRLLEAGIKPVYVFDGK PDLKKQELAKRYSKREDATKELTEAVEEGD	120
	*****:	
WB-CG_28	EDSVEKFSKR TVKITKEHNDGCKRLL RLMGV PVVEAPGEAEACAS LCKNHKAYAVASED	180
Aegilops	EDSVEKFSKR TVKITKEHNDGCKRLL RLMGVPI VEAPGEAEACAS LCKNHKAYAVASED	180
Brachypodium	EDSIEKFSKR TVKITKHNDDCKLL RLMGV PVVEAPGEAEACAS LCKNHKAYAVASED	180
Oryza_FEN1-B	EDLIEKFSKR TVKVTKKHNEDCKRLL SLMGV PVVQAPGEAEACAL CKNHKVFAIASED	180
Barley	TDALIEKFSKR TVKVTQHNDCKRLL RLMGV PVVEAPCEAE SQCAALCKSDKVYAVASED	180
Arabidopsis	KEDIEKYSKR TVKVTQHNDCKRLL RLMGV PVVEATSEAEACAL CCKSGKVYGVASED	180
Oryza_FEN1-A	KDALIEKFSKR TVKVTQHNEECKRLL RLMGV PVVEAPCEAEAE CAALCINDMVYAVASED	180
	:*:	
WB-CG_28	MDTLTFGAPR FLRHVTDLSFKKSPVTEFEV PKVLEELGLTMDQFIDL CILSGCDY CENIK	240
Aegilops	MDTLTFGAPR FLRHVTDLSFKKSPVTEFEV PKVLEELGLTMDQFIDL CILSGCDY CENIK	240
Brachypodium	MDSLTFGSLR FLRHITDLSFKRSPVTEFEV PKVLEELGLTMDQFIDL CILSGCDY CENIK	240
Oryza_FEN1-B	MDSLTFGAR FLRHLDLSFKRSPVTEFEV SKVLEELGLTMDQFIDL CILSGCDY CENIK	240
Barley	MDSLTFGAPR FVRHLDMPSSRKIPVMEFEV AKILEELEFTMDQFIDL CILCGDYCDSIK	240
Arabidopsis	MDSLTFGAPK FLRHLDMPSSRKIPVMEFEV AKILEELQ LTMDFIDL CILSGDYCDSIR	240
Oryza_FEN1-A	MDSLTFGAPR FLRHLDMPSSKIPVMEFEV AKVLEELE LTMDFIDL CILSGDYCDSIK	240
	**:	
WB-CG_28	GIGGQ RALKLIRQHGCIEE VVQNLN-KRYTVPEDWPYQEVRTL FKPQPNVCTEI--PDFQW	297
Aegilops	GIGGQ RALKLIRQHGCIEE VVQNLH-KRYTVPEDWPYQEVRTL FKPQPNVCTEI--PDFQW	297
Brachypodium	GIGGQ RALKLIRQHGCIEE VVQNLN-NRFTVPEDWPYQEVRTL FKEPNVCTEI--PDFQW	297
Oryza_FEN1-B	GIGGQ RALKLIRQHG YIEE VVQNL SQT RY SVPEDWPYQEV RALFKEPNVCTDI--PDFLW	298
Barley	GIGGL TALKLIRQHGSIEG ILENINKD RYQIPEDWPYQEAR RMFKEPSVTLDI--PELKW	298
Arabidopsis	GIGGQ TALKLIRQHGSIE TLENLNKERY QIPEEWPYNEAR KLFKEPDVITDEEQLDIKW	300
Oryza_FEN1-A	GIGGQ TALKLIRQHGSIE SLENINKD RYQIPEDWPYQEAR RLFKEPNVTLDI--PELKW	298
	**** *:	
WB-CG_28	TSADKEGLVN FLAFENSFS SDRVEKAVEK IKAASDRYSPAGRAKLL TPVANLSGST---E	354
Aegilops	TSADKEGLVN FLAFENSFS SDRVEKAVEK IKAASDRYSPAGRAKLL TPVANLSGST---D	354
Brachypodium	TSVDKEGIVN FLAIENSFS SDRVEKAVQ K IKAARD RYSP-GRVKLL TPVANLSGSTI--TK	354
Oryza_FEN1-B	TPPDEEGLIN FLAAENNFSPDRV VKSVEK IKAANDK FSL-GRGKLL TPVANLTGSTSTAG	357
Barley	TAPDEEGLVN FLVKENGFS QDRVTKAIEK IKSANKSS QGRCLSHFSSQLLAHQCH---	354
Arabidopsis	TSPDEEGIVQ FLVNENGFNIDRVTKAIEK IKTAKNKSS QGRLESFFKPVANSVPAKRKG	360
Oryza_FEN1-A	NAPDEEGLVE FLVKENGFNQDRVTKAIEK IKFAKNKSS QGRLESFFKPVVSTVPLKRKD	358
	. *:	
	Ala ³⁷³ Thr	
WB-CG_28	KESKCVLGASG-QGLRSRTAVQVCSSSSSGFRYGSS--SSKPLVM-GRQ-----S	400
Aegilops	KESKCVLGASG-QGLRSRTAVQVCSSSSSGFRYGSS--SSKPLVL-GRQ-----S	400
Brachypodium	KEPECVLGSSG-QGLKSWALQVCRSSSSDFRYRSYY-SSKPLVL-GRQ-----S	401
Oryza_FEN1-B	KEPKCILGGPG-QVMKARSPLOVCKSSSLNFIHD---NSKAFML-GRR-----S	401
Barley	-----S	354
Arabidopsis	-NLICLVASEV IPNILDHRVPNACSGSIN---QPSA-IKSPCLMLLDGTPPITLLALGCS	415
Oryza_FEN1-A	-TSEKP-----S	363
WB-CG_28	GVHVKPPTFSFI-----	412
Aegilops	GVHVKPPTFSFI-----	412
Brachypodium	GFHGIPHAFSLI-----	413
Oryza_FEN1-B	GFLRISTYASI-----	412
Barley	-----	354
Arabidopsis	LYPGLP-TFRFTWLEEIPESTTKGAANKKTKGAGGRKKK	453
Oryza_FEN1-A	-----TKAVANKKTKGAGGRKKK	380

B)

N-domain	WB-CG_28	Aegilops	Brachypodium	Oryza_FEN-1 B	Barley	Arabidopsis
Aegilops	98.1 %					
Brachypodium	98.1 %	96.3 %				
Oryza_FEN-1 B	90.7 %	90.7 %	88.9 %			
Barley	68.5 %	68.5 %	67.6 %	66.7 %		
Arabidopsis	74.1 %	74.1 %	73.1 %	69.4 %	84.3 %	
Oryza_FEN-1 A	75.9 %	75.0 %	75.0 %	71.3 %	88.0 %	92.6 %

I-domain	WB-CG_28	Aegilops	Brachypodium	Oryza_FEN-1 B	Barley	Arabidopsis
Aegilops	99.3 %					
Brachypodium	93.4 %	92.7 %				
Oryza_FEN-1 B	86.1 %	85.4 %	88.3 %			
Barley	77.4 %	76.6 %	75.9 %	75.2 %		
Arabidopsis	77.4 %	76.6 %	76.6 %	77.4 %	89.1 %	
Oryza_FEN-1 A	80.3 %	79.6 %	78.8 %	80.3 %	89.1 %	87.6 %

C-terminal region	WB-CG_28	Aegilops	Brachypodium	Oryza_FEN-1 B	Barley	Arabidopsis
Aegilops	97.4 %					
Brachypodium	79.9 %	79.2 %				
Oryza_FEN-1 B	59.6 %	60.9 %	60.3 %			
Barley	30.2 %	30.2 %	28.1 %	31.6 %		
Arabidopsis	31.6 %	30.6 %	26.8 %	30.2 %	31.8 %	
Oryza_FEN-1 A	32.9 %	32.3 %	31.5 %	35.4 %	61.2 %	46.6 %

Figure B 10: Multiple sequence alignment of the WB-CG_28 homologs

A) The complete protein sequences, that were identified as candidate homologs of the indicated plant species, were aligned using the online tool 'Clustal Omega' with default settings. In case of rice the two homologs were labelled in accordance with the literature (Kimura *et al.*, 2003). The proteins of *Aegilops tauschii*, *Brachypodium distachyon* and WB-CG_28 were annotated as flap endonuclease (FEN)-1 B type proteins and the barley as well as the Arabidopsis homolog as FEN-1 A proteins, respectively. The composite alignment underwent minor hand editing and the conserved amino acids were coloured in grey. In case of differences between the conserved amino acids, the FEN-1 A conserved amino acids were coloured dark grey and FEN-1 B amino acids in light grey. Dashes denote gaps. The predicted XPG (Xeroderma Pigmentosum Complementation Group G) N-terminal domain and the XPG Internal-region were indicated by a solid red and green frame, respectively. The annotation of the I-domains of the two rice homologs was slightly longer (Kimura *et al.*, 2003) and it is indicated by dashed green frames. The blue coloured triangle represents the presence of the indicated amino acid exchange in allele 1 compared to allele 2. A mutation in the 5' untranslated region of allele 1 led to a new start codon and the respective amino acid sequence is depicted by a red triangle.

B) The protein sequences of the annotated N- and I-domains as well as of the C-terminal regions were aligned with the online tool 'EMBOSS Needle – protein alignment' to determine the sequences identities between the indicated homologs.

b) Additional tables

Table B 1: Quantification of the resistance response of the 459 barley Whealbi genotypes against the powdery mildew isolates D35/3 based on the development of macroscopic disease symptoms

Genotype	Median ¹	Resistance class ²	Genotype	Median ¹	Resistance class ²
WB-001*	75	s.	WB-050	52.5	s.
WB-002*	30	m. s.	WB-051*	25	m. r.
WB-003*	80	s.	WB-052*	0	r.
WB-004	45	m. s.	WB-053	45	m. s.
WB-005	50	m. s.	WB-054*	30	m. s.
WB-006	15	m. r.	WB-055*	25	m. r.
WB-007*	75	s.	WB-056*	20	m. r.
WB-008*	30	m. s.	WB-057	40	m. s.
WB-009*	20	m. r.	WB-058*	30	m. s.
WB-010*	20	m. r.	WB-059	50	m. s.
WB-011*	25	m. r.	WB-060*	30	m. s.
WB-012*	75	s.	WB-061*	60	s.
WB-013*	30	m. s.	WB-062	45	m. s.
WB-014*	60	s.	WB-063*	60	s.
WB-015	45	m. s.	WB-065*	0	r.
WB-016*	0	r.	WB-066*	5	m. r.
WB-017*	0	r.	WB-067	50	m. s.
WB-018*	0	r.	WB-068*	80	s.
WB-019*	0	r.	WB-069*	20	m. r.
WB-020*	77.5	s.	WB-070*	60	s.
WB-021	37.5	m. s.	WB-071	40	m. s.
WB-022*	25	m. r.	WB-072*	70	s.
WB-023*	30	m. s.	WB-073*	30	m. s.
WB-024*	25	m. r.	WB-074*	60	s.
WB-025	37.5	m. s.	WB-075*	70	s.
WB-026*	30	m. s.	WB-076*	85	s.
WB-027*	75	s.	WB-077	45	m. s.
WB-028*	30	m. s.	WB-078	50	m. s.
WB-029	50	m. s.	WB-079*	25	m. r.
WB-030	42.5	m. s.	WB-081	37.5	m. s.
WB-031*	0	r.	WB-082*	20	m. r.
WB-032	40	m. s.	WB-083	50	m. s.
WB-037	37.5	m. s.	WB-085*	5	m. r.
WB-038	45	m. s.	WB-086*	25	m. r.
WB-039*	80	s.	WB-087*	75	s.
WB-040*	30	m. s.	WB-088	50	m. s.
WB-042*	65	s.	WB-089	50	m. s.
WB-043*	0	r.	WB-090	45	m. s.
WB-044	40	m. s.	WB-091*	60	s.
WB-045*	20	m. r.	WB-092*	27.5	m. s.
WB-046	45	m. s.	WB-093*	60	s.
WB-047*	25	m. r.	WB-094*	60	s.
WB-048*	25	m. r.	WB-095	35	m. s.
WB-049*	10	m. r.	WB-097	45	m. s.

Table B 1 (continued)

Genotype	Median¹	Resistance class²	Genotype	Median¹	Resistance class²
WB-098	55	s.	WB-151*	62.5	s.
WB-099*	75	s.	WB-152*	25	m. r.
WB-101*	85	s.	WB-153*	75	s.
WB-102*	80	s.	WB-154*	80	s.
WB-103	35	m. s.	WB-155	47.5	m. s.
WB-104	75	s.	WB-156*	80	s.
WB-105*	0	r.	WB-157*	80	s.
WB-106*	15	m. r.	WB-158*	65	s.
WB-107*	0	r.	WB-159*	70	s.
WB-108	52.5	s.	WB-160*	15	m. r.
WB-109	40	m. s.	WB-161*	0	r.
WB-110*	60	s.	WB-162*	70	s.
WB-111*	75	s.	WB-163	50	m. s.
WB-112*	15	m. r.	WB-164	40	m. s.
WB-113*	60	s.	WB-165*	30	m. s.
WB-114*	70	s.	WB-166*	75	s.
WB-115	10	m. r.	WB-167*	5	m. r.
WB-116*	60	s.	WB-168*	20	m. r.
WB-117	50	m. s.	WB-169*	67.5	s.
WB-119*	75	s.	WB-170*	70	s.
WB-120*	0	r.	WB-171	35	m. s.
WB-121*	30	m. s.	WB-173	50	m. s.
WB-123*	25	m. r.	WB-174	50	m. s.
WB-124	0	r.	WB-175*	30	m. s.
WB-125	45	m. s.	WB-176	52.5	s.
WB-126*	15	m. r.	WB-177*	0	r.
WB-127	50	m. s.	WB-178	55	s.
WB-128*	75	s.	WB-179	50	m. s.
WB-129	50	m. s.	WB-181*	60	s.
WB-130*	70	s.	WB-182*	80	s.
WB-131*	80	s.	WB-183*	75	s.
WB-133*	20	m. r.	WB-184	45	m. s.
WB-135*	75	s.	WB-185*	30	m. s.
WB-136*	25	m. r.	WB-186*	60	s.
WB-138*	75	s.	WB-187*	70	s.
WB-139	50	m. s.	WB-188*	75	s.
WB-140	50	m. s.	WB-189*	25	m. r.
WB-141	50	m. s.	WB-190*	60	s.
WB-142*	80	s.	WB-191*	60	s.
WB-143*	85	s.	WB-192*	25	m. r.
WB-144*	85	s.	WB-193*	20	m. r.
WB-145	50	m. s.	WB-194*	25	m. r.
WB-146	35	m. s.	WB-195*	75	s.
WB-147*	30	m. s.	WB-196*	75	s.
WB-148*	10	m. r.	WB-197	47.5	m. s.
WB-149*	70	s.	WB-198	50	m. s.
WB-150	20	m. r.	WB-199*	60	s.

Table B 1 (continued)

Genotype	Median¹	Resistance class²	Genotype	Median¹	Resistance class²
WB-200*	65	s.	WB-249*	85	s.
WB-201*	60	s.	WB-250*	85	s.
WB-202	50	m. s.	WB-252*	80	s.
WB-203*	75	s.	WB-253*	70	s.
WB-204*	10	m. r.	WB-256	45	m. s.
WB-205	0	r.	WB-258*	65	s.
WB-206*	75	s.	WB-259*	12.5	m. r.
WB-207	50	m. s.	WB-260*	80	s.
WB-208*	75	s.	WB-261*	75	s.
WB-209	50	m. s.	WB-262*	30	m. s.
WB-210*	70	s.	WB-263*	30	m. s.
WB-211*	70	s.	WB-264	55	s.
WB-212	70	s.	WB-265	60	s.
WB-213	32.5	m. s.	WB-266	30	m. s.
WB-214*	15	m. r.	WB-267	50	m. s.
WB-215	45	m. s.	WB-269*	80	s.
WB-216	50	m. s.	WB-270*	65	s.
WB-217*	25	m. r.	WB-271	30	m. s.
WB-218*	70	s.	WB-272	45	m. s.
WB-219*	0	r.	WB-273*	75	s.
WB-220*	75	s.	WB-274*	85	s.
WB-221	55	s.	WB-275	60	s.
WB-222*	70	s.	WB-276*	70	s.
WB-223	50	m. s.	WB-277*	85	s.
WB-224*	60	s.	WB-279*	17.5	m. r.
WB-225	50	m. s.	WB-280*	30	m. s.
WB-226*	0	r.	WB-281*	15	m. r.
WB-227*	80	s.	WB-282*	30	m. s.
WB-228*	10	m. r.	WB-283	55	s.
WB-229*	60	s.	WB-284	55	s.
WB-230	55	s.	WB-285	50	m. s.
WB-232*	65	s.	WB-286	50	m. s.
WB-233	50	m. s.	WB-287*	85	s.
WB-234	60	s.	WB-288	50	m. s.
WB-235	40	m. s.	WB-289	55	s.
WB-236*	70	s.	WB-290*	75	s.
WB-237*	75	s.	WB-291	32.5	m. s.
WB-238	0	r.	WB-292	50	m. s.
WB-239	60	s.	WB-293	35	m. s.
WB-240	50	m. s.	WB-294	50	m. s.
WB-241*	70	s.	WB-295	32.5	m. s.
WB-242*	70	s.	WB-297*	72.5	s.
WB-243	50	m. s.	WB-298	50	m. s.
WB-244*	75	s.	WB-299*	85	s.
WB-245	55	s.	WB-300*	75	s.
WB-246	52.5	s.	WB-301*	75	s.
WB-247*	25	m. r.	WB-302*	10	m. r.
WB-248	50	m. s.	WB-303	55	s.

Table B 1 (continued)

Genotype	Median¹	Resistance class²	Genotype	Median¹	Resistance class²
WB-305*	0	r.	WB-354	60	s.
WB-306*	0	r.	WB-355*	75	s.
WB-307*	0	r.	WB-356*	75	s.
WB-308*	0	r.	WB-357*	70	s.
WB-309	60	s.	WB-358*	0	r.
WB-310	12.5	m. r.	WB-359	40	m. s.
WB-311*	75	s.	WB-360*	75	s.
WB-312*	70	s.	WB-361	40	m. s.
WB-313*	15	m. r.	WB-363*	70	s.
WB-314*	75	s.	WB-364	40	m. s.
WB-315*	65	s.	WB-365*	27.5	m. s.
WB-316*	75	s.	WB-366	47.5	m. s.
WB-317*	75	s.	WB-367	40	m. s.
WB-318	50	m. s.	WB-368	0	r.
WB-319*	30	m. s.	WB-370*	20	m. r.
WB-320*	27.5	m. s.	WB-371	50	m. s.
WB-321*	80	s.	WB-372*	25	m. r.
WB-322	50	m. s.	WB-374*	30	m. s.
WB-323	45	m. s.	WB-375	45	m. s.
WB-324*	75	s.	WB-376*	70	s.
WB-325*	65	s.	WB-377*	20	m. r.
WB-326	50	m. s.	WB-378*	15	m. r.
WB-327*	85	s.	WB-379	50	m. s.
WB-328	20	m. r.	WB-380	60	s.
WB-329*	85	s.	WB-381	35	m. s.
WB-330*	20	m. r.	WB-382	45	m. s.
WB-331	60	s.	WB-383	40	m. s.
WB-332	10	m. r.	WB-384	25	m. r.
WB-333*	75	s.	WB-385*	0	r.
WB-334	10	m. r.	WB-386	45	m. s.
WB-335	55	s.	WB-387	50	m. s.
WB-336	60	s.	WB-388*	80	s.
WB-337	55	s.	WB-390	25	m. r.
WB-338	50	m. s.	WB-391*	62.5	s.
WB-340*	30	m. s.	WB-392*	30	m. s.
WB-341	50	m. s.	WB-393	50	m. s.
WB-342	45	m. s.	WB-394	50	m. s.
WB-343	57.5	s.	WB-395	55	s.
WB-344	47.5	m. s.	WB-396	35	m. s.
WB-345	50	m. s.	WB-397*	25	m. r.
WB-346*	75	s.	WB-398	50	m. s.
WB-347	40	m. s.	WB-399	50	m. s.
WB-348	35	m. s.	WB-400*	20	m. r.
WB-349*	25	m. r.	WB-401*	25	m. r.
WB-350*	30	m. s.	WB-402	35	m. s.
WB-351*	22.5	m. r.	WB-403	40	m. s.
WB-352*	0	r.	WB-404	47.5	m. s.
WB-353	37.5	m. s.	WB-405	52.5	s.

Table B 1 (continued)

Genotype	Median ¹	Resistance class ²	Genotype	Median ¹	Resistance class ²
WB-406*	12.5	m. r.	WB-450*	15	m. r.
WB-407	50	m. s.	WB-451	50	m. s.
WB-408	40	m. s.	WB-452	45	m. s.
WB-409	25	m. r.	WB-453	47.5	m. s.
WB-410	50	m. s.	WB-454*	70	s.
WB-411*	30	m. s.	WB-455	60	s.
WB-413*	30	m. s.	WB-456*	30	m. s.
WB-414	42.5	m. s.	WB-457*	80	s.
WB-415*	25	m. r.	WB-458*	20	m. r.
WB-416	45	m. s.	WB-459	50	m. s.
WB-417	40	m. s.	WB-460*	25	m. r.
WB-418	55	s.	WB-461*	0	r.
WB-419*	77.5	s.	WB-462*	10	m. r.
WB-420	60	s.	WB-463	50	m. s.
WB-421	40	m. s.	WB-464	50	m. s.
WB-422	60	s.	WB-465*	15	m. r.
WB-423*	30	m. s.	WB-466*	0	r.
WB-424*	75	s.	WB-467*	27.5	m. s.
WB-425*	75	s.	WB-468*	0	r.
WB-426	47.5	m. s.	WB-469*	72.5	s.
WB-427*	75	s.	WB-470	45	m. s.
WB-428*	30	m. s.	WB-472*	20	m. r.
WB-429*	70	s.	WB-473*	20	m. r.
WB-430*	70	s.	WB-474*	0	r.
WB-431	50	m. s.	WB-475	47.5	m. s.
WB-432	60	s.	WB-476*	0	r.
WB-433*	25	m. r.	WB-477	52.5	s.
WB-434	10	m. r.	WB-478*	25	m. r.
WB-435*	70	s.	WB-483*	0	r.
WB-437	50	m. s.	WB-485	40	m. s.
WB-438	50	m. s.	WB-486*	30	m. s.
WB-439	50	m. s.	WB-490*	30	m. s.
WB-440*	30	m. s.	WB-497	40	m. s.
WB-441	35	m. s.	WB-498	12.5	m. r.
WB-442*	15	m. r.	WB-499*	0	r.
WB-443	47.5	m. s.	WB-500	32.5	m. s.
WB-444	20	m. r.	WB-501*	80	s.
WB-445	50	m. s.	WB-505	60	s.
WB-446*	20	m. r.	WB-506	50	m. s.
WB-447	45	m. s.	WB-510*	0	r.
WB-448	55	s.	WB-512	80	s.
WB-449*	22.5	m. r.			

¹ macroscopic disease symptoms represented as median value of the infected leaf area (in %)

² resistance classes according to Table M 3: r. – resistant; m. r. – moderate resistant; m. s. – moderate susceptible; s. – susceptible

* genotypes selected for the detached leaf assay with two powdery mildew isolates

Table B 2: Quantification of the resistance response of the 267 barley Whealbi genotypes against the powdery mildew isolates D35/3 and RiIII based on the development of macroscopic disease symptoms

Genotype	D35/3			RiIII			<i>Max</i> ⁴	<i>Max BLUE</i> ⁵	Resistance class ⁶
	\emptyset ¹	SD ²	BLUE ³	\emptyset	SD	BLUE			
WB-001	73.5	10.4	72.4	80.6	8.9	77.4	80.6	77.4	s.
WB-002	44.7	18.5	45.2	45.9	20.2	41.2	45.9	45.2	m. s.
WB-003	62.0	15.8	61.1	63.0	8.7	59.4	63.0	61.1	s.
WB-007	61.8	17.0	60.9	58.5	20.0	55.3	61.8	60.9	s.
WB-008	36.5	12.0	38.6	29.7	8.3	32.2	36.5	38.6	m. s.
WB-009	28.6	7.1	28.3	29.2	8.7	34.5	29.2	34.5	m. s.
WB-010	37.4	17.8	35.4	39.4	14.8	44.9	39.4	44.9	m. s.
WB-011	32.9	8.4	37.7	41.5	7.1	40.5	41.5	40.5	m. s.
WB-012	55.0	15.5	54.7	60.3	13.1	57.0	60.3	57.0	s.
WB-013	48.3	19.9	49.8	57.1	18.0	57.1	57.1	57.1	s.
WB-014	57.2	12.6	57.6	53.7	10.5	52.4	57.2	57.6	s.
WB-016 ⁸	0.0	0.0	NA ⁷	0.0	0.0	NA	0.0	NA	r.
WB-017 ⁸	0.0	0.0	NA	0.0	0.0	NA	0.0	NA	r.
WB-018 ⁸	0.0	0.0	NA	0.0	0.0	NA	0.0	NA	r.
WB-019 ⁸	1.5	2.2	NA	0.0	0.0	NA	1.5	NA	r.
WB-020	61.3	13.4	60.0	55.3	18.1	59.3	61.3	60.0	s.
WB-022	44.4	18.6	46.2	54.0	23.5	53.3	54.0	53.3	s.
WB-023 ⁹	43.7	17.3	NA	43.7	12.8	NA	43.7	NA	m. s.
WB-024	36.5	13.4	36.9	43.2	18.6	42.7	43.2	42.7	m. s.
WB-026	31.6	10.7	31.8	31.4	17.2	34.4	31.6	34.4	m. s.
WB-027	60.1	9.4	59.0	60.9	9.6	64.3	60.9	64.3	s.
WB-028	42.3	17.8	42.1	53.2	20.8	48.3	53.2	48.3	s.
WB-031	43.0	12.2	38.6	45.9	15.6	39.7	45.9	39.7	m. s.
WB-039	62.2	11.6	62.9	55.7	18.0	52.9	62.2	62.9	s.
WB-040 ⁺	36.5	24.6	38.1	47.9	23.5	44.1	47.9	44.1	m. s.
WB-042 ⁺⁺	39.2	19.3	38.9	37.9	22.1	42.3	39.2	42.3	m. s.
WB-043 [*]	0.0	0.0	NA	0.0	0.0	NA	0.0	NA	r.
WB-045	26.6	11.6	26.8	40.1	15.3	37.3	40.1	37.3	m. s.
WB-047	29.2	8.7	29.5	52.8	24.6	47.6	52.8	47.6	s.
WB-048 ⁺	40.5	18.9	40.7	29.0	21.7	28.1	40.5	40.7	m. s.
WB-049 ⁺⁺	10.6	9.9	14.6	8.3	7.4	20.3	10.6	20.3	m. r.
WB-051	23.7	16.9	28.6	54.1	12.6	52.6	54.1	52.6	s.
WB-052 [*]	8.2	9.4	8.0	0.0	0.0	4.8	8.2	8.0	m. r.
WB-054 [*]	24.2	6.9	24.9	22.1	7.9	21.3	24.2	24.9	m. r.
WB-055 [*]	29.7	23.5	30.4	27.7	30.8	26.9	29.7	30.4	m. s.
WB-056	11.9	9.7	15.9	0.0	0.0	-0.4	11.9	15.9	m. r.
WB-058 [*]	25.3	11.9	27.2	29.0	19.1	37.5	29.0	37.5	m. s.
WB-060 ⁺	20.3	12.3	23.3	23.4	13.9	28.2	23.4	28.2	m. r.
WB-061 ⁺	50.7	15.3	49.7	58.3	14.8	55.0	58.3	55.0	s.
WB-063	51.9	16.2	50.5	42.0	12.5	45.7	51.9	50.5	s.
WB-065 ^{10*}	0.0	0.0	NA	0.0	0.0	NA	0.0	NA	r.
WB-066 [*]	13.4	11.1	15.8	18.5	17.5	25.8	18.5	25.8	m. r.
WB-068 ⁹	63.1	12.9	NA	57.8	14.9	NA	63.1	NA	s.
WB-069 [*]	29.3	15.3	30.5	38.2	15.7	37.9	38.2	37.9	m. s.
WB-070 [*]	42.7	14.6	41.9	49.5	16.7	45.7	49.5	45.7	m. s.
WB-072 ⁹	59.9	10.8	NA	64.2	14.1	NA	64.2	NA	s.
WB-073 ⁹	26.8	10.6	NA	38.6	14.9	NA	38.6	NA	m. s.

Table B 2 (continued)

Genotype	D35/3			RiIII			Max ⁴	Max BLUE ⁵	Resistance class ⁶
	Ø ¹	SD ²	BLUE ³	Ø	SD	BLUE			
WB-074*	46.7	15.8	45.3	52.2	14.8	48.4	52.2	48.4	s.
WB-075 ⁹	49.3	20.3	NA	28.2	21.4	NA	49.3	NA	m. s.
WB-076 ⁹	64.3	13.2	NA	60.4	12.6	NA	64.3	NA	s.
WB-079 ⁹	30.6	18.2	NA	43.9	18.6	NA	43.9	NA	m. s.
WB-082 ⁹	18.7	14.5	NA	1.1	2.1	NA	18.7	NA	m. r.
WB-085 ⁹	34.7	22.8	NA	54.8	18.8	NA	54.8	NA	s.
WB-086 ⁹	33.7	14.8	NA	46.4	19.1	NA	46.4	NA	m. s.
WB-087 ⁹	54.3	16.7	NA	13.6	14.3	NA	54.3	NA	s.
WB-091	50.2	12.8	49.0	33.6	11.0	37.3	50.2	49.0	m. s.
WB-092 ⁹	50.3	20.5	NA	53.1	21.6	NA	53.1	NA	s.
WB-093 ⁹	61.9	13.9	NA	51.1	14.1	NA	61.9	NA	s.
WB-094*	32.9	21.6	34.0	30.3	15.8	27.4	32.9	34.0	m. s.
WB-099	45.4	27.5	54.4	34.0	30.5	37.0	45.4	54.4	m. s.
WB-101*	71.7	8.0	70.8	68.1	11.2	64.4	71.7	70.8	s.
WB-102*	34.0	27.5	34.7	32.4	13.7	27.8	34.0	34.7	m. s.
WB-105 ⁸	0.0	0.0	NA	0.0	0.0	NA	0.0	NA	r.
WB-106	24.0	24.3	25.7	36.5	24.0	34.1	36.5	34.1	m. s.
WB-107 ⁸	0.0	0.0	NA	0.0	0.0	NA	0.0	NA	r.
WB-110 ⁹	56.8	14.8	NA	55.2	17.4	NA	56.8	NA	s.
WB-111	57.8	15.5	56.8	57.1	7.5	53.4	57.8	56.8	s.
WB-112 ⁹	27.5	16.8	NA	24.2	13.0	NA	27.5	NA	m. s.
WB-113*	50.3	14.4	50.0	54.8	12.1	51.7	54.8	51.7	s.
WB-114	50.5	14.0	49.8	47.9	10.0	44.0	50.5	49.8	m. s.
WB-116 ⁹	47.3	12.8	NA	50.4	12.8	NA	50.4	NA	m. s.
WB-119	65.7	10.0	64.7	74.0	10.3	68.2	74.0	68.2	s.
WB-120	0.0	0.0	7.0	43.1	29.6	45.9	43.1	45.9	m. s.
WB-121	50.7	22.2	49.5	69.1	9.5	65.2	69.1	65.2	s.
WB-123	34.1	11.3	35.3	43.2	20.8	42.7	43.2	42.7	m. s.
WB-126	32.2	21.5	29.7	48.9	12.5	45.3	48.9	45.3	m. s.
WB-128	65.0	11.2	64.2	64.2	9.6	62.0	65.0	64.2	s.
WB-130 ⁺	46.1	17.3	47.1	31.0	18.4	29.7	46.1	47.1	m. s.
WB-131	67.1	9.2	55.9	55.7	18.9	52.3	67.1	55.9	s.
WB-133 ⁺	29.9	12.5	29.6	37.8	9.6	34.9	37.8	34.9	m. s.
WB-135 ⁺⁺	65.6	12.6	64.8	66.6	11.6	63.0	66.6	64.8	s.
WB-136 ⁹	49.5	21.7	NA	47.6	20.1	NA	49.5	NA	m. s.
WB-137*	13.1	10.3	9.3	8.0	7.9	4.3	13.1	9.3	m. r.
WB-138 ⁺⁺	51.0	19.6	50.5	53.1	11.5	47.0	53.1	50.5	s.
WB-142 ⁺	49.4	13.1	48.4	66.0	18.2	63.2	66.0	63.2	s.
WB-143 ⁺	67.1	10.3	66.4	70.8	7.1	66.9	70.8	66.9	s.
WB-144 ⁺⁺	64.6	10.6	65.4	62.9	10.6	60.2	64.6	65.4	s.
WB-147 ⁺⁺	39.2	15.1	39.5	48.6	13.0	47.9	48.6	47.9	m. s.
WB-148 ⁺	16.3	19.4	16.8	31.6	30.5	29.7	31.6	29.7	m. s.
WB-149*	52.8	14.5	52.1	52.6	11.2	56.6	52.8	56.6	s.
WB-151*	59.2	12.8	57.1	59.4	18.2	58.0	59.4	58.0	s.
WB-152 ⁺⁺	23.8	12.5	23.8	18.7	13.2	24.2	23.8	24.2	m. r.
WB-153 ⁺⁺	56.8	21.5	56.4	53.9	17.8	58.3	56.8	58.3	s.
WB-154 ⁺	61.5	12.5	60.2	56.6	10.3	60.3	61.5	60.3	s.
WB-156 ⁺⁺	65.8	9.2	65.1	68.9	6.4	63.4	68.9	65.1	s.
WB-157 ⁺⁺	73.9	4.5	64.1	66.4	25.0	64.5	73.9	64.5	s.

Table B 2 (continued)

Genotype	D35/3			RiIII			Max ⁴	Max BLUE ⁵	Resistance class ⁶
	Ø ¹	SD ²	BLUE ³	Ø	SD	BLUE			
WB-158*	61.9	12.3	54.7	58.2	23.5	55.0	61.9	55.0	s.
WB-159	63.6	15.6	62.2	51.6	20.5	56.2	63.6	62.2	s.
WB-160	21.5	17.4	21.0	28.0	11.4	32.5	28.0	32.5	m. s.
WB-161*	10.3	14.5	21.8	11.1	15.5	15.6	11.1	21.8	m. r.
WB-162	50.9	19.1	49.5	35.9	18.4	40.3	50.9	49.5	m. s.
WB-165*	39.8	14.8	39.4	37.0	17.3	41.5	39.8	41.5	m. s.
WB-166*	64.4	9.6	63.4	63.6	9.8	60.4	64.4	63.4	s.
WB-167	19.2	16.6	21.0	35.9	21.4	36.4	35.9	36.4	m. s.
WB-168*	39.2	17.7	38.7	39.8	24.1	37.2	39.8	38.7	m. s.
WB-169*	68.2	7.8	67.4	69.5	8.5	66.9	69.5	67.4	s.
WB-170*	55.4	9.9	55.6	53.8	12.6	50.9	55.4	55.6	s.
WB-175	38.3	14.2	38.8	54.9	14.7	52.3	54.9	52.3	s.
WB-177 ¹⁰	0.3	0.9	NA	57.3	10.6	NA	57.3	NA	s.
WB-181*	57.8	10.1	57.9	57.1	18.0	54.5	57.8	57.9	s.
WB-182 ⁹	61.0	20.1	NA	4.2	4.1	NA	61.0	NA	s.
WB-183*	54.4	12.8	54.9	54.5	9.3	57.9	54.5	57.9	s.
WB-185	34.1	16.4	36.4	2.8	3.1	9.4	34.1	36.4	m. s.
WB-186*	52.5	12.2	48.0	50.5	21.1	46.7	52.5	48.0	s.
WB-187*	52.5	17.2	51.8	50.7	17.7	54.3	52.5	54.3	s.
WB-188*	52.6	18.3	52.4	59.2	18.6	61.3	59.2	61.3	s.
WB-189	41.9	17.7	44.1	58.6	12.6	59.7	58.6	59.7	s.
WB-190 ⁹	41.8	14.1	NA	39.3	17.3	NA	41.8	NA	m. s.
WB-191	46.1	12.7	44.9	5.9	4.5	1.9	46.1	44.9	m. s.
WB-192	19.1	9.9	22.4	39.1	18.7	40.3	39.1	40.3	m. s.
WB-193*	40.7	18.8	38.7	37.6	16.8	42.9	40.7	42.9	m. s.
WB-194	24.2	13.0	24.9	60.2	17.1	59.6	60.2	59.6	s.
WB-195	45.8	15.0	48.6	31.7	18.2	34.4	45.8	48.6	m. s.
WB-196*	53.4	14.6	54.6	47.3	12.6	44.0	53.4	54.6	s.
WB-199	60.5	13.4	59.0	47.6	22.2	51.7	60.5	59.0	s.
WB-200	49.6	18.7	48.2	56.9	15.3	60.3	56.9	60.3	s.
WB-201*	62.0	9.3	58.7	65.2	11.9	62.5	65.2	62.5	s.
WB-203*	43.6	18.3	43.0	39.4	12.8	37.4	43.6	43.0	m. s.
WB-204	22.4	14.9	21.9	47.8	13.3	52.9	47.8	52.9	m. s.
WB-206*	48.9	17.4	48.5	47.9	14.2	44.0	48.9	48.5	m. s.
WB-208	60.4	10.3	59.8	34.2	12.8	37.9	60.4	59.8	s.
WB-210*	56.7	11.4	57.9	56.9	14.6	53.7	56.9	57.9	s.
WB-211*	58.1	15.4	55.7	60.4	10.5	56.5	60.4	56.5	s.
WB-214	26.0	13.1	23.9	29.6	11.2	34.9	29.6	34.9	m. s.
WB-217	22.7	11.2	25.9	58.6	11.1	59.9	58.6	59.9	s.
WB-218	47.3	16.2	46.5	59.5	11.2	54.8	59.5	54.8	s.
WB-219 ⁸	0.0	0.0	NA	0.0	0.0	NA	0.0	NA	r.
WB-220*	66.1	13.2	65.4	59.6	10.7	56.4	66.1	65.4	s.
WB-222*	60.1	7.8	59.2	56.2	9.3	52.4	60.1	59.2	s.
WB-224*	51.7	17.7	50.7	46.7	17.4	41.6	51.7	50.7	s.
WB-226 ^{10*}	0.0	0.0	NA	0.0	0.0	NA	0.0	NA	r.
WB-227*	65.4	13.8	64.4	60.5	17.0	61.5	65.4	64.4	s.
WB-228	23.3	16.7	25.9	54.7	17.2	55.9	54.7	55.9	s.
WB-229	41.0	16.5	43.1	24.6	22.8	27.5	41.0	43.1	m. s.
WB-232*	56.8	13.6	55.8	50.2	18.8	47.0	56.8	55.8	s.

Appendix B

Table B 2 (continued)

Genotype	D35/3			RiIII			Max ⁴	Max BLUE ⁵	Resistance class ⁶
	Ø ¹	SD ²	BLUE ³	Ø	SD	BLUE			
WB-236	56.7	16.4	56.1	52.9	14.2	56.3	56.7	56.3	s.
WB-237	61.8	12.4	61.2	50.8	13.7	49.2	61.8	61.2	s.
WB-241*	40.6	23.1	40.1	41.8	19.2	37.6	41.8	40.1	m. s.
WB-242 ⁺	41.8	11.8	39.7	48.3	12.8	45.2	48.3	45.2	m. s.
WB-244	69.0	9.8	66.5	53.4	23.0	57.1	69.0	66.5	s.
WB-247	46.9	26.0	49.3	49.4	20.7	46.2	49.4	49.3	m. s.
WB-249	63.5	13.1	62.4	65.6	13.6	62.4	65.6	62.4	s.
WB-250*	72.9	8.5	71.9	72.0	10.2	68.7	72.9	71.9	s.
WB-252	50.5	29.6	52.1	29.8	32.0	38.7	50.5	52.1	m.s.
WB-253*	45.8	21.2	40.9	36.7	20.3	32.0	45.8	40.9	m. s.
WB-258*	57.5	13.8	57.0	63.9	11.2	59.2	63.9	59.2	s.
WB-259*	36.1	19.9	35.5	40.1	16.3	38.3	40.1	38.3	m. s.
WB-260	61.6	17.5	61.5	34.2	17.1	31.0	61.6	61.5	s.
WB-261*	60.2	14.8	58.7	57.4	20.0	55.7	60.2	58.7	s.
WB-262	20.8	17.3	22.6	21.0	18.6	27.7	21.0	27.7	m. r.
WB-263*	21.9	22.7	24.9	16.5	19.3	19.6	21.9	24.9	m. r.
WB-269*	56.7	17.0	55.2	57.1	16.1	61.0	57.1	61.0	s.
WB-270*	59.3	9.3	58.5	58.0	15.9	61.6	59.3	61.6	s.
WB-273	62.5	16.2	63.4	51.0	18.6	49.7	62.5	63.4	s.
WB-274*	67.2	13.9	66.7	66.2	8.2	62.1	67.2	66.7	s.
WB-276	64.2	8.7	60.6	69.5	8.3	68.9	69.5	68.9	s.
WB-277	57.4	12.7	55.8	49.3	14.4	46.2	57.4	55.8	s.
WB-279*	32.3	22.0	34.1	38.3	20.7	37.5	38.3	37.5	m. s.
WB-280*	48.2	19.4	47.9	50.9	17.8	48.3	50.9	48.3	m. s.
WB-281*	27.4	11.2	30.4	27.6	12.2	28.6	27.6	30.4	m. s.
WB-282*	44.8	17.2	44.9	46.1	18.0	45.7	46.1	45.7	m. s.
WB-287*	71.6	5.3	70.6	62.3	9.5	59.5	71.6	70.6	s.
WB-290*	59.3	16.7	58.0	59.1	15.7	62.9	59.3	62.9	s.
WB-297*	46.5	29.2	54.6	38.7	21.9	45.3	46.5	54.6	m.s.
WB-299	42.1	21.2	45.3	28.8	14.4	32.9	42.1	45.3	m. s.
WB-300*	69.1	11.5	68.0	69.7	7.5	66.0	69.7	68.0	s.
WB-301 ⁹	54.6	17.3	NA	41.0	13.5	NA	54.6	NA	s.
WB-302*	38.1	11.7	38.7	42.7	17.0	42.1	42.7	42.1	m. s.
WB-305 ^{3*}	0.0	0.0	NA	0.0	0.0	NA	0.0	NA	r.
WB-306	0.0	0.0	-0.7	22.0	10.6	19.0	22.0	19.0	m. r.
WB-307 ^{10*}	0.0	0.0	NA	0.0	0.0	NA	0.0	NA	r.
WB-308	0.0	0.0	-0.3	14.2	11.4	9.7	14.2	9.7	m. r.
WB-311*	61.5	9.4	60.5	59.1	15.4	62.7	61.5	62.7	s.
WB-312	60.4	19.8	60.2	49.6	26.4	54.0	60.4	60.2	s.
WB-313 ⁹	33.5	23.4	NA	65.0	11.0	NA	65.0	NA	s.
WB-314 ⁹	51.2	22.7	NA	37.5	25.5	NA	51.2	NA	s.
WB-315*	62.4	11.4	62.6	60.6	10.4	57.9	62.4	62.6	s.
WB-316	60.0	11.8	58.7	7.8	4.4	12.1	60.0	58.7	s.
WB-317	61.2	11.9	61.9	65.6	11.3	62.9	65.6	62.9	s.
WB-319*	40.9	17.7	42.3	42.0	19.0	39.3	42.0	42.3	m. s.
WB-320*	39.9	13.9	39.9	47.8	10.0	46.8	47.8	46.8	m. s.
WB-321 ⁺	64.3	12.3	65.1	53.3	15.3	50.5	64.3	65.1	s.
WB-324	52.2	17.7	53.4	50.4	15.7	47.7	52.2	53.4	s.
WB-325*	57.8	9.0	58.6	56.0	16.1	54.7	57.8	58.6	s.

Table B 2 (continued)

Genotype	D35/3			RiIII			Max ⁴	Max BLUE ⁵	Resistance class ⁶
	Ø ¹	SD ²	BLUE ³	Ø	SD	BLUE			
WB-327	64.0	9.3	59.2	55.8	21.5	58.4	64.0	59.2	s.
WB-329	73.3	14.9	71.8	72.4	12.6	75.1	73.3	75.1	s.
WB-330 ⁹	42.1	26.8	NA	68.2	14.0	NA	68.2	NA	s.
WB-333	73.7	4.9	69.1	58.9	15.9	55.7	73.7	69.1	s.
WB-340	54.9	21.8	55.6	68.8	14.4	68.3	68.8	68.3	s.
WB-346*	73.6	6.6	72.4	77.7	7.0	71.7	77.7	72.4	s.
WB-349	42.5	11.7	42.9	47.0	16.1	46.0	47.0	46.0	m. s.
WB-350	40.0	18.3	41.6	57.1	20.0	57.1	57.1	57.1	s.
WB-351	48.2	22.5	49.9	38.2	24.3	37.7	48.2	49.9	m. s.
WB-352 ^{8*}	0.0	0.0	NA	0.0	0.0	NA	0.0	NA	r.
WB-355*	64.9	12.9	63.9	57.3	11.0	54.0	64.9	63.9	s.
WB-356	61.4	13.3	59.5	68.9	6.9	65.6	68.9	65.6	s.
WB-357	59.8	14.8	59.1	64.3	11.1	64.6	64.3	64.6	s.
WB-358 ^{8*}	0.3	0.9	NA	1.2	1.9	NA	1.2	NA	r.
WB-360	52.9	16.0	52.0	50.7	19.3	49.4	52.9	52.0	s.
WB-363	60.6	20.1	59.7	46.2	19.1	42.4	60.6	59.7	s.
WB-365 ⁺	24.9	8.0	26.3	27.1	17.4	23.4	27.1	26.3	m. s.
WB-369 ^{9*}	38.2	16.1	NA	42.3	11.7	NA	42.3	NA	m. s.
WB-370	24.2	19.7	23.4	34.9	9.8	34.1	34.9	34.1	m. s.
WB-372	17.1	8.8	17.1	0.0	0.0	-1.1	17.1	17.1	m. r.
WB-374	29.5	17.2	30.2	62.3	21.1	63.2	62.3	63.2	s.
WB-376*	61.9	8.1	58.0	57.7	10.3	54.4	61.9	58.0	s.
WB-377*	35.0	12.8	37.1	40.3	15.2	39.6	40.3	39.6	m. s.
WB-378 ⁹	34.4	15.0	NA	49.4	17.1	NA	49.4	NA	m. s.
WB-385 ¹⁰	0.0	0.0	NA	0.0	0.0	NA	0.0	NA	r.
WB-388 ⁹	72.0	4.3	NA	66.5	14.2	NA	72.0	NA	s.
WB-391 ⁹	52.7	13.0	NA	53.0	18.9	NA	53.0	NA	s.
WB-392 ⁹	37.2	15.9	NA	46.4	16.3	NA	46.4	NA	m. s.
WB-397 ⁹	10.8	11.1	NA	19.7	14.1	NA	19.7	NA	m. r.
WB-400*	24.9	17.0	27.9	28.5	16.2	31.3	28.5	31.3	m. s.
WB-401	17.5	11.6	17.6	6.0	6.7	6.3	17.5	17.6	m. r.
WB-406 ⁹	41.4	19.4	NA	41.2	23.0	NA	41.4	NA	m. s.
WB-411 ⁹	40.4	17.9	NA	44.8	21.4	NA	44.8	NA	m. s.
WB-413 ⁹	31.6	19.5	NA	29.0	18.9	NA	31.6	NA	m. s.
WB-415 ⁹	45.4	21.3	NA	46.0	17.3	NA	46.0	NA	m. s.
WB-419 ⁹	50.9	19.7	NA	47.9	17.8	NA	50.9	NA	m. s.
WB-423 ⁹	40.4	13.8	NA	45.0	15.6	NA	45.0	NA	m. s.
WB-424	63.7	14.0	64.4	57.9	21.4	56.7	63.7	64.4	s.
WB-425 ⁹	63.6	8.6	NA	61.7	9.7	NA	63.6	NA	s.
WB-427	61.3	16.4	60.1	43.9	17.0	49.0	61.3	60.1	s.
WB-428	37.1	14.1	37.7	29.4	12.4	28.4	37.1	37.7	m. s.
WB-429 ⁹	43.6	19.6	NA	27.5	11.1	NA	43.6	NA	m. s.
WB-430 ⁹	61.1	12.8	NA	60.3	12.0	NA	61.1	NA	s.
WB-433 ⁹	44.1	17.9	NA	43.3	16.0	NA	44.1	NA	m. s.
WB-435 ⁹	50.9	14.2	NA	37.6	13.1	NA	50.9	NA	m. s.
WB-440 ⁹	28.3	10.5	NA	29.6	14.6	NA	29.6	NA	m. s.
WB-442 ⁹	24.8	11.4	NA	29.0	8.2	NA	29.0	NA	m. s.
WB-446	36.0	16.7	36.6	48.9	15.6	46.0	48.9	46.0	m. s.
WB-449	39.2	19.1	39.2	45.6	21.0	47.1	45.6	47.1	m. s.

Table B 2 (continued)

Genotype	D35/3			RiIII			Max ⁴	Max BLUE ⁵	Resistance class ⁶
	$\bar{\phi}$ ¹	SD ²	BLUE ³	$\bar{\phi}$	SD	BLUE			
WB-450	28.0	9.9	28.6	34.7	11.5	33.9	34.7	33.9	m. s.
WB-454	56.6	13.0	55.5	47.9	11.5	48.4	56.6	55.5	s.
WB-456	40.6	14.3	41.4	46.3	15.3	45.6	46.3	45.6	m. s.
WB-457	52.5	19.4	51.7	52.3	17.8	57.0	52.5	57.0	s.
WB-458	48.5	18.7	47.6	53.3	17.7	59.5	53.3	59.5	s.
WB-460	19.3	8.2	19.9	23.5	9.3	22.6	23.5	22.6	m. r.
WB-461 ⁸	0.0	0.0	NA	0.0	0.0	NA	0.0	NA	r.
WB-462	18.1	10.9	19.4	42.3	20.6	39.7	42.3	39.7	m. s.
WB-465	18.8	9.6	18.4	5.6	6.0	2.2	18.8	18.4	m. r.
WB-466 ⁸	0.0	0.0	NA	0.0	0.0	NA	0.0	NA	r.
WB-467	36.9	18.3	39.3	33.7	21.2	39.8	36.9	39.8	m. s.
WB-468 ⁸	0.0	0.0	NA	0.0	0.0	NA	0.0	NA	r.
WB-469 ⁺ *	53.9	17.5	53.9	60.1	19.6	57.5	60.1	57.5	s.
WB-472 ⁺ *	15.8	14.9	19.9	19.4	18.0	21.2	19.4	21.2	m. r.
WB-473 ⁺	16.9	6.7	17.5	16.8	7.9	15.9	16.9	17.5	m. r.
WB-474 ⁸	0.0	0.0	NA	0.0	0.0	NA	0.0	NA	r.
WB-476*	9.6	11.6	4.6	0.0	0.0	1.7	9.6	4.6	m. r.
WB-478*	30.4	9.2	31.1	32.9	8.3	34.6	32.9	34.6	m. s.
WB-483 ⁺	3.5	4.2	8.7	0.0	0.0	-0.1	3.5	8.7	m. r.
WB-486 ⁹	38.5	16.4	NA	50.7	26.6	NA	50.7	NA	m. s.
WB-490 ⁹	39.3	19.9	NA	40.9	10.2	NA	40.9	NA	m. s.
WB-499 ^{10*}	0.0	0.0	NA	0.0	0.0	NA	0.0	NA	r.
WB-501 ⁺	59.4	8.8	56.0	53.4	16.7	57.0	59.4	57.0	s.
WB-510 ⁸	0.0	0.0	NA	0.0	0.0	NA	0.0	NA	r.

¹ mean values of the normalized infected leaf area (in %)

² standard deviation of the normalized infected leaf area (in %)

³ calculated best linear unbiased estimation (BLUE) value

⁴ *in silico* generated maximal infection based on the selection of the higher infection value

⁵ *in silico* generated maximal infection based on the selection of the higher BLUE value

⁶ resistance classes according to Table M 3: r. – resistant; m. r. – moderate resistant; m. s. – moderate susceptible; s. – susceptible

⁷ not analysed

⁸ identified *mlo* carriers were excluded from the analysis

⁹ from these genotypes no exome capture data were available

¹⁰ identified race-specific resistant genotypes were excluded from the analysis

⁺ member of the subpopulation

* genotypes were selected for the field trials

Table B 3: Quantification of the resistance response of 102 barley genotypes against natural powdery mildew infection under field conditions and against the powdery mildew isolates D35/3 and RiIII under controlled conditions

Genotype	natural field infection ¹			D35/3 ¹		RiIII ¹		Max BLUE ⁷
	Gatersleben ²	Bergen ³	BLUE ⁴	Ø ⁵	BLUE ⁶	Ø ⁵	BLUE ⁶	
Morex	4.0	4.0	4.0	72.8	3.9	72.2	3.9	3.9
Roland	2.2	2.7	2.4	54.9	3.6	56.7	3.6	3.6
WB-042	3.3	4.0	3.6	39.2	2.7	37.9	3.0	3.0
WB-043	2.8	3.5	3.1	0.0	NA ⁸	0.0	NA	NA
WB-049	2.5	2.5	2.5	10.6	1.6	8.3	1.9	1.9
WB-052*	1.0	1.5	1.2	8.2	1.3	0.0	1.2	1.3
WB-054	1.8	2.5	2.1	24.2	2.1	22.1	1.9	2.1
WB-055	2.5	2.0	2.2	29.7	2.4	27.7	2.2	2.4
WB-058	2.3	2.8	2.5	25.3	2.3	29.0	2.8	2.8
WB-065	3.8	4.0	3.9	0.0	NA	0.0	NA	NA
WB-066*	1.5	2.0	1.7	13.4	1.7	18.5	2.1	2.1
WB-069	2.5	3.3	2.9	29.3	2.4	38.2	2.8	2.8
WB-070	3.5	4.0	3.7	42.7	3.0	49.5	3.2	3.2
WB-074	2.8	2.5	2.6	46.7	3.1	52.2	3.3	3.3
WB-094	1.8	2.3	2.0	32.9	2.6	30.3	2.4	2.6
WB-101	3.5	4.0	3.7	71.7	3.9	68.1	3.8	3.9
WB-102	1.8	3.5	2.6	34.0	2.4	32.4	2.3	2.4
WB-113	3.3	3.0	3.1	50.3	3.3	54.8	3.4	3.4
WB-135	4.0	4.0	4.0	65.6	3.8	66.6	3.7	3.8
WB-137	2.0	3.8	2.9	13.1	1.4	8.0	1.1	1.4
WB-138	4.0	4.0	4.0	51.0	3.2	53.1	3.4	3.4
WB-144	3.0	4.0	3.5	64.6	3.8	62.9	3.7	3.8
WB-147	4.0	4.0	4.0	39.2	2.9	48.6	3.3	3.3
WB-149	2.5	3.8	3.1	52.8	3.3	52.6	3.7	3.7
WB-151	3.8	4.0	3.9	59.2	3.6	59.4	3.6	3.6
WB-152	3.5	4.0	3.7	23.8	2.1	18.7	2.1	2.1
WB-153	2.8	4.0	3.4	56.8	3.5	53.9	3.6	3.6
WB-156	2.8	3.3	3.0	65.8	3.8	68.9	3.8	3.8
WB-157	3.0	4.0	3.5	73.9	3.6	66.4	3.6	3.6
WB-158	2.8	3.0	2.9	61.9	3.4	58.2	3.3	3.4
WB-161	2.8	4.0	3.4	10.3	2.0	11.1	1.7	2.0
WB-165	3.5	4.0	3.7	39.8	2.9	37.0	2.8	2.9
WB-166	3.8	3.8	3.7	64.4	3.8	63.6	3.7	3.8
WB-168	3.8	4.0	3.9	39.2	2.9	39.8	2.7	2.9
WB-169	4.0	4.0	4.0	68.2	3.8	69.5	3.8	3.8
WB-170	3.0	4.0	3.5	55.4	3.6	53.8	3.4	3.6
WB-181	2.8	2.5	2.6	57.8	3.7	57.1	3.4	3.7
WB-183	3.0	3.0	3.0	54.4	3.6	54.5	3.8	3.8
WB-186	3.0	3.0	3.0	52.5	3.3	50.5	3.1	3.3
WB-187	3.0	3.5	3.2	52.5	3.4	50.7	3.6	3.6
WB-188	3.0	3.5	3.2	52.6	3.3	59.2	3.7	3.7
WB-193	3.0	3.0	3.0	40.7	2.9	37.6	3.0	3.0
WB-196	2.8	2.3	2.5	53.4	3.5	47.3	3.1	3.5
WB-201	2.8	3.3	3.0	62.0	3.6	65.2	3.7	3.7
WB-203	3.0	2.8	2.9	43.6	2.9	39.4	2.9	2.9
WB-206	2.8	3.5	3.1	48.9	3.2	47.9	3.1	3.2
WB-210	2.5	2.8	2.6	56.7	3.7	56.9	3.5	3.7

Table B 3 (continued)

Genotype	natural field infection ¹			D35/3 ¹		R111 ¹		Max BLUE ⁷
	Gatersleben ²	Bergen ³	BLUE ⁴	Ø ⁵	BLUE ⁶	Ø ⁵	BLUE ⁶	
WB-211	3.3	3.0	3.1	58.1	3.5	60.4	3.7	3.7
WB-220	3.3	4.0	3.6	66.1	3.8	59.6	3.6	3.8
WB-222	2.3	3.3	2.7	60.1	3.7	56.2	3.5	3.7
WB-224	2.8	2.3	2.5	51.7	3.3	46.7	3.0	3.3
WB-226	2.8	3.8	3.3	0.0	NA	0.0	NA	NA
WB-227	2.5	2.8	2.6	65.4	3.8	60.5	3.7	3.8
WB-232	3.5	4.0	3.7	56.8	3.4	50.2	3.2	3.4
WB-236	3.5	3.3	3.4	56.7	3.5	52.9	3.7	3.7
WB-241	3.0	3.3	3.1	40.6	2.9	41.8	2.8	2.9
WB-250	3.0	3.0	3.0	72.9	3.9	72.0	3.8	3.9
WB-253	3.5	4.0	3.7	45.8	2.9	36.7	2.6	2.9
WB-258	3.3	3.8	3.5	57.5	3.6	63.9	3.7	3.7
WB-259	3.0	3.5	3.2	36.1	2.6	40.1	2.8	2.8
WB-261	4.0	4.0	4.0	60.2	3.6	57.4	3.4	3.6
WB-263	4.0	4.0	4.0	21.9	2.1	16.5	1.9	2.1
WB-269	2.8	3.3	3.0	56.7	3.5	57.1	3.8	3.8
WB-270	4.0	3.5	3.7	59.3	3.8	58.0	3.8	3.8
WB-274	3.0	4.0	3.5	67.2	3.7	66.2	3.7	3.7
WB-279	4.0	4.0	4.0	32.3	2.5	38.3	2.7	2.7
WB-280	3.3	4.0	3.6	48.2	3.2	50.9	3.2	3.2
WB-281	3.5	4.0	3.7	27.4	2.4	27.6	2.4	2.4
WB-282	4.0	4.0	4.0	44.8	3.1	46.1	3.1	3.1
WB-287	3.0	3.5	3.2	71.6	3.9	62.3	3.7	3.9
WB-290	3.3	3.3	3.2	59.3	3.5	59.1	3.9	3.9
WB-297	3.0	3.8	3.4	46.5	3.4	38.7	3.1	3.4
WB-300	4.0	4.0	4.0	69.1	3.9	69.7	3.8	3.9
WB-302	3.5	4.0	3.7	38.1	2.8	42.7	3.0	3.0
WB-305	1.8	2.0	1.9	0.0	NA	0.0	NA	NA
WB-307	1.5	2.0	1.8	0.0	NA	0.0	NA	NA
WB-311	4.0	4.0	4.0	61.5	3.7	59.1	3.8	3.8
WB-315	3.0	3.8	3.4	62.4	3.8	60.6	3.6	3.8
WB-319	4.0	4.0	4.0	40.9	3.0	42.0	2.9	3.0
WB-320	3.5	3.5	3.5	39.9	2.9	47.8	3.3	3.3
WB-325	2.5	3.3	2.9	57.8	3.7	56.0	3.5	3.7
WB-346	3.0	3.8	3.4	73.6	3.9	77.7	3.7	3.9
WB-352	1.3	1.0	1.1	0.0	NA	0.0	NA	NA
WB-355	2.8	3.5	3.1	64.9	3.8	57.3	3.5	3.8
WB-358	1.0	1.3	1.1	0.3	NA	1.2	NA	NA
WB-369	3.5	3.0	3.2	38.2	2.8	42.3	2.9	2.9
WB-376	4.0	4.0	4.0	61.9	3.7	57.7	3.6	3.7
WB-377	4.0	4.0	4.0	35.0	2.8	40.3	2.9	2.9
WB-400*	1.0	1.5	1.2	24.9	2.3	28.5	2.6	2.6
WB-424	4.0	4.0	4.0	63.7	3.8	57.9	3.5	3.8
WB-449	2.0	2.5	2.2	39.2	2.8	45.6	3.1	3.1
WB-450	3.5	4.0	3.7	28.0	2.3	34.7	2.6	2.6
WB-454	2.8	4.0	3.4	56.6	3.5	47.9	3.4	3.5
WB-456	3.0	4.0	3.5	40.6	3.0	46.3	3.2	3.2
WB-457	3.3	4.0	3.6	52.5	3.3	52.3	3.6	3.6
WB-458	4.0	4.0	4.0	48.5	3.2	53.3	3.7	3.7

Table B 3 (continued)

Genotype	natural field infection ¹			D35/3 ¹		RiIII ¹		Max BLUE ⁷
	Gatersleben ²	Bergen ³	BLUE ⁴	Ø ⁵	BLUE ⁶	Ø ⁵	BLUE ⁶	
WB-460	2.8	2.8	2.7	19.3	1.9	23.5	2.1	2.1
WB-469	3.5	4.0	3.7	53.9	3.4	60.1	3.4	3.4
WB-472	2.0	3.0	2.5	15.8	1.9	19.4	2.0	2.0
WB-476*	1.5	1.0	1.2	9.6	1.2	0.0	1.1	1.2
WB-478	3.0	3.8	3.4	30.4	2.5	32.9	2.6	2.6
WB-499	1.8	2.0	1.9	0.0	NA	0.0	NA	NA

¹ source of powdery mildew infection

² infection value of the field in Gatersleben (51°49'35.7"N 11°16'49.7"E, 110 m) based on four major resistant classes (Table M 4)

³ infection value of the field in Bergen/Wohlde (52°48'32.1"N 9°59'53.7"E, 80 m) based on four major resistant classes (Table M 4)

⁴ calculated best linear unbiased estimation (BLUE) value from adult plants (field data of both locations integrated)

⁵ mean value of the normalized infected leaf area (in %) from detached seedling leaves

⁶ calculated best linear unbiased estimation (BLUE) value from transformed data

⁷ *in silico* generated maximal infection based on the selection of the higher BLUE value from detached seedling leaves

⁸ not analysed

* genotypes were selected for the large isolate test

Table B 4: Resistance spectra of the four resistant field genotypes defined by the infection of detached seedling leaves with 27 powdery mildew isolates

Powdery mildew isolates ¹		Genotypes			
		WB-052	WB-066	WB-400	WB-476
75	RiIII	0	1-2	2	1/3
78	Ro93a	1	1-2	2-3	2
114		1	1	2-3	1
116		1	1	2-3	1
122		0	0	2-3	1
125	MH21	1	2	2-3	1/3
167		1	1	2-3	1
168		2	2	2-3	2-3
170		1	1	2-3	1-2
176		1	1-2	2-3	2
212		1	1	2-3	0/2-3
224	Si1	1	2-3	2-3	1-2/2-3
225		1	2	2-3	1
227	D2/4	1-2	2	2-3	1
229		2	1	2-3	1/2-3
231		1	2	2-3	0/2-3
232		1	2	2-3	1/3
233	D35/2	1-2	2	2-3	2
234		1-2	2	2-3	1
235		1	1	2-3	0/3
237		1	1	2-3	1
239		1	1-2	2-3	1
240	D4/6	0	1	2-3	1
241		0	1	2-3	2-3/1
242	D35/3	1	1-2	2-3	1
245		1-2	1-2	2-3	2-3
247	CH4.8	0	1-2	2	1-2

¹ represented by the official JKI numbers and in case of the nine previously used isolates by their work names

The test was performed in cooperation with the JKI Kleinmachnow and the infection types were scored on a scale from 0-4 (0= resistant; 4=highly susceptible).

Table B 5: Overview of all significant single nucleotide polymorphisms**i) significant single nucleotide polymorphisms (SNPs) of the *Max* trait**

Marker	Loci ¹	Candidate ²	-log ₁₀ (p-values)		
			<i>Max</i>	RiIII	D35/3
SNP7844730chr1H	1	1	4.75	3.01	4.16
SNP324191524chr1H	2	2	4.47	4.36	3.71
SNP437375879chr2H	3	3	5.13	4.82	3.83
SNP517799609chr2H	4	-	4.56	2.70	3.62
SNP519118124chr2H	4	-	4.56	2.77	3.36
SNP519526061chr2H	4	-	4.51	2.48	3.62
SNP519556675chr2H	4	-	4.70	2.78	4.20
SNP520255788chr2H	4	4	4.77	2.76	3.75
SNP669741419chr2H	5	5	4.84	5.36	4.32
SNP669741426chr2H	5	5	5.28	5.08	4.89
SNP669742305chr2H	5	5	4.46	4.84	3.97
SNP669742599chr2H	5	5	5.74	5.31	5.16
SNP669743745chr2H	5	5	5.29	5.70	4.29
SNP28690855chr3H	6	6	4.85	4.09	4.18
SNP491378587chr3H	7	7	5.59	4.22	4.32
SNP623759080chr3H	8	8	5.03	3.86	4.09
SNP623759155chr3H	8	8	5.12	3.90	4.28
SNP623759257chr3H	8	8	4.85	3.74	3.99
SNP623761291chr3H	8	9	4.77	3.47	4.05
SNP637689337chr3H	8	10	4.94	7.11	3.69
SNP637874133chr3H	8	-	6.01	6.16	4.60
SNP637874138chr3H	8	-	6.01	6.16	4.60
SNP637874201chr3H	8	-	5.00	5.54	3.75
SNP637874206chr3H	8	-	5.00	5.54	3.75
SNP637874220chr3H	8	-	5.00	5.54	3.75
SNP12462942chr4H	9	11	5.09	3.93	3.94
SNP420309355chr4H	10	12	4.50	4.64	3.42
SNP422058401chr4H	10	-	4.80	3.76	3.78
SNP422058430chr4H	10	-	4.48	3.94	3.41
SNP577041307chr4H	11	13	5.24	5.08	4.49
SNP577122735chr4H	11	-	4.55	5.06	3.36
SNP580096165chr4H	11	14	5.42	7.10	3.38
SNP580171165chr4H	11	-	4.74	6.16	3.03
SNP580172724chr4H	11	15	6.34	6.55	4.77
SNP633041853chr4H	12	16	4.61	4.94	2.82
SNP554456783chr5H	13	17	5.07	5.79	3.46
SNP554460428chr5H	13	18	5.06	5.57	3.54
SNP554461073chr5H	13	18	5.03	5.50	3.42
SNP554493706chr5H	13	-	4.75	5.14	3.32
SNP554738172chr5H	13	19	6.30	5.82	4.68
SNP643788587chr5H	14	20	5.87	5.85	5.09
SNP645843882chr5H	14	21	4.52	4.64	4.10
SNP647065503chr5H	14	-	4.54	3.81	4.43
SNP649184143chr5H	14	22	4.87	4.19	4.22
SNP649211044chr5H	14	23	4.83	3.89	4.36
SNP649380181chr5H	14	24	5.28	4.29	4.76
SNP649403811chr5H	14	-	4.60	3.99	4.07
SNP650946749chr5H	14	25	4.49	3.91	4.12

Table B 5i (continued)

Marker	Loci ¹	Candidate ²	-log ₁₀ (p-values)		
			Max	RiIII	D35/3
SNP650946767chr5H	14	25	4.49	3.91	4.12
SNP650946795chr5H	14	25	4.49	3.91	4.12
SNP650952559chr5H	14	26	4.49	3.91	4.12
SNP650956553chr5H	14	26	5.81	6.18	4.86
SNP650971235chr5H	14	27	6.15	5.75	5.24
SNP650973939chr5H	14	28	5.96	5.39	5.32
SNP650976700chr5H	14	28	7.38	6.68	6.34
SNP650998052chr5H	14	29	4.66	3.88	4.10
SNP651048872chr5H	14	30	4.49	3.91	4.12
SNP651049191chr5H	14	30	4.49	3.91	4.12
SNP651049830chr5H	14	30	4.49	3.91	4.12
SNP651050600chr5H	14	30	4.49	3.91	4.12
SNP651051756chr5H	14	30	4.49	3.91	4.12
SNP651514104chr5H	14	31	4.90	4.11	4.72
SNP651515931chr5H	14	31	6.15	5.75	5.24
SNP651518659chr5H	14	31	6.15	5.75	5.24
SNP651518986chr5H	14	31	6.15	5.75	5.24
SNP651519029chr5H	14	31	6.15	5.75	5.24
SNP651520044chr5H	14	-	6.21	6.01	5.29
SNP42371655chr6H	15	-	4.45	2.71	3.68
SNP561927407chr6H	16	32	4.72	3.50	4.21
SNP568471765chr6H	16	33	4.45	4.31	3.03

¹ annotated locus number² candidate number

Candidates are defined, when the corresponding SNP is located in an annotated gene model. The -log₁₀(p-values) above the significant threshold were highlighted in bold.

Table B 5 (continued)

ii) Single nucleotide polymorphisms (SNPs) that are only significant in the D35/3 or RiIII trait.

Marker	Loci ¹	-log ₁₀ (p-values)		
		Max	RiIII	D35/3
SNP42827chr1H	I	2.56	0.54	4.48
SNP291382chr1H	I	3.89	1.20	6.10
SNP3667470chr1H	I	3.89	2.80	4.53
SNP3667488chr1H	I	3.89	2.80	4.53
SNP3667491chr1H	I	3.89	2.80	4.53
SNP3667503chr1H	I	3.89	2.80	4.53
SNP3667516chr1H	I	3.89	2.80	4.53
SNP3667517chr1H	I	3.89	2.80	4.53
SNP3667520chr1H	I	3.89	2.80	4.53
SNP5013817chr1H	I	4.02	2.54	5.71
SNP324167645chr1H	2	4.29	4.64	3.53
SNP16803666chr2H	II	3.34	4.60	2.22
SNP16803672chr2H	II	3.34	4.60	2.22
SNP669741901chr2H	5	4.17	4.51	3.70
SNP669741993chr2H	5	4.27	4.69	3.82
SNP669742149chr2H	5	4.31	4.60	3.84
SNP732689879chr2H	III	3.24	1.14	4.71
SNP732722329chr2H	III	3.18	1.83	4.90
SNP732730198chr2H	III	4.30	3.55	4.47
SNP732730298chr2H	III	4.00	2.96	4.61
SNP732732141chr2H	III	4.00	2.96	4.61
SNP738838256chr2H	III	3.89	1.92	4.80
SNP760841462chr2H	IV	0.79	4.50	0.21
SNP760971467chr2H	IV	1.45	4.95	0.63
SNP760982349chr2H	IV	1.07	4.91	0.35
SNP760982369chr2H	IV	0.91	4.88	0.30
SNP760984635chr2H	IV	1.02	4.87	0.34
SNP760984640chr2H	IV	1.02	4.87	0.34
SNP760984641chr2H	IV	1.02	4.87	0.34
SNP760984653chr2H	IV	1.02	4.87	0.34
SNP760984654chr2H	IV	1.02	4.87	0.34
SNP760984657chr2H	IV	1.02	4.87	0.34
SNP760984662chr2H	IV	1.02	4.87	0.34
SNP760984686chr2H	IV	1.02	4.87	0.34
SNP760984694chr2H	IV	1.02	4.87	0.34
SNP761002172chr2H	IV	0.93	5.08	0.29
SNP761002177chr2H	IV	0.93	5.08	0.29
SNP761105520chr2H	IV	1.47	4.81	0.65
SNP761105999chr2H	IV	0.81	4.48	0.22
SNP761106781chr2H	IV	0.93	5.08	0.29
SNP761108435chr2H	IV	0.93	5.08	0.29
SNP761108447chr2H	IV	0.93	5.08	0.29
SNP761108638chr2H	IV	0.93	5.08	0.29
SNP761269553chr2H	IV	0.93	5.08	0.29
SNP761277368chr2H	IV	0.68	4.59	0.15
SNP761328115chr2H	IV	0.93	5.08	0.29
SNP761431182chr2H	IV	0.93	5.08	0.29
SNP761431478chr2H	IV	0.93	5.08	0.29

Table B 5ii (continued)

Marker	Loci ¹	-log ₁₀ (p-values)		
		Max	RiIII	D35/3
SNP761520864chr2H	IV	0.79	5.21	0.17
SNP761623684chr2H	IV	0.93	5.08	0.29
SNP761623897chr2H	IV	0.93	5.08	0.29
SNP761710272chr2H	IV	0.81	5.07	0.22
SNP761710284chr2H	IV	0.81	5.07	0.22
SNP761710448chr2H	IV	0.74	5.10	0.13
SNP761710568chr2H	IV	0.79	5.21	0.17
SNP761711485chr2H	IV	0.64	4.62	0.10
SNP761711575chr2H	IV	0.79	5.21	0.17
SNP762365252chr2H	IV	0.94	4.97	0.26
SNP762464939chr2H	IV	1.42	5.10	0.59
SNP762526722chr2H	IV	0.68	4.45	0.13
SNP762827652chr2H	IV	0.85	4.81	0.25
SNP762827706chr2H	IV	0.85	4.81	0.25
SNP762829664chr2H	IV	0.79	4.50	0.25
SNP762950592chr2H	IV	2.24	0.02	5.17
SNP762953341chr2H	IV	1.14	6.65	0.33
SNP762990427chr2H	IV	1.09	6.36	0.28
SNP762994715chr2H	IV	1.75	0.09	4.52
SNP763013435chr2H	IV	1.39	7.10	0.49
SNP763013662chr2H	IV	1.06	6.71	0.24
SNP763071590chr2H	IV	1.31	5.63	0.44
SNP763122863chr2H	IV	0.97	5.60	0.26
SNP763552030chr2H	IV	1.38	5.71	0.49
SNP763961891chr2H	IV	2.24	0.08	5.22
SNP763961892chr2H	IV	2.24	0.08	5.22
SNP763964127chr2H	IV	0.47	4.52	0.05
SNP764281778chr2H	IV	1.94	0.00	4.81
SNP32735164chr3H	V	4.43	6.17	3.28
SNP33152968chr3H	V	3.35	4.50	2.52
SNP33154454chr3H	V	3.35	4.50	2.52
SNP34231160chr3H	V	4.32	4.56	3.12
SNP558928861chr3H	VI	1.81	4.72	1.44
SNP558928888chr3H	VI	1.81	4.72	1.44
SNP558928915chr3H	VI	1.81	4.72	1.44
SNP558928922chr3H	VI	1.81	4.72	1.44
SNP558928924chr3H	VI	1.81	4.72	1.44
SNP558928936chr3H	VI	1.81	4.72	1.44
SNP558928951chr3H	VI	1.81	4.72	1.44
SNP637874211chr3H	8	4.16	4.72	3.20
SNP637874239chr3H	8	4.17	4.87	3.05
SNP580093689chr4H	11	3.96	5.28	2.72
SNP580095223chr4H	11	3.53	5.27	2.18
SNP580096976chr4H	11	3.99	5.33	2.50
SNP580097024chr4H	11	3.49	4.83	2.18
SNP580172809chr4H	11	3.06	4.55	1.85
SNP590349274chr4H	11	3.42	5.06	2.94
SNP590411556chr4H	11	3.08	4.67	2.66
SNP633043373chr4H	12	3.75	4.67	2.41

Table B 5ii (continued)

Marker	Loci ¹	-log ₁₀ (p-values)		
		Max	RiIII	D35/3
SNP75970509chr5H	VII	4.43	5.29	3.19
SNP82548792chr5H	VII	4.07	5.08	2.94
SNP554460742chr5H	13	4.40	4.61	3.16
SNP554463653chr5H	13	4.20	5.05	2.82
SNP554497408chr5H	13	3.98	4.77	2.54
SNP587154202chr5H	13	3.87	4.49	2.47
SNP639599345chr5H	14	2.87	4.93	2.48
SNP639599435chr5H	14	3.09	5.14	2.91
SNP639599438chr5H	14	3.09	5.14	2.91
SNP639604848chr5H	14	3.73	5.36	3.47
SNP639604878chr5H	14	3.29	4.98	3.02
SNP639726114chr5H	14	2.94	5.09	2.81
SNP639841468chr5H	14	2.82	4.99	2.61
SNP640005085chr5H	14	2.82	4.99	2.61
SNP640026000chr5H	14	2.82	4.99	2.61
SNP640069072chr5H	14	2.82	4.99	2.61
SNP640069186chr5H	14	2.82	4.99	2.61
SNP640161618chr5H	14	2.82	4.99	2.61
SNP640333693chr5H	14	2.82	4.99	2.61
SNP640333752chr5H	14	2.82	4.99	2.61
SNP640347202chr5H	14	2.82	4.99	2.61
SNP640347434chr5H	14	2.82	4.99	2.61
SNP640363997chr5H	14	2.82	4.99	2.61
SNP640364239chr5H	14	2.82	4.99	2.61
SNP640364443chr5H	14	2.95	4.82	2.74
SNP640367639chr5H	14	2.82	4.99	2.61
SNP640367827chr5H	14	2.80	5.04	2.53
SNP640367838chr5H	14	2.80	5.04	2.53
SNP640394500chr5H	14	2.80	4.50	2.57
SNP640715740chr5H	14	3.70	4.69	3.90
SNP640816258chr5H	14	4.31	4.47	4.05
SNP641063402chr5H	14	3.54	4.90	3.80
SNP643414588chr5H	14	3.55	4.46	3.01
SNP643414734chr5H	14	3.55	4.46	3.01
SNP643636039chr5H	14	3.39	4.50	2.89
SNP643637858chr5H	14	3.68	4.89	3.11
SNP643788268chr5H	14	3.39	4.50	2.89
SNP643788440chr5H	14	3.39	4.50	2.89
SNP643831460chr5H	14	3.39	4.50	2.89
SNP643831470chr5H	14	3.39	4.50	2.89
SNP645080880chr5H	14	2.71	4.66	2.70
SNP645395607chr5H	14	2.55	4.67	2.40
SNP645396646chr5H	14	2.59	4.55	2.48
SNP30214277chr6H	15	3.70	1.49	4.52
SNP30214310chr6H	15	3.66	1.43	4.53
SNP574366632chr6H	16	2.62	4.63	1.85
SNP578734108chr6H	16	3.66	5.40	2.30

¹ annotated locus number

Table B 6: Overview of the sequence identifiers for the defined candidates**i) most promising candidate genes**

Candidate	Nucleotide ¹	Protein ²
WB-CG_17 (HORVU5Hr1G078000)	<i>genes</i> ³	<i>barley</i> ⁶
	XM_020320876.1	HORVU5Hr1G078020
	XM_003578371.4	HORVU7Hr1G063660
	<i>cDNA</i> ⁴	<i>related species</i> ⁷
	AK365822.1	XP_020176465.1
	<i>ESTs</i> ⁵	XP_003578419.1
	HF13E21r	<i>Arabidopsis</i> ⁸
	HU05M08r	At5g11680.1
	HW01F09u	<i>rice</i> ⁹
		LOC_Os09g33800.1
WB-CG_19 (HORVU5Hr1G078330)	<i>genes</i>	<i>barley</i>
	XM_020320883.1	HORVU3Hr1G017960
	<i>cDNA</i>	<i>related species:</i>
	AK371013.1	XP_020176472.1
	AK371762.1	<i>Arabidopsis</i>
	AK367952.1	At1g48140.1
	<i>ESTs</i>	<i>rice</i>
	HO02F20S	LOC_Os02g51420.1
WB-CG_23 (HORVU5Hr1G116860)	<i>genes</i>	<i>barley</i>
	XM_003559157.3	HORVU5Hr1G116800
	<i>cDNA</i>	<i>related species</i>
	AK375834.1	XP_003559205.2
	<i>ESTs</i>	<i>Arabidopsis</i>
	HM05L23r	AT3G61600.1
	HF05C08r	AT2G46260.1
	HDP07C02w	<i>rice</i>
	LOC_Os02g16000.2 LOC_Os06g31100.1	
WB-CG_28 (HORVU5Hr1G117650)	<i>genes</i>	<i>barley</i>
	XM_020341159.1	HORVU1Hr1G079900
	XM_010240873.3	<i>related species</i>
	<i>cDNA</i>	XP_020196748.1
	AK249394.1	XP_010239175.2
	<i>ESTs</i>	<i>Arabidopsis</i>
	RUS41G07w	At5g26680.1
	HU06C07r	<i>rice</i>
	XP_015632894.1 XP_015639321.1	

Table B 6 (continued)**ii) additional 29 candidate genes**

Candidate	Nucleotide ¹
WB-CG_1 (HORVU1Hr1G003530)	<i>genes</i> ³ : XM_020301082.1, XM_010235099.3 <i>cDNA</i> ⁴ : AK354632.1 <i>ESTs</i> ⁵ : HF18D18r, RUS73G12w, HP05G23T
WB-CG_2 (HORVU1Hr1G044590)	<i>genes</i> : XM_020291725.1, XM_003574076.1 <i>cDNA</i> : AK363338.1 <i>ESTs</i> : RUS40F09w, HB16C24r
WB-CG_3 (HORVU2Hr1G064440)	<i>genes</i> : - <i>cDNA</i> : AK372600.1 <i>ESTs</i> : -
WB-CG_4 (HORVU2Hr1G072510)	no start & stop codon annotated
WB-CG_5 (HORVU2Hr1G095410)	<i>genes</i> : XM_020333308.1, XM_014903417.2 <i>cDNA</i> : AK368024.1 <i>ESTs</i> : HDP39D06w
WB-CG_6 (HORVU3Hr1G013300)	<i>genes</i> : XM_020315575.1, XM_003565287.4 <i>cDNA</i> : AK360084.1 <i>ESTs</i> : HC14P21w, HW04B19V
WB-CG_7 (HORVU3Hr1G064390)	<i>genes</i> : XM_020323606 <i>cDNA</i> : AK368295. <i>ESTs</i> : HDP17B17w, HD17B17T
WB-CG_8 (HORVU3Hr1G088110)	<i>genes</i> : XM_020298468.1, XM_024459289.1 <i>cDNA</i> : AK356032.1 <i>ESTs</i> : HDP35K18T, HB04C11r
WB-CG_9 (HORVU3Hr1G088120)	<i>genes</i> : XM_020298475.1 <i>cDNA</i> : AK249806.1 <i>ESTs</i> : HK03P18u
WB-CG_10 (HORVU3Hr1G092280)	<i>genes</i> : XM_020317166.1 <i>cDNA</i> : AK368067.1, AK371471.1 <i>ESTs</i> : -
WB-CG_11 (HORVU4Hr1G005530)	<i>genes</i> : XM_020301710.1 <i>cDNA</i> : AK365658.1 <i>ESTs</i> : HDP27M03w
WB-CG_12 (HORVU4Hr1G051290)	<i>genes</i> : XM_020306961.1, XM_003557950.1, KY461058 <i>cDNA</i> : AK251058.1 <i>ESTs</i> : RUS93B09w, HZ47A09r
WB-CG_13 (HORVU4Hr1G070630)	<i>genes</i> : XM_020302401.1 <i>cDNA</i> : AK251720.1, AK372666.1 <i>ESTs</i> : HDP27D19T, HDP14B11w; HY06C10v

Table B 6ii (continued)

Candidate	Nucleotide ¹
WB-CG_14 (HORVU4Hr1G071250)	<i>genes</i> ³ : XM_020331564.1 <i>cDNA</i> ⁴ : AK353996.1, AK360736.1 <i>ESTs</i> ⁵ : HU12B11r, HO19J08S, HO19J08w
WB-CG_15 (HORVU4Hr1G071290)	no results for the gene model, but for the genomic sequence <i>genes</i> : XM_020331565.1; XM_020331567.1 <i>cDNA</i> : AK363225, AK251078.1; - <i>ESTs</i> : HV11P18r, HI15C23r; HI08P01r, HI08P01w
WB-CG_16 (HORVU4Hr1G085960)	<i>genes</i> : XM_020338022.1, XM_003558918.1 <i>cDNA</i> : AK363167.1 <i>ESTs</i> : HY06G12V, HDP22E09w
WB-CG_18 (HORVU5Hr1G078100)	<i>genes</i> : XM_020320889.1 <i>cDNA</i> : AK360543.1 <i>ESTs</i> : GAN004K15f
WB-CG_20 (HORVU5Hr1G114400)	<i>genes</i> : XM_020293196.1 <i>cDNA</i> : AK371102.1 <i>ESTs</i> : HV14B03r, HC11C22y, HOO4I23w
WB-CG_21 (HORVU5Hr1G115160)	<i>genes</i> : XM_020306251.1 <i>cDNA</i> : AK370532.1 <i>ESTs</i> : HF13G09r, RUS118G08r
WB-CG_22 (HORVU5Hr1G116810)	<i>genes</i> : XM_020319101.1 <i>cDNA</i> : AK358688.1 <i>ESTs</i> : -
WB-CG_24 (HORVU5Hr1G116890)	<i>genes</i> : XM_020303942.1, XM_020330238.1 <i>cDNA</i> : - <i>ESTs</i> : HDP15011w
WB-CG_25 (HORVU5Hr1G117600)	<i>genes</i> : XM_020330053.1, XM_006664922.1 <i>cDNA</i> : AK365818.1 <i>ESTs</i> : -
WB-CG_26 (HORVU5Hr1G117610)	<i>genes</i> : XM_020316411.1, XM_003576606.3 <i>cDNA</i> : - <i>ESTs</i> : HX14P19r
WB-CG_27 (HORVU5Hr1G117630)	<i>genes</i> : XM_020341151.1, XM_014902741.2 <i>cDNA</i> : - <i>ESTs</i> : -
WB-CG_29 (HORVU5Hr1G117670)	<i>genes</i> : XM_020341149.1, XM_003562981.1 <i>cDNA</i> : AK368987.1 <i>ESTs</i> : GAN007K22u, RUS99G11w
WB-CG_30 (HORVU5Hr1G117690)	<i>genes</i> : XM_020335193.1, XM_010240584.1 <i>cDNA</i> : AK373768.1 <i>ESTs</i> : HDP33F24w, HV05F18r
WB-CG_31 (HORVU5Hr1G117970)	<i>genes</i> : XM_020293233.1, XM_003562894.4 <i>cDNA</i> : AK355984.1 <i>ESTs</i> : HZ42H04r, HDP33C08w

Table B 6ii (continued)

Candidate	Nucleotide ¹
WB-CG_32 (HORVU6Hr1G086670)	<i>genes</i> ³ : XM_020310049.1 <i>cDNA</i> ⁴ : AK373486.1 <i>ESTs</i> ⁵ : -
WB-CG_33 (HORVU6Hr1G089250)	<i>genes</i> : XM_020327357.1, XM_010236308.1 <i>cDNA</i> : AM039899.1 <i>ESTs</i> : RUS122C09r, HZ65G10r

¹ candidate homologs based on nucleotide sequence similarity

² candidate homologs based on protein sequence similarity

³ putative homologs in related species (*Aegilops tauschii* or *Brachypodium distachyon*) identified via 'blastn' analysis against the NCBI server

⁴ cDNA clones with high nucleotide sequence similarity identified via 'blastn' analysis against the IPK Barley BLAST server

⁵ expressed sequence tags (ESTs) with high nucleotide sequence similarity identified via 'blastn' analysis against the IPK Barley BLAST server

⁶ putative homologs in barley, predicted as potential off-targets by the si-Fi21 tool

⁷ corresponding protein sequences of the putative homologs in related species

⁸ putative homolog of *Arabidopsis thaliana* identified via 'blastn' analysis against the TAIR database

⁹ putative homolog of rice (*Oryza sativa ssp japonica cv. Nipponbare*) identified via 'blastn' analysis against the rice genome annotation project server

Table B 7: Overview of the defined alleles of 33 candidates

Genotype	WB-CG ¹																																			
	1	2	3	4	5	6	7	8	9	10	11	12	13	14	15	16	17	18	19	20	21	22	23	24	25	26	27	28	29	30	31	32	33			
WB-001	2 ³	2	2	1	4	2	2	2	2	2	2	2	2	2	2	2	2	2	2	2	2	2	2	2	2	2	2	2	2	2	2	2	2	2	2	
WB-002	2	2	2	1	4	2	2	2	2	2	2	2	2	2	2	n. ⁴	2	2	2	2	2	2	2	2	2	2	2	2	2	2	2	2	2	2	2	
WB-003	2	2	2	2	4	2	2	n.	2	2	2	2	2	2	2	2	2	2	2	2	2	2	2	2	2	2	2	2	2	2	2	2	2	2	2	
WB-007	2	2	2	2	4	2	2	2	2	2	2	2	2	2	2	2	2	2	2	2	2	2	2	2	2	2	2	2	2	2	2	2	2	2	2	
WB-008	2	2	2	1	4	2	2	1	1	2	2	2	2	2	2	1	2	2	2	2	2	2	2	2	2	2	2	2	2	2	2	2	2	2	2	
WB-009	2	2	2	1	4	2	2	1	1	2	2	2	2	2	2	1	2	2	2	2	2	2	2	2	2	2	2	2	2	2	2	2	2	2	2	
WB-010	2	2	2	1	4	2	2	1	1	2	2	2	2	2	2	2	2	2	2	2	2	2	2	2	2	2	2	2	2	2	2	2	2	2	2	
WB-011	2	2	2	1	4	2	2	2	2	2	2	2	2	2	2	2	2	2	2	2	2	2	2	2	2	2	2	2	2	2	2	2	2	2	2	
WB-012	2	2	2	1	4	2	2	2	2	2	2	2	2	2	2	2	2	2	2	2	2	2	2	2	2	2	2	2	2	2	2	2	2	2	2	
WB-013	2	2	2	1	4	2	2	1	1	2	2	2	2	2	2	2	2	2	2	2	2	2	2	2	2	2	2	2	2	2	2	2	2	2	2	
WB-014	2	2	2	1	4	2	2	2	2	2	2	2	2	2	2	2	2	2	2	2	2	2	2	2	2	2	2	2	2	2	2	2	2	2	2	
WB-020	2	2	2	1	4	2	2	2	2	2	2	2	2	2	2	2	2	2	2	2	2	2	2	2	2	2	2	2	2	2	2	2	2	2	2	
WB-022	2	2	2	1	4	1	2	2	2	2	2	n.	2	2	2	2	1	2	2	2	2	2	2	2	2	2	2	2	2	2	2	2	2	2	2	
WB-024	2	2	2	1	4	2	2	2	2	2	2	2	2	2	2	2	2	2	2	2	2	2	2	2	2	2	n.	2	2	2	2	2	2	2	2	
WB-026	2	2	2	1	4	2	2	2	2	2	2	2	2	2	2	1	2	2	2	2	2	2	2	2	2	2	2	2	2	2	2	2	2	2	2	
WB-027	2	2	2	1	4	2	2	2	2	2	2	2	2	2	2	2	2	2	2	2	2	2	2	2	2	2	2	2	2	2	2	2	2	2	2	
WB-028	2	2	2	1	4	2	2	1	1	2	2	2	2	2	2	1	2	2	2	2	2	2	2	2	2	2	2	2	2	2	2	2	2	2	2	
WB-031	2	2	2	2	4	2	2	1	n.	2	2	2	2	2	2	2	2	n.	2	2	2	2	2	2	2	2	2	2	2	2	2	2	2	2	2	
WB-039	2	2	2	2	4	2	2	1	1	2	2	2	2	2	2	2	2	2	2	2	1	1	1	1	1	1	1	1	1	1	1	1	1	1	1	
WB-040	2	1	1	1	1	2	2	2	2	2	2	1	2	1	2	1	2	2	2	1	2	2	2	2	2	n.	2	2	2	2	2	2	2	n.	2	2
WB-042	2	1	2	1	2	1	2	2	2	2	2	2	2	2	1	2	2	2	2	2	2	2	2	2	2	2	2	2	2	2	2	2	2	2	2	1

Table B 7 (continued)

Genotype	WB-CG ¹																																		
	1	2	3	4	5	6	7	8	9	10	11	12	13	14	15	16	17	18	19	20	21	22	23	24	25	26	27	28	29	30	31	32	33		
1H ²	1H	2H	2H	2H	3H	3H	3H	3H	3H	4H	4H	4H	4H	4H	4H	5H	5H	5H	5H	5H	5H	5H	5H	5H	5H	5H	5H	5H	5H	5H	5H	5H	6H	6H	
WB-045	2 ³	2	1	4	2	2	2	1	1	2	2	2	2	2	2	2	2	2	2	2	2	2	2	2	2	2	2	2	2	2	2	2	2	2	2
WB-047	2	2	2	1	4	2	2	n. ⁴	2	2	2	2	2	2	2	2	2	2	2	2	2	2	2	2	2	2	2	2	2	n.	2	2	2	2	2
WB-048	2	1	2	1	2	2	2	2	2	2	2	2	2	2	1	2	2	2	2	2	2	2	2	2	2	2	2	2	2	2	n.	2	2	2	1
WB-049	2	1	n.	1	n.	n.	2	2	2	2	1	2	2	2	1	2	2	2	2	2	2	2	2	2	2	2	2	2	2	n.	2	2	2	2	1
WB-051	2	2	2	1	n.	1	2	2	2	2	2	2	2	2	2	2	2	2	2	2	2	2	2	2	2	2	2	2	2	2	2	2	2	2	2
WB-052	2	1	1	2	4	1	2	2	2	1	2	1	1	1	1	1	1	1	1	1	1	1	1	1	1	1	1	1	1	1	1	1	1	1	2
WB-054	2	2	1	1	1	n.	2	2	2	1	2	1	1	2	2	2	1	1	1	2	1	1	1	1	1	1	2	2	2	2	2	2	2	2	1
WB-055	2	1	1	n	n.	1	2	2	2	1	2	1	1	1	1	2	1	1	1	1	1	1	1	1	1	1	1	1	1	1	1	1	1	1	2
WB-056	2	1	1	2	4	2	2	2	2	1	2	1	1	1	1	1	1	1	2	1	1	1	1	1	1	1	1	1	1	1	1	1	1	1	2
WB-058	2	2	2	2	4	2	2	2	2	2	2	2	2	2	2	2	2	2	2	2	2	2	n.	2	2	2	2	2	2	2	2	2	2	2	2
WB-060	2	1	1	1	n.	2	2	2	2	2	1	2	2	2	1	2	2	2	2	2	2	2	2	2	2	2	2	2	2	2	2	2	2	2	1
WB-061	2	2	2	2	1	2	2	2	2	2	2	2	2	2	2	2	2	2	2	2	2	2	2	2	2	2	2	2	2	2	2	2	2	2	1
WB-063	2	2	2	2	4	1	2	2	2	2	2	2	2	2	2	2	2	2	2	2	2	2	2	2	2	2	2	2	2	2	2	2	2	2	1
WB-066	2	2	2	1	4	2	1	2	2	2	2	2	2	2	2	1	2	2	2	2	2	2	2	2	2	2	2	2	2	2	2	2	2	2	2
WB-069	1	2	2	2	4	2	2	1	1	2	2	2	2	2	2	1	2	2	2	2	2	2	2	2	2	2	2	2	2	2	2	2	2	2	2
WB-070	2	2	2	1	4	n.	2	2	2	2	2	2	2	2	1	2	2	2	2	2	2	2	2	2	2	2	2	2	2	2	2	2	2	2	2
WB-074	2	1	n.	2	1	2	2	2	2	1	2	2	1	2	2	1	1	1	1	2	1	1	1	1	1	1	1	1	1	1	1	1	1	1	2
WB-091	2	2	2	2	4	1	2	2	2	2	2	1	2	1	1	2	2	2	2	2	2	2	2	2	2	2	n.	2	2	2	2	2	2	2	2
WB-094	2	2	2	1	4	2	1	2	2	2	2	2	2	2	2	2	2	2	2	2	2	2	2	2	2	2	2	2	2	2	2	2	2	2	2
WB-099	2	2	2	2	4	2	2	2	2	2	2	n.	2	2	2	1	2	2	2	2	2	2	2	2	2	2	2	2	2	2	2	2	2	2	2
WB-101	2	2	2	2	4	2	2	2	2	2	2	2	2	2	2	2	2	2	2	2	2	2	2	2	2	2	2	2	2	2	2	2	2	2	2

Table B 7 (continued)

Genotype	WB-CG ¹																																				
	1	2	3	4	5	6	7	8	9	10	11	12	13	14	15	16	17	18	19	20	21	22	23	24	25	26	27	28	29	30	31	32	33				
WB-102	2 ³	2	2	2	4	2	2	1	1	2	2	1	2	2	2	2	2	2	2	1	1	2	2	2	2	2	2	2	2	2	2	2	2	2	2		
WB-106	2	2	2	2	4	2	2	1	1	2	2	1	2	2	2	2	2	2	2	1	1	1	1	1	1	1	1	1	1	1	1	1	1	1	2		
WB-111	2	n. ⁴	2	1	4	2	2	2	2	2	2	1	2	2	2	1	2	2	2	2	2	2	2	2	2	2	2	2	2	2	2	2	2	2	2		
WB-113	2	2	2	1	4	2	n.	2	2	2	2	2	2	2	2	1	2	2	2	2	2	2	2	2	2	2	2	2	2	2	2	2	2	2	2		
WB-114	2	2	2	1	4	2	2	2	2	2	2	n.	2	2	2	2	2	2	2	2	2	2	2	2	2	2	2	2	2	2	2	2	2	2	2		
WB-119	1	2	2	2	1	2	2	2	2	2	2	2	2	2	2	2	2	2	2	2	2	2	2	n.	n.	n.	2	2	2	2	2	2	2	n.	2		
WB-120	2	2	2	2	4	2	2	2	2	2	2	2	2	2	2	2	2	2	2	2	2	2	2	2	2	2	2	2	2	2	2	2	2	2	2		
WB-121	2	2	2	2	4	2	2	2	2	2	2	2	2	2	2	2	2	2	2	2	2	2	2	2	2	2	2	2	2	2	2	2	2	2	2		
WB-123	2	2	2	2	4	2	2	2	2	2	2	2	2	2	2	2	2	2	2	2	2	2	2	2	2	2	2	2	2	2	2	2	2	2	2		
WB-126	2	2	2	2	4	2	2	2	2	2	2	2	2	2	2	1	2	2	2	2	2	2	2	2	2	2	2	2	2	2	2	2	2	2	2		
WB-128	2	2	2	2	4	2	2	2	2	2	2	2	2	2	2	2	2	2	2	2	2	2	2	2	2	2	2	2	2	2	2	2	2	2	2		
WB-130	2	1	2	2	2	2	2	2	2	2	2	2	2	2	2	2	2	2	2	2	2	2	2	2	2	2	2	2	2	2	2	2	n.	2	2		
WB-131	2	2	2	2	4	2	2	2	2	2	2	2	2	2	2	2	2	2	2	2	2	2	2	2	2	2	2	2	2	2	2	2	2	2	2	2	
WB-133	2	1	n.	1	2	2	2	2	2	2	1	2	2	2	1	2	2	2	2	2	2	2	2	2	2	2	2	2	2	2	2	2	2	2	2	1	
WB-135	2	2	2	2	1	1	2	2	2	2	2	2	2	2	2	2	2	2	2	2	2	2	2	2	2	2	2	2	2	2	2	2	2	2	2	2	
WB-137	1	1	1	1	4	2	1	1	1	1	2	1	1	1	1	1	1	1	1	1	1	2	1	1	1	1	1	1	1	1	1	1	1	1	1	2	
WB-138	2	2	2	2	1	2	2	2	2	2	2	2	2	2	2	2	2	2	2	2	2	2	2	2	2	2	2	2	2	2	2	2	2	2	2	2	
WB-142	2	2	2	2	1	2	n.	2	2	2	2	2	2	2	2	2	2	2	2	2	2	2	2	2	2	2	2	2	2	2	2	2	2	2	2	2	
WB-143	2	2	2	2	1	2	2	2	2	2	2	2	2	2	2	2	2	2	2	2	2	2	n.	2	2	2	2	2	2	2	2	2	2	2	2	2	
WB-144	2	2	2	2	1	2	2	2	2	2	2	2	2	2	2	2	2	2	2	2	2	2	2	2	2	2	2	2	2	2	2	2	2	2	2	2	
WB-147	2	2	2	1	4	2	2	2	2	2	2	1	2	2	2	2	2	2	2	2	2	2	2	2	2	2	2	2	2	2	2	2	2	2	2	2	1

Table B 7 (continued)

Genotype	WB-CG ¹																																			
	1	2	3	4	5	6	7	8	9	10	11	12	13	14	15	16	17	18	19	20	21	22	23	24	25	26	27	28	29	30	31	32	33			
WB-148	2 ³	2	2	1	4	2	2	2	2	2	1	2	2	2	2	2	2	2	2	2	2	2	2	2	2	2	2	2	2	2	2	2	2	2	1	
WB-149	2	2	2	2	4	2	2	2	2	2	2	2	2	2	2	1	2	2	2	2	2	2	2	2	2	2	2	2	2	2	2	2	2	2	2	
WB-151	2	2	2	2	4	2	2	2	2	2	2	2	2	2	2	2	2	2	2	2	2	2	2	2	2	2	2	2	2	2	2	2	2	2	2	
WB-152	2	1	2	1	4	2	2	2	2	2	2	1	2	2	1	2	2	2	1	2	2	2	2	2	2	2	2	2	2	2	n. ⁴	2	2	2	1	
WB-153	2	2	2	2	1	2	2	2	2	2	2	2	2	2	2	2	2	2	2	2	2	2	2	2	2	2	2	2	2	2	2	2	2	2	2	
WB-154	2	2	2	2	1	2	2	2	2	2	2	2	2	2	2	2	2	2	2	2	2	2	2	2	2	2	2	2	2	2	2	2	2	2	1	2
WB-156	2	2	2	2	1	2	2	2	2	2	2	2	2	2	2	2	2	2	2	2	2	2	2	2	2	2	2	2	2	2	2	2	2	2	1	2
WB-157	2	2	2	2	1	2	2	2	2	2	2	2	2	2	2	2	2	2	2	2	2	2	2	2	2	2	2	2	2	2	2	2	2	2	1	2
WB-158	2	2	2	1	4	2	2	2	2	2	2	2	2	2	2	2	2	2	2	2	2	2	2	2	2	2	2	2	2	2	2	2	2	2	2	2
WB-159	2	2	2	2	4	2	2	2	2	2	2	2	2	2	2	1	2	2	2	2	2	2	2	2	2	2	2	2	2	2	2	2	2	2	2	2
WB-160	2	1	2	1	4	2	2	1	1	1	2	2	1	2	2	2	2	2	2	2	2	2	2	2	2	2	2	2	2	2	2	2	n.	2	2	2
WB-161	2	2	1	1	4	1	2	1	1	2	2	1	2	2	2	1	1	1	1	1	2	2	2	2	2	2	2	2	2	2	2	2	2	2	2	2
WB-162	2	2	2	1	4	2	2	2	2	2	2	2	2	2	2	2	2	2	2	2	2	2	2	2	2	2	2	2	2	2	2	2	2	2	2	2
WB-165	2	2	2	2	4	2	2	2	2	2	2	2	2	2	2	1	2	2	2	2	2	2	2	2	2	2	2	2	2	2	2	2	2	2	2	2
WB-166	2	2	2	2	4	2	2	2	2	2	2	2	2	2	2	2	2	2	2	2	2	2	2	2	2	2	n.	2	2	2	2	2	2	2	2	2
WB-167	2	2	2	1	4	2	2	2	2	2	2	2	2	2	2	1	2	2	2	2	2	2	2	2	2	2	2	2	2	2	2	2	2	2	2	2
WB-168	2	2	2	1	4	2	2	1	1	2	2	2	2	2	2	2	2	2	2	2	2	2	2	2	2	2	2	2	2	2	2	n.	2	2	2	2
WB-169	2	2	2	2	4	2	2	2	2	2	2	2	2	2	2	2	2	2	2	2	2	2	2	2	2	2	2	2	2	2	2	2	2	2	2	2
WB-170	2	2	2	2	4	2	2	2	2	2	2	2	2	2	2	2	2	2	2	2	2	2	2	2	2	2	2	2	2	2	2	2	2	2	2	2
WB-175	2	1	2	2	4	2	2	2	2	2	2	2	2	2	2	1	2	2	2	2	2	2	2	2	2	2	2	2	2	2	2	2	2	2	2	2
WB-181	2	2	2	2	4	2	2	2	2	2	2	2	2	2	2	1	2	2	2	2	2	2	2	2	2	2	2	2	2	2	2	2	2	2	2	2

Table B 7 (continued)

Genotype	WB-CG ¹																																		
	1	2	3	4	5	6	7	8	9	10	11	12	13	14	15	16	17	18	19	20	21	22	23	24	25	26	27	28	29	30	31	32	33		
WB-183	2 ³	2	2	2	4	2	2	2	2	2	2	2	2	2	2	1	2	2	2	2	1	2	2	2	2	2	2	2	2	2	2	2	2	2	2
WB-185	2	2	2	2	4	2	2	1	1	2	2	2	2	2	2	1	2	2	2	1	1	1	1	1	1	1	1	1	1	1	1	1	1	1	2
WB-186	2	2	2	2	4	2	2	2	2	2	2	2	2	2	2	1	2	2	2	2	2	2	2	2	2	2	2	2	2	2	2	2	2	2	2
WB-187	2	2	2	2	4	2	2	2	2	2	2	2	2	2	2	1	2	2	2	2	2	2	2	2	2	2	2	2	2	2	2	2	2	2	2
WB-188	2	2	2	2	4	2	2	2	2	2	2	2	2	2	2	2	2	2	2	2	2	2	2	2	2	2	2	2	2	2	2	2	2	2	2
WB-189	2	2	2	2	4	2	2	2	2	2	2	2	2	2	2	1	2	2	2	2	2	2	2	2	2	2	2	2	2	2	2	2	2	2	2
WB-191	2	2	2	1	4	2	2	2	2	2	2	2	2	2	2	2	2	2	2	2	2	2	2	2	2	2	2	2	2	2	2	2	2	2	2
WB-192	2	2	2	2	4	2	2	2	2	2	2	2	2	2	2	1	2	2	2	2	2	2	2	2	2	2	2	2	2	2	2	2	2	2	2
WB-193	2	2	2	2	4	2	2	2	2	2	2	2	2	2	2	1	2	2	2	2	2	2	2	2	2	2	2	2	2	2	2	2	2	2	2
WB-194	2	2	2	2	4	2	2	2	2	2	2	2	2	2	2	1	2	2	2	2	2	2	2	2	2	2	2	2	2	2	2	2	2	2	2
WB-195	2	2	2	2	4	2	2	1	1	2	2	2	2	2	2	1	2	2	2	2	1	1	1	1	n ⁴	1	1	1	1	1	1	1	1	1	2
WB-196	2	2	2	2	4	2	2	2	2	2	2	2	2	2	2	1	2	2	2	2	2	2	2	2	2	2	2	2	2	2	2	2	2	2	2
WB-199	2	2	2	2	4	2	2	2	2	2	2	2	2	2	2	1	2	2	2	2	2	2	2	2	2	2	2	2	2	2	2	2	2	2	2
WB-200	2	2	2	2	4	2	2	2	2	2	2	2	2	2	2	1	2	2	2	2	2	2	2	2	2	2	2	2	2	2	2	2	2	2	2
WB-201	2	2	2	2	4	2	2	2	2	2	2	2	2	2	2	1	2	2	2	2	2	2	2	2	2	2	2	2	2	2	2	2	2	2	2
WB-203	2	2	2	2	4	2	2	2	2	2	2	2	2	2	2	1	2	2	2	2	2	2	2	2	2	2	2	2	2	2	2	2	2	2	2
WB-204	2	2	2	2	4	2	2	2	2	2	2	2	2	2	2	1	2	2	2	2	2	2	2	2	2	2	2	2	2	2	2	2	2	2	2
WB-206	2	2	2	2	4	2	2	2	2	2	2	2	2	2	2	1	2	2	2	2	2	2	2	2	2	2	2	2	2	2	2	2	2	2	2
WB-208	2	2	2	2	4	2	2	2	2	2	2	2	2	2	2	1	2	2	2	2	2	2	2	2	2	2	2	2	2	2	2	2	2	2	2
WB-210	2	2	2	2	4	2	2	2	2	2	2	2	2	2	2	1	2	2	2	2	2	2	2	2	2	2	2	2	2	2	2	2	2	2	2
WB-211	2	2	2	2	1	2	2	1	1	2	2	2	2	2	2	1	2	2	2	2	2	2	2	2	2	2	2	2	2	2	2	2	2	2	2

Table B 7 (continued)

		WB-CG ¹																																		
		1	2	3	4	5	6	7	8	9	10	11	12	13	14	15	16	17	18	19	20	21	22	23	24	25	26	27	28	29	30	31	32	33		
Genotype	1H ² 1H	2H	2H	2H	3H	3H	3H	3H	3H	3H	4H	4H	4H	4H	4H	4H	4H	5H	5H	5H	5H	5H	5H	5H	5H	5H	5H	5H	5H	5H	5H	5H	6H	6H		
WB-214	2 ³	1	2	2	4	2	2	2	2	2	2	2	2	2	2	2	1	2	2	2	2	2	2	2	2	2	2	2	2	2	2	2	2	2	2	
WB-217	2	2	2	2	4	2	2	1	1	2	2	2	2	2	2	2	1	2	2	2	2	2	2	2	2	2	2	2	2	2	2	2	2	2	2	
WB-218	2	2	2	2	4	2	2	2	2	2	2	2	2	2	2	2	1	2	2	2	2	2	2	2	2	2	2	2	2	2	2	2	2	2	2	
WB-220	2	2	2	2	4	2	2	1	n. ⁴	2	2	2	2	2	2	2	1	2	2	2	2	2	2	2	2	2	n.	2	2	2	2	2	2	2	2	
WB-222	2	2	2	2	1	2	2	1	1	2	2	2	2	2	2	2	1	2	2	2	2	2	2	2	2	2	2	2	2	2	2	2	2	1	2	
WB-224	2	2	2	2	4	2	2	2	2	2	2	2	2	2	2	2	1	2	2	2	2	2	2	2	2	2	2	2	2	2	2	2	2	2	2	
WB-227	2	2	2	2	4	2	2	2	2	2	2	2	2	2	2	2	1	2	2	2	2	2	2	2	2	2	2	2	2	2	2	2	2	2	2	
WB-228	2	2	2	2	4	2	2	1	1	2	2	2	2	2	2	2	1	2	2	2	2	2	2	2	2	2	2	2	2	2	2	2	2	2	2	
WB-229	2	2	2	2	4	2	2	1	1	2	2	2	2	2	2	2	1	2	2	2	2	2	2	2	2	2	2	2	2	2	2	2	2	2	2	
WB-232	2	2	2	2	4	2	2	2	2	2	2	2	2	2	2	2	1	2	2	2	2	2	2	2	2	2	2	2	2	2	2	2	2	2	2	
WB-236	2	2	2	2	1	2	2	2	2	n.	2	2	2	2	2	2	1	2	2	2	2	2	2	2	2	2	2	2	2	2	2	2	2	2	2	
WB-237	2	2	2	2	4	2	2	1	1	2	2	2	2	2	2	2	1	2	2	2	2	2	2	2	2	2	2	2	2	2	2	2	2	2	2	
WB-241	2	2	2	2	4	2	2	2	2	2	2	2	2	2	2	2	1	2	2	2	2	2	2	2	2	2	2	2	2	2	n.	2	2	2	2	
WB-242	1	2	2	2	4	2	2	2	2	2	2	2	2	2	2	2	2	2	2	2	2	2	2	2	2	2	n.	2	2	2	2	2	2	n.	2	2
WB-244	2	2	2	2	4	2	2	2	2	2	2	2	2	2	2	2	1	2	2	2	2	2	2	2	2	2	2	2	2	2	2	2	2	2	2	2
WB-247	2	2	2	1	4	2	2	1	1	2	2	2	2	2	2	2	2	2	2	2	2	2	2	2	2	2	2	2	2	2	2	2	2	2	2	2
WB-249	2	2	2	2	4	2	2	2	2	2	2	2	2	2	2	2	2	2	2	2	2	2	2	2	2	2	2	2	2	2	2	2	2	2	2	2
WB-250	2	2	2	n.	4	2	2	2	2	2	2	2	2	2	2	2	2	2	2	2	2	2	2	2	2	2	2	2	2	2	2	2	2	2	2	2
WB-252	2	2	2	2	4	2	2	1	1	2	2	2	2	2	2	2	1	2	2	2	2	2	2	2	2	2	2	2	2	2	2	2	2	2	2	2
WB-253	2	2	2	2	4	2	2	1	1	2	2	2	2	2	2	2	1	2	2	2	2	2	2	2	2	2	2	2	2	2	2	2	2	2	2	2
WB-258	2	2	2	2	4	2	2	2	2	2	2	2	2	2	2	2	n.	2	2	2	2	2	2	2	2	2	2	2	2	2	2	2	2	2	2	2

Table B 7 (continued)

Genotype	WB-CG ¹																																			
	1	2	3	4	5	6	7	8	9	10	11	12	13	14	15	16	17	18	19	20	21	22	23	24	25	26	27	28	29	30	31	32	33			
WB-259	2 ³	2	2	2	4	2	2	1	1	2	2	2	2	2	2	1	2	2	2	2	2	2	2	2	2	2	2	2	2	2	2	2	2	2	2	
WB-260	2	2	2	2	4	2	2	2	2	2	2	2	2	2	2	1	2	2	2	2	2	2	2	2	2	2	2	2	2	2	2	2	2	2	2	
WB-261	2	2	2	2	4	2	2	2	2	2	2	2	2	2	2	n. ⁴	2	2	2	2	2	2	2	2	2	2	2	2	2	2	2	2	2	2	2	
WB-262	2	2	1	1	4	2	2	2	2	2	2	1	2	2	2	1	2	2	2	2	2	2	2	2	2	2	2	2	2	2	2	2	2	2	2	
WB-263	1	2	2	1	4	1	2	1	1	1	2	2	2	2	2	2	2	2	2	2	2	2	2	2	2	2	n.	2	2	2	2	2	2	2	2	
WB-269	2	2	2	2	1	2	2	2	2	2	2	2	2	2	2	1	2	2	2	2	2	2	2	2	2	2	2	2	2	2	2	2	2	2	2	
WB-270	2	2	2	2	4	2	2	2	2	2	2	2	2	2	2	2	2	2	2	2	2	2	2	2	2	2	2	2	2	2	2	2	2	2	2	
WB-273	2	2	2	2	4	2	2	2	2	2	2	2	2	2	2	2	2	2	2	2	2	2	2	2	2	2	2	2	2	2	2	2	2	2	2	
WB-274	2	2	2	2	4	2	2	2	2	2	2	2	2	2	2	2	2	2	2	2	2	2	2	2	2	2	2	2	2	2	2	2	2	2	2	
WB-276	2	2	2	2	4	2	2	2	2	2	2	2	2	2	2	1	2	2	2	2	2	2	2	2	2	2	2	2	2	2	2	2	2	2	2	2
WB-277	2	2	2	2	4	2	2	2	2	2	2	2	2	2	2	2	2	2	2	2	2	2	2	2	2	2	2	2	2	2	2	2	2	2	2	2
WB-279	2	2	2	2	4	2	2	1	1	1	2	2	2	2	2	2	2	2	2	2	2	2	2	2	2	2	2	n.	2	2	2	2	2	2	2	2
WB-280	2	2	2	2	4	2	2	1	1	1	2	2	2	2	2	2	2	2	2	2	2	2	2	2	2	2	2	2	2	2	2	2	2	2	2	2
WB-281	2	2	2	2	4	2	2	2	2	2	2	2	2	2	2	2	2	2	2	2	2	2	2	2	2	2	2	2	2	2	2	2	2	2	2	2
WB-282	2	2	2	2	4	1	2	1	1	1	2	2	2	2	2	2	2	2	2	2	2	2	n.	2	2	2	2	2	2	2	2	2	2	2	2	2
WB-287	2	2	2	2	4	2	2	2	2	2	2	2	2	2	2	2	2	2	2	2	2	2	2	2	2	2	2	2	2	2	2	2	2	2	2	2
WB-290	2	2	2	2	4	2	2	2	2	2	2	2	2	2	2	2	2	2	2	2	2	2	2	2	2	2	2	2	2	2	2	2	2	2	2	2
WB-297	2	1	2	2	1	2	2	1	1	1	2	2	2	2	2	2	2	2	2	2	2	2	2	2	2	2	2	n.	2	2	2	2	2	2	2	2
WB-299	2	2	2	2	1	2	2	2	2	2	2	2	2	2	2	1	2	2	2	2	2	2	2	2	2	2	2	2	2	2	2	2	2	2	2	2
WB-300	2	2	2	2	1	2	2	2	2	2	2	2	2	2	2	1	2	2	2	2	2	2	2	2	2	2	2	2	2	2	2	2	2	2	2	2
WB-302	2	2	2	2	4	2	2	1	1	1	2	2	2	2	2	2	2	2	2	2	2	2	2	2	2	2	2	2	2	2	2	2	2	2	2	2

Table B 7 (continued)

		WB-CG ¹																																		
		1	2	3	4	5	6	7	8	9	10	11	12	13	14	15	16	17	18	19	20	21	22	23	24	25	26	27	28	29	30	31	32	33		
Genotype	1H ² 1H	2H	2H	2H	3H	3H	3H	3H	3H	3H	4H	4H	4H	4H	4H	4H	4H	5H	5H	5H	5H	5H	5H	5H	5H	5H	5H	5H	5H	5H	5H	5H	6H	6H		
WB-306	1 ³	2	2	2	4	2	2	1	1	2	2	2	2	2	2	2	1	2	2	2	1	1	1	1	1	1	1	1	1	1	1	1	1	2	2	
WB-308	1	2	2	2	4	2	2	1	1	2	2	2	2	2	1	1	1	2	2	2	1	1	1	1	1	1	1	1	1	1	1	1	1	2	2	
WB-311	2	2	2	2	4	2	2	2	2	2	2	2	2	2	2	2	2	2	2	2	2	2	2	2	2	2	2	2	2	2	2	2	2	2	2	2
WB-312	2	2	2	2	4	2	2	2	2	2	2	2	2	2	2	2	1	2	2	2	2	2	2	2	2	2	2	2	2	2	2	2	2	2	2	2
WB-315	2	2	2	2	4	2	2	2	1	n. ⁴	2	2	2	2	2	2	1	2	2	2	2	2	2	2	2	2	2	2	2	2	2	2	2	2	2	2
WB-316	2	2	2	2	4	2	2	2	1	1	n.	2	2	2	2	2	1	2	2	2	1	2	2	2	2	2	2	2	2	2	2	2	2	2	2	2
WB-317	2	2	2	2	4	2	2	2	2	2	2	2	2	2	2	2	2	2	2	2	2	n.	2	2	2	2	2	2	2	2	2	2	2	2	2	2
WB-319	2	2	2	2	4	2	2	2	2	2	2	2	2	2	2	2	2	2	2	2	2	2	2	2	2	2	2	2	2	2	2	2	2	2	2	2
WB-320	2	2	2	2	4	2	2	2	2	2	2	2	2	2	2	2	2	2	2	2	2	n.	2	2	2	2	2	2	2	2	2	2	2	2	2	2
WB-321	2	1	2	n.	n.	2	2	2	2	2	2	2	2	2	2	2	2	2	2	2	2	2	2	2	2	2	2	2	2	2	2	2	2	2	1	n.
WB-324	2	2	2	1	4	1	n.	2	2	2	2	2	2	2	2	2	2	2	2	2	2	2	2	2	2	2	2	2	2	2	2	2	2	2	2	2
WB-325	2	2	2	n.	4	2	2	2	2	2	2	2	2	2	2	2	1	2	2	2	2	2	2	2	2	2	2	2	2	2	2	2	2	2	2	2
WB-327	2	2	2	2	2	2	2	2	2	2	2	2	2	2	2	2	2	2	2	2	2	2	2	2	2	2	2	2	2	2	2	2	2	2	2	2
WB-329	1	2	2	2	1	2	2	2	2	2	2	2	2	2	2	2	2	2	2	2	2	2	2	2	2	2	n.	2	2	2	2	2	2	2	1	2
WB-333	2	2	2	2	4	2	2	2	2	2	2	2	2	2	2	2	2	2	2	2	2	2	2	2	2	2	2	2	2	2	2	2	2	2	2	2
WB-340	2	2	2	2	4	2	2	2	2	2	2	2	2	2	2	2	2	2	2	2	2	2	2	2	2	2	2	2	2	2	2	2	2	2	2	2
WB-346	2	2	2	2	1	2	2	2	2	2	2	2	2	2	2	2	2	2	2	2	2	2	2	2	2	2	2	2	2	2	2	2	2	2	2	2
WB-349	2	2	2	2	4	2	2	2	1	1	2	2	2	2	2	2	2	2	2	2	2	2	2	2	2	2	2	2	n.	2	2	2	2	2	2	2
WB-350	2	2	2	1	4	1	2	2	2	2	2	2	2	2	2	2	2	2	2	2	2	2	2	2	2	2	2	2	2	2	2	2	2	2	2	2
WB-351	2	2	2	1	4	2	2	2	2	2	2	2	2	2	2	2	1	2	2	2	2	2	2	2	2	2	2	2	2	2	2	2	2	2	2	2
WB-355	2	2	2	1	4	2	2	2	2	2	2	2	2	2	2	2	2	2	2	2	2	2	2	2	2	2	2	2	2	2	2	2	2	2	2	2

Table B 7 (continued)

Genotype	WB-CG ¹																																				
	1	2	3	4	5	6	7	8	9	10	11	12	13	14	15	16	17	18	19	20	21	22	23	24	25	26	27	28	29	30	31	32	33				
WB-356	1H ²	2	2	2	1	2	2	2	2	2	2	2	2	2	2	2	2	2	2	2	2	2	2	2	n. ⁴	2	2	2	2	2	2	2	2	2			
WB-357	2	2	2	2	4	2	2	2	2	2	2	2	2	2	2	2	2	2	2	2	2	2	2	2	2	2	2	2	2	2	2	2	2	2			
WB-360	2	2	n.	2	n	2	2	2	2	n.	2	2	1	2	2	2	2	2	2	2	2	n.	1	n.	2	2	2	2	2	2	2	2	2	2			
WB-363	2	2	2	n.	4	2	2	2	2	n.	2	2	2	2	2	2	2	2	2	2	2	2	2	2	2	2	2	2	2	2	2	2	2	2			
WB-365	2	1	2	2	4	2	2	2	2	2	1	2	1	2	1	2	2	2	2	2	2	2	2	2	2	n.	2	2	2	2	2	2	2	2	1		
WB-370	2	2	2	1	4	1	2	1	1	2	2	2	2	2	2	2	2	2	2	2	2	2	2	2	2	2	2	2	2	2	2	2	2	2	2		
WB-372	2	1	1	2	4	1	2	2	2	1	1	1	1	1	1	1	1	1	1	1	1	1	1	1	1	1	1	1	1	1	1	1	1	2	2		
WB-374	2	2	2	2	4	2	2	1	1	2	2	2	2	2	2	2	2	2	2	2	2	2	2	2	2	2	2	2	2	2	2	2	2	2	2	2	
WB-376	2	2	2	2	4	2	2	1	1	2	2	2	2	2	2	2	2	2	2	2	2	2	2	2	2	2	2	2	2	2	2	2	2	2	2	2	
WB-377	2	2	2	2	4	2	2	1	1	2	2	2	2	2	2	2	2	2	2	2	2	2	2	2	2	2	2	2	2	2	2	2	2	2	2	2	
WB-400	2	1	1	2	1	1	2	2	2	n.	1	1	1	2	2	1	n.	1	1	1	1	1	1	1	1	1	1	1	1	1	1	n.	2	2	2		
WB-401	2	1	1	2	4	1	2	2	2	1	2	1	1	1	n.	1	1	1	1	1	1	1	1	1	1	1	1	1	1	1	1	1	1	1	2	2	
WB-424	2	2	2	2	4	2	2	2	2	2	2	2	2	2	2	2	2	2	2	2	2	2	2	2	2	2	2	2	2	2	2	2	2	2	2	2	2
WB-427	2	2	n.	1	4	2	2	2	2	2	2	2	2	1	n.	2	2	2	2	2	2	2	2	2	2	2	2	n.	2	2	2	2	2	2	2	2	
WB-428	2	2	1	1	4	n.	1	2	2	2	2	2	2	1	1	1	1	n.	1	2	2	2	2	2	2	2	2	2	2	2	2	2	2	2	2	2	
WB-446	2	2	2	1	4	n.	1	2	2	2	2	2	2	2	2	2	2	2	2	2	2	2	2	2	2	2	2	2	2	2	2	2	2	2	2	2	
WB-449	2	2	2	1	4	2	2	2	2	2	2	2	2	2	2	2	2	2	2	2	2	2	2	2	2	2	2	2	2	2	2	2	2	2	2	2	
WB-450	2	2	2	1	4	2	1	1	1	2	2	2	2	2	2	2	2	2	2	2	2	2	2	2	2	2	2	2	2	2	2	2	2	2	2	2	
WB-454	2	2	2	2	4	2	2	2	2	2	2	2	2	2	2	2	2	2	2	2	2	2	2	2	2	2	2	2	2	2	2	2	2	2	2	2	
WB-456	2	2	2	1	4	2	2	2	2	2	2	2	2	2	2	2	2	2	2	2	2	2	2	2	2	2	2	2	2	2	2	2	2	2	2	n.	
WB-457	2	2	2	2	4	2	2	2	2	2	2	2	2	2	2	2	2	2	2	2	2	2	2	2	2	2	2	2	2	2	2	2	2	2	2	2	

Table B 7 (continued)

		WB-CG ¹																																		
		1	2	3	4	5	6	7	8	9	10	11	12	13	14	15	16	17	18	19	20	21	22	23	24	25	26	27	28	29	30	31	32	33		
Genotype	1H ²	1H	2H	2H	3H	3H	3H	3H	3H	3H	4H	4H	4H	4H	4H	4H	5H	5H	5H	5H	5H	5H	5H	5H	5H	5H	5H	5H	5H	5H	5H	5H	6H	6H		
WB-458	2 ³	2	2	2	4	2	2	2	2	2	2	2	2	2	2	2	2	2	2	2	2	2	2	2	2	2	2	2	2	2	2	2	2	2	2	
WB-460	2	1	1	2	1	n. ⁴	2	2	2	1	1	1	1	1	1	1	1	1	1	1	n.	1	1	1	1	1	1	1	1	1	1	1	1	2	2	
WB-462	2	1	1	2	4	1	2	2	2	1	2	1	1	1	2	2	1	1	1	1	1	1	1	1	1	1	1	1	1	1	1	1	1	2	2	
WB-465	2	1	1	1	4	1	2	2	2	1	1	1	1	1	2	2	1	1	1	1	1	1	1	1	1	1	1	1	1	1	1	1	1	2	1	
WB-467	2	2	2	2	4	2	2	2	2	2	2	2	2	2	2	2	1	2	2	2	2	2	2	2	2	2	2	2	2	2	2	2	2	2	2	
WB-469	2	2	1	1	4	2	2	2	2	2	2	2	2	2	2	2	2	2	2	2	2	2	2	2	2	2	n.	2	2	2	2	2	n.	2	2	
WB-472	2	1	1	1	4	1	1	2	2	1	2	2	1	2	1	2	2	2	2	2	1	1	n.	1	1	1	1	1	1	1	1	1	1	1	2	2
WB-473	2	1	1	1	4	2	1	1	n.	2	2	1	2	1	2	1	2	2	2	2	1	2	2	2	2	2	2	n.	2	2	2	2	2	2	1	
WB-476	2	2	2	1	4	1	1	1	1	1	2	2	2	2	2	2	2	2	2	2	2	2	2	2	2	2	2	2	2	2	2	2	2	2	2	
WB-478	2	2	2	1	4	1	1	2	2	1	2	2	2	2	2	2	1	2	2	2	2	2	2	2	2	2	2	2	2	2	2	2	2	2	2	
WB-483	1	1	1	2	4	2	1	1	2	1	1	1	n.	1	1	1	1	1	1	1	1	1	2	2	2	2	2	2	2	2	2	2	2	1	2	
WB-501	2	2	n.	2	3	2	2	2	2	2	2	2	2	2	2	1	1	2	2	2	2	2	2	2	2	2	n.	2	2	2	2	2	2	2	2	

¹ annotated candidate² corresponding chromosome number³ the defined alleles were numbered from 1-4⁴ alleles codified as n. could not be specified because of heterozygous single nucleotide polymorphism calls

Table B 8: Effect of the defined alleles on the infected leaf area

		Candidates			
		WB-CG_17	WB-CG_19	WB-CG_23	WB-CG_28
Allele 1	$\bar{\mu}^1$	22.89 %	24.76 %	28.38 %	24.24 %
	SD ²	12.26 %	11.38 %	15.58 %	13.12 %
	SEM ³	3.28 %	2.48 %	3.48 %	3.09 %
	n ⁴	14	21	20	18
	variation ⁵	23.4 %	31 %	16.7 %	27.3 %
Allele 2	$\bar{\mu}^1$	51.14 %	51.91 %	51.50 %	51.51 %
	SD ²	13.20 %	12.60 %	13.06 %	12.80 %
	SEM ³	0.97 %	0.94 %	0.98 %	0.95 %
	n ⁴	185	179	179	181

¹ mean value of the infected leaf area (in %)

² standard deviation of the infected leaf area (in %)

³ standard error of the mean of the infected leaf area (in %)

⁴ total number of genotypes

⁵ phenotypic variation which is explained by the allele

Acknowledgment

I want to express my sincere gratitude to my supervisor Dr. habil Patrick Schweizer. He gave me the chance to work on this interesting topic and to learn from him the work in an international research field in frame of the EU financed Whealbi project. He was always open for my ideas and provided me with constructive criticisms, support and valuable suggestions. I will be always grateful that he inspired me to go to science. Without his advice I would have never found the courage to choose this way and it is sad he never had the chance to see the final results of this study.

I would also express my deepest appreciation to Prof. Dr. Jochen C. Reif because he took the responsibility as my second supervisor. Especially, after Patrick's accident he was a great support and his continuous advice and encouragement helped me to finish this study. Additionally, I am grateful for the proof-reading of this thesis and the cooperation he initiated.

In frame of these cooperation, I want to thank Fang Liu for her contribution to the GWAS and Dr. Albert W. Schulthess for his support by the analysis of the data, in particular of the field trials. In addition, I very appreciated his valuable support and constructive criticism as my mentor. I could always ask questions and count on his advice. Furthermore, I want to thank him for the proof-reading of this thesis.

I would like to acknowledge Dr. Daniela Nowara for her help particularly in the beginning of my work. Without her guidance and support the first steps in the new environment would have been very difficult. Additionally, she also taught me essential methods which I used in this study and shared generously her experience and knowledge with me.

A special thanks goes to Dr. Kestin Flath from the JKI for the cooperation and the provision of the data of the large isolate test. I am grateful for the time she spent with me discussing the details of the results and her advice.

I would also express my appreciation to Carolin Stern from KWS Lochow for the cooperation in frame of the field trial.

Especially, I want to acknowledge Dr. habil Armin Djamei, the head of the new Biotrophy and Immunity group, for his support and advice regarding this thesis. I would like to thank Dr. Dimitar K. Douchkov and Stefanie Lück for their help and support by the data analysis, the cloning and the construct design. In addition, I want to appreciate the other group members of the former Pathogen Stress Genomics group for the positive atmosphere and the helpful discussions. Additionally, I am grateful for the technical support of the gardeners, mainly Kathrin Gramel-Koch and Kathrin Tiemann, concerning the greenhouse experiments and the field trial.

I would like to express my appreciation to the Whealbi consortium for the provision of the seeds and the exome capture data as well as for the support regarding the administrative questions.

A special thanks goes to my friends and former colleagues who helped me to find my place. Finally, I want to thank my family. Without the never-ending support of my mum, dad and sister this work would never have been possible.

Curriculum vitae

Name: Maria Pogoda
Date, place and country of birth: 06.08.1991 in Quedlinburg, Germany
Nationality: German
Gender: female

Education:

- 01/2016 to 10/2019 **Graduation** (Dr. rer. nat.)
Martin-Luther-University, Halle-Wittenberg

Thesis work has been carried out at the research group Pathogen Stress Genomics (PSG), now Biotrophy and Immunity (BIM) at the Leibniz Institute of Plant Genetics and Crop Plant Research (IPK)
- 10/2013 to 09/2015 **Master of Science, Biochemistry** (M.Sc. 120 LP)
Martin-Luther-University, Halle-Wittenberg (Sept. 2015)
- 10/2010 to 09/2013 **Bachelor of Science, Biochemistry** (B.Sc. 180 LP)
Martin-Luther-University, Halle-Wittenberg (Sept. 2013)

Professional experience:

- 01/2016 to 08/2019 **PhD student at the Leibniz Institute of Plant Genetics and Crop Plant Research (IPK)**
Department of Breeding Research
Research Group: Pathogen Stress Genomics & Biotrophy and Immunity

“Identification and validation of seedling powdery mildew resistance genes.”
- 03/2015 to 09/2015 **Master thesis in the Leibniz Institute for Plant Biochemistry (IPB)**
Department of Molecular Signal Processing
Research Group: Defense Metabolism/RNA Regulation

“Analysis of the role of the natural antisense long non-coding RNA encoded by the *At4g14548* gene from *Arabidopsis thaliana*”
- 03/2013 to 09/2013 **Bachelor thesis in the Leibniz Institute for Plant Biochemistry (IPB)**
Department of Cell and Metabolic Biology
Research Group: Jasmonate Function & Mycorrhiza

“Entwicklung der Staubblätter in Tomate: Pharmakologische Bestätigung der negativen Regulation von Ethylen und Jasmonate“

List of publications

J. Rajaraman, D. Douchkov, S. Lück, G. Hensel, D. Nowara, **M. Pogoda**, T. Rutten, T. Meitzel, J. Brassac, C. Höfle, R. Hüchelhoven, J. Klinkenberg, M. Trujillo, E. Bauer, T. Schmutzer, A. Himmelbach, M. Mascher, B. Lazzari, N. Stein, J. Kumlehn, Schweizer P. *Evolutionarily conserved partial gene duplication in the Triticeae tribe of grasses confers pathogen resistance*. Genome Biology (2018) 19:116
<https://doi.org/10.1186/s13059-018-1472-7>

Oral presentations and posters

- S. Höpfner, **M. Pogoda**, K. Seidel, J. Schuck, S-E. Beherns, S. Gago-Zachert
Deciphering the role of the natural antisense long non-coding RNA encoded by At4g14548 in IAA14 expression regulation. (Poster at the Plant Science Students Conference 2015)
- **M. Pogoda**, D. Nowara, P. Schweizer
Whealbi project: Mining for new powdery mildew resistance genes. (Poster at the Plant Science Students Conference 2016)
- **M. Pogoda**
Disease phenotyping of the Whealbi barley legacy collection. (Presentation at the Plant Science Students Conference 2017)
- **M. Pogoda**, F. Liu, J. Reif, P. Schweizer
From precision disease phenotyping to identification of quantitative powdery mildew resistance genes. (Poster at the German Plant Breeding Conference 2018)
- **M. Pogoda**, F. Liu, J. Reif, P. Schweizer
From precision disease phenotyping to identification of quantitative powdery mildew resistance genes. (Poster at the International Plant Immunity Symposium 2018)
- **M. Pogoda**
From precision disease phenotyping to identification of new powdery mildew resistance genes. (Presentation at the Plant Science Students Conference 2018)
- **M. Pogoda**
From disease phenotyping to identification of new powdery mildew resistance genes. (Presentation at the International Cereal Rusts and Powdery Mildews Conference 2018)

Declaration

I hereby declare that details above are true and correct to the best of my knowledge.

Place, date

Signature

Eidesstattliche Erklärung / *Declaration under oath*

Ich erkläre an Eides statt, dass ich die Arbeit selbstständig und ohne fremde Hilfe verfasst, keine anderen als die von mir angegebenen Quellen und Hilfsmittel benutzt und die den benutzten Werken wörtlich oder inhaltlich entnommenen Stellen als solche kenntlich gemacht habe. Des Weiteren erkläre ich, dass die gemachten Angaben wahrheitsgemäß sind und die wissenschaftliche Arbeit an keiner anderen wissenschaftlichen Einrichtung zur Erlangung eines akademischen Grades eingereicht zu haben. Hiermit erkläre ich, dass ich weder vorbestraft bin, noch dass gegen mich Ermittlungsverfahren anhängig sind.

I declare under penalty of perjury that this thesis is my own work entirely and has been written without any help from other people. I used only the sources mentioned and included all the citations correctly both in word or content. Further I declare that the above made statements are true and that this thesis was not submitted at another scientific institution to graduate. I hereby declare that I have no criminal record and that no preliminary investigations are pending against me.

Datum / Date

Unterschrift des Antragstellers / *Signature of the applicant*